IN VIVO NEUROCHEMICAL MONITORING WITH HIGH TEMPORAL AND SPATIAL RESOLUTION USING SEGMENTED FLOW MICROFLUIDICS

by

Meng Wang

A dissertation submitted in partial fulfillment
of the requirements for the degree of
Doctor of Philosophy
(Chemistry)
in the University of Michigan
2011

Doctoral Committee:

Professor Robert T. Kennedy, Chair
Professor Mark A. Burns
Professor Zhan Chen
Professor Margaret E. Gnegy
Associate Professor Kristina I. Håkansson

To my Grandmother:
May she enjoy health and peace in heaven

ACKNOWLEDGEMENTS

I would like to thank my research advisor, Dr. Robert Kennedy, for his continuous guidance and encouragement on my way towards this dissertation. As a graduate student, nothing is more rewarding than knowing that my advisor cares about my research and is excited with every little progress I have made. Bob is just such kind of advisor. When he learnt that I am interested in pursuing an academic career, he also did his best in providing me with the necessary information and sharing his experience with me as a professor, which has been extremely helpful for me to get to know this career path and to strengthen my mind of sticking to it.

I would also like to thank the other members of my doctoral committee including Dr. Kristina Håkansson, Dr. Zhan Chen, Dr. Mark Burns, and Dr. Margaret Gnegy for their comments and suggestions during my candidacy exam, data meeting, and dissertation preparation. Kristina and Peggy are both role models for me as female scientists who are leading successful academic careers. Prof. Chen and I are both alumni of Peking University and he has also established a good example for me as a Chinese researcher who has achieved reputable standing in the scientific community. I do appreciate very much the kindness of Prof. Burns for being so supportive and encouraging in every milestone on my road to this Ph.D. degree, even though he is almost always on an extremely busy schedule as the chair of the department of chemical engineering.

I am most grateful to the current and past members of the Kennedy group for their assistance. In particular, for my initial years in graduate school, I thank Dr. Gregory Roman for his excellent guidance in mentoring me to start with my research projects. I also thank Dr. Kristin Shultz, Dr. Maura Perry, Dr. Omar Mabrouk, Neil Hershey, and Thomas Slaney for their help with animal surgeries at different times throughout my later years.

I am forever indebted to my parents for all the love they have given to me. Although there is always some extra pressure on me to earn this degree, as both of them are chemistry graduates and mom is a Ph.D. in analytical chemistry, I feel lucky that I have finally made it to this point, with all the "chemistry genes" they have passed down to me. I especially thank them for being very understanding and open-minded parents who respect every decision I have made, and for raising me to be independent and mentally strong to face hardships in life.

At last, I would like to thank my friends in Ann Arbor and all over the United States for their accompany, which is indispensible for me to have so many enjoyable moments, although away from home, throughout the years in graduate school.

TABLE OF CONTENTS

LIST OF FIGURES

LIST OF ABBREVIATIONS

AA	Amino acid
aCSF	Artificial cerebral spinal fluid
BGE	Background electrolyte
BME	β- mercaptoethanol
CCD	Charge-coupled device
CE	Capillary electrophoresis/channel electrophoresis
CEC	Capillary electro-chromatography
CGE	Capillary gel electrophoresis
CIEF`	Capillary isoelectric focusing
CN	Cyanide
cP	Centipoise
CZE	Capillary zone electrophoresis
DMSO	Dimethyl sulfoxide
EA	Enzyme assay
EC	Electrochemical (detection)
EK	Electrokinetic
EOF	Electroosmotic flow
ESI	Electrospray ionization

FG	Flow-gated
FITC	Fluorescein isothiocyanate
f.p.	Freezing point
GABA	γ-aminobutyric acid
GOX	Glucose oxidase
HMDS	Hexamethyldisilazane
HP-β-CD	Hydroproxyl-β-cyclodestrin
HP-γ-CD	Hydroproxyl-γ-cyclodestrin
HPFA	High purity perfluoroalkoxy
HPLC	High performance liquid chromatography
HRP	Horseradish Peroxidase
HTS	High-throughput screening
i.d.	Inner diameter
i.p.	Intraperitoneal
LC	Liquid chromatography
LF-PPP	Low flow push-pull perfusion
LIF	Laser-induced fluorescence (detection)
LOD	Limit of detection
MALDI	Matrix-assisted laser desorption ionization
MD	Microdialysis
MEKC	Micellar electrokinetic chromatography
MS	Mass spectrometry/mass spectrometer
MWCO	Molecular weight cut-off

NAC	Nucleus accumbens
NDA	Naphthalene-2,3-dicarboxaldehyde
NMR	Nuclear magnetic resonance
o.d.	Outer diameter
PCR	Polymerase chain reaction
PDC	L-trans-pyrrolidine-2,4-dicarboxylic acid
PDMA	Polydimethylsiloxane
PET	Positron emission tomography
PFD	Perfluorodecalin
PMT	Photomultiplier tube
OPA	*o*-phthaldialdehyde
OTCS	Octadecyltrichlorosilane
RIA	Radioimmunoassay
RSD	Relative standard deviation
SD	Standard deviation
SEM	Standard error of the mean
SF	Segmented Flow
μTAS	Micro-total analysis system
UV	Ultroviolet (detection)

ABSTRACT

Monitoring the concentration dynamics of neurochemicals in the brain is a key tool in the effort to understand brain function, diseases, and treatments. A versatile and effective approach for in vivo monitoring of chemical messages is to couple sampling methods, such as microdialysis, to analytical measurements. Although this approach has proven invaluable, it is limited by poor temporal and spatial resolution. Temporal resolution is limited to about 60 s by the dispersion of sampled concentration zones during transportation. Spatial resolution is limited by the size of microdialysis probes which are typically 200 to 500 μm diameter and 1-4 mm long. As a result, some rapid chemical changes cannot be detected and the method cannot be used to probe smaller brain nuclei. To address the temporal resolution problem, a microfluidic device was developed that segmented a sample stream into plugs separated by fluorinated oil to prevent temporal distortion during transport. To quantify the chemical contents of the plugs, systems were developed for enzymatic and electrophoretic analysis. For enzyme assay, reagents were added to the plugs as they were formed and detected by fluorescence. For electrophoresis, a microfluidic device was developed that extracted plugs from the segmented flow stream and then injected them into a narrow channel for electrophoretic separation. The sampling and analysis systems allowed temporal resolution as good as 2 s. Alternatively, a capillary-based electrophoresis system could also be used to analyze dialysate plugs through a simple interface with 14 s on-line temporal resolution and

robust performances. To address the spatial resolution problem, the segmented flow analysis approach was coupled with miniauturized microdialysis probe with 0.5 mm sampling length. This system improved spatial resolution 2-8 fold over regular microdialysis while maintaining temporal resolution of 10-15 seconds. Dynamics of glucose and neuroactive amino acids were monitored in vivo with both anesthetized and freely-moving rats during pharmacological manipulations. These applications not only validated the robustness of this system, but also revealed different releasing pattern of taurine upon long term and short puffs of potassium infusion due to unprecedented spatial and temporal resolution it could offer.

CHAPTER 1

INTRODUCTION

In vivo Neurochemical Monitoring

Understanding normal and abnormal functioning of the brain is one of the greatest challenges facing science today. The brain contains a vast network of neurons that communicate with each other through neurotransmission between synapses (Figure 1-1). During neurotransmission, chemicals, or neurotransmitters, are released from a neuron into the extracellular space where they diffuse to the neighboring neurons to interact with receptors causing either excitation or inhibition of neurotransmitter release from the target neurons. Released neurotransmitters are removed from the extracellular space by either uptake through transporter proteins or enzymatic degradation.[1] Over 100 different compounds have been identified as neurotransmitters (or neuromodulators) including amino acids, peptides, small molecules like NO and acetylcholine, purines, catecholamines, and indoleamines.

In order to understand neurotransmission and its crucial role in brain functions, mental diseases and pharmacological treatments, great efforts have been made to measure neurotransmitter dynamics in the brain. Although ex vivo experiments on brain tissue slices and cultured cells have provided us with many valuable insights into neurotransmission, ultimately it is necessary to evaluate neurotransmitters in vivo. In vivo measurements make it possible to explore the regulation of neurotransmission from

different brain regions in the presence of complete neuronal circuits. Furthermore, in vivo measurementsallow the correlation of behavior and emotional state with neurotransmitter concentrations.

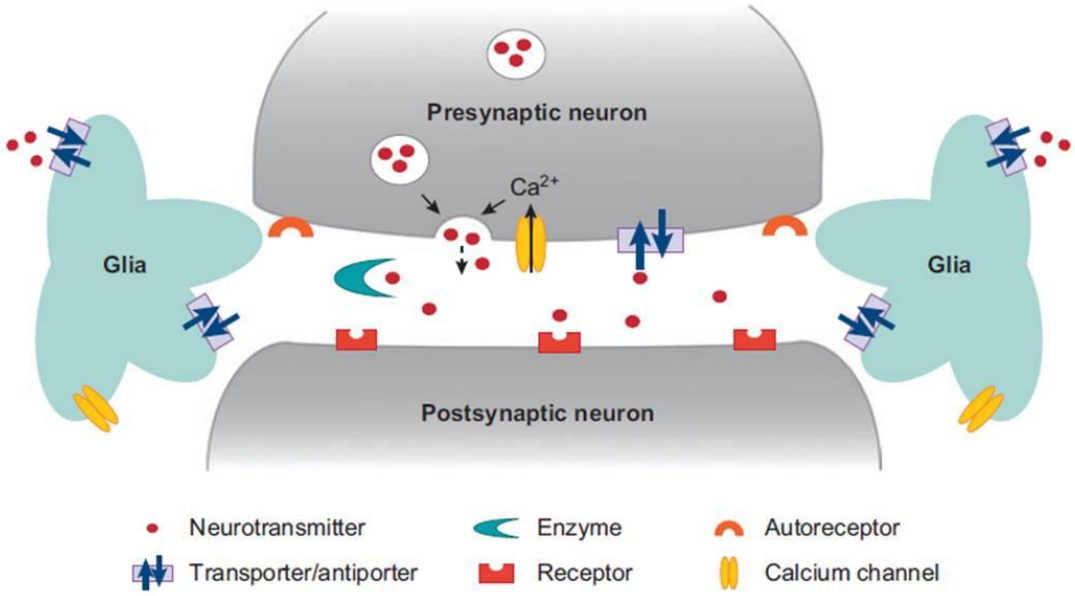

Figure 1-1. Neurotransmission at the synapse. Neurotransmitters diffuse across the synapse to interact with and bind to receptors on the postsynaptic neuron. These receptors can be on dendrites, cell bodies, or on another axon. If a neurotransmitter binds to an autoreceptor on the presynaptic neuron, a negative feedback loop is initiated to inhibit further release. Signaling is terminated via enzyme degradation or reuptake into the presynaptic terminal by transporter. Other supportive neuronal cells such as glia can also release and take up neurotransmitters (e.g., glutamate). Reprinted from Reference 2.

Criteria in Evaluating In vivo Monitoring Methods

In evaluating methodologies for in vivo monitoring, several criteria are of great importance, including sensitivity, selectivity, simultaneous measurement capability, spatial and temporal resolution. Since there are more than 100 neurotransmitters and

metabolites present in the extracellular space with concentrations ranging from pM to mM, the ability to selectively measure the targeted analyte without interference from others is indispensible. Simultaneously measurements of multiple neurotransmitters are also necessary in order to study interactions among them or to determine which neurotransmitters are involved in certain transmission event.

The brain is heterogeneous in neuronal functions and chemical compositions, which require measurements solely from the region of interest. Spatial resolution is important, because many brain structures, especially in experimental animals such as rats, are very small (several mm^3). Larger structures like striatum and cortex also have heterogeneity within themselves that can be lost with poor spatial resolution. As the mouse model has become highly interesting because of the many disease models based on genetic manipulations (e.g., gene knock-out) that have been made, the requirement put on spatial resolution becomes even higher since their brains are only ~1/3 the size of rat brains and therefore need micrometer resolution for localized measurements.

Finally, temporal resolution is critically important because fluctuations in neurotransmitter levels can occur on the millisecond time scale during exocytosis and reuptake/degradation process at the synaptic cleft, or on the second scale during behavior or pharmacological stimulations.[3-8] Accurate detection of these concentration changes is required to fully understand neurotransmission. At present only a few neurotransmitters have been measured with this temporal resolution.[3, 7, 9] It is the goal of this dissertation to significantly improve our ability to monitor neurotransmitters by developing novel analytical technology that allows simultaneous measurement of many neurotransmitters in vivo on the second time scale.

Current Monitoring Technologies

A variety of techniques to measure neurotransmitters in vivo have been developed, among which the prominently used ones are positron emission tomography (PET), microsensors, and microdialysis sampling .

PET is a noninvasive technique that uses trace amounts of radioactive isotopes to tag molecules of interest.[10] These molecules are injected into the bloodstream and monitored by their emission of positrons. Although PET is desirable because it does not cause damage to the area studied, it is expensive, has poor spatial and temporal resolution, detects a limited number of neurotransmitters, and is ill-suited for small laboratory animals such as rats and mice.

Microsensors and microdialysis sampling are both invasive methods that require implanting probes in the brain for direct monitoring or sample collection. Electrochemical microsensors[7, 8, 11, 12] provide high spatial and temporal resolution. However, only a few neurotransmitters out of more than 100 can be measurement with this method and selectivity is hard to verify. Furthermore, microsensors are not usually capable of simultaneously measuring multiple neurotransmitters, and are not reliably used for determining basal concentrations in vivo. As a result of these limitations, most in vivo neurotransmitter studies involve microdialysis sampling,[13, 14] which is discussed in more detail below.

Microdialysis Sampling

A microdialysis probe consists of two pieces of tubing as fluid inlet and outlet, and a piece of semi-permeable hollow-fiber membrane that is usually 200 to 500 μm in

diameter and 1 to 4 mm in length (Figure. 1-2).[13-16] During sampling, the probe is inserted into the brain region of interest. A buffer that has the similar ionic composition as the extracellular fluid, named as artificial cerebral spinal fluid (aCSF), is constantly perfused from the inlet tubing at 0.1 to 2 μL/min. A concentration gradient is established across the membrane, which induces components below the molecular weight cut-off (MWCO) of the membrane to diffuse into the perfusing buffer. Dialysate is collected in fractions and analyzed either on-line or off-line by appropriate techniques such as enzyme assay (EA), high performance liquid chromatography (HPLC), radioimmunoassay (RIA), and capillary electrophoresis (CE). Compared to PET and microsensors, microdialysis excels in terms of selectivity and multi-analyte measurement capability. In theory, it can be used to measure any kind of neurotransmitters, due to its sampling property and a wide selection of analysis methods. Weaknesses of microdialysis include difficulty with quantification,[17-19] poor temporal resolution[20, 21] and poor spatial resolution.

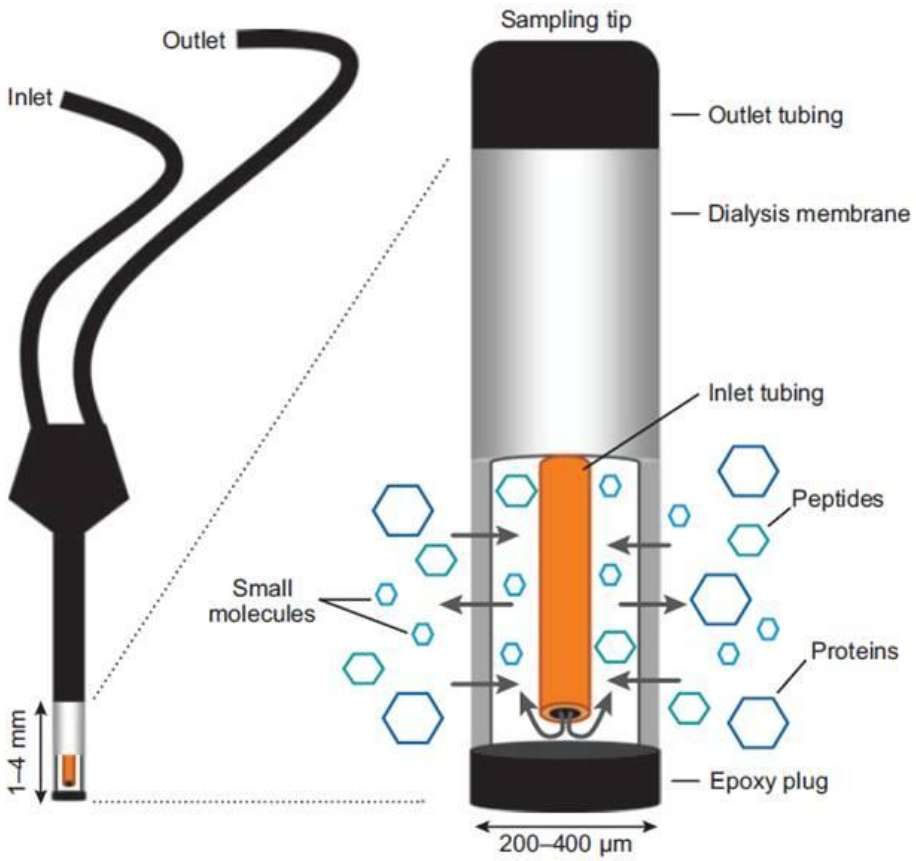

Figure 1-2. Microdialysis sampling with a concentric probe. A perfusion buffer that mimics the ionic content of the extracellular space is pushed into the inlet. When this buffer flows past the active area of the membrane, this creates a concentration gradient between the tissue and the lumen of the probe. Analytes that have a mass below the MWCO of the membrane diffuse into the probe and can be collected for further analysis. Dialysate exits the probe through the outlet to be collected off-line into a vial or to be sent directly toward the instrument's detector. Local pharmacological manipulations can also be performed simultaneously by adding the agent to the perfusion buffer. Reprinted from Reference 2.

Temporal Resolution

Temporal resolution in microdialysis sampling is usually limited by mass sensitivity of the analytical method coupled to the probe i.e., sample must be collected

long enough to obtain a detectable quantity. When techniques such as HPLC are used, the temporal resolution is often 10-30 min. However, coupling microdialysis to nanoscale analytical techniques such as capillary electrophoresis (CE) and capillary liquid chromatography (LC) have shortened sampling times to 3-30 second.[6, 20-32] Both on-line[20, 24, 29, 31, 33] and off-line[5, 6, 27, 34] analysis have been demonstrated with such temporal resolution.

With the high sensitivity of these analytical methods, other factors can begin to limit temporal resolution. With on-line analysis, temporal resolution may become limited by the separation speed, which is problematic for complex separations.[35] With off-line analysis, the problem lies in sample handling. For example, only 12 samples will be generated in 1 hr with 5 min temporal resolution. This number rapidly reaches to 360 if temporal resolution is increased to 10 s.[2] Smaller sample volume (e.g. from μL to nL) and larger sample load create substantial demands on the fraction collection and analysis system, and can also limit sampling period to no more than a few minutes.

In both on-line and off-line systems, an inherent factor limiting temporal resolution is Taylor dispersion, i.e. the broadening of sample zones as they are transferred from the sampling probe to the analytical system.[36] This problem is especially acute when using low flow rates (desirable for use with smaller probes or quantification, as discussed below) or long connector tubing (as in freely moving animal experiments or clinical applications). Under low flow conditions, temporal resolution may be worsened to 2-4 min because of zone broadening.[29] In this dissertation, an approach that eliminates Taylor dispersion to achieve higher temporal resolution is reported.

Spatial Resolution

Microdialysis is also limited in terms of spatial resolution due to its relatively large sampling area, which is generally 200-500 μm in diameter and 1-4 mm in length. In addition, when probes are operated at high flow rates, such as 1-3 μL/min, they will remove compounds from a relatively large area around the probe, creating concentration gradient several millimeters away from the membrane surface, thus further decreasing spatial resolution. This makes microdialysis sampling only applicable to experimentation on large rodents such as rats. Some alternative sampling techniques, such as low flow push-pull perfusion (LF-PPP)[37] and direction sampling[38] have been introduced. As sampling only occurs at the tip of these probes, it is proposed that they offer ~500 fold improvement in spatial resolution compared to microdialysis.[39] However, so far they are not routinely used for in vivo studies, probably due to the fragility in probe handling during animal experiments. As an alternative, further shrinkage of the size of microdialysis probes (e.g. micrometer sampling area) to improve spatial resolution is possible. However, low sampling flow rates (e.g., <100 nL/min) are needed for such small probes so as to collect enough sample concentration in the dialysate (i.e. higher relative recovery) to be detectable. As a result, temporal resolution has to be compromised, because Taylor dispersion becomes severe under such low flow rates. In this dissertation, methods to alleviate the temporal resolution disadvantage of small probes are reported, thus allowing high temporal and spatial resolution simultaneously.

Recovery and Quantification

Analyte recovery by the microdialysis probe is an important issue to consider in evaluating the effectiveness of sampling. Recovery can be defined as absolute or

relative. Absolute recovery refers to the mass of analyte collected over a period, while relative recovery is defined as the concentration of analyte in dialysate divided by the actual extracellular concentration. Both absolute and relative recovery are strongly dependent on flow rate, with higher flow rate resulting in higher absolute recovery but lower relative recovery (Figure 1-3). In high temporal resolution monitoring, sample collection time is short, thus making relative recovery more important in order to satisfy the mass sensitivity of the detector. With flow rates commonly used in microdialysis practices, e.g. 0.5-2 μL/min, relative recovery is normally less than 50%. The fact that relative recovery is not 100% complicates quantification of extracellular levels, since in vitro determinations of relative recovery do not accurately reflect in vivo relative recovery.[14, 17, 19, 21, 40, 41] The reason for this discrepancy is that active control over extracellular concentrations in vivo affects the concentration profiles towards the probe and hence the recovery. To circumvent this problem, in vivo calibration method such as no-net-flux is commonly used.[17-19, 21, 42] However, this method requires many measurements and is very cumbersome. Another calibration method is the low flow rate method in which the flow rate through the probe is low enough (e.g., <100 nL/min) to yield nearly quantitative recovery (>90%).[43-45] This method is easy to implement but would sacrifice temporal resolution due to amplified Taylor dispersion at the low flow rates used. In vivo monitoring with quantitative recovery while simultaneously obtaining temporal resolution as good as 20 s has been shown in this dissertation.

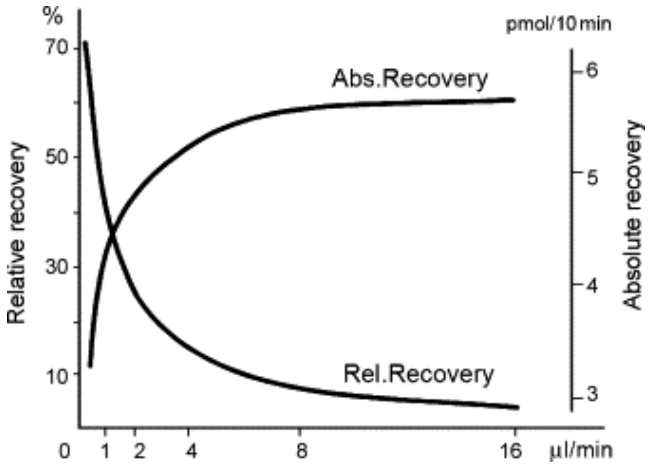

Figure 1-3. Relative and absolute recoveries as a function of sampling flow rate (from "Microdialysis-principles of recovery" by Agneta Eliasson, 1991). Reprinted from Reference 46.

On-line and Off-line Methods

Dialysate samples can either be analyzed on-line or off-line. In on-line analysis, dialysate stream from the probe is directly pumped to the detector. In off-line mode, a specified volume of dialysate (usually 1-20 μL) is collected in vials or tubes for later analysis. On-line methods offer the advantage of minimal manual sample handling because the dialysate is continuously pumped to the analysis system. In addition, with an on-line method, it is possible to monitor the output during the experiment to ensure proper sample collection. On-line monitoring is also useful for providing rapid feedback in certain situations such as chemical monitoring during surgery. However, on-line analysis places strict requirements on the speed of the analytical method. Thus, analysis time can become the limiting factor of the temporal resolution, even if Taylor dispersion or mass sensitivity is not a problem.

Off-line methods have the advantage of maintaining temporal resolution, even if the analysis time is longer than the collection time of each sample fraction. This is realized by decoupling the sampling step from the analysis and detection. Due to such flexibility, sample manipulations before analysis, such as derivatization and digestion that might require long reaction time or specific incubation conditions, can also be conveniently performed. Off-line methods are also indispensible in collaboration projects, where sample collection and analysis may be performed at different locations. In additional, multiple detection methods with various dynamic ranges may be used if sample fractions can be divided into several portions, thus expanding the number of measurable species. Major drawbacks of off-line analysis include manual sample handling, which can be labor-intensive. Sample loss due to degradation and adsorption to containers during collection and storage can also hinder our ability to probe accurate in vivo information. In addition, although temporal information may be conserved with off-line methods, throughput is traded off due to long analysis time.

Analysis of the Dialysate

As a sampling method, microdialysis can virtually be coupled to any analytical technique. Commonly used ones include enzyme assays, HPLC and CE. Enzyme assays have good sensitivity and selectivity, but are only available for the detection of a limited number of compounds, such as glutamate,[47, 48] acetylcholine,[49] glucose,[50, 51] and lactate.[52] To take advantage the multi-analyte detection capability offered by microdialysis, separation-based techniques such as HPLC and CE are more popular. HPLC coupled to UV detection[53] is most widely used because of the variety of developed separation methods, commercially available instrument and ruggedness of the set-up. Conventional

LC column have large inner diameter (e.g. 4.6 mm) and typically requires 20-30 μL of sample for injection, which limits temporal resolution to 20-30 min. Capillary LC needs less sample volume, and together with the use of sensitive detector such as electrochemical (EC) or laser induced fluorescence (LIF), temporal resolution up to 10 s has been reported.[20, 25, 54] Coupling capillary LC to mass spectrometry (MS) is an even more powerful approach due to the high mass sensitivity of MS and the capability of identifying novel species by using tandem MS to analyze chemical structures.[55] This method has nearly become the only practical means to detect endogenous neuropeptides,[56-60] whose in vivo concentrations can be as low as several pM, which is ~10^6 fold lower than amino acids neurotransmitters.[28] Due to relatively long separation time, most in vivo measurements with LC are performed off-line.[57]

For the detection of neurotransmitters with higher in vivo level, such as amino acids, CE coupled to LIF or EC is a feasible approach for fast analysis. In state-of-the-art techniques, separation time in CE can be as short as less than one second.[61] Although typical separation times are 1-60 s, CE is still substantially faster than LC and is more suitable for on-line in vivo measurements with high temporal resolution. Details of CE coupled to microdialysis sampling will be discussed in the following section.

Capillary Electrophoresis for Dialysate Analysis

Ever since electrophoretic separation was first performed in open tubular capillaries reported by Jorgensen and Lukacs in 1981,[62] many electrophoresis-based separation modes have been developed, including capillary zone electrophoresis (CZE), micellar electrokinetic capillary chromatography (MEKC), capillary isoelectric focusing

(CIEF), capillary gel electrophoresis (CGE), and capillary elecro-chromatography (CEC). CZE, which is also known as free-solution CE or simply referred to as CE, is the simplest yet most widely used format of all. Analytes in CZE migrate in the background electrolyte (BGE) buffer when an electric field is applied across the capillary. Under an electric field, the speed and the direction of migration are determined by both electroosmotic mobility (μ_{eo}) of the buffer and the electrophoretic mobility (μ) of the analyte. Electroosmotic mobility (μ_{eo}) is the result of ionized silanol groups on the inner capillary wall that cause a net positive charge for the buffer, which, under the electric field (E), pushes the bulk solution toward cathode as electroosmotic flow (EOF):

$$v_{eo} = \mu_{eo} E = \frac{\varepsilon \xi}{\eta} E$$

where ε is the permittivity and η is the viscosity of the solution, and ξ is the potential in the Helmhotz plane.

Electrophoretic mobility μ is the intrinsic property of the analyte and is described by:

$$\mu = \frac{q}{6\pi\eta r}$$

where q is the charge of the ion and r is the Stoke's radius of the ion in the buffer. The overall migration velocity (v) of the analyte is then governed by electric field and the apparent mobility μ_{app}:

$$v = \mu_{app} E = (\mu_{eo} + \mu) E$$

Different analyte will have different migration velocity, thus being separated based on their charge-to-size ratio.

Compared to HPLC, which utilizes pressure-driven flow with a parabolic velocity profile, EOF in CE has a plug-shaped profile that results in less band broadening of sample zone and more plates generated per unit length. This is considered to be the major merit of CE, which, together with its simple instrumentation and small sample consumption, has given rise to its widespread application in the separation of various classes of analytes ranging from small molecules to peptides and proteins.[63] Separation in traditional CE, however, is slow, which might take anywhere from tens of minutes to hours depending on the complexity of the sample. In order to make CE an appropriate choice for in vivo chemical monitoring where fast analysis is always welcomed, high-speed CE separation is necessary.

Principle of Fast Capillary Electrophoresis

In the case where diffusion is the only source of band broadening, simple CE theory dictates that both separation speed and efficiency can be simultaneously increased by increasing the voltage dropped across the separation channel.[54] This principle is demonstrated by the equations for theoretical plates (N) and migration time (t_{mig}):

$$t_{mig} = {}^{l}/_{v} = {}^{L}/_{V\mu_{app}}$$

$$N = {}^{\mu_{app}V}/_{2D}$$

Where l is the separation length, L is the total capillary length and V is the voltage dropped across L, D is the diffusion coefficient of the analyte. From these equations, it is apparent that N is proportional to voltage and t_{mig} is inversely proportional to voltage. The equations also show that separation efficiency is independent of column length.

Therefore, as long as the same voltage is applied, separation column can be shortened for faster runs with the same plate number.

In actual applications, however, other sources of band broadening limit the benefit of higher voltages on efficiency. These sources of band broadening have to be suppressed to obtain diffusion-limited efficiency. Their effect can be evaluated by considering the definition of efficiency:

$$N = {t_{mig}^2}\Big/{\sigma_{tot}^2}$$

where σ_{tot}^2 is the zone variance from all sources of band broadening. In CE, σ_{tot}^2 can be expressed as:

$$\sigma_{tot}^2 = \sigma_{diff}^2 + \sigma_{inj}^2 + \sigma_{det}^2 + \sigma_{heat}^2 + \sigma_{ads}^2 + \sigma_{ed}^2$$

where σ_{diff}^2, σ_{inj}^2, σ_{det}^2, σ_{heat}^2, σ_{ads}^2, σ_{ed}^2 are the variances caused by longitudinal diffusion, sample injection, detection, Joule heating, adsorption, and electromigration dispersion (or "sample overloading"), respectively. Under diffusion-limited conditions, the expression for σ_{tot}^2 simplifies to:

$$\sigma_{tot}^2 = \sigma_{diff}^2 = 2Dt_{mig}$$

However, when t_{mig} is small, which reduces the magnitude of σ_{diff}^2, it is difficult to achieve diffusion-limited efficiency. Consequently, great care must be taken to reduce the contribution from other band broadening sources.

Joule Heating Joule heating generates radial temperature gradient inside the separation capillary because heat is only dissipated through the capillary surface. Such temperature gradients result in band broadening due to uneven electromigration rates and convection. Separation capillary with small inner diameter (e.g., < 10 μm) is more desirable in fast-

CE due to its higher surface-to-volume ratio for more effective heat dissipation. Dissipation rate can be further enhanced with external cooling sources such as air or liquid coolant. Using low-conductivity BGE is also an effective way to reduce current under fixed electric field, thus reducing heating.

Detection In order to minimize extra-column band broadening, virtually all fast separations employ on-column detection. However, the use of small bore capillaries for suppressed Joule heating places stringent requirements on the choice of detector due to the short path length that results in small absorbance. Therefore, laser induced fluorescence (LIF) has become the most popular detection method in fast CE because its sensitivity is concentration-dependent. After derivatization with appropriate fluorogenic reagents, amino acids with subattomole concentrations can be detected with a sheath-flow cell,[64] making this approach valid for in vivo experiments. Other detection methods for fast CE include electrochemical (EC)[65] or electrospray ionization-mass spectrometry (ESI-MS)[66] detection, which also offer sufficient sensitivity to be used with small columns.

Sample Injection In fast CE, very narrow plugs of sample are required to be loaded onto separation column, as variance due to injection is often the largest contributor to band broadening.[61, 67] The variance contributed by sample injection can be expressed as:[68]

$$\sigma_{inj}^2 = {h^2}/{12}$$

where *h* is the initial width of the sample plug. In order to reduce injection variance in fast CE, the injected sample volume should be on the order of hundreds of picoliters (10^{-12} L). Optically-gated injection and flow-gated injection are two major options for

precise and repeatable small volume sample loading. In optical-gated CE,[69] sample is fluorescently tagged and continuously photo-bleached by an intense laser beam (gating beam). Injection is made by briefly blocking the gating beam with the shutter to allow a narrow plug of fluorescently labeled analytes into the separation column for electrophoresis and LIF detection. In flow-gated CE,[70] separation buffer is pumped through the gap between the sample inlet and the separation column inlet, so as to prevent the incoming sample stream from entering the separation column during separation mode. For injection, the buffer flow is temporally stopped and sample is drawn into the separation capillary by electrokinetic effects. In comparison, optical gate excels in rapid injection and faster separation, while flow gate has the advantage of less-expensive set-up and wider range of applications (not limited to fluorescently-tagged samples).

Adsorption Adsorption to capillary walls generates chromatographic retention and band-broadening to electrophoretic separation, whose effects increase with the speed of migration. For CE performed in fused silica capillaries, adsorption is generally not a problem with small molecules or DNAs, which consist most examples of fast CE. However, when separating peptides and proteins in fused silica capillaries, or when using capillaries (or microfabricated channels) made from materials other than glass (e.g., polymer), special procedures are need to coat the capillary walls in order to suppress adsorption.

Fast Electrophoresis on Microfluidic Device

"Microfluidics" refers to the science and technology of manipulating fluidics in networks of channels with micrometer dimensions.[71] Performing chemical analysis on a microfuidic device not only reduces sample and reagent consumption, but also enables

sample manipulation and even detection in an automated fashion.[72] Chips for carrying out channel electrophoresis (CE) are mainly fabricated from glass or quartz due to their suitable surface chemistry to generate stable EOF and optical transparency.[73, 74] Although polymers like polydimethylsiloxane (PDMS) have also been used for CE,[75] separation performance comparable to that of glass or quartz chips is yet to be demonstrated.

While high-speed CE on chips follows the same principles and cautions as those with capillary systems in terms of reducing sources of band-broadening, one major advantage of chip based devices is the capability of using electrokinetic pumping to manipulate and inject samples in picoliter scale. Various injection schemes have been developed based on the needs of applications,[76] such as T-type injection,[77] pinched injection[78] and gated injection.[79] In gated injection, sample stream is diverted from the entrance of the separation channel by EOF pumped cross-flowing buffer, while injection is made by floating the potentials of the buffer and sample waste reservoir for a very short time.[80] This scheme has the advantage of making computer-controlled automatic injections repetitively with the minimal number of voltage sources,[81] which is most suitable for chemical sensing such as in vivo monitoring, where serial injections are required. Due to the nature of electrophoretic flow, injection bias is observed in both the sample loading and dispensing steps, with neutral analytes being preferentially injected over anionic analytes.[82, 83] The bias can be alleviated by loading the sample for sufficiently long time.[84]

Compared to capillary system, CE on a chip can have an additional source of band broadening that comes from the geometry of separation channels. In order to

maintain a compact footprint yet sufficient separation length for desirable resolution, turns or bends are often included in the design of lengthened separation channel. These turns or bends can cause additional zone dispersion by electric field enhanced "racetrack" effect for individual molecules in the analyte band,[78, 85] where molecules on the inside wall of the turn travel not only a shorter distance but also faster than molecules along the outside wall because of a higher potential field. The amount of dispersion introduced by a turn can be quantified using a one-dimensional model:[85, 86]

$$\sigma_{geo}^2 = \left[2\theta\omega \left(1 - exp\left(- {\omega^2 v_c r_c}/{2D\theta\left(r_c + {\omega}/{2}\right)^2} \right) \right) \right]^2 \Big/ 24$$

where θ is the angle of the turn in radians, ω is the width of the channel, v_c is the velocity of the analyte, r_c is the radius of curvature along the centerline of the turn, and D is the analyte diffusion coefficient. This equation reveals that with fixed CE separation conditions, reducing the channel width at the turn and increasing the radius of the turn are two practical means to suppress geometry dispersion. Both spiral shaped separation channel (large radius turns)[86] and tapered channel at the turns[87] have been demonstrated for high-efficiency microchip separation. In general practice, including an even number of tapered turns with alternating directions in the design can cancel out the racetrack effect at a single turn, resulting in more uniform sample bandwidth.

Capillary/Channel Electrophoresis for the Analysis of In vivo Dialysate

The rapid development of fast CE technologies, which makes separation duration ranging from several second to a few minutes a common practice, has made CE an attractive choice for the analysis of microdialysis samples. Microdialyisis sampling coupled to on-line CE (MD-CE) have been used to continuously monitor neurobiological processes with excellent temporal resolution.[2, 46, 57, 88] This technique is alternatively named as "separation-based sensor",[21, 89] due to the its similarity to traditional chemical sensors in terms of continuously outputting real-time information of chemical components, yet providing significant performance enhancements including high selectivity and multi-chemical monitoring capability.

To interface CE with on-line dialysate stream, both flow gate[24, 90] and optical gate[61, 91] have been employed. LIF is the most popular detection method due to its high sensitivity for detecting trace amount of analytes in vivo. A large number of reagents are commercially available for fluorescence derivatization of amines, thiols, carbohydrates and other functional groups, such as fluorescein isothiocyanate (FITC), naphthalnene-2,3,-dicarboxaldehyde (NDA) and *o*-phthalaldehyde (OPA). The latter two are more commonly used for on-line MD-CE due to their fast reaction kinetics (<240 s).[92] Amino acids are the most studied neurotransmitters using on-line CE-LIF and the continuous monitoring of neuroactive amino acids like glutamate, aspartate, γ-aminobutyric acid (GABA) and taurine with 5-90 s temporal resolution have been reported.[24, 29, 31, 33, 90, 93, 94] Monoamines such as dopamine have also been monitored with this approach using NDA derivatization and 90-s MEKC separation.[35]

Electrochemical (EC) detection, in the mode of either amperometry or conductivity, is also commonly used for MD-CE. It is especially suitable for the measurements of monoamines (e.g., dopamine, norepinephrine, epinephrine, and other catecholamines), whose structures lend themselves readily to oxidation/reduction at the electrode surface.[95]

Besides on-line monitoring, off-line measurements of dialysate fractions are also feasible with CE, especially when sample manipulation or separation is not fast enough for desired temporal resolution. Examples with both amino acids and catecholamines using either LIF or EC detection have been reported.[22, 96-101]

In the same manner, microchip CE can be used in place of capillary system for coupling to microdialysis sampling, with the effort of integrating sample manipulation, separation and detection into a miniaturized total analysis device for on-animal sensing. Both Lunte's group[102, 103] and Kennedy's group[104] have reported on-line sampling, derivatization and CE-LIF for monitoring amino acids on glass chips with comparable temporal resolution (30-40s) as the capillary system. Use of the microfluidics approach also offers the convenience of fabricating valves and pumps in situ to drive dialysate fluid within channel networks. For example, peristaltic pump made from multilayer soft lithography technique on PDMS[105] was used to sample from a push-pull probe and to inject dialysate onto a fused silica separation capillary through an on-chip flow-gate interface.[39] Such solenoid-controlled pneumatic valving method in dialysate manipulation and injection was also used in a series of other reports.[106, 107] Although LIF is a popular detector of choice for microchip CE due to the exceptionally low detection levels that are possible, amperometric detection was also demonstrated for dopamine

analysis.[106] Actually, there has been great interest in coupling EC detection to microfluidic devices due its compatibility with microfabrication technologies and inherent miniaturization and portability.[108]

Droplet-based Microfluidics and Segmented Flow

Droplet-based microfluidics, or segmented flow, in which sample droplets or plugs are carried by an immiscible fluid, has received considerable interest in recent years because of its potential for improving sample manipulation and chemical reaction control in low volume systems.[109-115] Droplets or plugs from femtoliter to microliter volume can be reproducibly generated using several channel geometries such as co-axial injectors,[116, 117] flow-focusing nozzles,[118, 119] and T-junctions,[120, 121] by either passive pumping[122-124] or active fluidic control.[125-128] Various fluidic manipulations of segmented flow have also been demonstrated, such as in-plug mixing,[129-133] fusion and merging,[134-141] fission and splitting,[141-145] sorting,[146-148] heating and freezing,[149-151] shrinkage and expansion,[152-154] trapping and incubation,[139, 155-157] reagent addition,[129, 158, 159] de-segmentation and droplet extraction.[160-163]

Compared to single phase microfluidic stream, droplet microfluidics owns unique properties, including reduction of axial dispersion between adjacent plugs,[164] rapid mixing within a plug due to induced recirculation,[132, 133, 164, 165] large interfacial areas that contribute to high mass or energy transfer,[109] and the ability to conveniently tune droplet/plug volume and frequency for a spectrum of femliter to microliter droplet/plugs at sub-one to thousands of hertz.[166, 167] These properties, together with the elegant manipulations of segmented flow, have enabled numerous droplet/plug-based

applications. For example, various chemical reactions can be carried out in droplets/plugs, which provides rapid mixing of reagents, control of the timing of reactions, control of interfacial properties and the ability to perform reactions in a high-throughput fashion.[111] Applications include enzyme assays,[168, 169] DNA analysis,[170-175] PCR,[176, 177] protein crystallization,[178, 179] organic and nanopartical synthesis,[129, 130, 180-182] etc. Biological species including cells[148, 183-186] and worms[187] can be compartmentalized in droplets/plugs for further manipulations such as cell lysis[183, 185] and nanosurgery.[188] Due to the high-throughput nature of segmented flow, there have been numerous reports on using droplets/plugs in place of 96-well plates for high throughput screening (HTS).[189] A variety of screening subjects such as enzyme reactivity,[190, 191] reaction condition,[180, 192] protein crystallization condition,[178, 193] and drug susceptibility to bacteria[194] have been demonstrated. Large interfacial area between droplets/plugs and the carrier phase has also proven valuable in small-scale interfacial synthesis,[195, 196] liquid-liquid extraction[197-199] and pH sensing.[200] Furthermore, from a computational perspective, droplets/plugs can be considered as units of information, which is analogous to electronics, thus bridging chemistry with computation for process control.[201-203]

Conserving Temporal Information with Segmented Flow

In the studies discussed above, avoiding dispersion or mixing of discrete samples is often cited as an advantage of segmented flow. Indeed, in real-world chemical analysis, due to unavoidable physical distance between sampling and detection points, or the necessity of sample manipulation (reactions, incubations, etc) prior to measurements, temporal information is often distorted by dispersion during sample transportation or reaction in continuous flow system. Segmented flow turns out to be an ideal solution to

such concern. Several studies have therefore focused on the ability of using segmented flow to improve temporal resolution in chemical monitoring. For example, enzyme kinetics can be monitored with millisecond temporal resolution, where substrate and enzyme were rapidly mixed upon droplet/plug formation and the reaction mixture was monitored at different points downstream, representing various reaction times.[168] A more comprehensive droplet/plug processing system with off-chip incubation was also demonstrated to characterize catalytic activity of in vitro translated protein.[169] In a different study, zinc secretion from pancreatic islets was monitored with ~1 s temporal resolution by converting perfusion buffer into plugs shortly after sampling from the islet, which revealed both short (~20-60 s) and long (~5-10 min) pulses in secretion profile.[204]

Besides the commonly used "sampling-droplets" approach, a novel device termed the "chemistrode" was operated in the reverse way, i.e. "droplets-sampling".[205] In this method, perfusion buffer with or without stimulant was pre-formed into plugs prior to sampling from the islet via a V-shaped interface. Sampling and stimulation were made possible by the coalescence of buffer plug with the wetting layer above the hydrophilic substrate.[206] By delivering the buffer plugs at 20 Hz frequency, temporal resolution of the system was 50 ms.

Another useful application of droplet microfluidics in conserving temporal information lies in the compartmentalization of chemically separated components from CE or HPLC.[207-209] By collecting CE or HPLC effluents as nanoliter or picoliter plugs, both temporal resolution and separation resolution could be preserved. This approach has proven invaluable in two-dimensional separations,[207-209] and would also be helpful for post-column derivatizations.

Despite the above applications, there has been no report on coupling segmented flow with microdialysis sampling to improve temporal resolution of in vivo chemical measurements. This topic is therefore thoroughly studied in this dissertation.

Methods to Probe the Chemical Information in Droplets/Plugs

Although there has been considerable research effort aimed at manipulating sample droplets/plugs and applying them to technical problems, relatively few methods exist for analyzing the chemical contents of droplets/plugs, which greatly limits their potential utility. Most studies discussed above relied on optical probing of droplets/plugs by fluorescence, X-ray diffraction or absorbance. While many useful assays can be developed with this approach, higher resolving power is often necessary for complex mixtures or for the detection of multiple analytes simultaneously. Mass spectrometry (MS) is a competent detector with great sensitivity and resolving power. One approach in coupling droplet microfluidics to MS is to deposit plugs onto MALDI plate for off-line MALDI-MS analysis.[180, 189, 205] However, the sample deposition step could be time-consuming and labor-intensive. On the other hand, droplet/plug analysis by electrospray ionization (ESI) can be operated in a high-throughput fashion, which has been demonstrated by several research groups. It has been shown that both air-segmented flow[210] and oil-segmented flow[191, 208] could be directly infused into ESI emitter tip, although careful selection of the carrier phase and operational flow rate was necessary in the latter situation.[208] Alternatively, to avoid carrier phase interference with ESI, sample droplets/plugs could also be extracted from the carrier phase prior to MS analysis.[163, 211, 212] Besides MS, electrochemical detection[213] and NMR[214] of droplets/plugs have also been reported.

Another powerful approach to analyzing droplets/plugs would be capillary/channel electrophoresis. Edgar et al[215] reported the first seminal study on this concept by injecting picoliter sample plugs into CE channel through an immiscible boundary between the carrier phase and the separation buffer. Electrophoretic separation of FITC-labeled amino acid standards was demonstrated using this PDMS-based device. Niu et al[209] also adopted a similar approach to separate protein mixtures in plugs, while an additional "comb" structure was included to remove carrier phase prior to sample plug loading, so that sample injection could be operated repetitively by continuous pumping. The Wheeler group reported two generations of interface for coupling CE with digital microfluidics.[216, 217] The newer generation was a multilayer hybrid device which used glass substrate for electrophoresis to achieve better separation efficiency.[217]

These interesting methods were proven useful, but were either unsuitable for sampling from a continuous stream of plugs to achieve high throughput analysis, or had unsatisfactory separation efficiency due to the use of PDMS substrate or lack of proper scheme for efficient sample injection, rendering the methods incompetent to resolve complex mixtures. Therefore, in Chapter 3 of this dissertation, a CE device that provides high throughput and high efficiency CE analysis of segmented flow steams, which is suitable for complex sample such as in vivo dialysate, is introduced.

Dissertation Overview

This dissertation addressed several important technical innovations on using segmented flow microfluidics to improve the temporal and spatial resolution of in vivo neurochemical monitoring. In Chapter 2, segmented flow microdialysis (SF-MD) was

demonstrated for the first time and its ability to maintain temporal resolution independent of the length of transfer tubing was verified. An enzyme assay was integrated and applied to monitoring glucose dynamics in vivo with 30 s temporal resolution, which testified the robustness of the method .

Chapter 3 introduced a novel microfluidic design that extracts water plugs from segmented flow before analyzing the plug content by channel electrophoresis. Differential etching and selective patterning are two key factors leading to complete phase separation. High efficiency CE analysis with more than 200,000 plates can be obtained with the design, which is the highest among reported segmented flow CE (SF-CE) methods. On-line coupling of this SF-CE device with SF-MD allowed 30-40 s overall temporal resolution.

In Chapter 4, a new generation of dialysate segmentation chip with smaller footprint and lower connection dead volume was described. Temporal resolution achieved with this dialysis/plug sampler was up to 2 s, which is the highest so far with microdialysis sampling and is almost comparable to that of some microsensors. To avoid the limitation of overall temporal resolution by slow CE separation step, 2 nL dialysate plugs were collected off-line in removable Teflon tubing and pumped to the SF-CE chip at a lower flow rate. 9 s temporal resolution was demonstrated in vivo using this approach.

Chapter 5 answered several important questions regarding off-line in vivo monitoring using segmented flow microdialysis, This includes sampling from freely-moving animals for behavioral studies, using small microdialysis probes for 2-8 fold higher spatial resolution, and freezing dialysate plugs to extend analysis window to 4

days. The combination of these features made the method applicable to collaboration projects, which would allow other pharmacologists to take advantage of the achievements of this dissertation.

In Chapter 6, segmented flow microdialysis was coupled to a capillary-based electrophoresis system with a flow-gated injection interface. The system offered better electrophoresis performance than microchip CE including faster separation, lower detection limit, and longer operation life. Phase separation before flow-gated injection was realized by the insertion of a hydrophilic side-capillary. In vivo applications involved the comparison of the effect of long term and short puffs of potassium stimulation on the responses of multiple neuroactive amino acids, which revealed a different releasing mechanism of taurine.

Chapter 7 described several future directions that can potentially improve the usability of the method for routine pharmacological analysis. The feasibility of coupling SF-CE with low flow push-pull sampling[37, 39] was also initially proven. The combination would realize high temporal resolution monitoring with ~500 fold higher spatial resolution compared to microdialysis.

CHAPTER 2

IMPROVED TEMPORAL RESOLUTION FOR IN VIVO MICRODIALYSIS BY USING SEGMENTED FLOW

Introduction

Microdialysis sampling is widely used in for in vivo monitoring of chemicals in extracellular space of tissues such as heart, fat, liver, and brain.[15, 218, 219] In chemical monitoring applications, temporal resolution is a key figure of merit because analyte concentrations can change rapidly.[20, 220, 221] When using microdialysis sampling, temporal resolution is usually limited by mass sensitivity of the analytical method coupled to the probe i.e., sample must be collected long enough to obtain a detectable quantity. When techniques such as HPLC are used, the temporal resolution is often 10-30 min;[16] however, coupling microdialysis to nanoscale analytical techniques such as capillary electrophoresis (CE), microbore liquid chromatography (LC), and electrochemical sensors have shortened sampling times to seconds.[6, 20-23, 25-30]

When using high sensitivity analytical methods, other factors can begin to limit temporal resolution achievable with microdialysis sampling. One inherent limitation is broadening of sample zones due to Taylor dispersion as they are transferred from

sampling probe to analytical system.[36] The effect of Taylor dispersion can be ameliorated by using high flow rate through the probe; however, this decreases relative recovery thus decreasing the concentration of analytes measured. Higher flow rates are also incompatible with smaller probes and alternative sampling methods such as low flow push-pull perfusion[37] or direct sampling[38] that improve spatial resolution. Taylor dispersion can also be decreased by shortening the length of tubing connections; however, this approach is impractical for experiments involving freely moving animals. Thus, although temporal resolution of 3 s has been described for sampling from an anesthetized animal at high dialysis flow rates; temporal resolution is increased to 90 s for low flow rates or work with awake and freely moving animals.[29] In this work, we describe coupling microdialysis probes to a microfluidic segmented flow system to avoid these limitations. Segmented flow can eliminate Taylor dispersion by localizing samples as aqueous droplets or plugs formed in a stream of water-immiscible carrier fluid.[109, 222-224]

A surge of recent research into segmented flows has shown the potential of this approach for chemical measurement. Droplets or plugs from femtoliter to microliter volume can be reproducibly created using a variety of microfluidic geometries including tee junctions,[165] Y-junctions,[223] and nozzles.[225] Furthermore, plugs can be manipulated for chemical analysis through reagent addition,[129, 158, 159] rapid on-chip mixing,[129, 159] and transfer to outside tubing.[129, 159, 179, 226] Recent applications of such systems include kinetic measurement,[168, 227] synthesis,[129, 130, 182] protein crystallization,[226, 228] DNA analysis,[229] PCR,[176] cell sorting[148] and cell encapsulation.[185, 230] Although avoiding dispersion or mixing of discrete samples is often cited as an advantage of segmented flow,

this approach has not been described for chemical monitoring applications such as in vivo microdialysis.

The goal of this chapter was to combine in vivo microdialysis sampling with a segmented flow microfluidic device to conserve temporal resolution while sample plugs were transported from the probe to a downstream detection system. We determined conditions for obtaining dialysate flow segmentation on the scale needed for in vivo analysis, tested the effects of flow segmentation on temporal resolution, and demonstrated use of the system for analytical measurements by coupling it to an on-line enzyme assay for monitoring glucose in the brain of living rats. We demonstrate that temporal resolution of 15 s is possible and that this resolution is independent of both time to transport sample to the analytical system and dialysis flow rate.

Experimental Section

Chemicals

All chemicals were used as received. Perfluorodecalin, fluorescein, hexamethyldisilazane (HMDS), octadecyltrichlorosilane (OTCS), n-hexadecane, and methanol were purchased from Sigma-Aldrich (St. Louis, MO). Salts for artificial cerebral spinal fluid (aCSF) were purchased from Fisher Scientific (Chicago, IL). A glucose assay kit consisting of Amplex® red reagent, dimethylsulfoxide (DMSO), horseradish peroxidase (HRP), glucose oxidase (GOX), D-glucose, concentrated reaction buffer (0.05 M sodium phosphate, pH 7.4), and H_2O_2 was purchased from Invitrogen (Carlsbad, CA). All aqueous solutions were prepared with water purified and deionized

to 18 MΩ resistivity using a Series 1090 E-pure system (Barnstead|Thermolyne Cooperation, Dubuque, IA).

Microdialysis Probes

Side-by-side microdialysis probes were constructed in-house as described elsewhere.[14, 45] Briefly, two 40 μm i.d. x 100 μm o.d. fused silica capillaries (Polymicro Technologies, Phoenix, AZ), held in place by a 250 μm i.d. capillary sleeve, were inserted into a 1 cm length of 200 μm diameter hollow fiber dialysis tubing that was sealed at one end with polyimide resin (Alltech Biotechnology, State College, PA). The dialysis tubing was made from regenerated cellulose and had 18 kDa molecular weight cut-off (Spectrum Laboratories, Rancho Dominguez, CA). Polyimide was used to coat the outside of the dialysis tubing except for the sampling region. A piece of 718 μm o.d. x 502 μm i.d. stainless steel tubing (Small Parts, Inc., Miramar, FL) was sleeved over the outside of the 250 μm capillary sheath to strengthen the probe. The probes had a 2 mm sampling tip unless stated otherwise.

Microchip Fabrication and Interface to Microdialysis

Sample plugs were formed by flowing dialysate and perfluorodecalin as an oil carrier phase into separate arms of a microchannel tee formed in PDMS as illustrated in Figure 2-1. Microchannels were formed by casting PDMS on silicon masters[231, 232]. Silicon masters were fabricated using photolithography methods as described in detail elsewhere[232-235]. Briefly, AZ 50XT photoresist (AZ Electronic Materials, Somerville, NJ) was spin-coated onto a 3-inch silicon wafer (HMDS vapor pre-treated, International Wafer Service, Colfax, CA) and exposed to UV radiation for 20 s (365 nm mercury line,

45 mJ/cm^2 power, Optical Associates, Inc. Milpitas, CA) through a mask to generate the desired pattern before development in AZ 400 K developer (AZ Electronic Materials, Somerville, NJ). The channels employed were 80 μm deep unless stated otherwise. Main channels (oil flow that carried plugs) were 250 μm wide and increased to 320 μm wide downstream in order to facilitate connection to silica capillaries. Inlet channels carrying aqueous flow were 125 μm wide for each branch. After casting PDMS over the molds, the layer containing channels was removed and treated with corona discharge (Model BD-20, Electro-Technic Products, Inc., Chicago, IL). The treated PDMS layer was sealed to an un-patterned PDMS layer. The sealed device was placed in a 120 ^{o}C oven for 10 min to ensure bonding and restore native hydrophobicity to the PDMS walls.

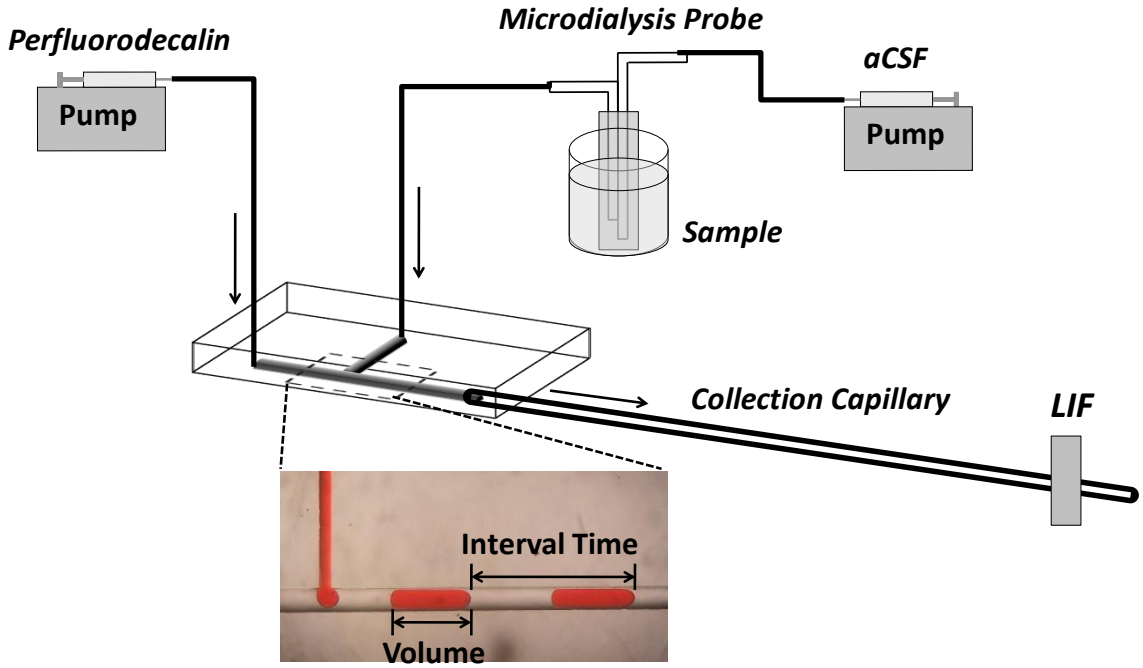

Figure 2-1. Microdialysis/segmented flow system. Arrows indicate direction of flow. Micrograph illustrates plug generation at a tee junction. (Aqueous stream contains

orange food dye for visualization.) Aqueous channels had a width of 125 μm and main channel with segmented flow had a width of 250 μm.

Chips had fused silica capillary connected for inlet flows of aqueous dialysate sample and oil carrier phase. Access ports for these connections were created using a blunt 18-gauge needle to punch holes through the PDMS over the appropriate channels (see Figure 2-1).[39] Fused silica capillaries with 360 μm o.d. were inserted into the holes and used for connection to syringe pumps (Model 402, CMA Microdialysis, North Chelmsford, MA) via Valco unions (1/16" o.d. tubing, 0.15 mm bore, Houston, TX). Where microdialysis sampling was used, the 40 μm i.d. outlet capillary of the microdialysis probe was directly inserted into the port. The total length of this tube was 3.5 cm. Segmented flow was pumped out of the chip into a collection capillary consisting of a 40 or 70 cm long piece of 250 μm i.d. x 360 μm o.d. fused silica tubing. The inner surface of this capillary was made hydrophobic by pumping 1% (V/V) OTCS in n-hexadecane for 10 min at 6 μL/ min. After derivatization the capillary was rinsed by pumping hexane, methanol and air through it in succession.[236] The modified capillary, with polyimide coating removed at one end, was inserted into the 320 μm wide channel between the two layers of the chip i.e., in the same plane as the main channel. After making all connections to fused silica capillaries, a sealant layer of PDMS was poured on top of the chips and cured on a hot plate at 85 ^{o}C for 3 h to seal capillaries to the chip.[39] Cyanoacrylate cement was applied to PDMS surface around inlet capillaries to prevent fluid leakage.

LIF Detection and Data Analysis

For visual inspection and monitoring of sample plugs, the chip or collection capillary was mounted on a Nikon inverted microscope (Eclipse TS100, Melville, NY). Photographs were taken through the microscope using a digital camera (FinePix F30, Fujifilm, Japan). When detecting fluorescence, the collection capillary or chip was mounted on an epi-illumination inverted microscope (Axiovert 100, Carl Zeiss Inc.). Fluorescence was excited using a 488 nm line of an Ar^+ laser (Melles Griot, Carlsbad, CA) for fluorescein or the 543.5 nm line of a He-Ne laser (Melles Griot, Carlsbad, CA) for Amplex® red. Fluorescence was collected through a 10x objective through appropriate filter sets and detected using a photometer (R3896, Hamamatsu Photonics, Bridgewater, NJ) mounted on the microscope. The photometer was set to low pass filter at 250 Hz. Fluorescence signals were collected via a data acquisition card (PCI-6036E, National Instruments, Austin, TX) at 1000 Hz using LabView program written in-house. Microsoft Excel 2007 (Microsoft, Redmond, WA), Igor Pro 6.01 (Wavemetrics, Inc., Lake Oswego, OR), and Cutter 7.0[237] were used for data analysis and graphing.

Testing of Temporal Resolution

The temporal response of the microdialysis/ segmented flow system shown in Figure 2-1 was tested by equilibrating the dialysis probe in a solution of fluorescein dissolved in aCSF (145 mM NaCl, 2.68 mM KCl, 1.01 mM $MgSO_4$, 1.22 mM $CaCl_2$, 1.55 mM Na_2HPO_4, 0.45 Mm NaH_2PO_4, pH 7.4) and then rapidly altering the fluorescein concentration by using pipettes to quickly change the solution surrounding the probe while monitoring fluorescence of sample plugs either on the chip or downstream in the

collection capillary. In some experiments, oil flowing through the main channel was replaced with aCSF to determine the effect of segmentation on temporal resolution.

Computational Modeling of Microdialysis Sampling

Microdialysis probe sampling dynamics were modeled using COMSOL Multiphysics ® 3.3 (Comsol, Inc., Burlington, MA). 1 and 2 mm long probes were approximated as 200 μm wide cylinders with a 40 μm i.d. by 100 μm o.d. capillary inserted to within 50 μm of the bottom of the probe, a similar capillary outlet at the top of the probe and a 10 μm thick membrane. The boundary layer (i.e., quiescent solution) around the probe was approximated to be 50 μm thick for a well stirred solution (assuming Re ~ 100).[238] Diffusion was treated as uniform throughout the boundary layer, membrane and probe volume. All models were solved in three dimensions by modeling mass transport from the edge of the boundary layer into the perfusing flow in the probe as a function of time for 1 minute. The net concentration out of the probe was fit to a Hill equation by nonlinear regression using Origin® 6.0 (Microcal Software, Inc., Northhampton, MA) to generate data traces. The outlet capillary from the probe was modeled as a 3.5 cm long by 40 μm i.d. capillary in two dimensions. Analyte concentration and response times were determined from the time-dependent concentration profile at the end of the capillary model. Constants used in the model were 4.25×10^{-6} cm^2/s as diffusion coefficient for fluorescein,[239] 993 kg/m^3 for density of water, and 6.90×10^{-4} Pa s for viscosity of water (37 ^oC).

In Vitro Glucose Assay

Glucose assays were performed on-line by mixing reagents and dialysate within a chip to form sample plugs that were pumped to a detection zone in a collection capillary downstream of the mixing/plug formation point. Reagents were prepared from stock solutions of Amplex® red (10 mM in DMSO), GOX (100 U/mL in 0.05 M sodium phosphate reaction buffer, pH 7.4) and HRP (10 U/mL in reaction buffer, as described above) according to vendor instructions. Stock solution was stored frozen at -80 ^{o}C as single-use aliquots. For each day's experiment, stock solution aliquots were thawed on ice and then diluted with reaction buffer to produce reagents of 6 U/mL GOX and 0.6 U/mL HRP in one vial and 0.3 mM Amplex® red in another vial. These working solutions were kept on ice and shielded from light by aluminum foil at all times. To ensure activity of reagents, solutions were replaced every two hours.

For the on-line glucose assay, the aqueous inlet channel shown in Figure 2-1 was modified to have 3 channels (one for HRP/GOX solution, one for Amplex® red solution, and one for dialysate) that merged to a single channel just before the tee intersection (details given in text). The flow rate for sample stream was 200 nL/min and for each reagent stream 50 nL/min. Oil flow rate was 1000 nL/min. With these flow rates, each plug was expected to contain the concentrations recommended by the vendor, i.e. 0.1 U/mL HRP, 1 U/mL GOX and 50 μM Amplex® red. To test and calibrate the on-line assay, glucose solutions with concentrations ranging from 0.1 mM to 5 mM were prepared in aCSF and sampled by microdialysis. Fluorescence of each resulting sample plug was detected 40 cm downstream using LIF as described above.

Surgery and in vivo Glucose Monitoring

In vivo microdialysis experiments were performed on male Sprague-Dawley rats (Harlan, Indianapolis, IN) weighing 200-250 g. Rats were anesthetized with intraperitoneal (i.p.) injections of ketamine (65 mg/kg) and domitor (0.5 mg/kg) and mounted on a stereotaxic apparatus (Kopf Instruments, Tujunga, CA). Rats were maintained under anesthesia for the entire experiment by giving i.p. injections of ketamine (32.5 mg/kg) and domitor (0.25 mg/kg) as needed. The probe was inserted into the nucleus accumbens (NAC) at coordinates +1.6 mm anterior, +1.2 mm lateral, and -8.1 mm ventral, measured from bregma, according to a rat brain atlas.[240] After inserting the dialysis probe, the system was equilibrated by perfusing aCSF through the probe at 200 nL/min for 1 h before beginning measurements.

Glucose was measured in vivo similarly to the in vitro assay described above with some modifications. The length of the collection capillary from the chip to the detection window was increased to 70 cm to accommodate space requirements of the in vivo experiment. Flow rates were adjusted to 300 nL/min through sampling probe, 75 nL/min for each reagent stream and 1500 nL/min for oil to achieve a 17 min reaction time (i.e., time from the collection capillary to detection zone). A 6-port valve (Valco, Cheminert 04Y-0000H) was plumbed between the dialysate syringe pump and sampling probe to allow the dialysis perfusion solution to be switched. Solutions containing either aCSF or high K^+ aCSF (100 mM KCl, 50 mM NaCl, 1.2 mM $CaCl_2$, 1.2 mM $MgSO_4$, 0.4 mM NaH_2PO_4, pH 7.40) could be selected. In vitro calibration with glucose of known concentrations was performed prior to in vivo measurements.

Results and Discussion

Effect of Flow Rates on Plug Volume and Time Interval

In a segmented flow system integrated with on-line sampling and analysis, parameters such as sample plug volume, interval between plugs, and plug generation frequency have a large impact on both the temporal information that can be obtained and the analytical methods that should be adopted. The sample plugs must be large enough that the amount of analyte in them is higher than the mass detection limits of the analytical method. Sample plug generation frequency sets the upper limit to temporal resolution obtainable, e.g. a system that generates one sample plug every 10 s will have a temporal resolution no higher than 10 s. If on-line analysis is used, then the interval between plugs that are created must be longer than the minimum time required for each analysis (e.g., separation time in LC). In this work we used a microfluidic tee to segment flow from the dialysis probe. As demonstrated previously,[121, 164] plugs generated in a tee can be controlled by changing relative flow rates of the sample and carrier fluid as well as dimensions of the channels. Although models have been developed to predict plug generation,[121] we found that experimentation was required to obtain the desired plug formation dynamics.

For this work, we sought to generate plugs from sample stream flow rates in the 0.1 to 1 μL/min range at 1 to 10 s intervals to yield samples with low nanoliter volumes. This flow rate is typical for microdialysis and the plug formation frequency represents significant improvement in temporal resolution while generating plugs that are easily manipulated and analyzed. As shown in Figure 2-1, a tee with 125×80 μm inlet channel and 250×80 μm main channel allowed such plugs to be formed. For a given sample flow

rate, increasing the oil flow rate decreased plug volumes and intervals (Figure 2-2). Decreasing the sample flow rate generated smaller plugs at longer intervals. The dynamic range of intervals was approximately 0.6 to 10 s. Plugs were reproducible with < 5% RSD in volume and < 8% RSD in interval time. Chip dimensions could also be varied to yield different ranges that might be appropriate for different applications. For example, with 50×12 μm channels we generated plugs of 50 to 200 pL at < 1 s intervals. In some cases, it may be desirable to independently control sample size and interval between plugs; however, this is not possible with the tee junction. An active system where plugs are formed by a trigger would allow such independent control but would also necessitate a more complex instrument.

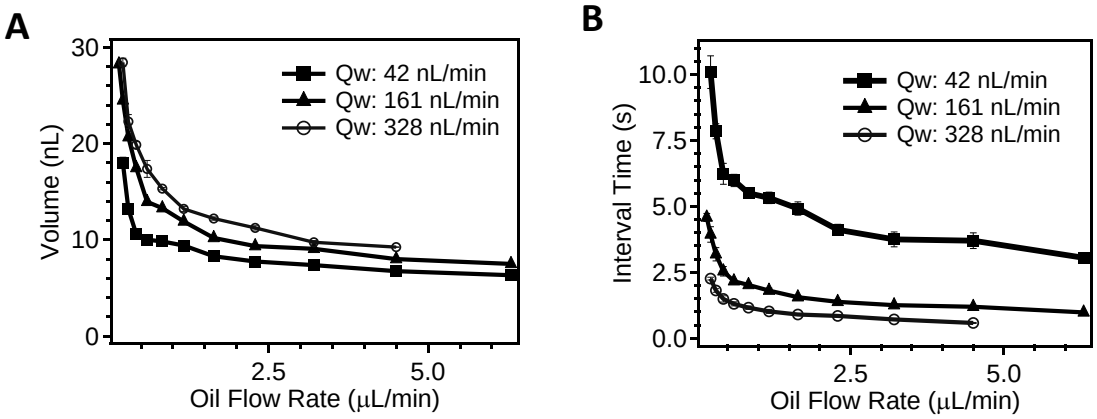

Figure 2-2. Dependence of plug volume (A) and frequency (B) on flow rate. Aqueous flow rate (Q_w) were chosen within the range of commonly used low sampling flow rates for microdialysis. The graphs were made with the structure shown in Figure 1-1.

Conservation of Temporal Resolution with Segmented Flow System

After demonstrating controlled sample plug formation, we tested the potential to preserve temporal resolution in comparison to a continuous flow system during microdialysis sampling. For these experiments, step changes in fluorescein concentration were made at the probe surface while recording response curves by LIF detection. A dialysis flow rate of 200 nL/min was used representing a relatively low flow rate that generates high relative recovery (approximately 53% for glucose) but is usually not associated with good temporal resolution. For the continuous flow system the oil flow was replaced by aCSF. Recordings were made both near the tee junction and 40 cm downstream for both continuous flow and segmented flow (see Figure 2-3 (A-B)). A comparison between upstream and downstream response curves for both systems demonstrates the advantage of segmented flow over continuous flow for conserving temporal resolution. (Temporal resolution and response time in this discussion refer to the time from the initial increase in signal to the steady state signal and does not include the delay time associated with flowing from the probe to the detection window.) With segmented flow, on-chip and downstream detection produced response curves that exactly overlapped (Figure 2-3 (C)), verifying prevention of axial dispersion between plugs and conservation of temporal resolution after sampling. In contrast, severe deterioration in temporal resolution, represented as a broadened transition zone, was observed with continuous flow (Figure 2-3 (D)), due to axial dispersion of sample zones during transport at low flow rate through a capillary.

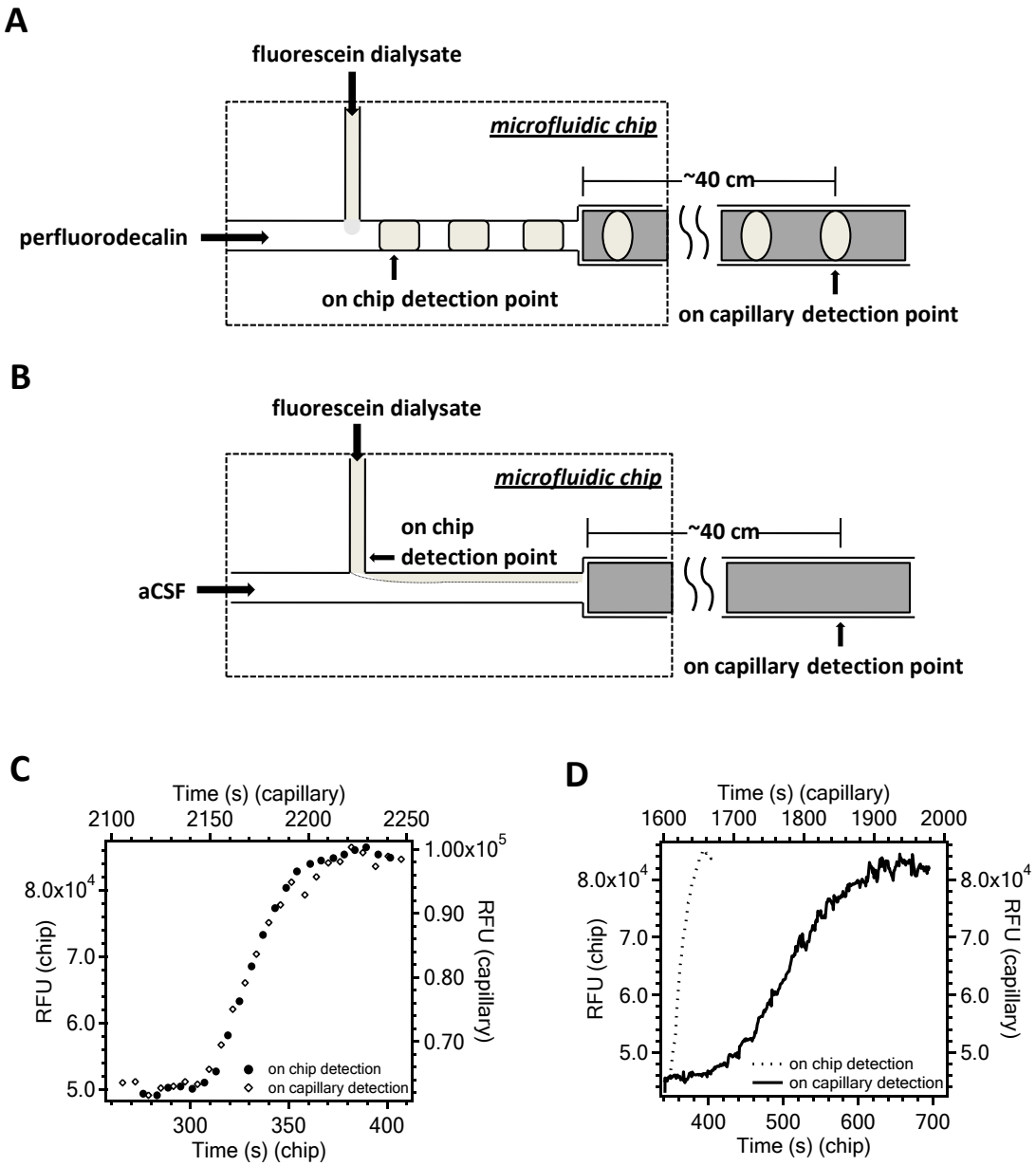

Figure 2-3. Comparison of Taylor dispersion during sample transfer using segmented flow and continuous flow. Step change of fluorescein concentration from 50 nM to 100 nM was made at the probe surface and response curves at the two detection points shown in (A) and (B) were recorded for segmented flow (C) and continuous flow (D). For (C), the data points represent the maximal fluorescence recorded from each sample plug as it passed through the detector. The top time axis is for the downstream (capillary) detection point and the bottom for the on-chip detection point in both graphs. Sampling flow rate was 200 nL/min and cross-sectional flow rate (PFD or aCSF) was 1 μL/min.

We next explored the upper limits of temporal resolution with this system. To do this, we repeated the step change experiment but with stirred solutions and probes equilibrated to 37 ^{o}C. Stirring is expected to decrease the distance required for analyte to diffuse to the probe while the elevated temperature increases diffusion coefficients. Using this approach we observed response times of ~ 30 s (time from 10-90% of maximal signal) at 200 nL/min dialysis flow rates (see Figure 2-4 (A)). Increasing the dialysis flow rate to 1 μL/min did not improve the temporal resolution (Figure 2-4 (B)). Decreasing the dialysis probe length by half to 1 mm resulted in an approximately 2-fold improvement in response time to 15 s at both flow rates (Figure 2-4 (C-D)). Thus, response time scaled with membrane length rather than flow rate. These results suggest that mass transport across the membrane limits temporal resolution rather than Taylor dispersion under these conditions.

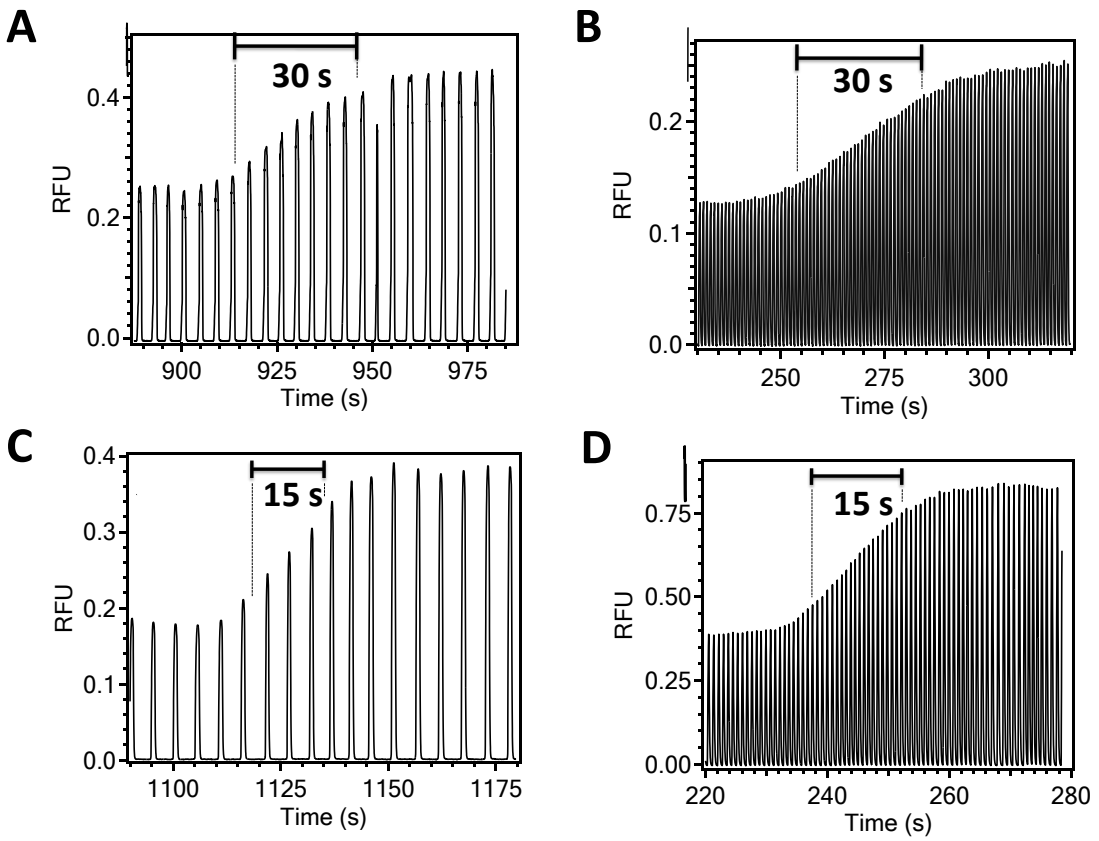

Figure 2-4. Responses obtained at both low and high sampling flow rate with microdialysis probes with different membrane lengths. (A) 2 mm probe at 200 nL/min; (B) 2 mm probe at 1 μL/min; (C) 1 mm probe at 200 nL/min; (D) 1 mm probe at 1 μL/min. Fluorescein concentration was changed from 2 μM to 5 μM at the probe surface. Cross-sectional flow rates were 1 μL/min for 200 nL/min sampling rate and were 4 μL/min for 1 μL/min sampling rate. Data traces are raw output from LIF detector and show detection of individual sample plugs. Temporal resolution, defined as the time during which signals increased from 10% to 90% of the maximum intensity, is marked on each graph.

To further explore this effect, we modeled the response of a dialysis probe to step changes in concentration in a stirred solution at 37 ^{o}C. The model was based on the geometry of the probe (see Experimental section and Figure 2-5 (A)). The system was considered to have a 50 μm boundary layer and diffusion coefficient within the

membrane was considered to be the same as solution. These conservative estimates have the effect of making the observed responses limited primarily by flow and diffusion within the probe and tubing and not transport across the membrane. As shown in Figure 2-5 (B), this model predicts response times of 11.9 s for a 2 mm probe at 0.2 μL/min. Increasing the flow rate to 1 μL/min decreased the response time to 3.5 s. Cutting the probe length in half yielded a small decrease in response time to 8.0 and 2.1 s with 0.2 and 1 μL/min flow rates, respectively. Thus, when the transport across the membrane is not limiting, the response times are faster than measured experimentally. Furthermore, in contrast to experimental results, the dialysis flow rate has a bigger effect on response time than membrane length. This result further supports the conclusion that transport across the membrane is a limiting factor in response time in this system. Reduced effective diffusion coefficients through the membrane,[36, 241] adsorption to the membrane, and flow leakage through the membrane are all factors that can slow transport and therefore alter response time. Accurate knowledge of these processes would be required to correctly predict response times. This work suggests that improved membranes or sampling without membranes, such as direct[38] or push-pull sampling,[37] would be required to further improve the temporal resolution.

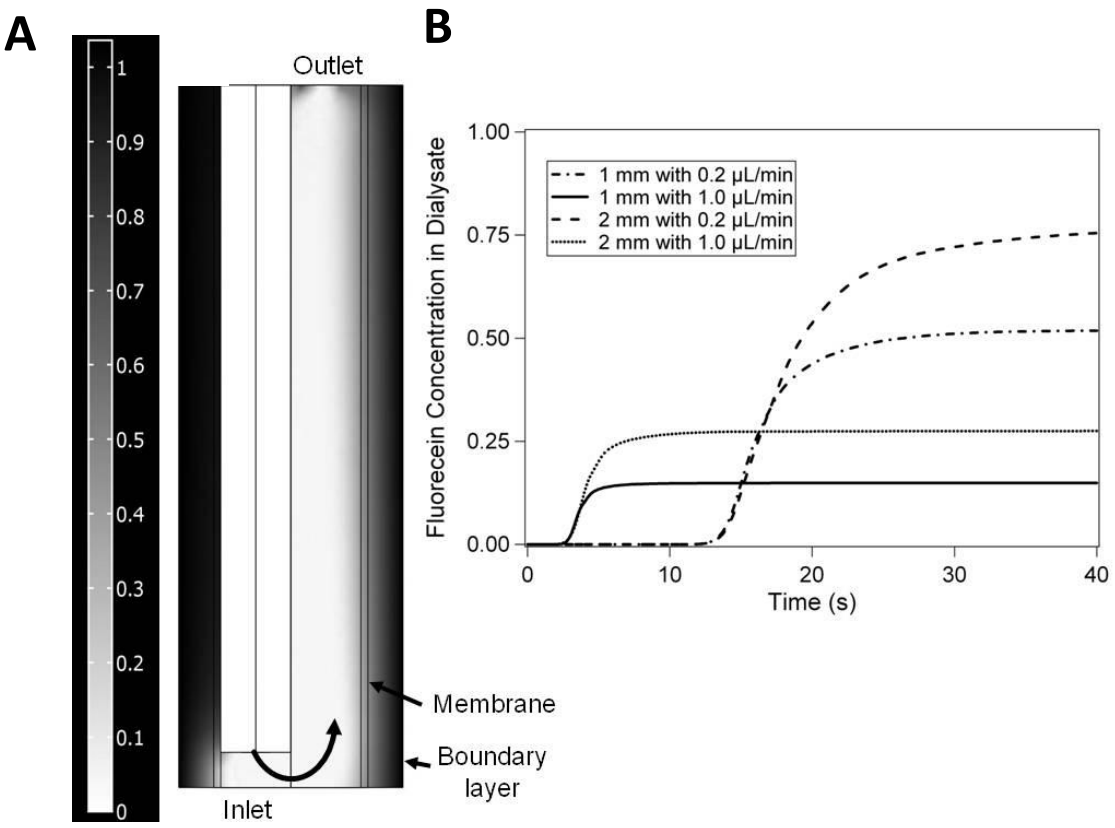

Figure 2-5. Simulation of response to step change in fluorescein concentration at a microdialysis probe using COMSOL. (A) The geometry of the dialysis probe was the same as those used experimentally i.e., 200 μm inner diameter, 220 μm outer diameter, side-by-side inlet-outlet capillaries and a 40 μm i.d. by 3.5 cm long exit capillary. The steady state concentration gradients at unit concentration is shown over the geometry in this illustrate. (B) The response shown is the concentration change at the outlet of the exit capillary following a step change from zero to unit concentration at time zero. The probe lengths and dialysis flow rates used are shown in the legend.

On-Chip Glucose Assay with Segmented Flow

To demonstrate the potential of the microdialysis to segmented flow system for chemical analysis, we integrated an on-line glucose enzyme assay. The sampling chip was modified with a triple-branch inlet to enable addition of assay reagents to the sample stream 1 mm upstream of the plug formation point. As illustrated in Figure 2-6 (A),

sample stream from the microdialysis probe flowed in the middle branch while enzymes (GOX, HRP) and dye (Amplex® red) were infused from the two side branches. Sample stream flow rate was 200 nL/min while the reagent stream flows were 50 nL/min each. This net flow rate resulted in sample plugs forming at 4 s intervals. After mixing at the tee junction, enzymatic reaction took place to form a fluorescent product (see Figure 2-6 (B) for reaction scheme) within plugs as they were transported in a piece of hydrophobic capillary from the microfluidic chip to detection window. Reaction time could be adjusted by varying the length of the capillary as well as oil flow rate. Although the assay kit suggested a 30 min incubation time before detection, we found that 17 min was enough to distinguish different glucose concentrations. This reaction time could be achieved by a 40 cm capillary at 1 μL/min oil flow rate. An illustration of the raw fluorescence signal from the plug enzyme assay at the detection point during a step change from 0.2 to 1 mM glucose is shown in Figure 2-6 (C). This trace illustrates the uniformity of signal intensities across different plugs for a given glucose concentration. Indeed, the assay yielded 2.3% RSD (n = 56) at 1 mM glucose. The assay also had a linear response up to 2 mM glucose and a detection limit of 50 μM glucose (see Figure 2-6 (D)). The trace in 5C also illustrates the preservation of temporal resolution for this experiment even though the sample plugs required 17 min for transport from the sampling to detection points. This effect represents a substantial advantage of the segmented flow system for assays that require long reaction times. This result further illustrates that the segmented flow system can maintain temporal resolution regardless of downstream processes.

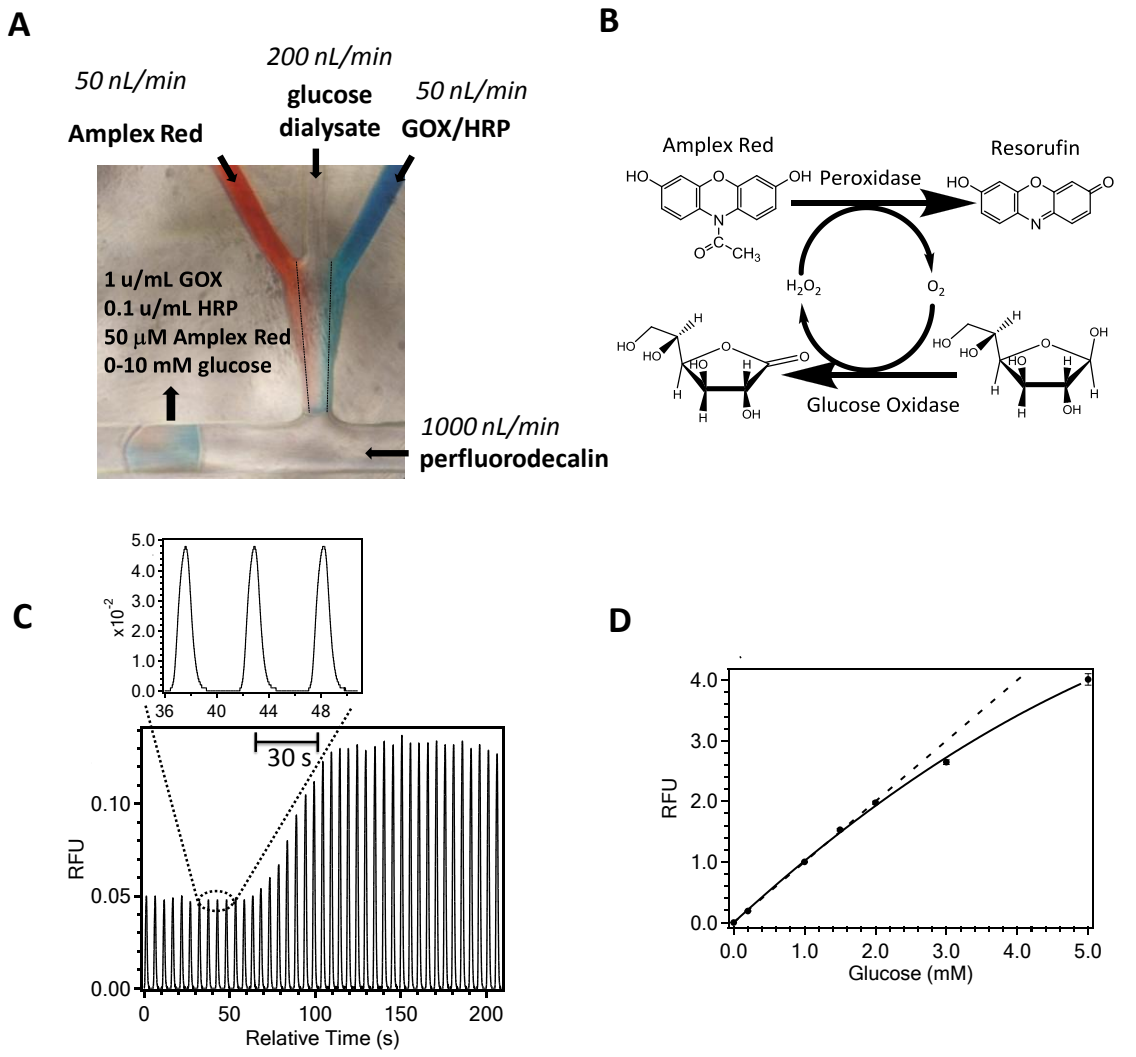

Figure 2-6. Glucose assay with segmented flow system. (A) Micrograph of microchannel network used for enzymatic assay within plugs. Food dye has been added to the Amplex® red and GOX/HRP streams for visualization. (B) Reaction scheme for the enzymatic assay. (C) LIF response when glucose concentration was changed at the probe from 0.2 to 1 mM. The inset shows an amplified view of the trace. Data are raw traces showing detection of individual plugs. (D) Calibration curve for glucose sampled by microdialysis and assayed using this system. Glucose concentrations are sampled concentrations.

In vivo Monitoring of Extracellular Glucose in Rat Brain

We next investigated if the system with glucose assay was robust enough for in vivo measurements. Glucose plays a critical role for providing energy to the brain. Regional cerebral activity, for example during cognition, has been associated with local glucose utilization.[242-244] Brain glucose concentrations also change with infarct[245] and spontaneous depolarization after head injury.[30] Therefore, glucose dynamics is of interest for research and clinical applications.

In this preliminary trial to couple the segmented flow system to an animal, probes were inserted into the NAC of anesthetized rats and perfused at 300 nL/min with aCSF. Basal concentrations of glucose measured by the method were 1.5 ± 0.1 mM (n = 3), in agreement with previous work.[246] To evoke a change in glucose concentration, 100 mM K^+ was perfused through the probe. As illustrated in Figure 2-7, after a 24 minute delay (7 min for perfusion solution to reach rat brain and 17 min for samples to reach the detection point), the concentration of glucose began to decrease reaching a minimum of 43 ± 9% (n = 4) of basal concentration after 30 min of exposure. Re-perfusion with regular aCSF brought glucose concentration back to basal level in less than 10 min. The results of this experiment coincide well with previous reports which showed 70% decrease of glucose in NAC over 60 min and 25% decrease in striatum over 30 min.[247, 248] Differences in conditions such as use of anesthetized animals in this experiment versus awake animals in other reports likely accounts for the small quantitative differences observed.

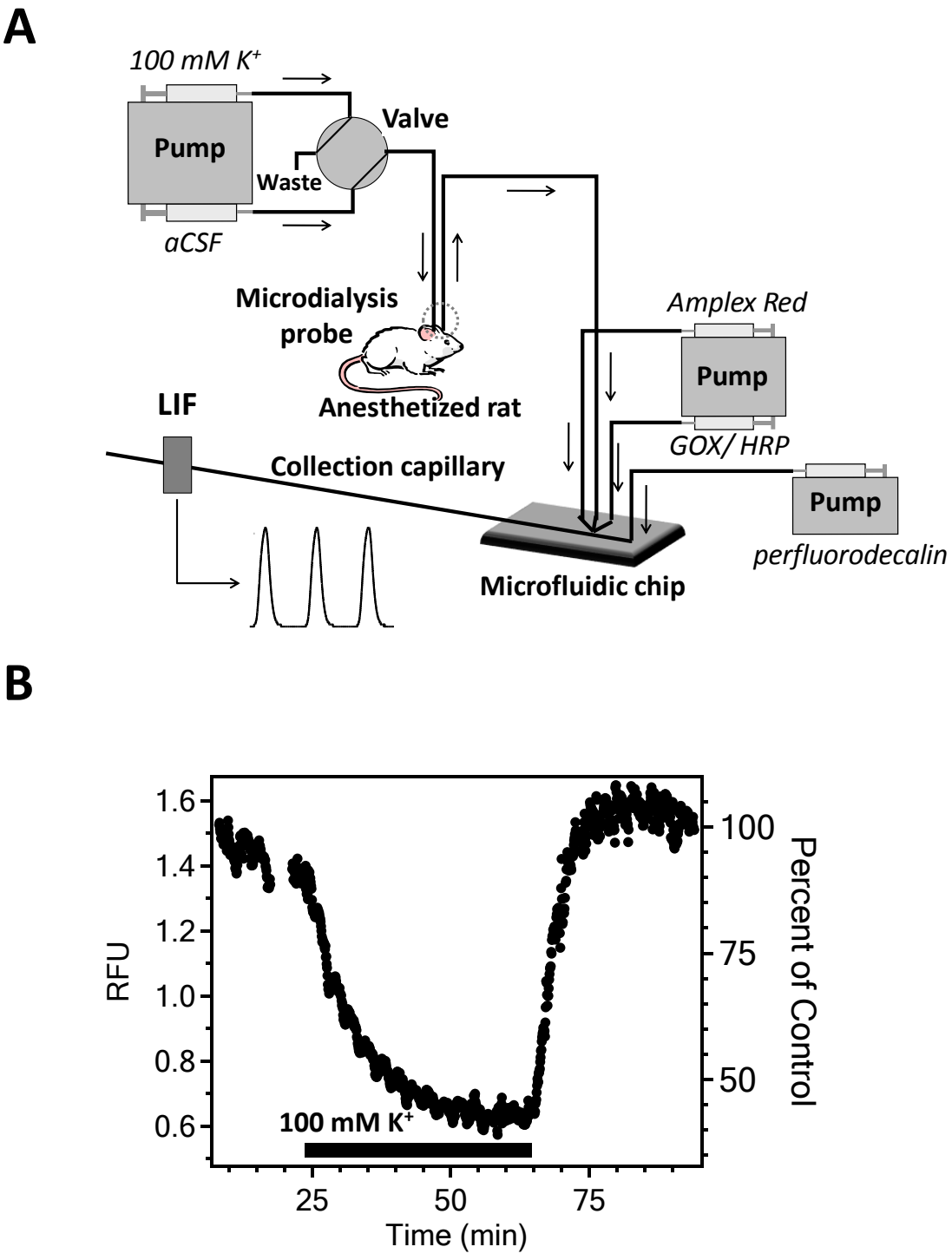

Figure 2-7. In vivo glucose assay. (A) System set-up overview. (B) Time course of extracellular glucose concentration in the NAC of rats infused high K^+ (100 mM) aCSF through the probe. Time on axis is time since switch was made to high K^+. Black bar indicates application of K^+ corrected dead volume of system. Axis on the left is relative

fluorescence unit (RFU) for the maximal signal in each plug while right axis expresses data as the percentage of basal glucose concentration.

The purpose of these in vivo experiments was to illustrate that the system could be used in a practical application to measure chemical dynamics. In view of pre-existing glucose assays that can be coupled on-line to microdialysis,[30, 245] and the observation that extremely rapid changes were not observed in this experiment, it is not likely that this method will have primary application for in vivo glucose monitoring. The flow-segmented approach will have more impact as assays are developed for neurotransmitters and other compounds that are expected to have faster concentration changes. Indeed, a particular advantage of the approach described here compared to sensors is the ease with which the assay can be changed to target other analytes. We also believe that the general concept of using sampling with segmented flow to preserve temporal resolution will have utility beyond brain chemistry to monitoring other environments, such as chemical reactions or other biological systems.

Conclusion

Segmented flows have received significant attention in chemical analysis in recent years primarily for their potential in high-throughput analysis. In this chapter, we pioneered in practicing the possibility that microfluidic segmented flows can be used to prevent temporal distortion in a sampling and monitoring experiment. Temporal resolution for microdialysis was maintained at 15 s even though samples were transported across long capillaries thus allowing good temporal resolution to be maintained for

experiments requiring long connection capillaries (such as freely moving animals) or assays that involve long reaction times. The use of segmented flow with sampling represents a significant advance for sampling approaches because it decouples analysis time from the temporal resolution that is possible. It also provides a convenient approach for manipulating the nanoliter volume fractions that are generated with performing high temporal resolution measurements. Our experiments suggest that future research aimed at improving the temporal resolution should be directed towards improving sampling membranes or using other sampling probes. Furthermore, coupling to other assay systems will be important in allowing this approach to extend beyond enzyme assays. Extension of the method to other assays and coupled to different sampling probes will likely yield systems with temporal resolution that approaches that of many sensors.

CHAPTER 3

A MICROFLUIDIC CHIP FOR HIGH EFFICIENCY ELECTROPHORETIC ANALYSIS OF SEGMENTED FLOW FROM A MICRODIALYSIS PROBE AND IN VIVO CHEMICAL MONITORING

Introduction

Microdialysis sampling coupled to analytical methods such as high performance liquid chromatography (HPLC) or capillary electrophoresis (CE) is a powerful approach for in vivo monitoring.[16, 249] High temporal resolution is often an important goal in developing a microdialysis analytical method.[20, 21, 29, 99, 250, 251] For example, correlating neurotransmitter fluctuations in the brain with behavior requires temporal resolution on the time scale of behavior changes which is often in the seconds range.[2, 90, 99] An inherent limitation to obtaining high temporal resolution with microdialysis is broadening of sample zones due to Taylor dispersion that occurs between the sampling probe and the analytical platform.[252] Although temporal resolution of 3-30 s using microdialysis has been reported,[6, 25, 29, 99, 102, 250] these studies used some or all of the following features: 1) high sampling flow rate (e.g. over 1 μL/min); 2) anesthetized subjects placed close to the detection system; or 3) short, small-bore connector capillaries for connecting the subject and analytical system to minimize dispersion during sample transfer. For many cases

though, lower sampling flow rate (e.g. 50-300 nL/min) is useful to obtain higher relative recovery, better sensitivity, and quantitative sampling.[43] Longer connector tubing is often necessary for clinical applications[250, 251] and for behavioral experiments. When using long connector tubing, larger bores are necessary to reduce back pressure exerted on microdialysis membrane and prevent leaks or ultrafiltration. Under conditions of long, large bore connecting tubing and low flow rates, Taylor dispersion becomes significant and obtaining high temporal resolution remains a challenge. In this work we describe a system that avoids these problems by coupling microdialysis with segmented flow to an electrophoresis chip for in vivo neurochemical monitoring.

Segmented flow analysis (also called continuous flow analysis[253]), in which sample plugs are carried by an immiscible fluid, is an excellent way to solve this problem because it prevents axial dispersion during transportation and storage. One approach to using segmented flow is to create a train of plugs on the inlet side of a sampling probe and pump them through the probe so that each plug collects sample at a point in time.[205] Although this approach achieves sub-second temporal resolution in sampling, coupling it with microdialysis membranes and in vivo sampling remains an unsolved problem. Previous work in our group has demonstrated that dialysate can be segmented immediately after sampling[252] to achieve temporal resolution as good as 15 s regardless of the downstream processing and connector tubing.

Previous work with microdialysis coupled to segmented flow has been limited to using enzyme assay for analysis of the plugs. To make microdialysis with segmented flow practically useful, it is necessary to couple segmented flow to more powerful, multi-analyte methods such as CE with laser-induced fluorescence (LIF).[23, 24, 29, 31, 254] Several

previous methods have been reported for electrophoretic analysis of plugs;[215, 255] however, they have not yet been coupled to microdialysis nor do they have the analytical performance in terms of separation efficiency to be used for complex samples collected in vivo.

In this chapter we describe a system that segments dialysis flow, derivatizes the analyte stream with naphthalene-2,3-dicarboxaldehyde (NDA)/CN^-, transfers the samples to a glass microfluidic chip, and serially injects samples for electrophoretic analysis with >200,000 plates at 20 s intervals. This system required 3 technical innovations: 1) reliable transfer of plug flow to a glass chip; 2) efficient extraction of aqueous plugs from segmented flow; and 3) electrophoretic injection suitable for high efficiency separation with minimal dilution of sample. This microfluidic system was proven suitable for on-line in vivo chemical measurements of amino acids from the brain with ~30 s temporal resolution offering the combined advantages of maintained temporal resolution with segmented flow and high resolving power of electrophoresis.

Experimental Section

Chemicals

All chemicals were purchased from Sigma-Aldrich (St. Louis, MO) with the following exceptions. Salts for artificial cerebral spinal fluid (aCSF) were purchased from Fisher Scientific (Chicago, IL). NDA was purchased from Invitrogen (Eugene, OR). All aqueous solutions were prepared with water purified and deionized to18 MΩ resistivity using a Series 1090 E-pure system (Barnstead Thermolyne Cooperation, Dubuque, IA). Amino acid standards of γ-aminobutyric acid (GABA), taurine (Tau),

serine (Ser), glycine (Gly), glutamic acid (Glu) aspartic acid (Asp) were dissolved in aCSF. Octadecyletrichlorosilane (OTCS) was stored in a desiccator and was opened in dry N_2 atmosphere in an Aldrich Atmosbag (St. Louis, MO)

Microdialysis Probes

Side-by-side microdialysis probes with 18 kDa molecular weight cut-off membranes made from regenerated cellulose hollow-fibers were made in-house as described elsewhere.[45] Probes had 200 μm diameter, 2 mm sampling length and 40 μm i.d. x 100 μm o.d. fused silica capillaries for inlet and outlet tubing.

PDMS Chip Fabrication

The overall scheme of the system, which used two different chips, is illustrated in Figure 3-1. Fabrication of the PDMS chip with integrated microdialysis probe was previous described.[252] The segmented flow channel was 150 μm wide x 90 μm deep and the channels for NDA, dialysate, and KCN/EDTA were 75 μm wide x 90 μm deep. The 40 μm i.d. outlet capillary (3 cm total length) of the microdialysis probe was directly inserted into an access port on the PDMS chip. Other fluids were transferred to the chip through 50 μm i.d. x 360 μm o.d. capillaries. Segmented flow was pumped out of the chip into a 60 cm length of 150 μm i.d. x 360 μm o.d. high purity perfluoroalkoxy plus (HPFA+) tubing (Upchurch Scientific, Oak Harbor, OR) through a glass adaptor (Hampton Research, Aliso Viejo, CA).

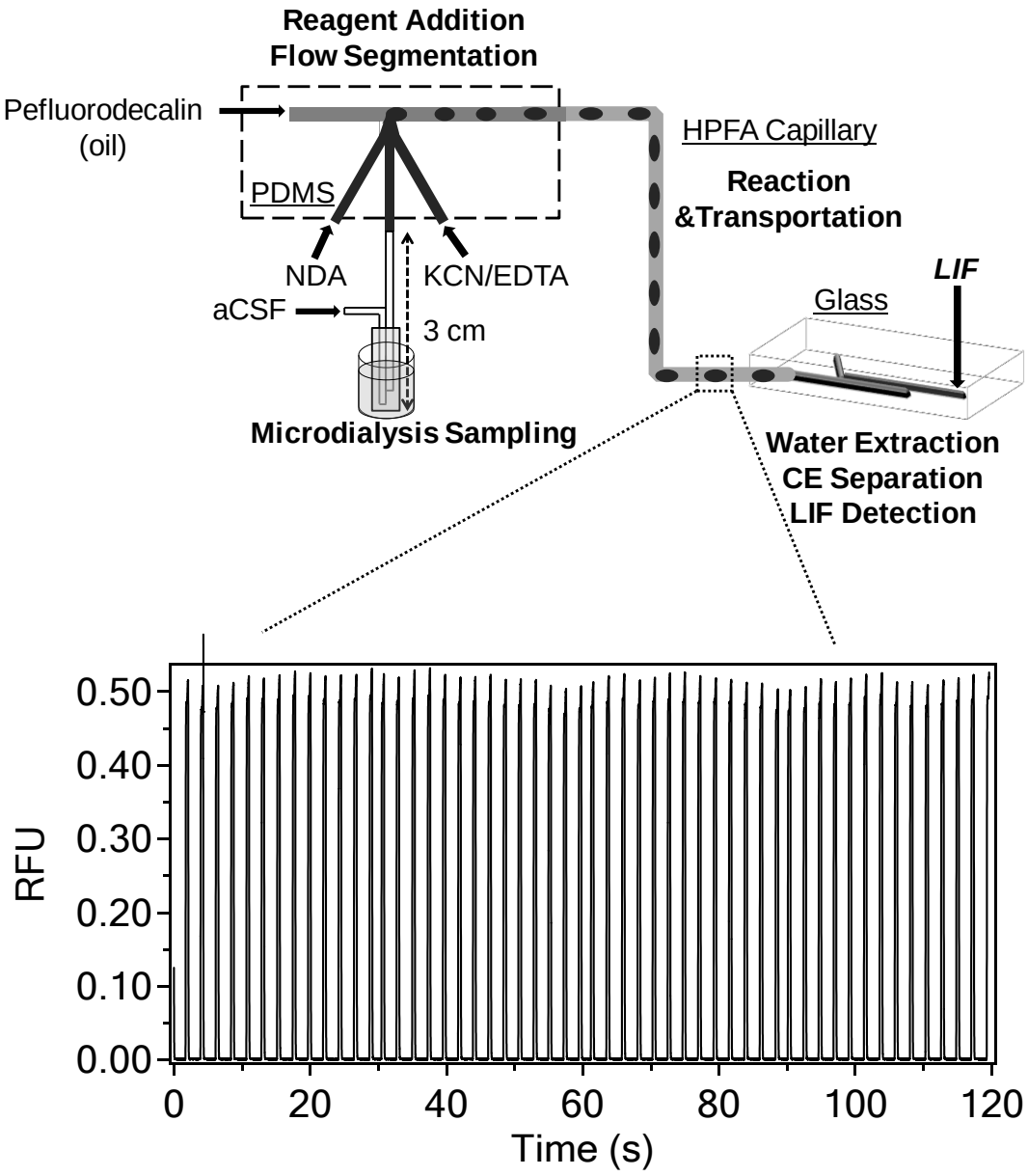

Figure 3-1. Dual-chip system for electrophoretic analysis of segmented dialysate flow. Inset graph shows reproducible total fluorescence intensity of plugs containing NDA derivatized amino acids as they pass through the HPFA connector tubing. RSD for peak height is 1.4%.

Glass Chip Fabrication

Layout of the glass chip is shown in Figure 3-2, with channel network filled with blue dyes for visualization.

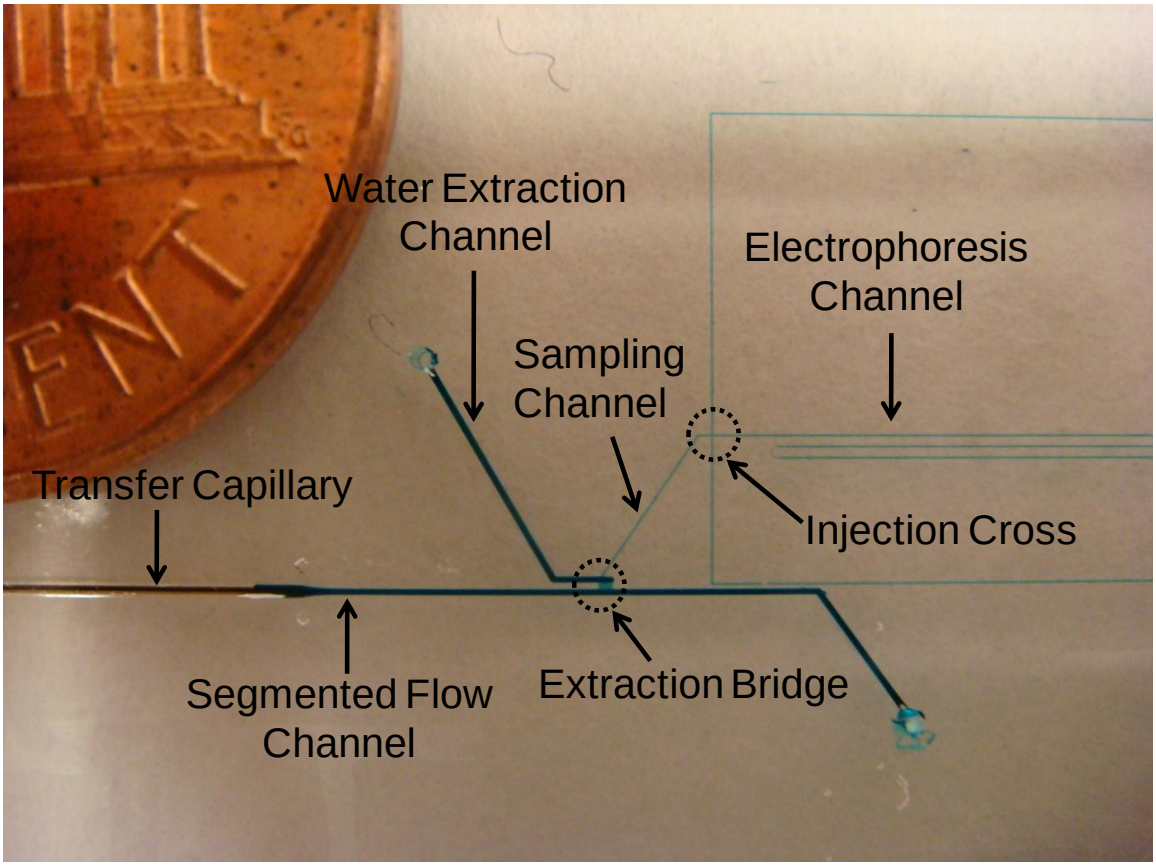

Figure 3-2. Picture of the channel network of segmented flow CE chip. Channels were filled with blue dyes for visualization. Channel names indicating their functions are labeled in the picture. The chip was photographed next to a one cent coin.

Standard photolithography and wet-etching techniques[73, 256] were used for chip fabrication. Two glass slides were etched with different channel patterns as illustrated in Figure 3-3 (A). Except for insertion channels, which were 90 μm deep on both slides,

features on slide (i) had a depth of 70 μm and features on slide (ii) had a depth of 6 μm. Since insertion channels required the largest depth and subsequently the longest etching time, other features were blocked by HF resistant tape (Semiconductor Equipment Corp., Moorpark, CA) after reaching their designed depths while only insertion channels were further exposed to HF until desired depth was obtained. After etching, access holes were drilled on slide (a) by #79 diamond drill bits from Tartan Tool Company (Troy, MI) using a Cameron micro drill press (Sonora, CA). The resulting glass slides were prepared for bonding by soaking them in piranha solution (sulfuric acid / hydrogen peroxide (30%) 4:1 v:v) for 20 min and then in heated RCA solution (ammonium hydroxide / hydrogen peroxide (30%) / water 1:1:5 v:v:v) for 40 min. After the acid and base baths the slides were thoroughly rinsed with water and aligned under a microscope such that extraction bridge overlaid both segmented flow and water extraction channels as shown in Figure 3-3(A) and Figure 3-3 (B i).

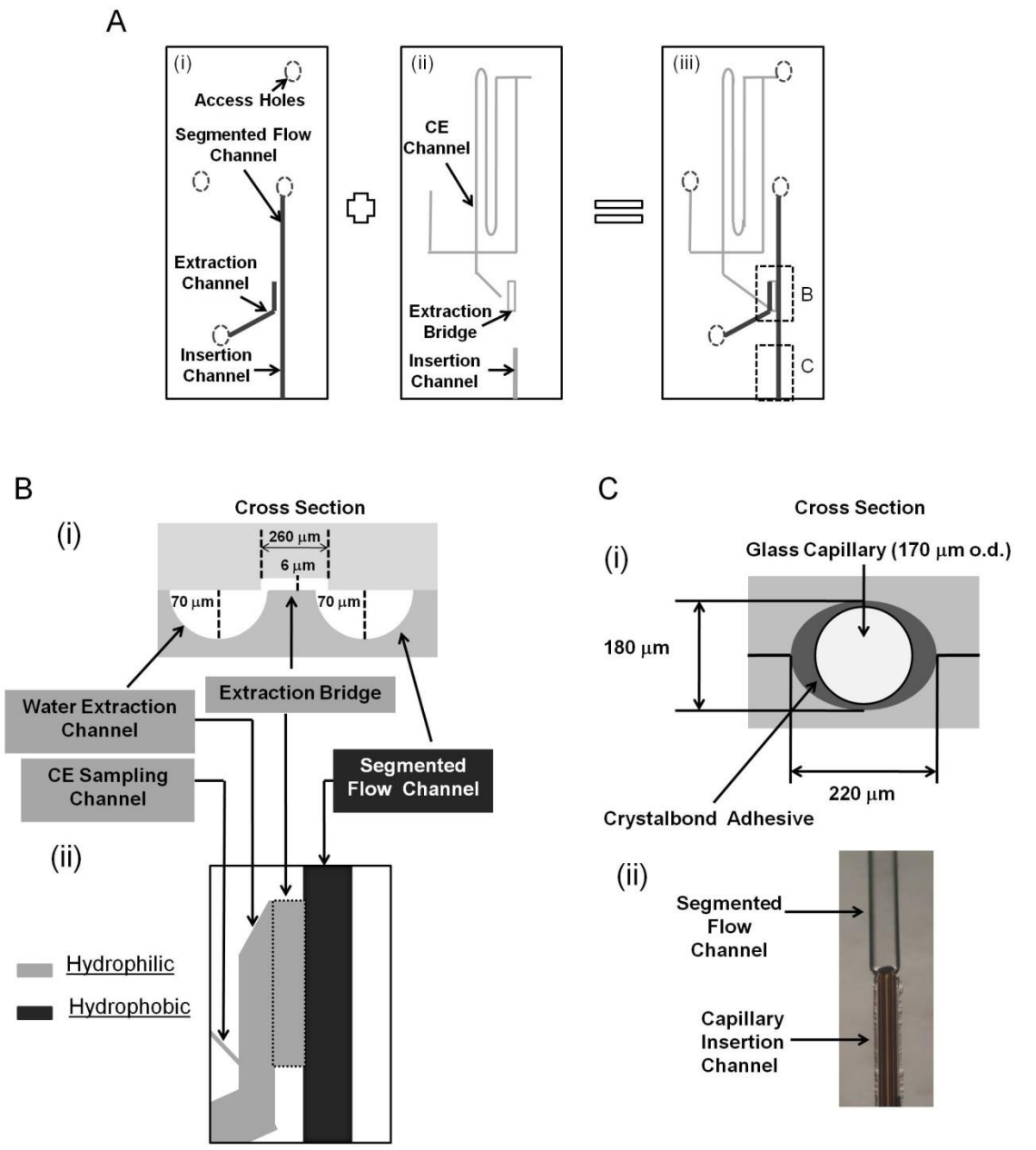

Figure 3-3. Fabrication of the CE chip. (A) Channels of different depths are etched on separate substrates and are aligned and bonded as shown. Regions enclosed by dashed box are shown in B and C. (B) Detail of extraction bridge. **i.** Cross section of the fabricated device at the extraction bridge. Widths of segmented flow channel, water extraction channel and extraction bridge are all 260 μm. **ii.** Top view of extraction bridge showing surface property of different regions. Segmented flow channel is patterned to be hydrophobic by OTCS while the other channels are left with the native hydrophilic surface of glass. (C) Detail of capillary-chip junction. **i.** Cross section of the capillary insertion channel. Both the top and bottom slides are etched to 90 μm to form an

elliptical channel after superposition to accommodate circular capillary. **ii.** Bright field image of the capillary-channel connection area.

After air dried for 1 h, chips were visually checked for Newton rings indicating an unsealed area and, if necessary, were separated and the cleaning cycle repeated. Chips were left in air overnight to eliminate water trapped in pinholes that might prevent successful bonding. The aligned slides were placed in a Neytech Centurian Qex furnace (Pacific Combustion, Los Angeles, CA) for bonding at 610 ºC. Reservoirs and Nanoports from Upchurch (Eugene, OR) were applied above the access holes using the manufacturer's protocol. To provide a connection for transferring sample plug trains to the glass chip, a short piece (~10 cm) of 100 μm i.d. x 170 μm o.d. fused silica capillary was inserted into the insertion channel and sealed using Crystalbond 509 adhesive (SPI Supplies, West Chester, PA), as illustrated in Figure 3-3 (C). Upon heating above 120 ^{o}C, Crystalbond melted and was drawn into the interstice between insertion channel and capillary by applying vacuum to the outlet of segmented flow channel. The wicking front of the adhesive was stopped several μm before capillary-channel interface by rapid N_2 cooling. This fused silica capillary was connected to Teflon tubing coming out of the PDMS chip via a short Teflon sheath. To generate a heterogeneous surface for phase separation and to stabilize segmented flow in glass channel, the deeper segmented flow channel was selectively derivatized with octadecyltrichlorosilane (OTCS) using previously described procedures.[236, 255] Figure 3-3 (B ii) illustrates patterned channels after derivatization.

Device Operation

aCSF (145 mM NaCl, 2.68 mM KCl, 1.01 mM $MgSO_4$, 1.22 mM $CaCl_2$, 1.55 mM Na_2HPO_4, 0.45 Mm NaH_2PO_4, pH 7.4) was pumped through a microdialysis probe and into one channel of the PDMS chip at 300 nL/min flow rate. NDA in 50:50 mixture (v:v) of acetonitrile and 20 mM borate and cyanide with 0.5 M EDTA in 20 mM sodium borate at pH 9.5 were pumped through separate channels at 150 nL/min each (see Fig. 1). These reagent conditions are based upon previous work.[92, 257, 258] The resulting solutions combined to form plugs at 0.3-0.5 Hz with 8-10 nL volume when perfluorodecalin was pumped at 1.5 μL/min through the cross-channel. The train of plugs flowed through 60 cm of 150 μm i.d. HPFA connector tubing to the glass chip for electrophoretic analysis.

All channels and reservoirs on the glass chip were filled with electrophoresis buffer (10 mM sodium tetraborate, 0.9 mM hydroxypropyl-β-cyclodextran (HPβCD), pH 9.7) prior to use. Voltage for performing electrophoresis was applied using a CZE1000R power supply (Spellman, Hauppague, NY). High-voltage relay for controlling electrokinetic-gated injection was from Kilovac (Santa Barbara, CA). Prior to use, channels of the glass chip were conditioned by using electroosmosis to pump 0.1 M NaOH for 15 min followed by deionized water for 15 min, and then electrophoresis buffer for 15 min through all channels.

Confocal LIF Detector and Data Analysis

Detection on chip was accomplished using an in-house built confocal LIF detector.[104] Excitation was provided by a 440-nm line from a 15 mW solid-state laser (CrystaLaser, Reno, NV) directed through a 436 ± 10 nm band-pass filter. Emission was

spectrally filtered with a 490 ± 10 nm band-pass filter and detected by a photomultiplier tube (R1477, Hamamatsu, Bridgewater, NJ). Current from the PMT was amplified and filtered (10 Hz low-pass) by a Stanford current preamplifier (Sunnyvale, CA), sampled at 100 Hz and analyzed using LabVIEW programs written in-house (National Instruments, Austin, TX).[237] Microsoft Excel 2007 (Microsoft, Redmond, WA), Igor Pro 6.01 (Wavemetrics, Inc., Lake Oswego, OR), and Cutter 7.0[237] were used for data analysis. When required, imaging of plug flow was accomplished using an inverted epi-fluorescence microscope (IX71, Olympus America, Inc., Melville, NY) with a 4X objective and was recorded with an electron-multiplying CCD camera (C9100-13, Hamamatsu Photonic Systems, Bridgewater, NJ).

Testing of Temporal Resolution

The temporal response of the whole system was tested by equilibrating the microdialysis probe in a solution of amino acid standards dissolved in aCSF, which was constantly stirred at 37 ^{o}C. The concentration of the surrounding solution was then quickly altered by using pipettes to remove and infuse solutions in the reservoir while monitoring the intensity of peaks in electropherograms. In continuous flow experiments, a Valco Cheminert cross (150 μm inner bore) was used to mix dialysate with derivatization reagents and to flow the mixture into a piece of 60 cm 150 μm i.d. × 360 μm o.d. fused silica capillary. Total fluorescence change was monitored near the outlet of the capillary.

Surgery and in vivo Experiments

In vivo microdialysis experiments were performed on male Sprague-Dawley rats (Harlan, Indianapolis, IN) weighing 200-250 g. Rats were anesthetized with intraperitoneal (i.p.) injections of ketamine (65 mg/kg) and domitor (0.5 mg/kg) and mounted on a stereotaxic apparatus (Kopf Instruments, Tujunga, CA). Rats were maintained under anesthesia for the entire experiment by giving i.p. injections of ketamine (32.5 mg/kg) and domitor (0.25 mg/kg) as needed. The probe was inserted into the striatum at following coordinates: +1.0 mm anterior of bregma, +2.0 mm lateral of midline, and 8.0 mm deep from dura.[240] After inserting the microdialysis probe, the system was equilibrated by perfusing aCSF through the probe at 300 nL/min for 1 h before beginning measurements.

A 6-port Valco valve (Cheminert 04Y-0000H) was plumbed between the dialysate syringe pump and sampling probe to allow the dialysis perfusion solution to be switched. Solutions of either aCSF or 400 μm L-trans-pyrrolidine-2,4-dicarboxylic acid (PDC) in aCSF could be selected. In vitro calibration with standards was performed after in vivo measurements.

Results and Discussion

NDA Reaction on PDMS Chip with Flow Segmentation

The dialysis probe integrated with PDMS chip allowed NDA/CN^- reagent to be added to a dialysate stream as it was segmented yielding 8-10 nL dialysate fractions that were derivatized as they flowed through the transfer tubing as illustrated in Figure 3-1. For this experiment, 10 μM amino acid solutions were sampled and the fluorescent

product detected 6 min later in the transfer tubing as a series of fluorescent spikes corresponding to individual plugs. The NDA reaction with amino acids generally takes 3 min or less to complete[257] and we were able to confirm that the 6 min transit time within plugs was sufficient for complete reaction (data not shown). Although all in vivo experiments were performed on anesthetized animals, the 60 cm of tubing connecting probe and analysis chip is sufficient for many awake animal studies. We have previously used the PDMS chip shown in Figure 3-1 to add reagents for a glucose assay to dialysate as it was segmented.[252] This approach to reagent addition is similar to that used for on-chip dilution of plugs as they are formed.[168] Figure 3-1 shows that the NDA/CN^- reaction could be performed in the same way.

Performing NDA derivatization using droplets was advantageous in at least two ways. NDA is hydrophobic and susceptible adsorbtion by native PDMS. Previous attempts to perform NDA derivatization of amino acids in continuous phases on a PDMS chip had to utilize channel surface treatment to increase its hydrophilicity.[259] With segmented flow, this is unnecessary since the reaction mixture was protected from contacting PDMS walls by a thin layer of perfluorinated oil. Another problem often encountered when using NDA/CN is precipitation.[92] Although this problem can be avoided with some capillary systems,[35, 258, 260] we found that on-line reaction in chips with continuous phases was frequently plagued with chip clogging due to precipitate formation. In this work, precipitation would occur where CN^- and saline solutions were brought into contact; however, these precipitates did not disrupt the formation of plugs, affect plug frequency or affect product yield for at least 2h. We believe that the elastomeric property of PDMS and relatively high oil cross flow both contributed to the

continuation of segmented sample flow even in the presence of precipitates. No precipitate was found within plugs. Consequently, downstream CE analysis was not affected.

Transfer of Segmented Flow to Glass Chip

To achieve high-performance separation, it was desirable to use glass chips for electrophoretic analysis. This required developing a system for smooth transfer of segmented flows to glass chips. Commercially available glass chip connections are a convenient option for regular fluid access to microfluidic channels, but they are typically mounted on the surface of the chip and generate a 90 degree turn in the fluid path which causes plugs to coalesce producing irregular plug frequency. We elected therefore to use in-line transfer similar to that used in microchip CE-electrospray ionization (CE-ESI) applications.[261, 262] Such connections are prepared by etching a channel in the same plane as fluidic connections and gluing connecting capillaries in place (Figure 3-3 (C)). Unlike CE-ESI connection that tolerates little dead-volume, transport of segmented flow did not require rigorous seal at the capillary-channel interface. For this application, hydrophobic channel walls helped with smooth transfer of plugs. Images of plug transfer without cross-contamination are shown in Figure 3-4. This in-line configuration is a simple connection that assists the manipulation of segmented flow from outside tubing to glass-based microchips.

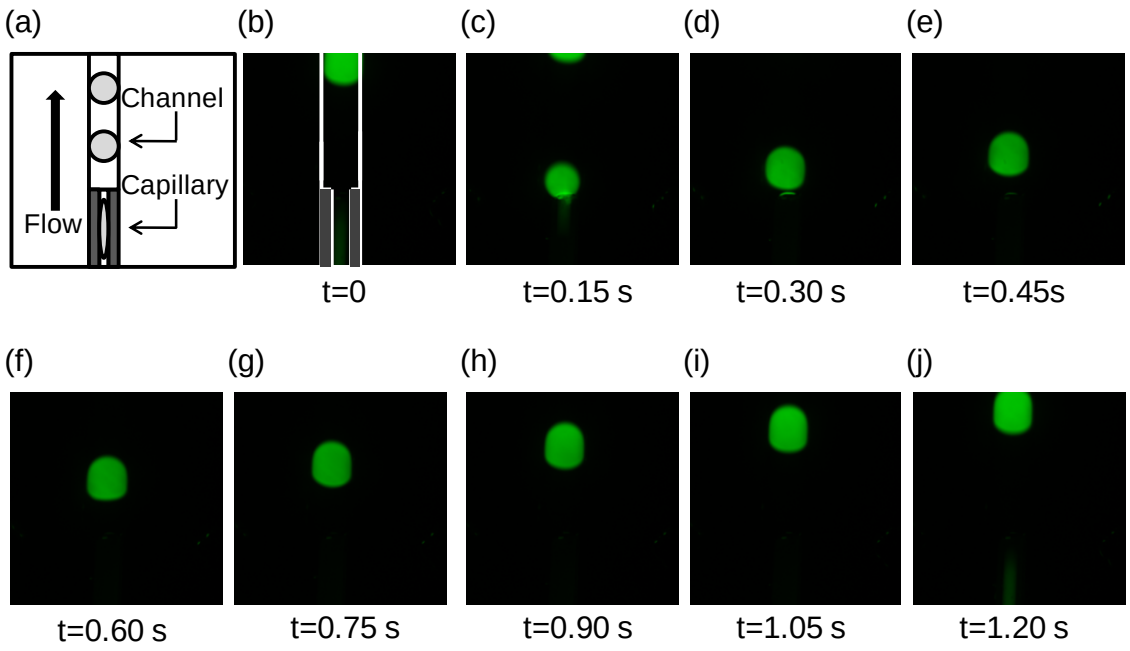

Figure 3-4. Transfer of plugs from capillary to electrophoresis chip. (a) Schematic drawing shows the interface between insertion capillary and segmented flow channel. (b)-(j) Series of fluorescence images show the transfer of plugs containing fluorescein from inlet capillary to the segmented flow channel of glass chip. Relative time points are indicated under each image. Images b, c, and j show a plug in the capillary.

Desegmentation through Extraction Bridge

A key to electrophoretic analysis of segmented flow is to collect sample from aqueous plugs and transfer it to the electrophoresis channel. One approach is to transfer the plug directly to the electrophoresis channel. This method has not yet yielded separations with sufficiently high efficiency to be used for complex dialysate samples.[215, 216, 255] The second approach is to "desegment" the plug flow to create a continuous aqueous sample stream that is then injected using a conventional microfluidic injection scheme.[255] Desegmentation is suitable for the dialysis application as long as the loss of temporal resolution due to recombining the plugs is less than that lost due to the sampling

and rate of electrophoretic analysis. Thus far desegmenting injection has shown more promise for achieving high efficiency separations. Previously this approach has yielded ~50k plates for an 18 s separation, compared to ~1k plates for injection of discrete plugs.[255]

In this work we developed an improved desegmenting and injection design for segmented flow electrophoresis shown in Figure 3-5. In this method, aqueous plugs are removed from a segmented flow and transferred to a separate channel using an "extraction bridge". The extraction bridge is a shallow, hydrophilic channel that connects two deep channels, a hydrophobic one for incoming segmentation flow and a hydrophilic one for extracted aqueous flow (Figure 3-3 (B)). When aqueous plugs contact the bridge, they experience both capillary force from the shallow depth of the bridge and lower surface energy induced by hydrophilic channel walls, which guides the aqueous fraction preferentially through the bridge. Using this method, the entire aqueous plug is consistently transferred through the extraction channel as illustrated in Figure 3-5. Oil is prevented from entering the extraction bridge by the high flow resistance and high surface energy of hydrophilic bridge area for organic phase.

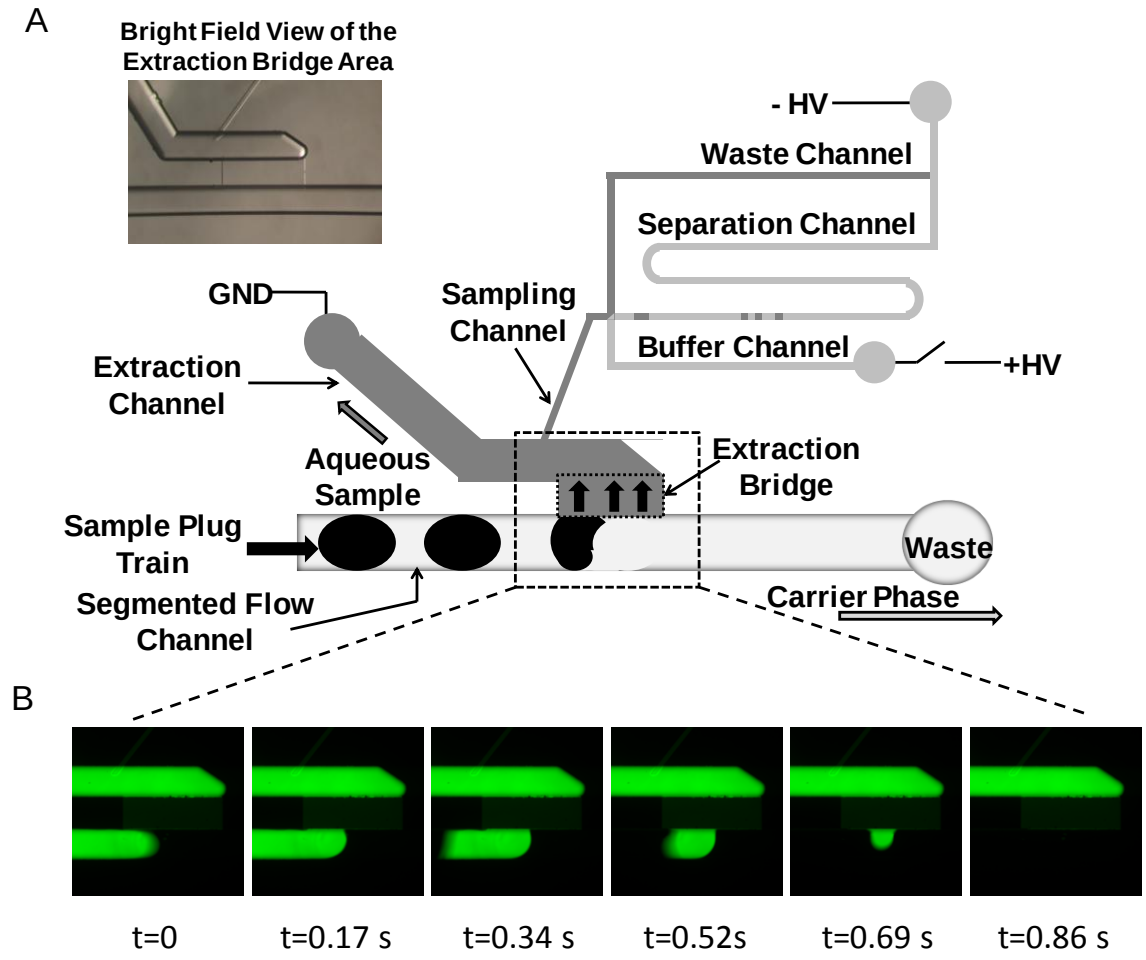

Figure 3-5. Operational scheme of the CE chip. (A) Incoming sample plugs reach the extraction bridge interface and are separated from carrier phase. By applying negative high voltage to the CE outlet and grounding the sample outlet reservoir, sample is drawn to the injection cross by electroosmotic flow and is gated by a cross-flowing buffer stream that is connected to positive high voltage through a relay. As the relay position is changed from closed to open for 60-200 ms, injection is made and electrophoresis separation is carried out. Inset is the bright field picture of the extraction bridge interface. All the sampling and electrophoresis channels are 42μm wide by 6 μm deep. (B) Series of micrographs illustrating the approach and extraction of plugs through extraction bridge. Black region in the segmented flow channel represents the continuously flowing carrier phase.

This phase separation method shares some similarity with previously reported work in terms of using capillary force to separate either gas-liquid flow[222, 263] or liquid-

liquid flow.[161, 162, 224] However, it better met the need of carrying out subsequent high performance electrophoresis of the plug content by building the device on glass substrate instead of PDMS, PTFE or silicon.

High Efficiency CE Separation of Amino Acids.

After phase separation, plugs fill the extraction channel (see Figure 3-5) which acts as a reservoir supplying sample to the sampling channel and cross-style CE injector. The volume of the extraction channel (9.5 nL) is such that each plug fills it and washes the previous plug past the sampling channel. The flow resistance of the sampling channel (6 μm deep x 42 μm wide x 4 mm long) is about 10^4 higher than the extraction channel (70 μm deep x 260 μm wide x 6.5 mm long) so that virtually no hydrodynamic flow occurs in the sampling channel.

Electrokinetic injection[81] was employed using the voltage scheme shown in Figure 3-5. With a negative high voltage applied to the CE outlet and ground at the sample outlet reservoir, sample extracted from the segmented flow was drawn toward the injection cross by EOF through the sampling channel. This stream was gated by a cross-flowing buffer stream connected to positive high voltage through a relay. Changing the relay from closed to open (float) allowed sample to be injected onto the channel for separation. Figure 3-6 is an example of electropherograms of the separation of six amino acids dissolved in aCSF with 11.1 cm separation distance, 60 ms injection time, and 720 V/cm applied to the separation channel. Injection was reproducible with an average of 4.4% RSD in peak height for 50 serial injections. Detection limits were 90-180 nM at the sampling probe for six amino acids.

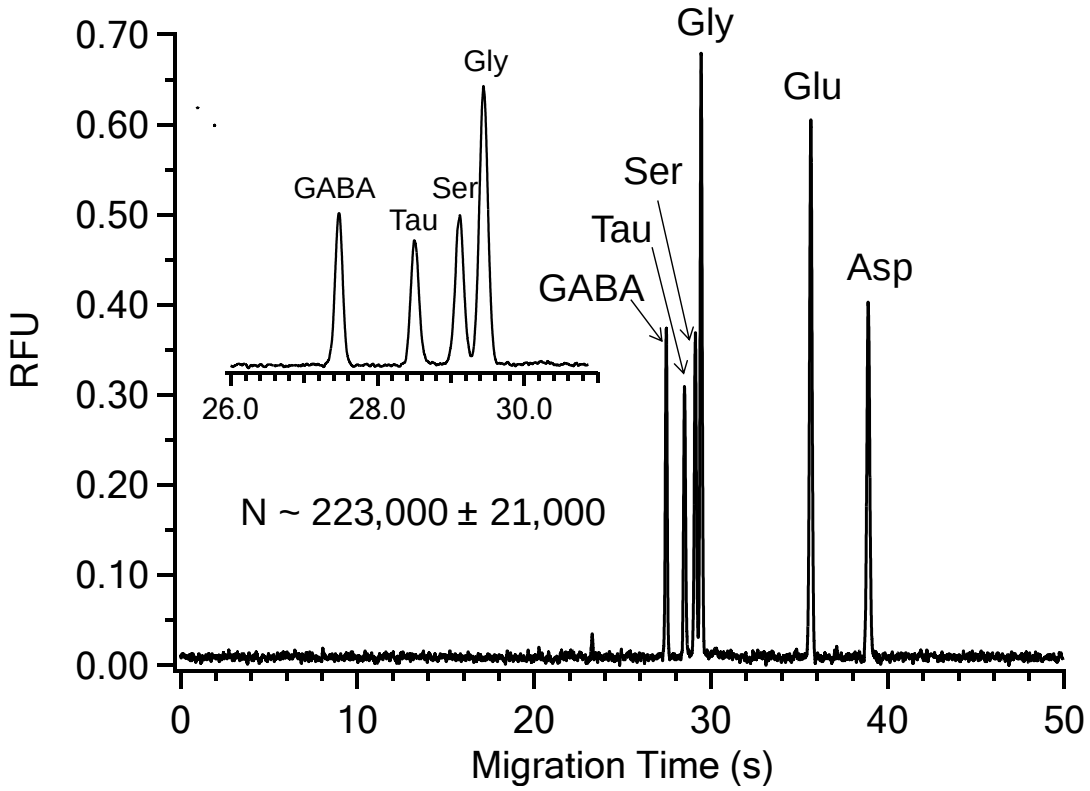

Figure 3-6. Electropherogram showing high efficiency separation of six amino acid standards dissolved in aCSF. Amino acid concentration was 50 μM. Separation buffer was 10 mM sodium tetraborate, 0.9 mM HPβCD at a pH of 9.7. Electric filed strength was 720 V/cm and injection width was 60 ms. Detection was made at 11.1 cm after injection cross. Inset is the enlargement of early migrating peaks.

Separation efficiency was over 200k theoretical plates even though samples contain high salts from the aCSF. This is a significant improvement over the 50k plates previously reported for a desegmenting injector.[255] It is also a significant improvement over previous chip-based electrophoretic analysis of microdialysate that used continuous phase flow.[102, 104, 106] Compared to previous methods of electrophoresis analysis of plugs, this device offered three major advantages. First, the entire plug was extracted without dilution, allowing shorter injections for improved separation efficiency as well as better

LOD. Second, there was no hydrodynamic cross flow that was prone to leaking into the sampling channel, which resulted in higher theoretical plates and better reproducibility. Third, the chip layout allowed for application of higher electric field before bubbles formed, which also helped with higher separation efficiency.

To better understand the factors that limit separation efficiency in the current design, we examined the relationship of peak variance with both injection width and migration time along the channel length. GABA and Glu were chosen as model analytes because of their large difference in mobility. As shown in Figure 3-7 (A), peak variance decreased linearly with decreasing injection width until a minimum value of ~6×10^{-4} cm^2 was reached at 80 ms injection width suggesting that below this injection time the injector does not contribute significantly to peak width.

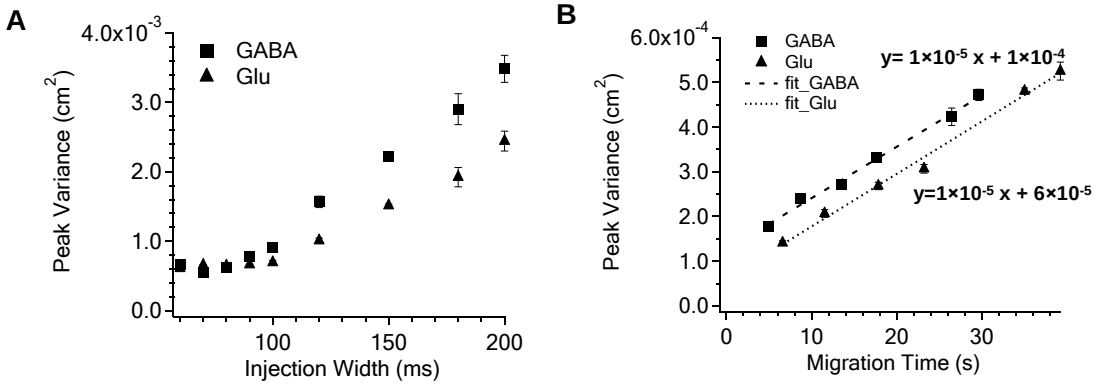

Figure 3-7. Effect of injection width and migration time on peak variance. Glutamate (Glu) and GABA are shown as examples. Data in (A) were obtained at 11.1 cm migration distance, while injection time was altered. Data in (B) were obtained with 80 ms injection width, while migration distance was altered and migration times were recorded. The field strength was kept at 720 V/cm. Separation buffer was the same as in Figure 3-6.

Plotting variance of zones against migration time (achieved by recording variance at different lengths along the channel) yields a linear trend with a slope of 10^{-5} cm^2/s (Figure 3-7 (B)). This value is double the estimated diffusion coefficient of ~5 x 10^{-6} cm^2/s for a small molecule, which is expected if diffusion is the dominant source of band broadening.[86] The small *y*-intercept of 10^{-4} cm^2 indicated that extracolumn effects contributed only 10-20% of the total bandwidth over 11.1 cm separation length. On the basis of these considerations, further improvement in efficiency would require higher fields; however, electric field higher than 720V/cm generated Joule heating. Therefore, future effort to improve efficiency should be directed towards improving heat dissipation.

Conservation of Temporal Resolution with CE Separation

In previous work, we found that temporal resolution with a 2 mm microdialysis probe using segmented flow was 30 s.[252] In such a case, temporal resolution is limited by broadening that occurs during sampling[241] and is fixed once segmented flow was formed. Because plugs were recombined prior to injection in this work, special care was required to not introduce extra mixing of contents of adjacent plugs that would further distort temporal distribution. To achieve this purpose, the sampling channel was placed as close as practical to the extraction bridge so that a desegmented plug could be immediately sampled once it entered water extraction channel. The dead end of the extraction channel was also designed with a triangular shape to fit the flow trajectory of sample plug as it entered water extraction channel through extraction bridge, facilitating rapid transfer with minimal unswept volume . With the above considerations, the final device proved to conserve temporal resolution as shown in Figure 3-8 (A). For this test, back-to-back injections were made every 7 s and separation length was 1.5 cm. A step change in

concentration at the dialysis probe was recorded as about a 35 s change in the electrophoresis traces, compared to 30 s before the extraction, suggesting minimal temporal distortion due to desegmenting. For more complex samples, it is desirable to use the full efficiency of the system. When we moved the detection point to 11.1 cm (Figure 3-8 (B)), where the six amino acids could be fully resolved, injection could be made every 20 s. As expected, the concentration change finished in two electropherograms or 40 s. Temporal response was limited by the separation time in this situation. Further enhancement of the separation speed would be required to be able to analyze each droplet that is formed.

If no flow segmentation was employed but other conditions remained the same, temporal resolution worsened to 90 s for a step increase (Figure 3-8 (C)) and was 130 s for a step decrease (Figure 3-8 (D)). Segmented flow was eliminated this bias allowing measurement of concentration dynamics in either direction with both good fidelity and high temporal resolution.

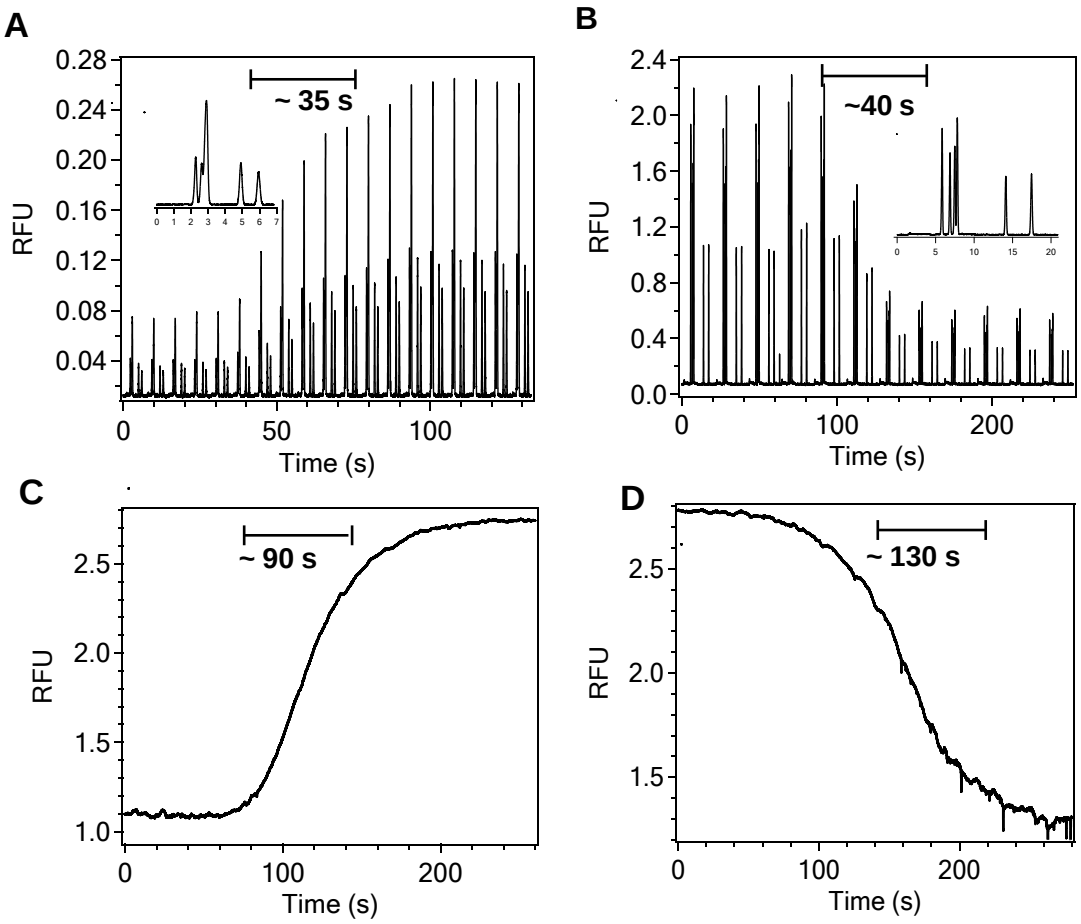

Figure 3-8. Comparison of temporal responses obtained using segmented flow and continuous flow. (A) and (B) were from segmented flow-CE system. Electropherograms in (A) were collected every 7 s at 1.5 cm. Electropherograms in (B) were collected every 20 s at 11.1 cm. Electric field and separation buffer were the same as described in Figure 3-6. Temporal responses in (C) and (D) were obtained at the end of 60 cm 150 μm i.d. capillary after microdialysate were mixed with NDA derivatization reagents at PEEK cross. Step changes of concentration were made between 10 μM and 50 μM amino acid standard solutions following the protocol describe in Experimental section. Temporal resolutions are denoted on the graphs.

In vivo Monitoring of Neurotransmitters

To test this system for in vivo chemical monitoring, we measured amino acids collected from rat brain during a pharmacological treatment. Figure 3-9 (A) illustrates a

typical electropherogram collected in vivo. Serine, glycine, glutamate, and aspartate were resolved. The basal concentration of the four resolved species were found to be 34.1 ± 4.4, 6.0 ± 1.1, 1.8 ± 0.4, 0.7 ± 0.3 μM (mean ± SEM, n = 3), respectively. These values are in good agreement with previous reports.[264, 265] Interferences were found for GABA and taurine; however, optimization of the electrophoresis buffer is likely to allow these neuroactive amino acids to be resolved.

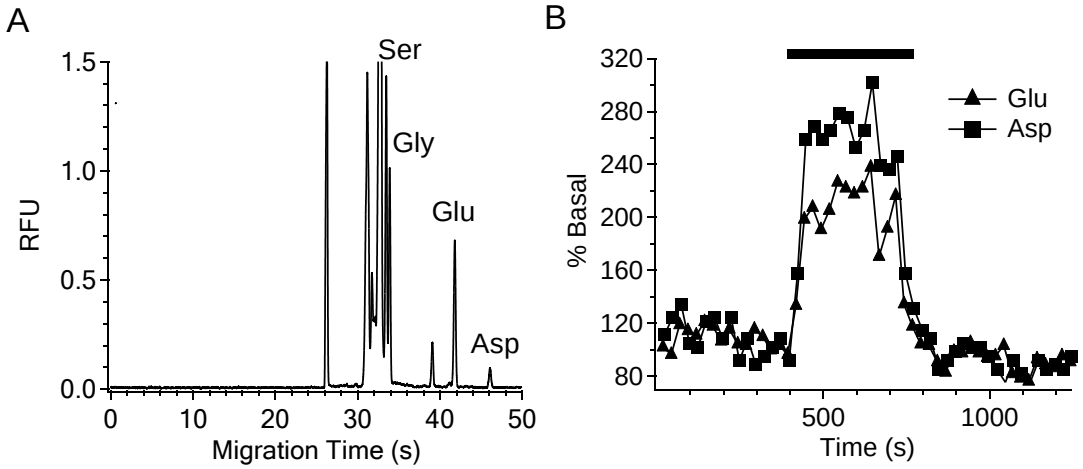

Figure 3-9. In vivo measurements of amino acids. (A) Typical electropherogram obtained in vivo from the rat striatum with on-line derivatization using the set-up. Peaks for serine (Ser), glycine (Gly), glutamate (Glu) and aspartate (Asp) are labeled in the graph. Electric field was 647 V/cm. Injection width was 80 ms. (B) Effect of PDC infusion on glutamate and aspartate basal levels. The black bar denotes infusion of PDC corrected for dead time (~6.5 min). Each point represents peak height of glutamate or aspartate from one electropherogram collected every 25 s.

To demonstrate the capability of the system to detect rapid changes of neurotransmitter levels, 400 μM 1-*trans*-pyrrolidine-2,4-dicarboxylic acid (PDC), a glutamate transport inhibitor[266] was infused into the striatum by reverse microdialysis.

Figure 3-9 (B) is an example of the chemical changes resulted from 5 min PDC stimulation. As expected, glutamate concentration in striatum was elevated to 206 ± 34% (mean ± SEM, n = 3) of basal upon PDC infusion. Aspartate also increased by 238 ± 19% (mean ± SEM, n = 3).[267] No changes in serine and glycine levels were observed.[266] Reperfusion of regular aCSF brought both neurotransmitter concentrations back to basal. The increase of glutamate and aspartate in response to PDC stimulation occurred at the limit of temporal resolution, illustrating a rapid achievement of steady-state concentrations after drug application. While the number of replicates is too low for a complete pharmacological study, the good reproducibility of the basal concentration and evoked changes show that the method has acceptable reproducibility for animal work.

A number of improvements could be made that might further improve temporal resolution. Faster separation in the on-line system would be one approach. This would require a method to avoid the effects of Joule heating. Another approach would be to use this method in off-line mode in which case the connector tubing is used as a fraction collector. NDA products are stable for several hours,[257] so in principle the sample plugs could be stored in tubing and analyzed later by pumping stored samples into the chip. In this case, the samples could be pumped into the electrophoresis chip more slowly to allow more time for analysis; however, this would also require long analysis times. Temporal resolution of sampling might be improved by better connections between dialysis probe and chip. Indeed, we have recently found that small changes in connections and droplet formation can improve temporal resolution to 10 s or better. Even more improvement could be obtained by using plugs created before the sampling probe[205] or by membraneless sampling methods such as push-pull perfusion.[37]

Conclusion

Work in this chapter successfully demonstrates the feasibility of coupling segmented microdialysate flow with CE analysis on a chip for near real-time in vivo chemical monitoring. This method takes advantage of both conserved temporal resolution with segmented flow and high resolving power of CE. The system offers a significant improvement in separation efficiency over previous dialysis-chip CE combinations and previous systems for electrophoretic analysis of multiphase flow. Although this work used anesthetized rats, we envision that as the engineering challenge of securely mounting the plug generator to animals is overcome, the system can be applied to freely-moving rats for behavior, pharmacology and physiology investigations. With optimization of separation conditions more transmitters can be measured. Improvement in temporal resolution may be possible leading to systems that approach the temporal resolution of many sensors, yet offering greater versatility and capacity for chemical analysis.

CHAPTER 4

COLLECTION OF NANOLITER MICRODIALYSATE FRACTIONS IN PLUGS FOR OFF-LINE IN VIVO CHEMICAL MONITORING WITH UP TO 2 S TEMPORAL RESOLUTION

Introduction

The study of brain function and pathologies requires the accurate characterization of neurochemical concentration dynamics in response to external and pharmacological stimuli. Coupling microdialysis sampling to analytical methods such as high performance liquid chromatography (HPLC) or capillary electrophoresis (CE) is an effective approach for such measurements.[16, 249] In developing a microdialysis method, achieving high temporal resolution is an important goal because neurotransmitter release events are observed on the order of seconds.[5, 90] These rapid changes in neurotransmitter release may also be behaviorally relevant and involved in disease states. An inherent limit to temporal resolution is Taylor dispersion, i.e. broadening of concentration zones due to flow and diffusion, during transfer from the dialysis probe to the analytical system (on-line methods) or fraction collector (off-line methods). The effects of Taylor dispersion can be minimized by decreasing the length and volume of connection tubing and by using high sampling flow rates (1-2 μL/min). Under such conditions, a temporal

resolution of 3-30 s has been realized with on-line analysis systems.[6, 25, 29, 102, 250] However, with on-line analysis the analytical method must be rapid enough to maintain this high temporal resolution.

Another approach to reduce dispersion is to segment the dialysate stream into discrete aqueous sample plugs carried by an immiscible oil phase.[252] This approach allows sufficient temporal resolution that is nearly independent of flow rate and completely independent of tubing inner diameter (i.d.) or length. For example, this approach was used to obtain 35 s temporal resolution with a 60 cm length of connector tubing and sampling flow rate of 200-300 nL/min[255, 268] with on-line analytical systems. Segmented flow provides other practical advantages such as compatibility with lower flow rates for higher recovery, larger bore tubing to prevent excessive back-pressure and leaking of the dialysis probe, and longer tubing for coupling to freely-moving subjects or other situations where the analytical system cannot be placed close to the subject.

A potential advantage of collecting dialysate fractions as plugs is storage and off-line analysis. Although on-line monitoring has significant advantages such as real-time data output, on-line analysis is not always possible or desirable. For example, analysis time could become the limiting factor of temporal resolution if using relatively slow assays operated in on-line mode, whereas with off-line measurements, fractions can be collected at the temporal resolution required and then analyzed at a slower pace. Off-line analysis is also desirable if the analytical instrument cannot be located near the subject as might occur in collaborative projects or clinical applications.[251]

Off-line analysis of dialysate collected at high temporal resolution is challenging because of the difficulty of manipulating the nanoliter samples generated. One approach

to this problem has been to collect dialysate and naphthalene-2,3-dicarboxaldehyde/cyanide (NDA/CN) mixtures directly to a commercial CE sample vial and to analyzed the samples by commercial CE instrument.[99] In that study, a 940 nL mixture was collected over 20 s, corresponding to 667 nL dialysate at 2 μL/min sampling flow rate. Another approach is to collect dialysate (collected at 1 μL/min) and fluorescein isothiocyanate (FITC) derivatization solutions together in a piece of collection capillary.[5] The capillary is then cut into 4 mm pieces and the liquid sample in each segment, corresponding to only 30 nL volume and 1 s sampling time, is transferred to a test tube for incubation and CE analysis. These two approaches significantly decreased collection volume from minutes to seconds. However, using these methods requires relatively high flow rates to reduce collection time, improve temporal resolution, and maintain sufficient volume for manipulation. In the second report, a multiple post-collection manipulations added complexity to the operation.

In this chapter, we report a new fraction collection method that used nanoliter plugs segmented by an immiscible oil as "collection vials". Dialysate and NDA/CN derivatization solutions were compartmentalized into 2 nL plugs carried by perfluorinated oil after microdialysis sampling. The plug train was collected into a capillary, which was then removed and pumped at a slower flow rate into a microfluidic chip for CE analysis.[268] Using this method, unprecedentedly low fraction volume was collected without using high sampling flow rate. Temporal resolution was only limited by the sampling probe and was as good as 2 s. The collection and manipulation of these sample fractions were automated and required little manual intervention.

Experimental Section

Chemicals

All chemicals were purchased from Sigma-Aldrich (St. Louis, MO) except the salts for artificial cerebral spinal fluid (aCSF) were from Fisher Scientific (Chicago, IL) and NDA was from Invitrogen (Eugene, OR). All aqueous solutions were prepared with water purified and deionized to18 MΩ resistivity using a Series 1090 E-pure system (Barnstead Thermolyne Cooperation, Dubuque, IA). Amino acid standards were dissolved in aCSF. Octadecyletrichlorosilane (OTCS) was stored in a desiccator and was opened in dry N_2 atmosphere in an Aldrich Atmosbag (St. Louis, MO).

Microdialysis Probes

Side-by-side microdialysis probes with 18 kDa molecular weight cut-off membranes made from regenerated cellulose hollow-fibers were made in-house as described elsewhere.[45] Probes had 200 μm diameter, 2 mm sampling length and 40 μm i.d. x 100 μm outer diameter (o.d.) fused silica capillaries for inlet and outlet tubing.

PDMS Chip Fabrication

A microfluidic chip made from polydimethylsiloxane (PDMS) that was integrated with the microdialysis probe was used to segment the dialysate stream and add reagents to the plugs. A brightfield picture of the PDMS chip layout is shown in Figure 4-2 (A). Channels were molded using standard photolithography described elsewhere [235, 252]. Channels for the delivery of dialysate, NDA and KCN/EDTA solutions were 75 μm wide x 70 μm deep while the segmented flow channel for oil delivery and plug flow was 100 μm wide x 70 μm deep. 40 μm i.d. x 100 μm o.d. fused silica capillaries (Polymicro,

Phoenix, AZ) were inserted into three aqueous delivery channels. The dialysate delivery capillary was the outlet of microdialysis probe and was about 4 cm from the probe tip. Capillary for oil delivery was 40 μm i.d. x 100 μm o.d. Plugs were collected into high-purity perfluoroalkoxy (HPFA) tubing (Upchurch Scientific, Oak Harbor, OR) with 150 μm i.d. x 360 μm o.d. The whole chip with capillaries inserted was encased in PDMS, leaving the other ends of capillaries and tubing extending outward for connections.

Glass Chip Fabrication

Detailed descriptions of the design and fabrication of glass microfluidic chip for sampling and electrophoretic separation of segmented dialysate flow has been reported.[268] For the chips used in the current work, the following changes were made: the size of segmented flow channel was 120 μm wide x 50 μm deep; the size of water extraction channel was 110 μm wide x 50 μm deep; the size of extraction bridge was 300 μm wide x 300 μm long x 6 μm deep. Consequently, the volume between extraction bridge and sampling channel was 1.8 nL. Selective patterning of channel surface with OTCS to create an hydrophobic segmented flow channel was also the same as that described before.[236, 255, 268]

Temporal Resolution and Relative Recovery

aCSF (145 mM NaCl, 2.68 mM KCl, 1.01 mM $MgSO_4$, 1.22 mM $CaCl_2$, 1.55 mM Na_2HPO_4, 0.45 Mm NaH_2PO_4, pH 7.4) was pumped through a microdialysis probe at a flow rate of 0.1 to 2 μL/min into the PDMS chip. NDA and cyanide solutions[257, 268] were pumped through separate channels, each at half the flow rate of microdialysate (see Figure 4-2 (A)). Carrier phase (FC-77) flow rate was chosen to maintain a fixed water

fraction (the ratio between aqueous flow rate and total flow rate) of 0.29. Plugs formed at the junction were transferred to a piece of 40 cm HPFA tubing connected to segmented flow channel. Total fluorescence signal of plugs were detected at the end of the tubing.

To determine temporal resolution, the microdialysis probe was dipped into 10 μM standard solution of amino acid mixture (γ-aminobutyric acid (GABA), taurine (Tau), serine (Ser), glycine (Gly), glutamic acid (Glu), and aspartic acid (Asp)) constantly stirred at 37 ^{o}C. Sampling flow rate was varied between 0.1 - 2 μL/min. At each flow rate, step change of concentration from 10 μM to 50 μM was made at the surface of the probe by rapidly spiking the solution with amino acids. During this time, the total fluorescence intensity of plugs were recorded downstream. Temporal resolution was defined as the time between 10% to 90% of the maximal signal.

PDMS Chip Characterization

Pure water was pumped into three aqueous delivery capillaries of the PDMS chip. Visual inspection and monitoring of plugs flowing in HPFA tubing was carried out with a Nikon inverted microscope (Eclipse TS100, Melville, NY). Photographs and videos were taken through the microscope using a digital camera (FinePix F30, Fujifilm). Photographs of plug were analyzed with ImageJ (NIH) to obtain the volume. Videos of plugs were analyzed with VirtualDub (Avery Lee) for frequency information.

To test the ability of the PDMS chip to form plugs with different analyte concentration, 0.2 mM fluorescein was pumped into dialysate delivery capillary while water was pumped into the other two water capillaries. Carrier phase flow rate was kept at 3 μL/min while total aqueous flow rate was kept at 1.2 μL/min. Relative flow rate of

fluorescein and water was varied and the fluorescence signal intensity of resulted plug was recorded. Fluorescein fraction was defined as the ratio of fluorescein flow rate and total water flow rate.

In Vitro Experiments

Sample plugs formed on PDMS chip were transferred to 10 cm HPFA tubing permanently connected to it (fixed tubing). Another 30 cm HPFA tubing (removable tubing) was connected to the fixed tubing through a Teflon adaptor. After completing the collection of plugs, the removable tubing was then disconnected from the PDMS chip body. NDA reaction in each plug was allowed to complete by leaving the tubing in darkness for 5 min before analysis. When plugs were to be analyzed by CE, the removable tubing was connected to another syringe filled with FC-77 and the plug train was pumped onto the glass chip at a slower flow rate (100 or 200 nL/min) (Figure 4-1). In the electrophoresis chip, segmented flow enters a large channel that has been rendered hydrophobic by selective derivatization. At the extraction bridge (indicated by region with heavy arrows in Figure 4-1 (B)), the channels are hydrophilic and shallower. As a result, the aqueous samples are extracted across this bridge while the oil continues to flow past. The aqueous channel fills the sample region of the chip (indicated by light gray) and is ultimately injected onto the electrophoresis channel at the injection cross (further details of operation are given in Chapter 3). Implementation of CE separation, LIF detection with home-built epi-confocal microscope and data processing were the same as reported in the earlier work.[268] Separation buffer consisted of 10 mM sodium borate at pH 10. When only total fluorescence signal was to be collected for off-line analysis, detection was made at the end of the removable tubing.

Surgery and In vivo Experiments

In vivo microdialysis experiments were performed on male Sprague-Dawley rats (Harlan, Indianapolis, IN) weighing 250-350 g. Rats were anesthetized with intraperitoneal (i.p.) injections of ketamine (65 mg/kg) and domitor (0.5 mg/kg) and mounted on a stereotaxic apparatus (Kopf Instruments, Tujunga, CA). Rats were maintained under anesthesia for the entire experiment by giving i.p. injections of ketamine (32.5 mg/kg) and domitor (0.25 mg/kg) as needed. The probe was inserted into the striatum at following coordinates: +1.0 mm anterior of bregma, +2.0 mm lateral of midline, and 5.5 mm deep from dura.[240] After inserting the microdialysis probe, the system was equilibrated by perfusing aCSF at 0.3 μL/min flow rate through the probe for 1 h before beginning measurements.

200 nL of either 10 mM PDC or high potassium aCSF (145 mM KCl, 2.63 mM NaCl, the other components were the same as aCSF) was delivered into the brain through a capillary (4.5 cm long x 20 μm i.d. x 90 μm o.d. fused silica capillary) by applying 78 psi air pressure for 4 s using an electrically actuated solenoid (Picospritzer, General Valve, Fairfield, NJ). A piece of 0.8 cm 100 μm i.d. x 200 μm o.d. capillary was sleeved over the outside of the 90 μm o.d. capillary near the tip. Both the microinjector assembly and the microdialysis probe were then threaded through a piece of 502 μm i.d. x 718 μm o.d. stainless steel tubing (Small parts, Inc., Miramar, FL) and were glued together. The tip of the microinjector was placed laterally 150 μm and vertically 1 mm above the tip of the probe. The microinjector was prefilled with drug solution before the microinjector-microdialysis probe assembly was inserted into the brain.

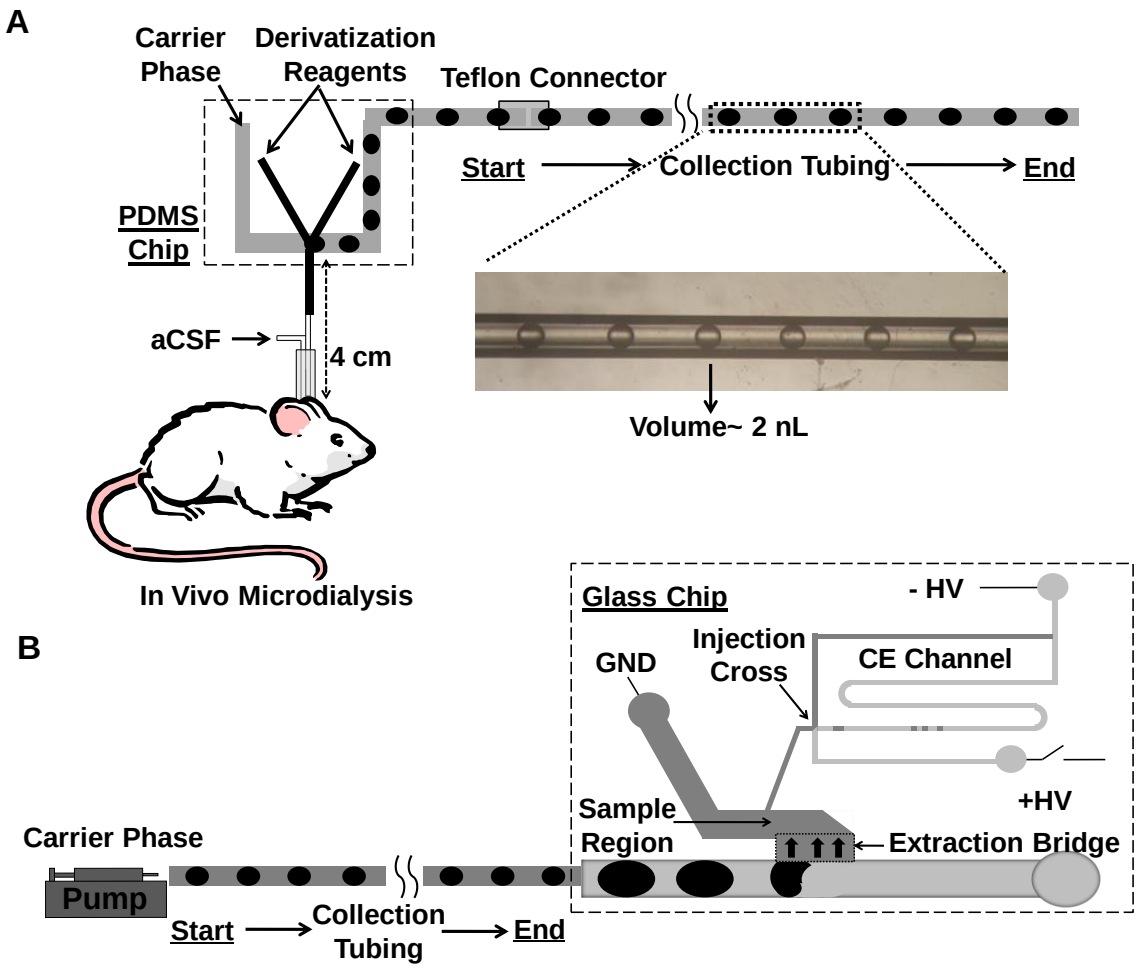

Figure 4-1. Operational scheme of off-line CE-based in vivo sensing using plugs as fraction collector. (A) In vivo dialysate was derivatized on-line and stored in collection tubing. (B) Plugs in the tubing was pumped to microfluidic chip for electrophoretic analysis. The inset shows a brightfield picture of sample plugs stored in 150 μm i.d. HPFA tubing. The volume of each plug is about 2 nL.

Results

Plug Generation with PDMS Chip

A PDMS chip integrated with the microdialysis probe was used to create plugs of dialysate mixed with fluorogenic reagent (Figure 4-1 (A) and 4-2 (A)). This design is a modification of previous reports, where a T-geometry channel with multiple water inlets was used for creating plugs of mixed composition.[168, 252] The new chip is designed to be compatible with sampling from freely moving animal by arranging the dialysate inlet and fluorogenic reagent inlets on opposite sides of the segmented flow channel (Figure 4-2 (A)). In this way, when the microdialysis probe is placed downward into the brain of the animal the other fluid access tubing is brought out from the top and therefore does not interfere with animal movement. The system also uses fused silica capillaries inserted along PDMS channels as conduits for solution delivery. We found that this method, as opposed to using the PDMS channel itself, was necessary to form plugs of uniform composition resulting from the merging of dialysate and derivatization reagents streams on different sides. This effect was attributed to the need for hydrophilic nature of the fused silica tubing.

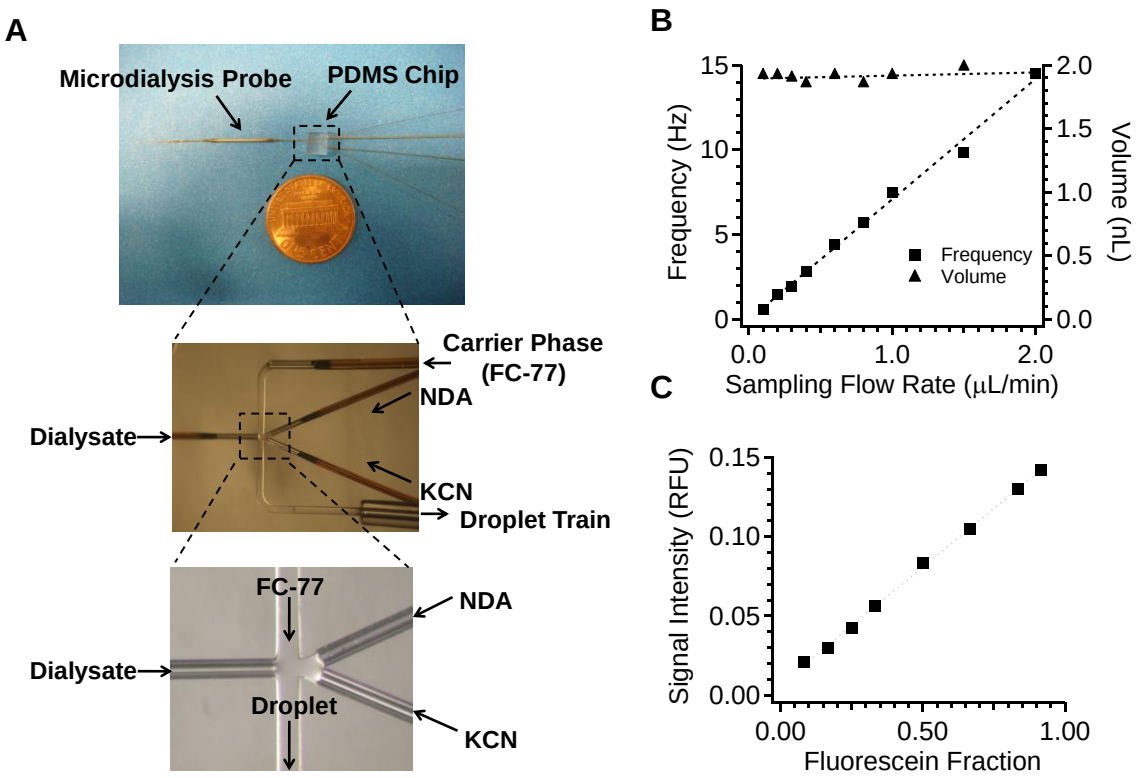

Figure 4-2. Fabrication and characterization of the dialysis/plug sampler. (A) Picture of dialysis/plug sampler placed next to a one-cent coin, brightfield picture of the PDMS chip network and enlarged picture of plug generation region. (B) Relationship between plug volume, frequency and sampling flow rate. Sum flow rate of derivatization reagents equaled to sampling flow rate and water fraction of segmented flow was 0.29. (C) Dependence of detected fluorescence signal on fluorescein fraction in plugs. Oil flow rate was 3 μL/min and total water flow rate was 0.6 μL/min. Fluorescein fraction is defined as the ratio between flow rate of fluorescein to total water flow rate.

To characterize plug generation with the device, sampling flow rate was varied from 0.1 to 2 μL/min. Reagent and oil flow rate were varied concurrently to keep a constant water fraction of 0.29. Figure 4-2 (B) shows the relationship of plug volume and time interval with dialysate flow rate. Because the water fraction was kept constant, the plug volume, which was around 2 nL, did not change with flow rate, while plug frequency increased with increasing flow rate, as expected. We also examined the ability

of this device to achieve stable on chip dilution by varying the relative flow rate of fluorescein (from dialysate inlet) and water diluent (from reagent inlets). Figure 4-2 (C) shows that average signal intensity of plugs measured at the end of the collection tubing formed a linear relationship with the calculated fluorescein fraction in those plugs. These results demonstrate reliable plug generation and dilution with this design.

Temporal Resolution and Relative Recovery with Integrated Microdialysis-PDMS Chip

In continuous flow microdialysis sampling, a trade-off is made between temporal resolution and relative recovery as a function of flow rate i.e., higher flow rate results in better temporal resolution, but lower concentration in the sampling stream.[29] The dialysis/plug sampler had a similar trade-off as illustrated by Figure 4-3. However, because any dispersion in the connection tubing between the probe and the analysis platform was eliminated with segmented flow,[252] the temporal resolution obtained with this device depended only upon dispersion associated with the probe itself. Thus, the temporal resolution only varied from 2 to 19 s over the whole range of flow rates (0.1-1 μL/min) tested. These results demonstrate that good temporal resolution can be achieved while achieving high recovery.

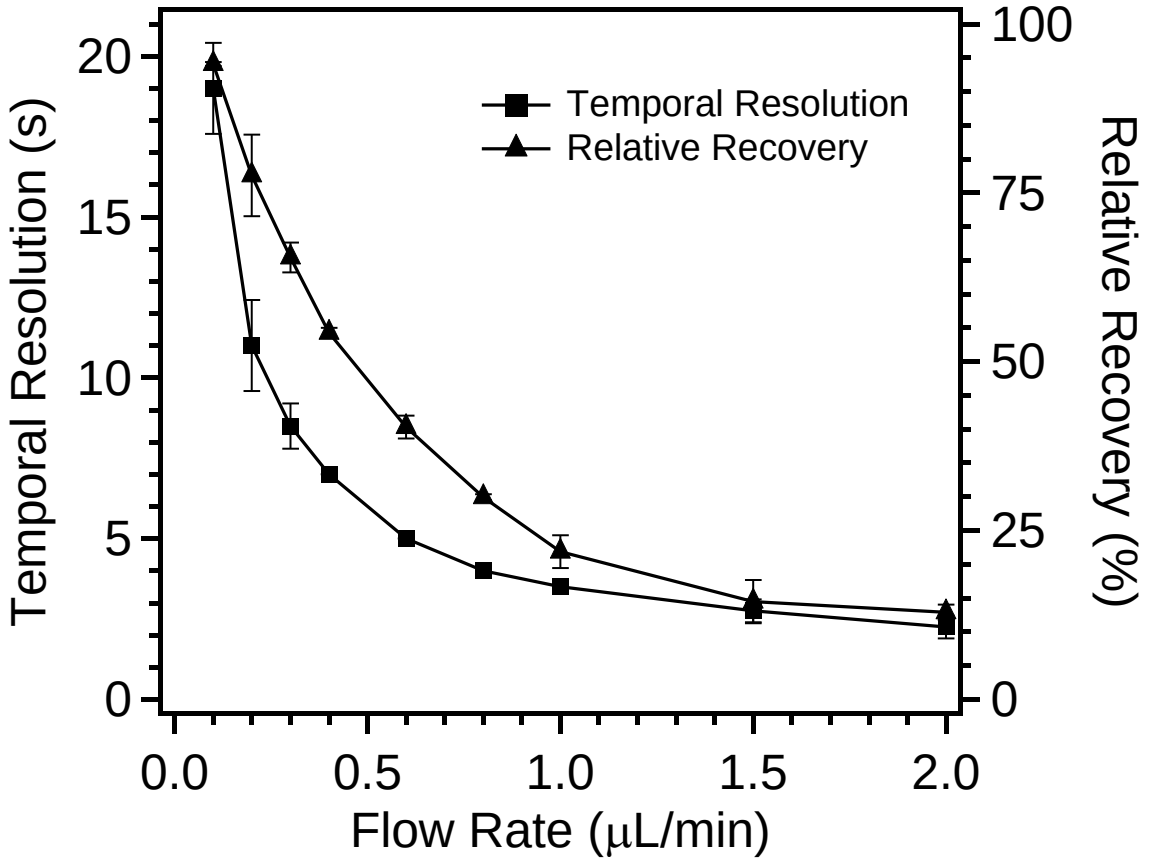

Figure 4-3. Dependence of temporal resolution and relative recovery on sampling flow rate. Microdialysis probe sampling length was 2 mm. Water fraction was 0.29. n=3 and error bars indicate standard deviation.

Off-line Analysis Using Plug as Fraction Collector

Next, we evaluated the potential for off-line analysis of the collected fractions. In previous work, we have shown on-line analysis of plugs, i.e. plugs were directly pumped into an electrophoresis chip for analysis. However, the on-line method is limited because it requires that the analysis time be as fast as the temporal resolution. With the dialysis/plug sampler, we have obtained up to 2 s temporal resolution in sampling, placing great constraints on the analytical system for on-line analysis. Off-line analysis

would allow slower assays to be used with the rapidly collected fractions. The small size of the plugs (~2 nL) means that off-line analysis cannot be performed by collecting fractions into separate tubes for analysis. Therefore, the fractions were stored in a collection capillary, then pumped into an analytical chip at a flow rate low enough to allow full analysis without affecting temporal resolution.

Figure 4-4 and Figure 4-5 illustrate the effectiveness of off-line analysis at generating more time for analysis with the plug system while preserving temporal resolution. Figure 4-4 shows that a step change in concentration of amino acids at a microdialysis probe with on-line monitoring of the plug fluorescence yields a 5 s temporal resolution recorded over 20 plugs when using a total flow rate of 4.2 μL/min (dialysis, derivatization, and oil flow rates of 0.6 μL/min, 0.6 μL/min, and 3 μL/min respectively). By pumping the collected plug train off-line at an ~20-fold lower flow rate (0.2 μL/min), the time available for analysis of the 5 s concentration change is increased 20-fold to 100 s (Figure 4-4 (B)). This plug train was then pumped at 0.2 μL/min into a CE chip while acquiring electropherograms at 50 s intervals. As shown in Figure 4-4 (C), the resulting step change in concentration is recorded over 2 electrophoregrams or 100 s (corresponding to 5 s of actual collection time), showing preservation of temporal resolution with this type of analysis. In each electrophoresis run, 11 amino acid standards including GABA, taurine, serine, glycine, glutamate, and aspartate were resolved in 50 s (Figure 4-4 (D)). Thus, it was possible to monitor all of these compounds at 5 s temporal resolution even though each electropherogram required 50 s.

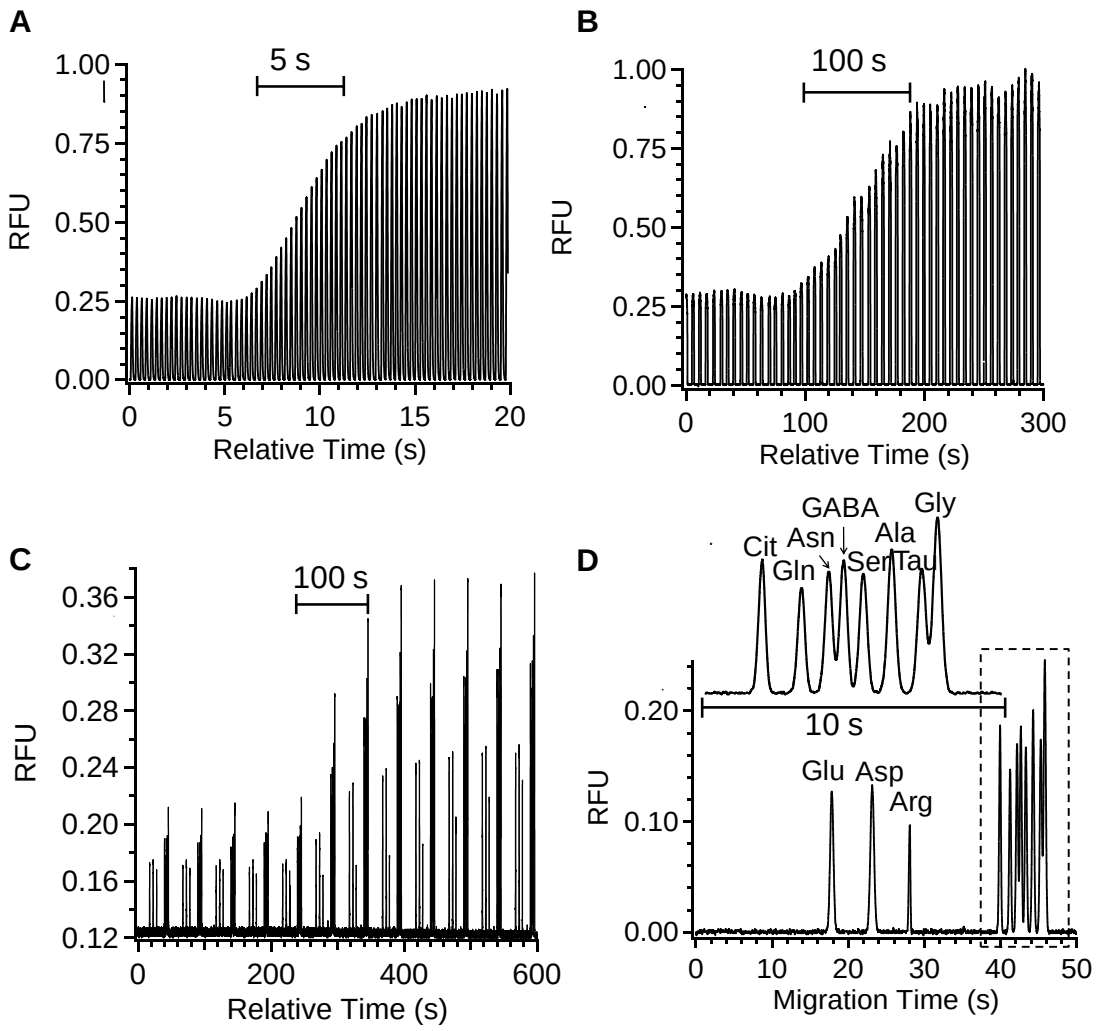

Figure 4-4. Validation of off-line operation with in vitro analysis (0.6 μL/min). Step change of amino acid solution concentration was made from 10 to 50 μM. Sampling flow rate and off-line pumping flow rate were 0.6 μL/min and 0.2 μL/min. Water fraction was kept at 0.29 in all cases. (A) On-line total fluorescence signal of plugs detected at the end of collection tubing; (B) Fluorescence signal of plugs detected at the end of collection tubing when plug train was pumped off-line; (C) Consecutive electropherograms collected when the plug train was off-line pumped to CE chip at the same flow rate as in (B); (D) Individual electropherogram showing the resolution of 11 amino acids. Insets show enlarged electropherograms in the dotted box. Separation buffer was 10 mM sodium borate at pH 10. Separation distance was 11 cm and electric field was 650 V/cm.

Figure 4-5 illustrates a similar example for collecting samples at 0.3 μL/min (total flow rate of 2.1 μL/min), yielding 9 s temporal resolution, and then performing off-line analysis at 0.1 μL/min to yield 180 s for analysis. These examples show the versatility for manipulating plugs and analysis time with off-line analysis by changing pumping flow rates.

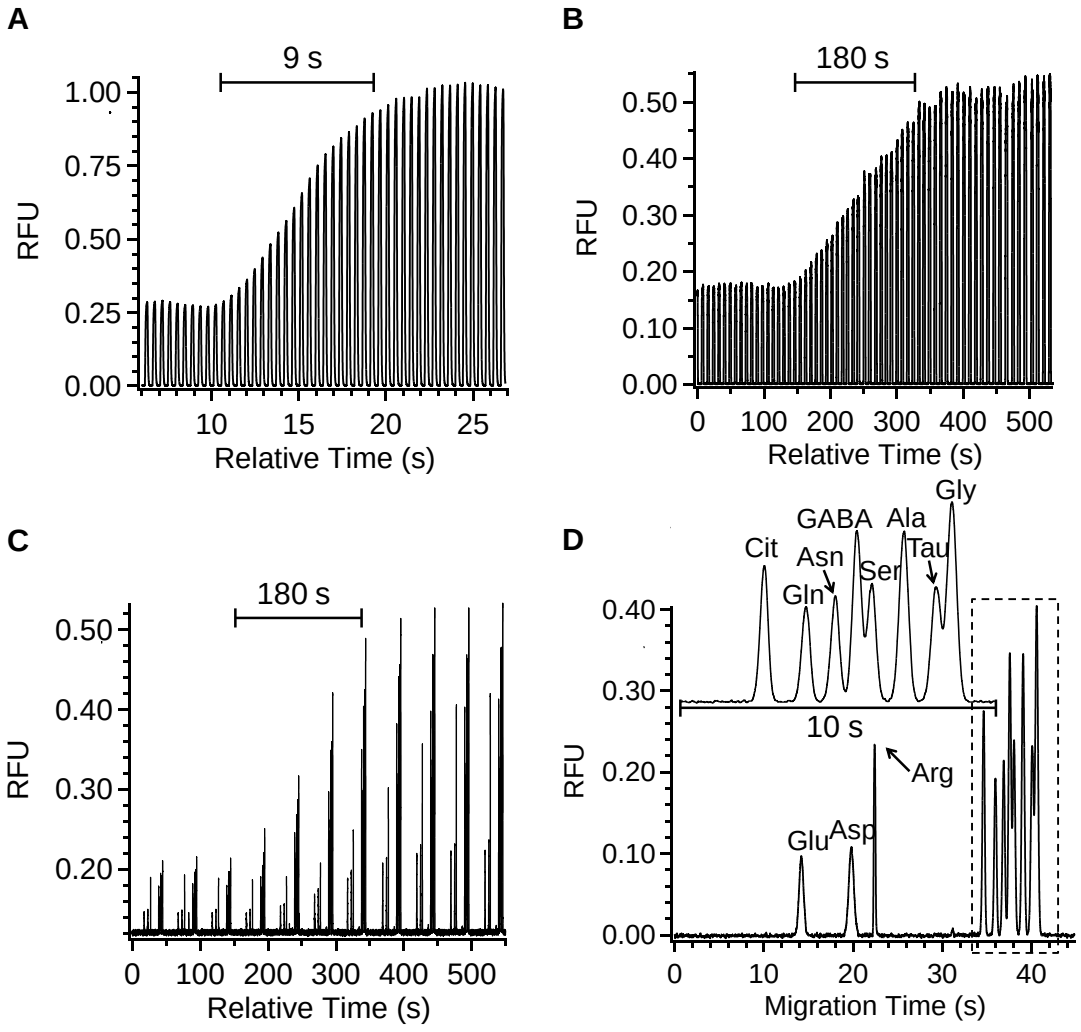

Figure 4-5. Validation of off-line operation with in vitro analysis (0.3 μL/min). Sampling flow rate and off-line pumping flow rate were 0.3 μL/min and 0.1 μL/min, respectively. Other conditions were the same as in Figure 4-4.

High Temporal Resolution Off-line Monitoring Neurotransmitters In vivo

To demonstrate the validity of the method in vivo, it was applied to monitoring amino acids in anaesthetized rats during microinjection of pharmacological agents. Microinjections were chosen over reverse microdialysis for drug delivery because dispersion at the moving front of the drug before it reached microdialysis probe resulted in relatively slow concentration changes in the brain. 200 nL of either 10 mM PDC, a glutamate uptake inhibitor, or 145 mM K^+ were microinjected over 4 s into the brain while sampling at 0.3 μL/min. The resulting collected fractions were then pumped into the electrophoresis chip at 0.2 μL/min. Figure 4-6 shows in vivo electropherograms of dialysate collected at basal (A) and levels obtained during PDC (B) or K^+ (C) stimulations. Basal dialysate concentrations of serine, taurine, glycine, glutamate, and aspartate were found to be 27.6 ± 1.8, 9.9 ± 1.0, 5.1 ± 0.5, 2.9 ± 0.1, 0.3 ± 0.1 μM (mean ± SEM, n = 8), respectively, which were in good agreement with previous reports [43, 264, 265] when accounting for the differences in recovery at different flow rates. GABA was not quantified due to its low basal level and incomplete resolution from serine. Optimization of electrophoresis buffer and the use of more sensitive detectection methods will be necessary to monitor GABA reliably.

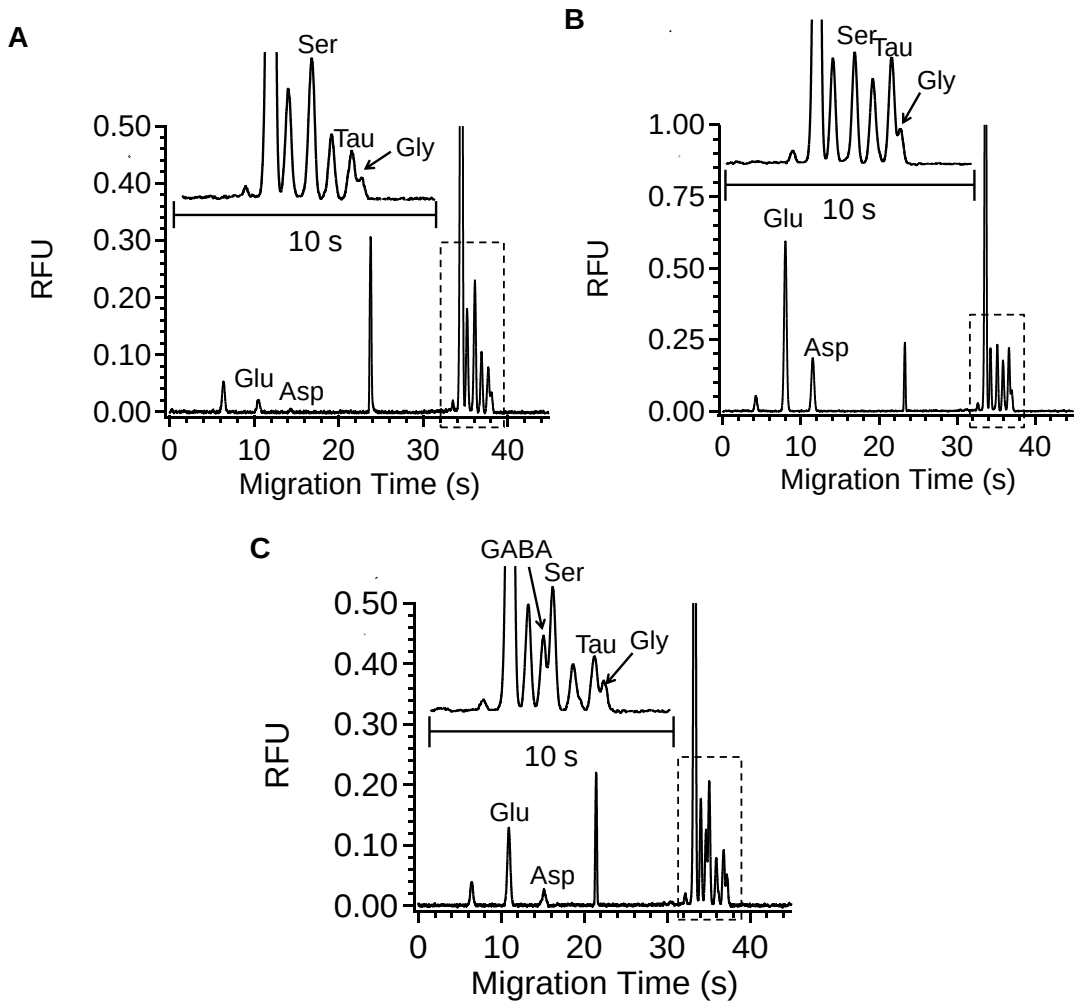

Figure 4-6. In vivo electropherograms collected from the striatum of anesthetized rats. (A) basal level; (B) elevated level during PDC stimulation; (C) elevated level during K^+ stimulation. Insets show enlarged electropherograms in the dotted box. Separation conditions were the same as in Figure 4-4.

Figure 4-7 shows response of glutamate (A), aspartate (B), taurine (C), and glycine (D) upon PDC microinjection. The first injection produced the highest percentage of increase, which was 4320 ± 250% in glutamate, 5000 ± 720% in aspartate, 300 ± 40% in taurine, and 170 ± 20% in glycine (mean ± SEM, n = 3), while the second and third injections produced an attenuated response. Average increase in the second

stimulation was 1370 ± 60% in glutamate, 1400 ± 80% in aspartate, 230 ± 20% in taurine, 150 ± 30% in glycine and in the third stimulation was 1160 ± 40% in glutamate, 1100 ± 100% in aspartate, 200 ± 30% in taurine, 150 ± 20% in glycine. For all amino acids, it took ~20 s to reach peak concentrations.

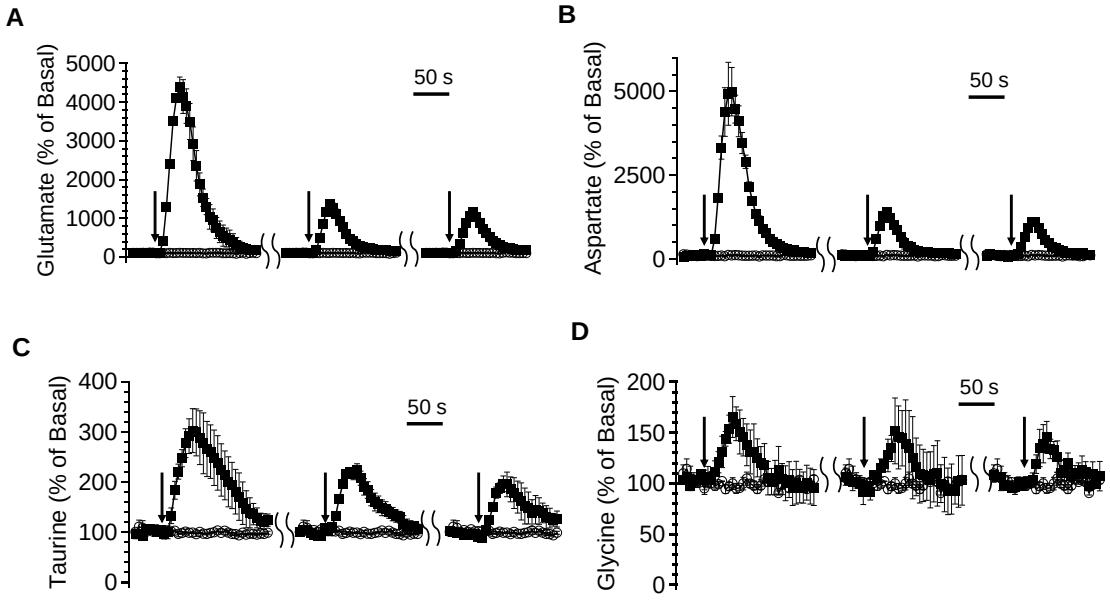

Figure 4-7. The effect of PDC on selected amino acids in the striatum of anesthetized rats. 200 nL 10 mM PDC was microinjected over 4 s for multiple times, with 30 min apart. Data are expressed as percentage of basal level (mean ± SEM, n=3) for glutamate (A), aspartate (B), taurine (C), and glycine (D). Each solid square represents a peak height value of corresponding amino acid in one electrophoresis run. Traces in empty circle are from control experiments when only aCSF was injected. Black arrows indicate the start of microinjection.

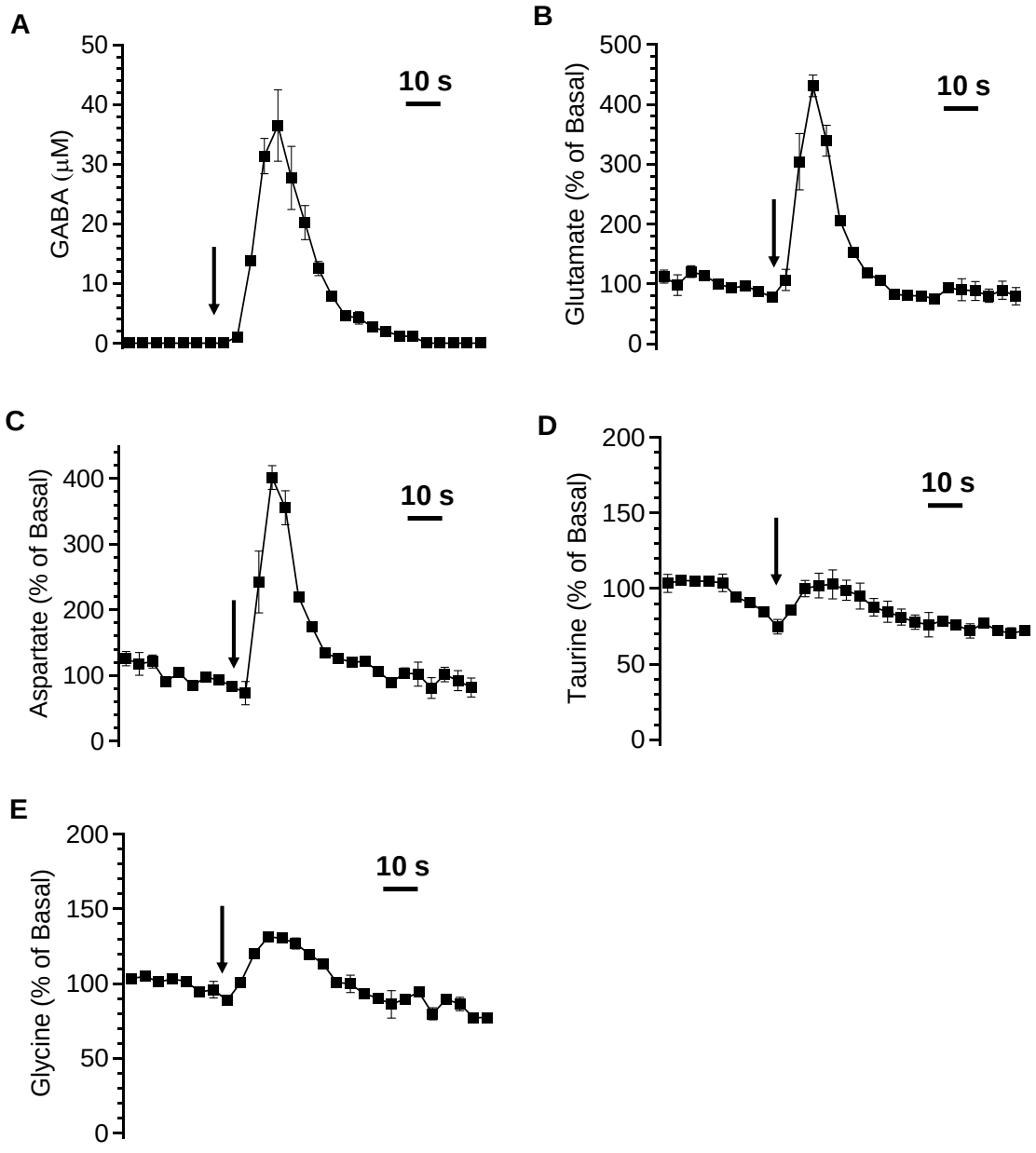

Figure 4-8. The effect of potassium on selected amino acids in the striatum of anesthetized rats. 200 nL 145 mM K^+ aCSF was microinjected over 4 s. GABA response (A) is expressed as concentration (μM) (mean ± SEM, n=3) in the dialysate and its baseline value is treated as zero. Responses of glutamate (B), aspartate (C), taurine (D), and glycine (E) are expressed as percentage of basal. The other conditions were the same as in Figure 4-7.

Figure 4-8 shows the response of GABA (A), glutamate (B), and aspartate (C) upon 145 mM K^+ stimulation. Elevated GABA level could be observed in vivo and on average reached a maximum of 37 ± 6 μM (mean ± SEM, n=3) in the dialysate. Glutamate and aspartate increased to 430 ± 20 and 400 ± 40% (mean ± SEM, n=3) of basal level, respectively. The rise time for K^+ response was faster compared that of PDC at about 9-12 s.

Discussion

Methodology

Improving temporal resolution of microdialysis sampling with off-line analysis creates multiple challenges. As the temporal resolution is increased, the volume of fractions decreases and the number of fractions that must be analyzed increases. Thus, efficient methods of manipulating low volume samples are necessary to achieve temporal resolution better than 10 s. This paper describes the use of segmented flow to collect dialysate fractions as plugs that are stored in a length of tubing for subsequent off-line analysis. This approach is an easy way to precisely and reproducibly collect and manipulate sample fractions down to 2 nL which is impractical with conventional methods using sample vials. Furthermore, this method is compatible with low sampling flow rate, which is important because low flow rates improve relative recovery and sensitivity.

The best temporal resolution possible by this method is ~ 2 s (Figure 4-3). By generating plugs at the immediate exit of the dialysis probe, the temporal resolution is independent of the tubing length used after the probe. Instead, temporal resolution is

only determined by the sampling flow rate and the volume of the probe, which reflects true microdialysis temporal resolution with little effect of the post-sampling section (e.g. transportation and analysis system). We previously reported a limit of 15 s in temporal resolution with segmented flow microdialysis.[252] However, the current work pushed this limit to 2 s because the dead volume between the sampling tip and the flow segmentation point was decreased with the newly designed dialysis/plug sampler. It is likely that the 2 s limit is determined by the mass transportation of analytes across the dialysis membrane, which is found to be the limiting factor at high sampling flow rate.[241] Further improvement of temporal resolution beyond 2 s would require the use of smaller, membrane-less probes with lower dead volume.

The use of segmented flow also means that the length of collector tubing can be varied to collect fractions for an arbitrary period. In the current work, we used 30 cm removable tubing because it was enough to collect fractions for 4 min (at 0.3 μL/min sampling flow), which was the time required for the microinjection experiments. However, the length of the collection tubing can be increased on demand, as long as its induced back pressure is tolerable for the dialysis membrane. This feature makes it more suitable for long term monitoring than the method of collecting sample in a capillary and then cutting the resulting capillary into short sections to create fractions.[5] In that method, the capillary had to be kept short (16 cm long) to prevent excessive dispersion during collection. As a result, time for collecting sample was limited (40 s collection time).

The current method uses reagent addition as the fractions were collected like other reports for off-line fraction collection.[5] This is important in this case because it facilitates reagent addition to the small fractions that are collected. On-line reagent addition is not

likely to be necessary however as methods for adding reagents to pre-formed plugs have been reported.[158] The fractions collected were analyzed immediately after the derivatization reaction was complete (~5 min); therefore, the stability of samples over time was not investigated. Preliminary results from our laboratory suggest that longer term storage of plugs is feasible; however, further study is required to identify robust conditions.

The method was coupled off-line to electrophoretic analysis. Although electrophoresis can provide rapid separations, which has been used to advantage in on-line analysis,[24, 29, 102, 269, 270] resolving multiple compounds often requires times longer than the 2-19 s temporal resolution achieved by segmented flow fraction collection. Thus, off-line analysis is necessary to preserve the high temporal resolution represented in the collected fractions. Although off-line analysis allows preservation of high temporal resolution, it is still desirable to use a relatively fast assay because of the time required to analyze the many fractions collected. The electrophoresis chip was designed to be compatible with this challenge. We determined the size of the channels so that dead volume between extraction bridge and sampling channel was only 1.8 nL. As this volume was smaller than average plug volume (~2.0 nL), the incoming plug content would sweep the previous one away from the sampling point, which introduced little extra mixing at this de-segmentation region and preserved temporal resolution stored in plug train. This plug extraction design, which was described in detail in our earlier publication,[268] is not limited to coupling to CE. It can also act as a preceding step before analytical techniques such as capillary liquid chromatography and electrospray ionization

mass spectrometry, which expands the number of available analysis methods for segmented sample flow to as many as those for continuous flow.

In vivo Experiments

The in vivo experiments (Figure 4-6 , 4-7, 4-8) demonstrate the potential utility of this method for amino acid measurements with high temporal resolution. PDC is a glutamate uptake inhibitor that is expected to increase excitatory amino acid efflux in the brain. Such changes were recorded with glutamate and aspartate as in Figure 4-7 (A) and (B). The percentage of increase of glutamate, which is around 4500%, is comparable to the reported value with similar microinjection procedure,[99] but is significantly higher than our previously obtained value using reverse microdialysis, which is around 200%.[268] We speculate that this difference come from different concentrations of PDC that are generated in the vicinity of the probe as well as the different methods for drug delivery. Levels of taurine and glycine were also observed to increase (Figure 4-7 (C) and (D)). The increase in taurine and glycine suggests a positive interaction between excitatory amino acids and inhibitory amino acids when the concentration of glutamate and aspartate are sufficiently elevated as previously studied.[271, 272] The time for neurotransmitters to reach peak level was around 20 s for most of the injections, which was larger than the 9 s temporal resolution of the sampling and analysis system. In agreement with the argument that glutamate evokes the release of taurine, we observed that the increase in taurine was delayed by ~ 9 s relative to the increase in glutamate. These results illustrate how the method can be used to study interactions of neuroactive compounds in vivo.

We also examined microinjection of 145 mM K^+ solution because this has previously been reported to yield even faster concentration changes in the brain.[273] A substantial effect was seen with GABA, which became detectable after stimulation (Figure 4-6 (C)). The average rise time for neurotransmitters was 9-12 s. This time range approaches the temporal resolution limit of the system under the flow condition used. Potassium evoked glutamate release recorded using a microelectrode[273, 274] has been shown to reach a peak value in only 1-3 s and last for 10-20 s before returning to baseline. Therefore, we speculate that the slower response we observed is due to the limitation imposed by the microdialysis sampling probe. Nevertheless, these results highlight how a dialysis system can approach the temporal performance of a microelectrode while offering a different complement of components to be measured. For example, our measurements reveal high K^+ microinjection evokes a much larger increase in GABA than Glu or Asp. Interestingly, Tau is not elevated by this injection. Infusion of K^+ through a microdialysis probe has been reported to elevate Tau.[43, 275] With higher temporal resolution, we have found that this increase is slower than the changes in Glu, Asp, and GABA (data not shown). These results suggest that the brief microinjection of K^+ does not provide sufficient depolarization to evoke release of Tau. We can also conclude that the increased efflux of Glu evoked by the microinjection of K^+ is insufficient to increase efflux of Tau, which is supported by the fact that Tau is significantly elevated during PDC injection when concurrent Glu increase is around 4000%, 10 times higher than that induced by K^+ injection. These results hint a different mechanism of release for Tau than Glu, Asp, and GABA.

Although the current work used anesthetized rats, this method should be applicable to freely moving animals. We are presently engineering the plug generator chip for robust mounting on freely moving rats. The combination of freely-moving animals and the proposed off-line analysis method will enable us to correlate neurochemical dynamics to behavioral changes on a second to second timescale.

Conclusion

In this chapter, we have developed and validated an off-line CE analysis method using nanoliter plugs as sample fraction collector to monitor multiple neurotransmitters in vivo. With off-line approach, temporal resolution is determined by sampling condition and is not limited by separation speed. Information with up to 2 s temporal resolution can be stored with an unprecedentedly low 2 nL fraction volume. This is the best temporal resolution reported so far using microdialysis sampling, which demonstrates that one can achieve sensor-like temporal resolution while still benefit from the high selectivity, high sensitivity, and multi-analyte detection capability that microdialysis sampling could offer.

CHAPTER 5

COLLECTION, STORAGE AND ELECTROPHORETIC ANALYSIS OF NANOLITER MICRODIALYSATE SAMPLES COLLECTED FROM FEELY-MOVING ANIMALS IN VIVO

Introduction

Microdialysis is a widely used in vivo sampling technique that has become especially useful for studying brain function and pathologies. When coupled to analytical methods such as high performance liquid chromatography (HPLC) or capillary electrophoresis (CE), microdialysis is an effective approach to characterize dynamics of neurochemical concentration in response to stimuli.[16, 249] An important figure of merit for in vivo monitoring is temporal resolution. Because neurotransmitter release events related to behavior or disease states are often observed on the order of seconds,[5, 90] it is necessary that our monitoring methods have comparable temporal resolution in order to accurately follow these dynamics. In state-of-the-art technology, an inherent limitation to obtaining high temporal resolution with microdialysis is Taylor dispersion, i.e. broadening of concentration zones due to flow and diffusion, during transfer from the dialysis probe to the analytical system or fraction collector.[252] Although temporal resolution of 3-30 s using microdialysis has been reported,[6, 25, 29, 99, 102] these studies were generally performed using high sampling flow rate (e.g. over 1 μL/min), anesthetized subjects, or short, small-bore connector capillaries. These procedures could suppress

Taylor dispersion, but often at the price of sacrificing other useful features such as higher relative recovery for better sensitivity that requires low sampling flow rate (50-300 nL/min),[43] or the possibilities of conducting behavioral experiments or clinical applications where long and larger bore connector capillaries are necessary.[250, 251]

Use of segmented flow coupled with microdialysis can reduce Taylor dispersion.[252] In this approach, a dialysate stream is converted into a train of discrete aqueous sample plugs carried by an immiscible oil phase, to prevent mixing between adjacent plugs during transport or storage. This approach allows temporal resolution that is largely independent of flow rate and tubing inner diameter (i.d.) or length.[276]

Segmented flow microdialysis has been coupled to microchip CE to monitor dynamics of neuroactive amino acids from anesthetized animals. In an on-line method, temporal resolution was limited by CE separation time, which was 25-50 s.[268] In off-line method (i.e., fraction collection separate from analysis), higher temporal resolution, such as 9 s in vivo, could be obtained by manipulating the flow rate that segmented samples were pumped to the chip to allow enough time for analysis.[276] Off-line analysis is also desirable if the analytical instrument cannot be located near the subject, as might occur in collaborative projects or clinical applications.[251]

Despite of the usefulness of off-line segmented flow microdialysis, several practical aspects the method remains unanswered. While dialysate plugs could be collected in tubing and analyzed shortly after, methods for storing these sample fractions over a long time (e.g. several days) has not been developed. Previous in vivo applications of segmented flow microdialysis have been carried out with anaesthetized animals, but demonstration on freely-moving animals, which is necessary for behavioral

and emotional studies, has yet to be shown. It is also desirable to optimize CE conditions for fast and high resolution separation of neuroactive amino acids, so as to increase throughput of off-line analysis.

In this paper, we report progress in these directions. A procedure to preserve uniform segmented flow format in HPFA tubing after freezing dialysate plugs at -80^{o}C was found. A dialysis/plug sampler[276] was integrated into a headpiece that is robust enough to be mounted onto freely-moving rats. Electrophoresis times were reduced to 30 s using higher electric field, chip cooling, and novel buffer additives. In addition, to achieve both high temporal and spatial resolution, we characterized microdialysis probes with only 0.5 mm active sampling length. By using segmented flow, low sampling flow rate (50 or 100 nL/min) compatible with small probes could be used while temporal resolution was still better than 15 s.

Experimental Section

Chemicals

All chemicals were purchased from Sigma-Aldrich (St. Louis, MO) except the salts for artificial cerebral spinal fluid (aCSF) were from Fisher Scientific (Chicago, IL) and NDA was from Invitrogen (Eugene, OR). All aqueous solutions were prepared with water purified and deionized to18 MΩ resistivity using a Series 1090 E-pure system (Barnstead Thermolyne Cooperation, Dubuque, IA). Amino acid standards were dissolved in aCSF (145 mM NaCl, 2.68 mM KCl, 1.01 mM $MgSO_4$, 1.22 mM $CaCl_2$, 1.55 mM Na_2HPO_4, 0.45 Mm NaH_2PO_4, pH 7.4). Octadecyletrichlorosilane (OTCS) was

stored in a desiccator and was opened in dry N_2 atmosphere in an Aldrich Atmosbag (St. Louis, MO).

Microdialysis Probes

Side-by-side microdialysis probes with 18 kDa molecular weight cut-off membranes made from regenerated cellulose hollow-fibers were made in-house as described elsewhere.[45] Probes had 200 μm diameter, 0.5 mm sampling length and 40 μm i.d. x 100 μm outer diameter (o.d.) fused silica capillaries for inlet and outlet tubing. Microdialysis probes were integrated with a guide cannula (Plastics One, Inc., Roanoke, VA) for later fixation onto the skull of freely-moving rats.

Headpiece for Freely-Moving Animals

Samples were segmented and reagents added as the dialysate emerged from the probe using a microufluidic chip. Details of the fabrication procedure and dimensions of the polydimethylsiloxane (PDMS) based dialysis/plug sampler, shown in Figure 5-1 (right), can be found in previous report.[276] Microdialysis probes were integrated with a guide cannula (Plastics One, Inc., Roanoke, VA) for later fixation onto the skull of freely-moving rats. To make the system compatible with freely moving animals, tubing on the opposite side to the microdialysis probe (including capillaries for the delivery of FC-77, NDA, and cyanide and perfluoroalkoxy (HPFA) tubing (Upchurch Scientific, Oak Harbor, OR) for plug transfer) were threaded through a hole drilled at the bottom of a 0.6 or 1.5 mL Fisher clear microcentrifuge tube (cap removed) until the PDMS chip was loosely stuck in the middle of the tube. The hole was then sealed with Loctite super glue gel (Henkel Consumer Adhesives, Inc., Avon, OH) before injecting uncured PDMS mixture

into the tube with a syringe until the whole tube was filled with PDMS. The whole device was left in room temperature for two days or until PDMS was fully cured. (See Figure 5-1, middle)

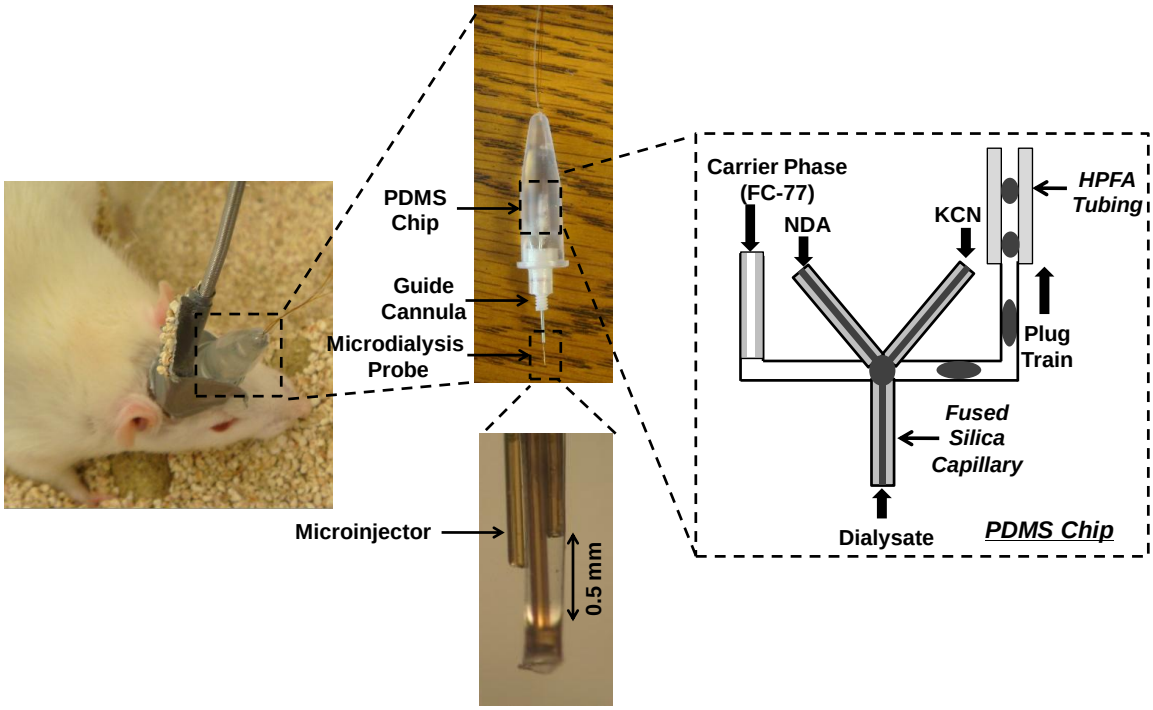

Figure 5-1. Illustration of headpiece for segmented flow microdialysis on freely moving animals. Left: picture of a freely-moving rat with the headpiece mounted on his head during experiment. Middle: picture of finished headpiece after encasing dialysis/plug sampler with guide cannula in a microcentrifuge tube (with enlarged picture of the sampling area of a 0.5 mm probe with a microinjector). Right: schematic drawing of channel network and connection tubing for the dialysis/plug sampler.

Segmented Flow CE Chip

The electrophoretic chip for analysis of segmented flow was the same as described before.[268] Selective patterning of channel surface with OTCS to create an

hydrophobic segmented flow channel was also the same as that described before.[236, 255, 268]

Temporal Resolution and Relative Recovery

To measure temporal resolution, dialysate was collected at 0.05 to 0.6 μL/min sampling flow rate and mixed on-line with NDA and cyanide solutions.[257, 268, 276] At each flow rate, step change of the concentration of a mixture of amino acid standards (γ-aminobutyric acid (GABA), taurine (Tau), serine (Ser), glycine (Gly), glutamic acid (Glu), and aspartic acid (Asp)) from 10 μM to 50 μM was made at the surface of the probe by rapidly spiking the solution with amino acids. The total fluorescence intensity of plugs were recorded downstream on HPFA tubing. Temporal resolution was defined as the time between 10% to 90% of the maximal signal. Relative recovery at each sampling flow rate was determined as the ratio of fluorescence intensity by microdialysis sampling 10 μM standards to the fluorescence intensity by directly infusing 10 μM standards.

Electrophoresis Conditions

The operational scheme of segmented flow electrophoresis chip as well as the configuration of epi-confocal microscope for laser induced fluorescence (LIF) detection have been reported before.[268] The chip uses a separation length of 11 cm in a channel that is 42 μm x 6 μm deep. Fisherbrand Tite-Seal caps with Pt electrodes fixed in the middle were used to cover buffer reservoirs. To prevent arcing at the high voltages used, exposed metal parts (e.g., electrodes or metal alligator clips) were wrapped by PVC electrical insulating tape and a 1" x 1"piece of glass was placed vertically between gating

buffer reservoir and electrophoresis waste reservoir where positive and negative voltages were applied. To suppress Joule heating caused by high electric field, nitrogen gas was forced along the bottom of the chip. Initial separation buffer consisted of 10 mM sodium tetraborate at pH 10. Hydroproxyl-β-cyclodextrin (HP-β-CD), HP-γ-CD, 1-butyl-2, 3-dimethylimidazolium tetrafluoroborate, or tetrabutylphosphonium methanesulfonate was added to the initial buffer at different concentrations for separation optimization. Resolutions between neuroactive amio acids and possible interference from other amino acids in dialysate were evaluated at each buffer composition using 10 μM amino acid standard solution.

Storage of Dialysate Plugs and Test of Sample Stability

A 30 cm length of 150 μm i.d. x 360 μm o.d. HPFA tubing was used to collect dialysate plugs. After collection, the ends of the tubing were sealed by capillary wax (Hampton Research, Aliso Viejo, CA). The tube of plugs was then immersed in a bottle filled with de-gassed hexane. A stir bar was placed in the bottle for use in future thawing step. The bottle was then wrapped in aluminum foil to keep out light and stored in -80 ^{o}C freezer.

Off-line CE was performed on selected days after sample collection. On the day of analysis, the bottle containing tube of sample plugs was taken out of the freezer and immediately immersed in a beaker filled with room temperature water. The beaker was placed on a stir plate to constantly stir hexane in the bottle using the pre-placed stir bar. After 10-15 min, the bottle was removed from the water bath. The tube with plugs was removed from the bottle and connected to another syringe filled with FC-77. The plug train was pumped onto CE chip at 100 or 200 nL/min for analysis.

To test the stability of NDA-AAs, 10 μM standard solution was derivatized and was either stored at -80 ^{o}C or room temperature (also immersed in hexane and kept in dark). Peak height of each amino acid on 1-3 days after sample collection was recorded and compared. With NDA labeled in vivo dialysate, measurements were performed through 8 days after sample collection. Calibration curve was made on each analysis day to quantify the concentration of amino acids over storage period.

Surgery and In vivo Experiments

In vivo microdialysis experiments with freely-moving rats were performed on male Sprague-Dawley rats (Harlan, Indianapolis, IN) weighing 250-350 g. For the implantation of a guide cannula, rats were anesthetized with a combination of ketamine (65 mg/kg; Fort Dodge Animal Health, Fort Dodge, IA) and medetomidine (0.5 mg/kg; Pfizer Animal Health, New York, NY) i.p. Using aseptic technique, a guide cannula was implanted anterior +1.0 mm from bregma, lateral +2.0 mm from midline, ventral -5.5 mm from dura[240] and secured in place with dental cement (A-M Systems, Inc., Sequim, WA). The guide cannula was sealed by means of a solid metal stylet (Plastics One, Inc.). Animals were allowed to recover for 2–3 days before experimentation.

On the day of experiment, the animal was weighed, briefly anesthetized with isoflurane (Baxter Healthcare Corporation, Deerfield, IL), and the dialysis/plug sampler headpiece was inserted with the probe extending 5 mm past the tip of the guide cannula. The animal was placed in a Ratturn (Bioanalytical Systems, Inc., West Lafayette, IN) to prevent the headpiece from being disturbed by normal movements of the animal (Figure 5-1 (left)). The system was equilibrated by perfusing aCSF at 0.1 μL/min flow rate through the probe for 1 h before beginning measurements. 200 nL of 75 mM potassium

aCSF was delivered into the brain through a microinjector (4.5 cm long x 20 μm i.d. x 90 μm o.d. fused silica capillary) by applying 80 psi air pressure for 4 s using an electrically actuated solenoid (Picospritzer, General Valve, Fairfield, NJ). The microinjector was pre-filled with test solution and glued next to the dialysis probe as shown in Figure 5-1(middle).

Results and Discussion

Dialysis/Plug Sampler Headpiece for Freely-Moving Animals

The dialysis/plug sampler headpiece used in this work was similar to that used previously but engineered to be suitable for mounting on freely moving animals.[276] As before, the dialysate inlet and derivatization reagent outlets were placed on opposite sides of the segmented flow channel (Figure 5-1, right). In this way, when the microdialysis probe is placed downward into the brain of the animal, the other fluid access tubing is brought out from the top and therefore does not interfere with animal movement. To give strength to the device and prevent breakage during animal movement, we encased the whole chip in a microcentrifuge tube (Figure 5-1, middle). The total weight of the device was 2-3 g, which is light enough to be carried by the rat on the head (Figure .5-1, left). The encasing PDMS was cured under room temperature to prevent shrinkage of HPFA tubing by heat, which was found to be the major cause of leakage at the HPFA-PDMS connection and failure of the device. With these precautions, the dialysis/plug sampler headpiece proved to be robust and we experienced no device failures.

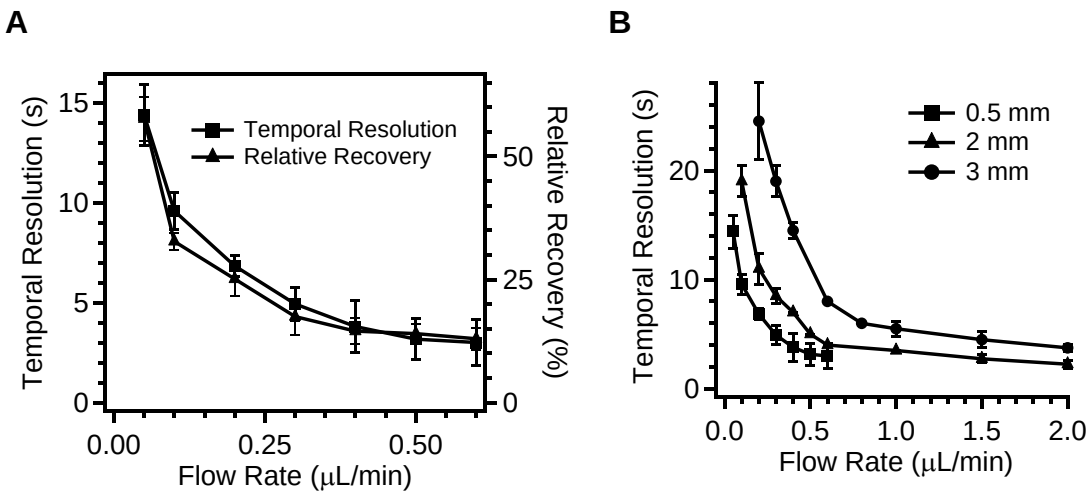

Figure 5-2. Characterization of 0.5 mm microdialysis probe. (A) Dependence of temporal resolution and relative recovery on sampling flow rate using 0.5 mm microdialysis probes. (B) Comparison of temporal resolution of 0.5 mm, 2 mm and 3 mm microdialysis probes at different flow rate. In both (A) and (B), water fraction was 0.29. n=3 and error bars indicate standard deviation.

Temporal Resolution and Relative Recovery of 0.5 mm Microdialysis Probes

Microdialysis sampling is generally considered to have poor spatial resolution due to its large probe size, i.e. 1-4 mm in length, which makes it impractical to accurately implant a dialysis probe in brain regions smaller than a few mm^3. In traditional continuous flow microdialysis, shorter probe (e.g. < 1 mm) would result in lower relative recovery and lower sensitivity. Although this can be partially compensated by using lower sampling flow rate (e.g. 50-300 nL/min), temporal resolution is generally worsened due to excessive Taylor dispersion at low flow rate and after long transport time. On the contrary, segmented flow microdialysis could maintain good temporal resolution even at low flow rate, which makes it suitable to be coupled to miniaturized microdialysis probes. In this work, we used microdialysis probes that have only 0.5 mm sampling length. As

shown in Figure 5-2 (A), at 0.6 - 0.05 μL/min sampling flow rates, temporal resolution of 3 - 15 s and relative recovery of 10 - 60 % could be obtained, which were not substantially inferior to regular 2 mm probes. Notably, at 0.05 μL/min, relative recovery was reasonably high at ~60%, which generated sufficient analyte concentration in the dialysate, and temporal resolution was still better than 15 s. When we compared attainable temporal resolutions with 0.5, 2, and 3 mm microdialysis probes (Figure 5-2 (B)), they all fell between 2 - 25 s, although within different flow rate ranges. Smaller probes had better temporal resolution than large ones under low flow rates, because temporal resolution depended only upon dispersion within the probe itself.[252] These results demonstrate that with segmented flow, miniaturized microdialysis probes can be used to improve spatial resolution without sacrificing temporal resolution or relative recovery.

CE resolution of NDA-AAs

NDA is an attractive fluorogenic reagent to label amino acids and primary amines in dialysate for CE-LIF detection, because its derivatives exhibit good stability, high quantum yields, and fast reaction kinetics (120-240 s).[92, 99, 103, 257, 259] Compared to another widely used fluorogenic reagent *o*-phthaldialdehyde (OPA), NDA offers 10-50 fold improvement in detection sensitivity.[24, 99, 257, 277] This is especially useful in LIF detection on microchip, where detection limits are generally higher than capillary-based systems.[24, 64, 104] However, in contrast to a free zone CE method to successfully resolve neuroactive OPA-AAs such as GABA, glutamate, aspartate, taurine and glycine in vivo,[24] reports of rapid and satisfactory CE separation of NDA-AAs have been scarce. A micellar electrokinetic chromatography (MEKC) method was proven effective in

simultaneously monitoring those neurotransmitters in vivo by capillary-based system.[92] However, from our experience, it was not very suitable for microchip CE, which only holds a small volume of buffer supplies in its reservoirs, as analyte migration order in MEKC can be sensitive to slight changes in buffer composition or pH during operation. Other reported methods based on free zone CE of NDA-AAs in vivo have only been able to resolve a subset of these compounds.[99, 258, 268, 278]

We searched for a CE buffer condition that was capable of simultaneously resolving all the NDA-AAs mentioned above in vivo. Initially, we found that 10 mM sodium tetraborate buffer at pH 10 without any additives roughly met our needs, although resolution in GABA/serine and taurine/glycine pairs were less than 1.5 (Figure 5-3 (A) bottom).[276] In order to improve resolution, cyclodextrins (HP-β-CD or HP-γ-CD) and ionic liquids (IL)[279, 280] (1-butyl-2, 3-dimethylimidazolium tetrafluoroborate or tetrabutylphosphonium methanesulfonate) were added at different concentrations to the initial borate buffer. Of these conditions, 10 mM 1-butyl-2, 3-dimethylimidazolium tetrafluoroborate (abbreviated as IL in Fig. 3) could improve resolutions of GABA/serine and taurine/glycine pairs (Figure 5-3 (A) top) without significantly altering the migration order of amino acids compared to plain borate buffer. Test with the separation of 21 NDA-AAs in vitro using this buffer condition also suggested that no interference from other amino acids would be expected in vivo (Figure 5-3 (B)). Therefore, 10 mM sodium tetraborate with 10 mM 1-butyl-2, 3-dimethylimidazolium tetrafluoroborate at pH 10 was chosen as the electrophoresis buffer.

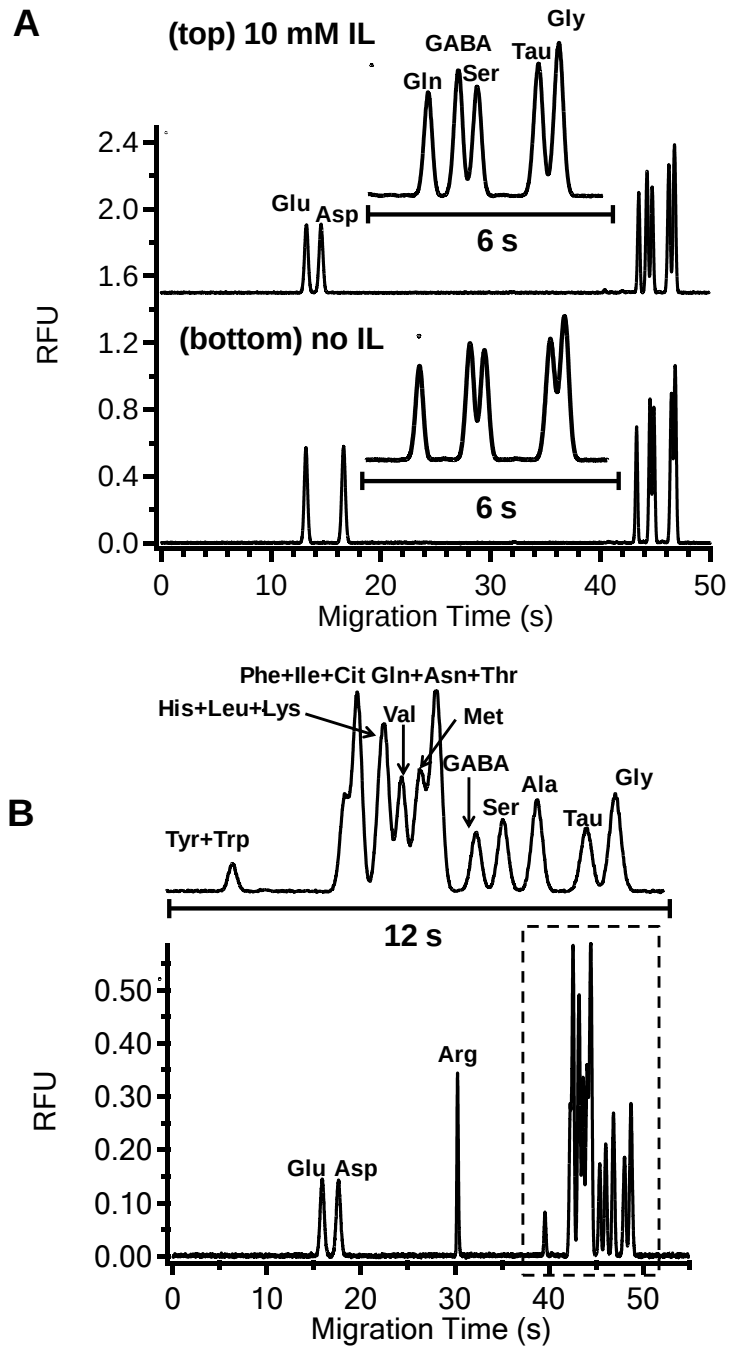

Figure 5-3. Optimization of CE separation buffer. (A) Comparison of the electropherograms of 7 neuroactive amino acid standards with or without ionic liquid (IL) as additive in running buffer. (B) Electropherogram of 21 amino acid standards using optimized separation buffer (10 mM sodium tetraborate and 10 mM 1-butyl-2, 3-dimethylimidazolium tetrafluoroborate, pH 10). Separation distance was 11 cm. Electric field was 720 V/cm. Injection time was 0.08 s.

To accelerate separation and increase analysis throughput, electric field up to 1.1 kV/cm (-14 kV separation voltage and +10 kV gating voltage) was applied after taking precautions to avoid arcing (Figure 5-4 (A)). The effect of Joule heating observed above 650 kV/cm was eliminated with forced gas cooling as shown in Figure 5-4 (B). Under these conditions, separations could be achieved in 30 s (Figure 5-4 (C)). At even higher electric field, though, electrolysis at the surface of Pt electrodes became more significant and rendered continuous operation unstable.

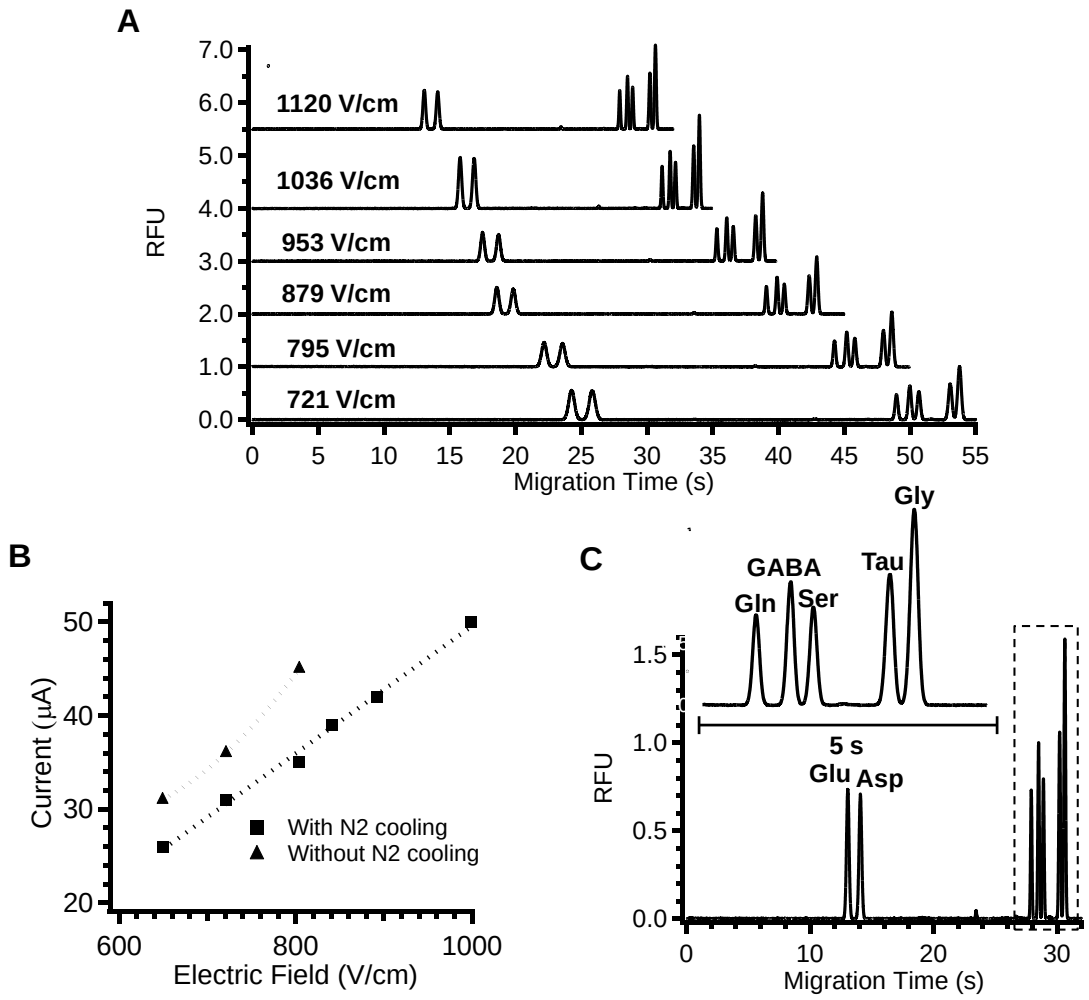

Figure 5-4. Optimization of CE electric field. (A) Serial electropherograms of 7 amino acid standards at different electric field. (B) Dependence of current on electric field with or without air cooling. (C) Electropherogram of 7 amino acid standards at 1.1 kV/cm electric field. Other conditions were the same as in Figure 5-3.

Conditions for Freezing Segmented Samples

The dialysis/plug sampler used in our experiment could generate 2 nL plugs with 5 nL oil gaps. Therefore, an array of ~760 dialysate plugs could be stored in a 30 cm length of 150 μm i.d. HPFA tubing, which corresponded to ~15 min sampling at 0.1

μL/min sampling flow rate (or 3 min at 0.5 μl/min). Such sample collection time would be enough for the study of fast neurotransmitter dynamics in response to short infusions of chemical agents into the brain.

In order to preserve neurotransmitters in these dialysate fractions for later off-line analysis, they should be stored at low temperature, preferably frozen at -80 ^{o}C.[281] However, freezing and thawing nanoliter plugs segmented by oil poses challenges and special procedures were necessary to keep uniform plugs during or after freezing. Placing the tube of plugs directly in the freezer often resulted in air bubbles in either aqueous or oil phase (FC-77) after thawing (Figure 5-5 (A)). We hypothesized that this was due to air permeable HPFA allowing gas exchange during freeze-thaw. To avoid this effect, we stored the tube in a liquid filled glass container to prevent such exchange. Hexane was chosen as the liquid because it does not freeze at -80 ^{o}C and is immiscible with either aqueous plugs or the carrier phase. This property eliminates the possibility of sample concentration change by water evaporation through HPFA walls to the storage media during long term storage. It was found that after storing plug tubes in degassed hexane, no air bubbles were observed after thawing (Figure 5-5 (B-C)).

Another problem was plug coalescence due to plugs moving at different velocities during thaw. This phenomenon was believed to be due to uneven heating rate in different sections of the tube that caused temperature-induced flow. Therefore, ensuring even and steady temperature increase throughout the whole tube during the thawing process was essential in reducing or eliminating coalescence problem. To achieve this, the hexane filled bottle was placed in a water bath and stirred to prevent rapid and uneven

temperature changes. With these procedures, uniform segmented flow format could be observed throughout most, if not all, parts of the tube (Figure 5-5 (B)).

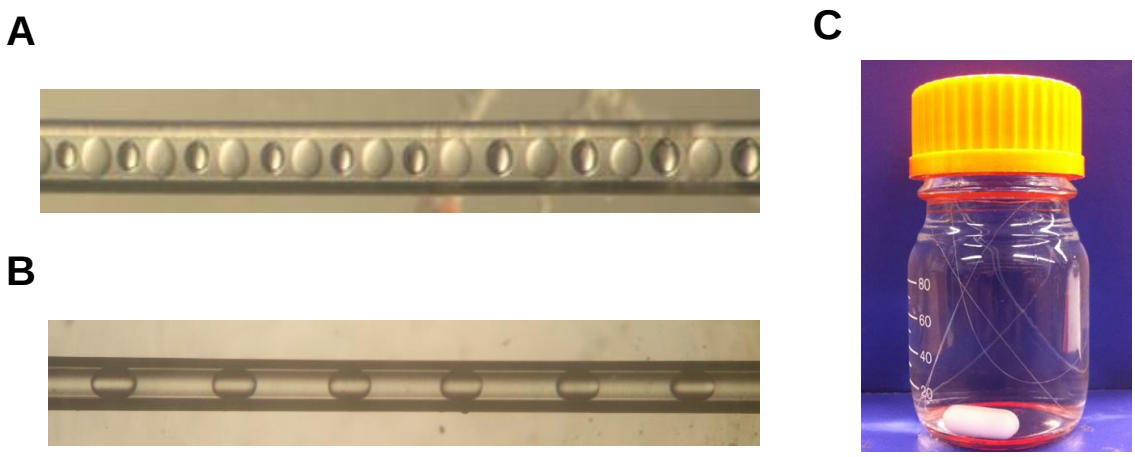

Figure 5-5. Brightfield pictures of plugs in HPFA tubing after freezing at -80 ^{o}C overnight. (A) Air bubbles were formed in carrier phase when the tube of plugs was directly placed in the freezer. (B) Segmented flow remained uniform after storage with optimal procedures described in text. Carrier phase was FC-77. (C) Picture of HPFA tubing filled with plugs immerged in hexane in a glass container with pre-placed stir bar.

FC-77 has a freezing point of -95 ^{o}C making it suitable for storage at -80 ^{o}C. We also tested other commonly used carrier phases such as FC-40, FC-70, FC-3283 and perfluorodecalin (PFD), which all have a freezing point higher than -80 ^{o}C, and would therefore freeze together with aqueous plugs. We found that a non-freezing oil like FC-77 had a higher success rate of keeping uniform plugs throughout the tube than oils that freeze at -80 ^{o}C. This observation can probably be explained by the abrupt volume change during solid-liquid phase conversion. FC-77 would not undergo such phase conversion, thus reducing the possibility of plug movement or coalescence.

The viscosity of the carrier phase also has an impact on plug uniformity. When plugs were stored at -20 ^{o}C, FC-70 (f.p. -25 ^{o}C), FC-40 (f.p. -50 ^{o}C) and FC-3283 (f.p. -

50 ^{o}C) could also be used as non-freezing carrier phases. Under such condition, we observed that more viscous oils like FC-70 resulted in higher success rate of keeping uniform plug array. This is probably because temperature-induced flow is more difficult with viscous oils, making plug coalescence less likely. However, due to large viscosity of FC-70 (24 cp) and the high back pressure it will induce in plug collection, it is unsuitable to be used with segmented flow microdialysis sampling. However, results from this study can be useful for freezing plug array in other applications where more viscous oils and higher storage temperatures (e.g. > -20 ^{o}C) are feasible.

Stability of NDA-AA Adducts In Vitro and In vivo during Long Term Storage

In our experiment, we derivatized samples prior to storage. We first examined the stability of NDA adducts of amino acid standards. 10 μM amino acids including glutamate, aspartate, GABA, taurine, and glycine were derivatized by NDA/cyanide and stored in the dark either at -80 ^{o}C or room temperature for 1-3 days. As shown in Figure 5-6 (A), samples stored at -80 ^{o}C remained intact throughout the period. The percentage of loss calculated from a two-sample t-test (α=0.05) was less than 7% for all the analytes. On the contrary, analysis of samples stored at room temperature presented a drastic plunge in peak height only after one day (Figure 5-6 (B)).

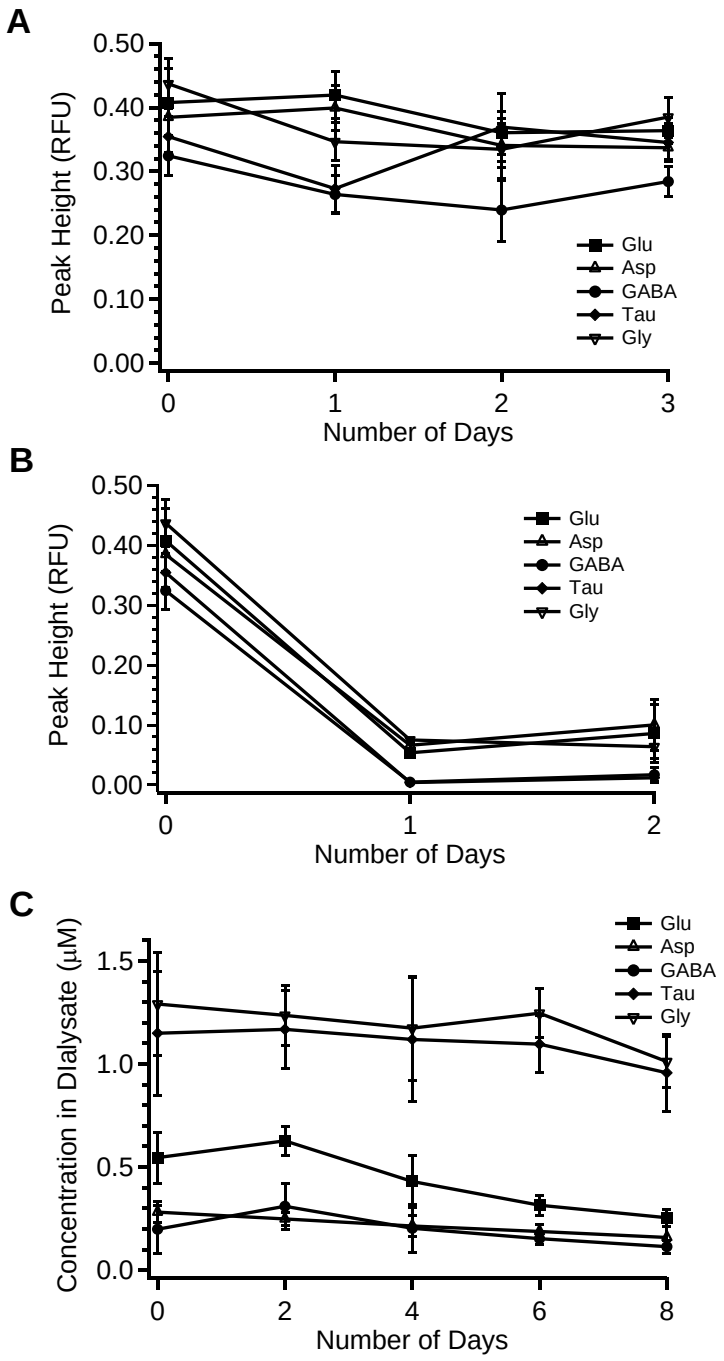

Figure 5-6. Stability of NDA-AAs after storage under different conditions. (A) Peak height of 10 μM NDA-AA standards stored at -80 ^{o}C for three days. (B) Peak height of the same standards stored at room temperature. (C) Measured concentration of amino acids in brain dialysate after derivatized by NDA/CN and stored at -80 ^{o}C for 8 days. Measurements were made on the 2nd, 4th, 6th, and 8th days after sample collection. Dialysate was collected from the striatum of a freely-moving rat using 0.5 mm microdialysis probe at 0.1 μL/min sampling flow rate. Data was the average of at least

20 electropherograms while sample plugs were pumped at 0.2 μL/min into the CE chip. Error bar = ± 1 standard deviation.

We then examined the stability of NDA-AAs from in vivo dialysate frozen at -80 ^{o}C. Figure 5-6 (C) shows measured concentrations of the same set of neuroactive amino acids from the striatum of an awake rat stored over 8 days (n=20 sample plugs). On the 4th day, no obvious decrease was observed in the measured concentration of GABA, taurine or glycine, while 10% of glutamate and aspartate was degraded. After 4 days, however, degradation in low concentration analytes such as glutamate, aspartate and GABA became statistically significant ($p < 0.05$).

These results suggest that in order to accurately quantify the absolute concentration of amino acids in the dialysate, it is desirable to analyze fractions soon after collection. On the other hand, however, freezing NDA derivatized amino acids could be an useful approach to extend the window of sample analysis when percent change of analyte with respect to its basal concentration is of more interest (i.e. analyte's basal concentration acts as the internal standard), which is often the case in many in vivo applications. This is based on the assumption that the decomposition rate of an NDA-AA adduct is independent of the concentration of the amino acid. Under such situation, dialysate could be stored for up to 4 days, without severe degradation in amino acids that might harm their detectability.

Off-line Measurements of Potassium Stimulated Neurotransmitter Efflux in the Striatum of Freely-Moving Rats

To demonstrate the suitability of the off-line method for monitoring rapid changes, we microinjected potassium into the striatum of freely-moving rats and analyzed the responses using off-line CE method after sample storage. 75 mM K^+ was microinjected over 4 s into the brain while sampling with a 0.5 mm probe at 0.1 μL/min. Under these conditions, temporal resolution was 9.5 s and relative recovery was ~30%. Dialysate fractions were stored for 1-4 days and then pumped into the electrophoresis chip at 0.1 μL/min. As the total flow rate of segmented flow during sample collection was 0.7 μL/min, the analysis time was 7 times greater than collection time. Figure 5-7 shows in vivo electropherograms of dialysate collected at basal (A) and levels obtained during K^+ stimulation (B). Basal dialysate concentrations of glutamate, aspartate, GABA, taurine and glycine in freely-moving rats were found to be 0.33 ± 0.17, 0.19 ± 0.07, 0.20 ± 0.05, 1.7 ± 1.1, 1.3 ± 0.4 μM (mean ± SEM, n = 4), respectively, which were in good agreement with previous reports[272, 282] when accounting for the differences in relative recovery in different works.

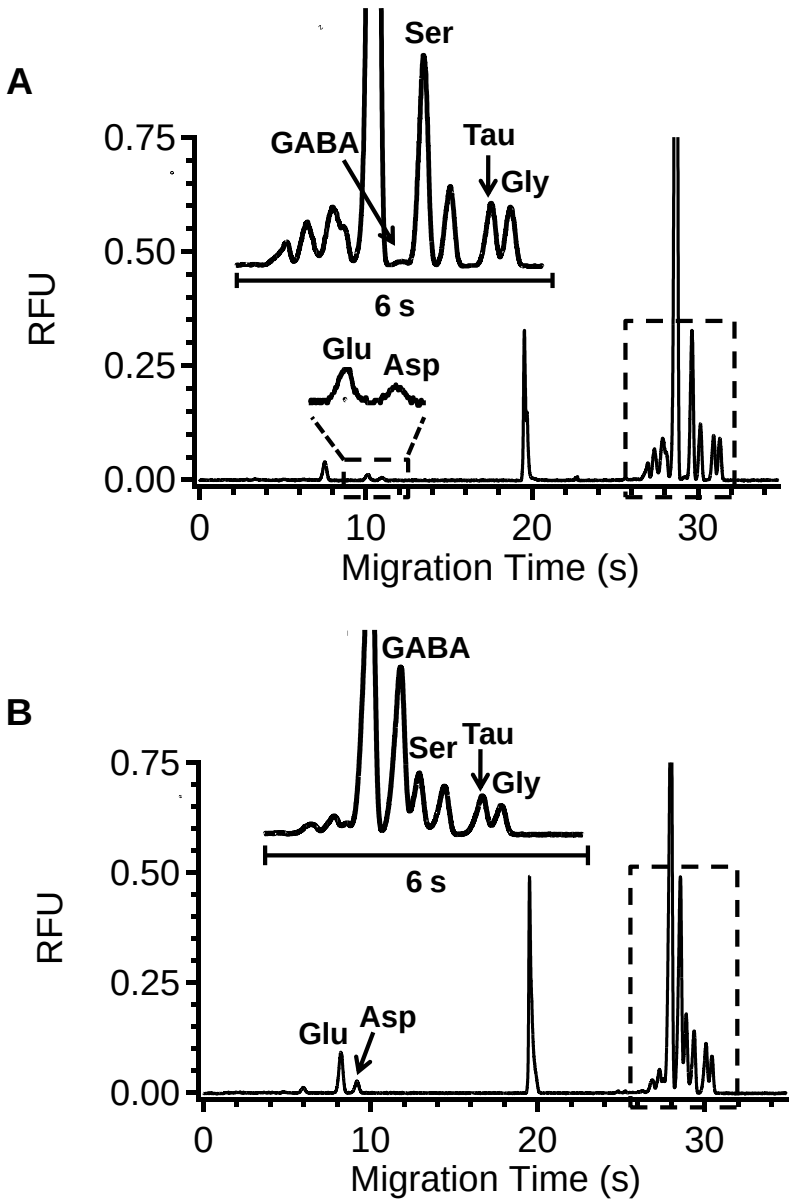

Figure 5-7. In vivo electropherograms collected from the striatum of freely moving rats. (A) basal level; (B) elevated level during K^+ stimulation. Insets show enlarged electropherograms in the dotted box. Sampling flow rate was 0.1 μL/min with 0.5 mm microdialysis probe. Separation conditions were the same as in Figure 5-3.

Figure 5-8 shows responses of glutamate (A), aspartate (B), GABA (C), taurine (D), and glycine (E) upon K^+ microinjection. On average, extracellular level was

elevated by 1570 ± 90 % in glutamate, 530 ± 80 % in aspartate, 7000 ± 1400 % in GABA, 180 ± 40 % in taurine, and 180 ± 20% in glycine (mean ± SEM, n = 4). For glutamate, aspartate, GABA and glycine, it took ~10 s to reach peak concentrations, which was the same as in our previous report [276] using similar experiment procedures with anaesthetized rats. The increase induced in taurine, however, was slower, both in the time to show the increase after injection and in the time it took to reach peak concentration. The results reveal differences in the dynamics of neurochemicals in response to the same stimulation.

Interestingly, the smaller probes used here resulted in significant differences from experiments performed following microinjection at larger probes. For example, in our previous report using 2 mm probes, no increase in taurine was observed, while glutamate and GABA were elevated to a few hundred percentage relative to basal level.[276] Using 0.5 mm probes in this work, however, not only ~180 % increase in taurine became obvious, measured release of glutamate and GABA also increased to a few thousand percentage of basal level. Since the former tests were done with anesthetized rats, we repeated the procedure on freely-moving rats using a slightly different CE system and obtained the same results (data not shown), which suggests that anesthetization was not the main reason leading to such differences. We speculate that this is because smaller probes can focus the sampling region to the center of the liquid stimulus sphere resulted from microinjection, where the strongest response was likely to be induced, while larger probes average the responses from both the center and the peripheral regions of the stimulus sphere. This further suggests that using miniaturized probes with improved spatial resolution is useful in revealing true dynamics induced by locally applied stimuli.

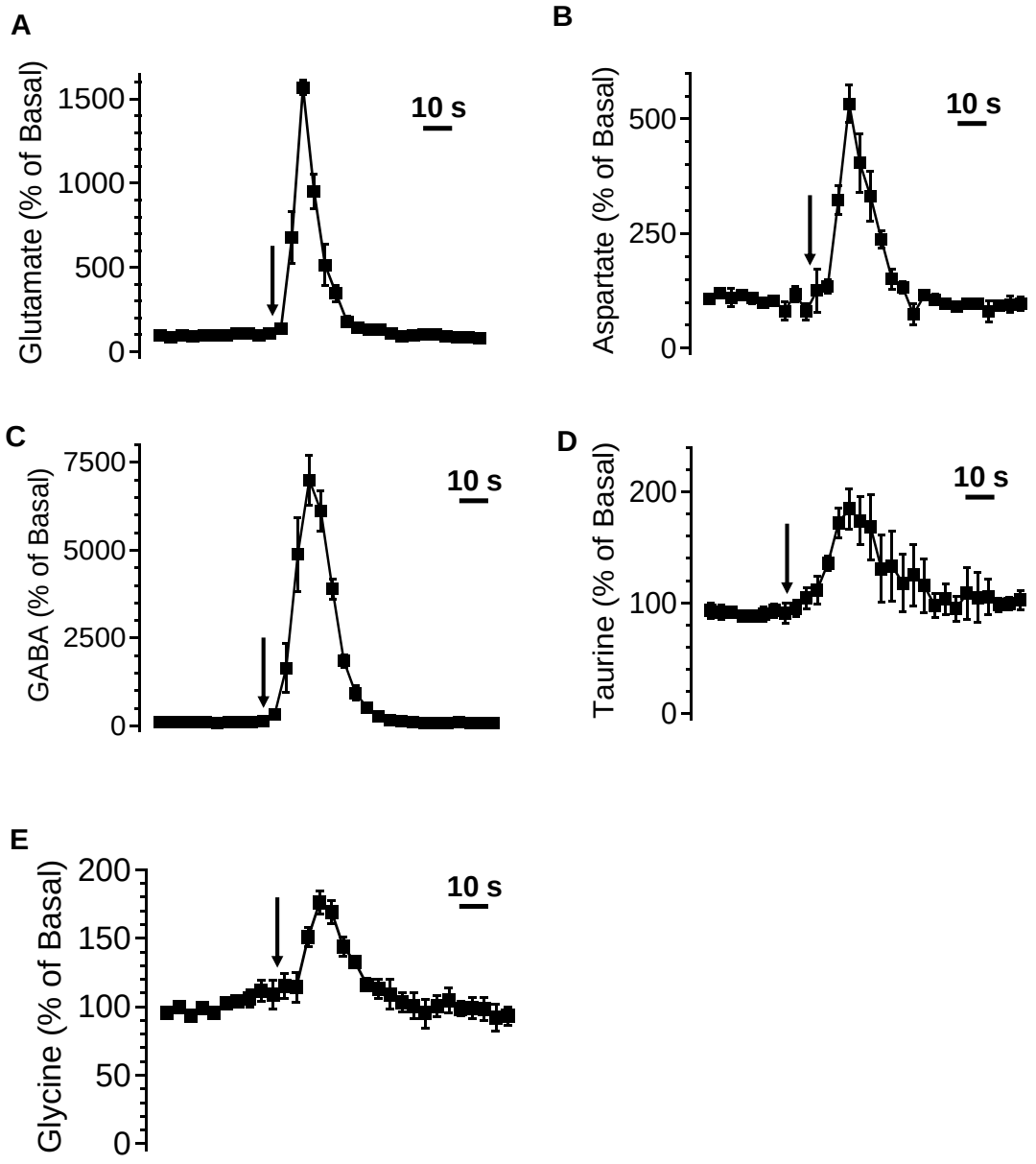

Figure 5-8. The effect of microinjecting 200 nL 75 mM potassium on selected amino acids. (A) glutamate. (B) aspartate. (C) GABA. (D) taurine. (E) glycine. Data are expressed as percentage of basal level (mean ± SEM, n=4). Black arrows indicate the start of microinjection.

Conclusion

In this chapter, we have discussed improvements made in some practical aspects of off-line segmented flow microdialysis. Demonstration of the technique with freely-moving animals extended its application to behavioral studies. By using miniaturized probes, spatial resolution was improved without sacrificing temporal resolution or sensitivity. Combining off-line fraction collection and long term storage of samples allows animal experiments to be separated from the analytical measurements in both time and space. Thus, conditions for both types of experiments can be optimized. Work flow efficiency may be improved because both aspects of the experiment (animal and analytical) do not need to be working at the same time. Finally, collaborations are facilitated by allowing both parts of the experiments to be performed in different locations. These improvements open the door for other neuroscientists and pharmacologists to use our method and to benefit from these technical advancements.

CHAPTER 6

ON-LINE ANALYSIS OF DIALYSATE PLUGS FROM FREELY-MOVING ANIMALS BY FLOW-GATED CAPILLARY ELECTROPHORESIS

Figure 6-6 was produced by Neil O. Hershey

Introduction

Microdialysis sampling coupled to analytical measurements is a versatile and effective approach for monitoring neurochemicals in vivo, which is a key tool in the effort to understand brain function, diseases, and treatments.[16, 249] In order to accurately record the concentration dynamics of neurotransmitters related to behavior and external stimuli, which can occur on the order of seconds,[2, 5, 90] developing methods that offer high temporal resolution is of great importance. "Separation-based-sensing" is one such method that couples microdialysis to on-line fast capillary electrophoresis (CE),[54, 283] in which dialysate could be periodically analyzed at an interval of 2-30 s.[6, 24, 29, 61, 102, 250] Although the analysis time was short, Taylor dispersion, i.e. broadening of concentration zone that occurs between the dialysis probe and the analytical system, began to limit temporal resolution, especially when low sampling flow rate for higher sensitivity[43] or long connection tubing for awake subjects and clinical application[250] was necessary. Under such conditions, temporal resolution could be worsened to several minutes.

To avoid Taylor dispersion, segmented flow was adopted to convert continuous dialysate stream into a train of discrete aqueous sample plugs carried by an immiscible oil

phase.[252] This approach prevents cross-contamination between adjacent plugs no matter how long they are transported in the tubing. Temporal resolution is therefore only related to the probe size and membrane material, and is nearly independent of flow rate and completely independent of tubing size or length.[276] For example, up to 2 s temporal resolution could be achieved with regenerated cellulose membrane (MWCO 18 kD) with various probe sizes (see Chapter 5).[276] To analyze the content of digitized dialysate, a microchip CE device was also developed,[268] which was capable to remove carrier phase prior to EK injection onto electrophoresis channels. Under optimized conditions, naphthalene-2,3-dicarboxaldehyde tagged neuroactive amino acids (NDA-AAs) were resolved in 30 s. Segmented flow microdialysis (SF-MD) coupled to microchip CE was demonstrated in both on-line[268] and off-line[276] in vivo monitoring of neurotransmitter dynamics in anesthetized[268, 276] or freely-moving rats (see Chapter 5).

Analyzing dialysate plugs by microchip CE, although proved effective in conserving second range temporal resolution, still has some practical obstacles for its widespread usage by other researchers First, the fabrication of the microchip CE device requires cleanroom facilities and trained personnel with good microfabrication skills, which might not be accessible for many laboratories. Second, CE performances on a microfluidic device is generally inferior to capillary based system in several aspects, such as continuous operation time, separation speed, separation efficiency, limit of detection (LOD), etc. For example, our CE chip mounted on a confocal microscope for LIF detection[268] could resolve NDA-AAs including glutamate, aspartate, γ-aminobutyric acid (GABA), taurine, glycine and serine in 30 s at a maximum electric field of 1.1 kV/cm with an LOD of 80-100 nM (see Chapter 5). On the other hand, a capillary based CE

system in our lab using flow-gated injection interface[70] and sheath flow cuvette for LIF detection[64] has been demonstrated to resolve *o*-phthaldialdehyde (OPA) tagged AAs in only 14 s at 2.1 kV/cm electric field with an LOD of 10-40 nM.[24, 90] The capillary system has also been shown to continuously operate throughout the day for on-line monitoring of neurotransmitter dynamics during animal behavior studies.[90] Therefore, it is desirable that SF-MD can be coupled to such capillary based CE system, so that we can still take advantage of the robust performance and easy accessibility of the capillary system while acquiring better temporal resolution by using SF-MD.

In this chapter, we have introduced a simple, cleanroom-free interface that is used to couple SF-MD to flow-gated capillary electrophoresis (FG-CE). In this T-shaped polydimethylsiloxane interface (PDMS-T), carrier phase and aqueous sample in the incoming segmented flow stream would select different flow pathways based on their contact angle on different surface of outlet tubing. Dialysate plugs were therefore re-combined into continuous stream without losing temporal information obtained at the sampling stage. Conditions for successful phase separation using PDMS-T and conditions for reproducible FG injections were explored and described. At 0.3-1 μL/min sampling flow rate, 14 s temporal resolution could be obtained with the system for routine pharmacological studies.. This method was applied to the on-line monitoring of neurotransmitter dynamics from the striatum of freely-moving rats during both long term and short puffs of K^+ stimulations, which revealed a different releasing mechanism of taurine.

Experimental Section

Chemicals

All chemicals were purchased from Sigma-Aldrich (St. Louis, MO) except the salts for artificial cerebral spinal fluid (aCSF) were from Fisher Scientific (Chicago, IL) and NDA was from Invitrogen (Eugene, OR). All aqueous solutions were prepared with water purified and deionized to18 MΩ resistivity using a Series 1090 E-pure system (Barnstead Thermolyne Cooperation, Dubuque, IA). Amino acid standards were dissolved in aCSF (145 mM NaCl, 2.68 mM KCl, 1.01 mM $MgSO_4$, 1.22 mM $CaCl_2$, 1.55 mM Na_2HPO_4, 0.45 Mm NaH_2PO_4, pH 7.4).

Microdialysis Probes

Side-by-side microdialysis probes with 18 kDa molecular weight cut-off membranes made from regenerated cellulose hollow-fibers were made in-house as described elsewhere.[45] Probes had 200 μm diameter, 2 or 3 mm sampling length and 40 μm i.d. x 100 μm outer diameter (o.d.) fused silica capillaries for inlet and outlet tubing.

Headpiece for Freely-Moving Animals

Details of the fabrication procedure and dimensions of the PDMS based dialysis/plug headpiece can be found in previous reports (refer to Chapter 5).[276] A slightly modified design with only one inlet channel for derivatization reagent was used in the current experiment for the delivery of pre-mixed solution of 10 mM OPA and 40 mM β-mercaptoethanol (BME) (in 40 mM borate buffer, pH 10.5).

PDMS-T Interface for Coupling Segmented Flow to FG-CE

The PDMS-T interface as illustrated in Figure 6-1 (A) was fabricated by pouring PDMS pre-polymer onto pre-assembled capillary tubing scaffold. A piece of ~ 3 cm 360 μm o.d. fused silica capillary was placed in a glass petri-dish with clean inner surface. Another piece of ~3 cm 185 μm o.d. capillary sheathed with ~ 2 cm 200 x 360 μm capillary in the middle was placed vertically relative to the previous 360 μm o.d. capillary to form a T-shaped scaffold. Both pieces were taped in place onto the petri-dish. 10:1 ratio of PDMS prepolymer (RTV 615, MG Chemicals, Surrey, B.C., Canada) was poured onto the tubing mode and cured at 170 ^{o}C for 10 min. The whole piece of PDMS with the tubing scaffold was then carefully flipped over. Another layer of PDMS pre-polymer was poured and cured in the same manner. A ~1 x 1 cm squire piece around the T-junction was then carefully cut out of the bulk PDMS slab with a scalpel. Capillaries was also pulled out from the T network during this process.

After obtaining the PDMS square with T shaped network, a piece of 4.5 cm 50 x 185 μm capillary (100 x 200 μm capillary when PDMS T was operated without being connected to the flow gate) was inserted into the vertical channel (Figure 6-1 (A)) till the T junction, used as aqueous sample outlet (or extraction capillary). A piece of 12 cm (or adjusted as needed) 150 x 360 μm HPFA capillary (Upchurch Scientific, Oak Harbor, WA) was inserted into one end of the horizontal channel as the carrier phase outlet. HPFA capillary of the same size for transportation of dialysate plugs was inserted into the other end. A square area of PDMS channel surface was left at the intersection of the three tubing, as shown in the picture of the T junction area after tubing assembly in Figure 6-1 (A).

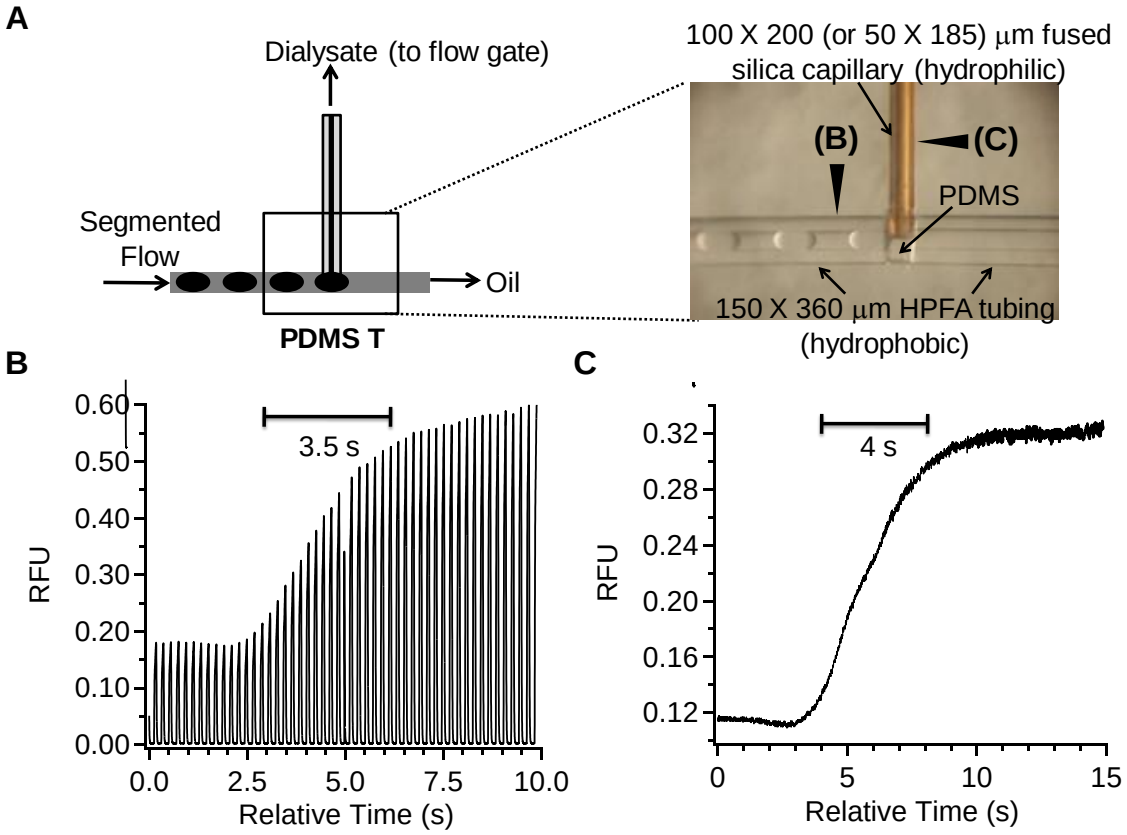

Figure 6-1. Layout and characterization of the PDMS-T interface. (A) Illustration and picture of the PDMS-T interface with assembled fused silica and HPFA capillary outlets. A train of plugs were coming in through HPFA tubing from the left. (B) LIF signal of individual plugs recorded in point (B) in (A). (C) LIF signal of de-segmented continuous sample recorded in point (C) in (A). Distance between point (C) and fused silica capillary inlet was around 2 cm. Sampling flow rate was 1 μL/min with a 2 mm microdialysis probe. Samples are standard mixture of amino acid solutions of 10 or 50 μM.

Test of Temporal Resolution after Desegmentation

At a fixed sampling flow rate (e.g. 1 μL/min in the example shown in Figure 6-1), LIF detection was made on both HPFA tubing with segmented flow (point (B) in Figure 6-1 (A)) and on extraction capillary right after phase separation (point (C) in Figure 6-1

(A)) to record signal change when a concentration change of amino acid standards from 10 μM to 50 μM was made at the surface of a 2 mm probe. Flow rate of OPA/BME solution was kept the same as the sampling flow rate and the water fraction of segmented flow was 0.29.

Electrophoresis Conditions

Figure 6-2 is an illustration of SF-MD from freely-moving rats coupled to on-line FG-CE. The FG-CE system with LIF detection was the same as the one used in the previous report.[24] The outlet of the extraction capillary from PDMS-T was aligned with inlet of the CE separation capillary in a Plexiglas block, leaving a gap of approximately 30 μm. A 0.3 mL/min cross-flow of separation buffer (40 mM sodium borate, 0.9 mM hydroproxyl-β-cyclodextrin (HP-β-CD), pH 10.5) was applied between the capillaries using a syringe pump (Harvard Apparatus, Holliston, MA, USA), which carries the sample solution to waste. To inject a plug of sample, the separation voltage was reduced to zero (0.5 s) and then the crossflow was stopped using a solenoid valve (Cole Palmer, Vernon Hills, IL, USA) allowing the sample to cross the gap between capillaries (0.5 s). The voltage was then raised to 2 kV for 200 ms to inject a plug of dialysate onto the separation capillary. After injection, the gating cross-flow was resumed and the separation voltage was ramped to 20 kV over 500 ms. The flow-gate was held at ground to isolate the animal from the voltage dropped across the separation capillary. The solenoid and voltage supply were controlled by software written in-house using Lab-View 5.0 (National Instruments, Austin, TX, USA), a DAC board (National Instruments), and a PC (Dell Computer Corporation, Austin, TX, USA).

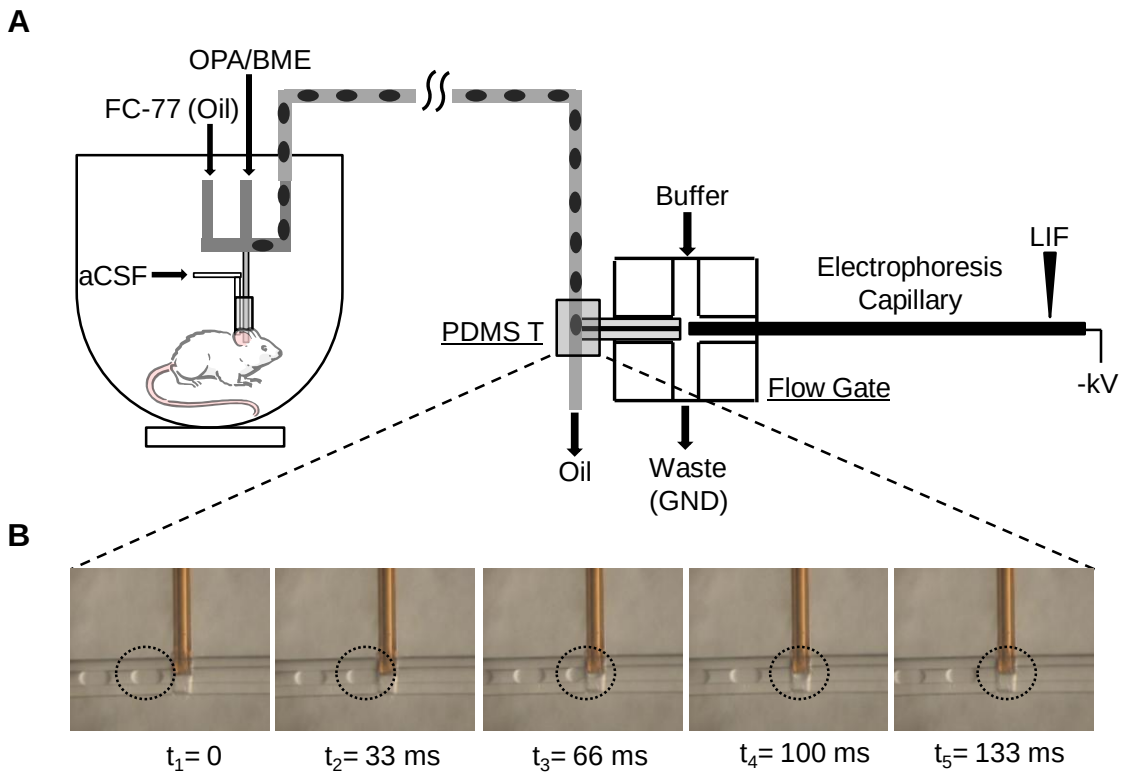

Figure 6-2. Overall scheme of system step-up. (A) Segmented flow microdialysis sampling from freely moving rats followed by flow-gated capillary electrophoresis using PDMS-T as the interface. (B) Series of pictures following the trajectory of a plug being extracted to the flow gate at the T interface.

CE was carried out in a 9.5 cm long, 10 μm i.d. x 150 mm o.d. fused silica capillary. The dead volume at the outlet of the separation capillary was reduced by grinding the outlet to a point using a high-speed grinder (Dremel Tool). A separation voltage of -20 kV was applied at the outlet of the separation capillary using a CZE1000R high voltage power supply (Spellman High Voltage Co., Hauppauge, NY, USA). The OPA-AAs were detected using LIF in a sheath-flow detector cell.[284] The outlet of the separation capillary was inserted into a 2 mm x 2 mm square outer diameter, 200 μm x 200 μm square inner bore quartz cuvette (Mindrum Precision, Inc., Rancho Cucamonga,

CA, USA). Sheath buffer was siphoned around the outside of the separation capillary outlet using gravity flow (15 cm height difference between buffer reservoir levels). Analytes migrated off the end of the separation capillary with a laminar flow profile and were detected in this flow using LIF. Fluorescence was excited using the 351 nm line (30 mW total UV) of an argon-ion laser (Enterprise II 622; Coherent Laser Group, Santa Clara, CA, USA) focused onto the analytes using a 1X fused silica lens (Newport Corp., Irvine, CA, USA). Emission was collected at 90^{o} using a 60 X, 0.7 N.A. long-working distance objective (Universe Kogaku (America) Inc., Oyster Bay, NY, USA), spatially filtered using an iris, passed through a 450 ± 25 nm bandpass filter (Melles Groit, Irvine, CA, USA) and collected on a photomultiplier tube (PMT, R1477; Hamamatsu, Bridgewater, NJ, USA). Current from the PMT was amplified and filtered (10 ms rise-time) using a current-amplifier Keithley Instruments, Cleveland, OH, USA) and sampled with the same software and hardware used for controlling the injections.

In Vitro Test of Injection Stability and Temporal Resolution Using SF-MD Coupled to FG-CE

In in vitro experiments, the animal represented in Figure 6-2 was replaced by amino acid standard solutions constantly stirred at 37 ^{o}C. Dialysate plugs were transported to the PDMS-T interface and extracted by 4.5 cm 50 x 180 μm capillary to the flow gate (shown in Figure 6-2 (B)). Cross buffer flow through the flow gate was kept at 1 mL/min until stable de-segmentation at the PDMS-T was established, after which normal injection conditions were applied. Sampling flow rate was varied between 0.3 to 1 μL/min while repeated injections at 11 s intervals were made. Stability of

injections was evaluated as relative standard deviation (RSD) of peak height of 2 μM glutamate under different sampling flow rate and plug frequencies.

To test the total temporal resolution of the system, amino acid standard solution at the surface of the 3 mm probe was switched between 2 and 10 μM for several times while signal responses reflected in periodic CE injections were recorded.

Surgery and In vivo Experiments

Detailed procedures for surgery and probe implantation was the same as practiced in Chapter 5. Briefly, male Sprague-Dawley rats (Harlan, Indianapolis, IN) weighing 250-350 g was used for experiments. A guide cannula (Plastics One, Inc., Roanoke, VA) was implanted anterior +1.0 mm from bregma, lateral +2.0 mm from midline, ventral -5.5 mm from dura[240] in the striatum. Animals were allowed to recover for 5–8 days before experimentation.

On the day of experiment, the dialysis/plug sampler headpiece was mounted on the rat skull by inserting the probe through the guide cannula. The animal was placed in a Ratturn (Bioanalytical Systems, Inc., West Lafayette, IN) to prevent the headpiece from being disturbed by normal movements of the animal. The system was equilibrated by perfusing aCSF at 1 μL/min flow rate through the probe for 1 h before beginning measurements. In long term K^+ stimulation, 75 mM potassium aCSF was delivered by reverse microdialysis to the brain for 10 min. In short puffs of K^+ stimulation, 200 nL of 75 mM potassium aCSF was delivered into the brain through a microinjector (4.5 cm long x 20 μm i.d. x 90 μm o.d. fused silica capillary) by applying 78 psi air pressure for 4 s using an electrically actuated solenoid (Picospritzer, General Valve, Fairfield, NJ).

Results and Discussion

Phase Separation Using PDMS-T Interface

A critical and necessary step in analyzing segmented dialysate flow by CE is to extract aqueous sample from the carrier phase before CE injection.[255, 268] This also applies to other analytical methods such as mass spectrometry, where oil would interfere with the analysis.[163, 211, 212] In all previous reports, this step was performed on a microfluidic device, [163, 211, 212, 255, 268] which either relied on external energy input,[212] or, more commonly, utilized heterogeneous surface properties and channel depths,[163, 211, 255, 268] to guide aqueous and oil phases through different flow pathways. In order to exempt this step from laborious microfabrication procedures, we considered the possibility of using capillary tubing with different surface properties to achieve the same goal. For example, fused silica capillaries with hydrophilic inner wall and HPFA capillaries with hydrophobic inner wall could be assembled to mimic selectively patterned channel surfaces in microfluidic devices. Through experimentation, a T shaped PDMS network proved to be the best configuration to put together the HPFA tubing for incoming segmented flow, hydrophilic fused silica capillary for extracting aqueous sample, and hydrophobic HPFA capillary for removing oil phase. As illustrated in Figure 6-1 (A), when the segmented flow guided by HPFA tubing approached the T-junction, which was an exposed area of bare PDMS, aqueous plugs got in touch with the inlet of a vertically placed fused silica capillary and were extracted through it due to capillary force and lower energy between water/fused silica interface. Oil phase flew forward through the HPFA tubing outlet, due to its preferential wetting of hydrophobic HPFA surface, as well as the Laplace pressure it experienced at the inlet of fused silica capillary. A series of

pictures showing the trajectory of one plug during extraction process is shown in Figure 6-2 (B).

Cautions should be taken in choosing appropriate capillary sizes and lengths in order to achieve complete phase separation with preserved temporal resolution. For the choice of fused silica capillary, its inner diameter should be large enough, and its length short enough, in order to completely extract the residing sample plug before the next one comes in, so as to prevent mixing between plugs at the junction that will harm temporal resolution. However, the extraction capillary should not be too large or too short so as not to produce enough pressure resistance to deter oil. From another perspective, though, shorter and smaller i.d. capillary is preferred to suppress Taylor dispersion of sample zone after desegmentation but before FG injection. Through practice we found that 2-3 cm 100 μm i.d. capillaries worked best for the above purpose when the end of the extraction capillary was left free in air. This was also the case when pictures were taken in Figure 6-1 (A) and 6-2 (B). However, during in vivo experiments as in Figure 6-2 (A), when the outlet of the extraction capillary was coupled to a flow gate, high speed cross-flowing buffer (e.g. 1 mL/min) generated vacuum at the outlet of the extraction capillary and produced additional force to draw fluid through it. Under such conditions, fused silica capillary with 50 μm i.d. was a better choice due to its smaller inner diameter and higher resistance to prevent oil intrusion. Considering the size of the flow gate, the shortest practical length of the extraction capillary was about 4.5 cm.

The size and length of the HPFA tubing for oil removing were tailored based on the choice of fused silica extraction capillary. In our practices, we used 150 x 360 μm HPFA tubing since it was readily available. The length of the tubing should be short

enough so that the pressure drop of oil flowing across it was less than the Laplace pressure between oil/water interface at the inlet of fused silica capillary. If the HPFA tubing was too long and generated to much flow resistance for oil, oil would intrude into sample extraction capillary. However, HPFA tubing should not be too short so that even water plugs began to flow through this outlet due to its low flow resistance, without being extracted by the fused silica capillary. When 4.5 cm 50 μm i.d. extraction capillary was used with PDMS-T coupled to the flow gate, optimal HPFA tubing length was around 12 cm (when FC-77 was used as oil phase at a flow rate of 5 μL/min). Using different oil phases or different flow rates might raise the need to alter this length, so as to keep the balance between the pressure drop and Laplace pressure. This could be done easily by inserting another piece of tubing or by cutting the currently one short with a razor blade.

After tailoring the size and length of both outlet capillaries based on the criteria and situations discussed above, stable phase separation could be established and maintained for several hours without interruption, which has been proved in animal experiments demonstrated in later parts.

Conserving Temporal Resolution after Desegmentation

We examined through experiments if this desegmentation method could function without altering temporal information. As shown in Figure 6-1, we monitored the fluorescence signal both at point (B) for segmented flow and at point (C) for continuous flow when a step change of sample concentration was made at a 2 mm microdialysis probe sampling at 1 μL/min. Temporal resolution was 3.5 s with segmented flow (Figure 6-1 (B)) and still remained as 4 s after sample extraction (Figure 6-1 (C)). Therefore, no severe band broadening was introduced by this desegmentation approach. In this test, the

distance between detection point (C) and the inlet of extraction capillary (100 μm i.d.) was around 2 cm. In animal experiment, the dispersion effect should be evaluated at 4.5 cm downstream of a 50 μm i.d. capillary. Under the sampling flow rate we used, i.e. 1 μL/min, Taylor dispersion was negligible in either situation. Of course, the effect of dispersion could become obvious when extremely slow flow rate was used. However, in implementation of SF-MD coupled to FG-CE using this interface, relative high sampling flow rate (0.3-1 μL/min) was necessary, which was explained in the next section. Therefore, no severe deterioration of temporal resolution was expected after sample extraction.

Conditions for Reproducible CE Injections

When segmented flow was coupled to FG-CE using PDMS-T interface, sample supply to the flow gate injection cross was pulsed, which was different from the continuous supply of sample at a constant flow rate using convention microdialysis sampling.[24] This phenomenon, if not carefully evaluated, could create a bias in the amount of sample being injected onto the separation column. As illustrated in Figure 6-3, under the separation mode, all incoming sample was flushed to the waste by cross flowing buffer. When the buffer flow was stopped for 0.5 s in injection mode, sample was allowed to fill the gap between the extraction capillary and the separation column, during which process two extreme conditions could occur: if a plug happened to be extracted at the time, named as “extracting” in Figure 6-3, there would be flow at the end of the extraction capillary and a large amount of sample would fill the gap; if no plug was being extracted at the time, named as “idle” in Figure 6-3, no sample would flow from

the extraction capillary or accumulate in the gap. Therefore, when a voltage was applied to electrokinetically inject fluid in the gap onto the separation column, there could be a huge difference in the actual amount of sample being loaded between "extracting" and "idle" situations, which would result in irreproducible injections.

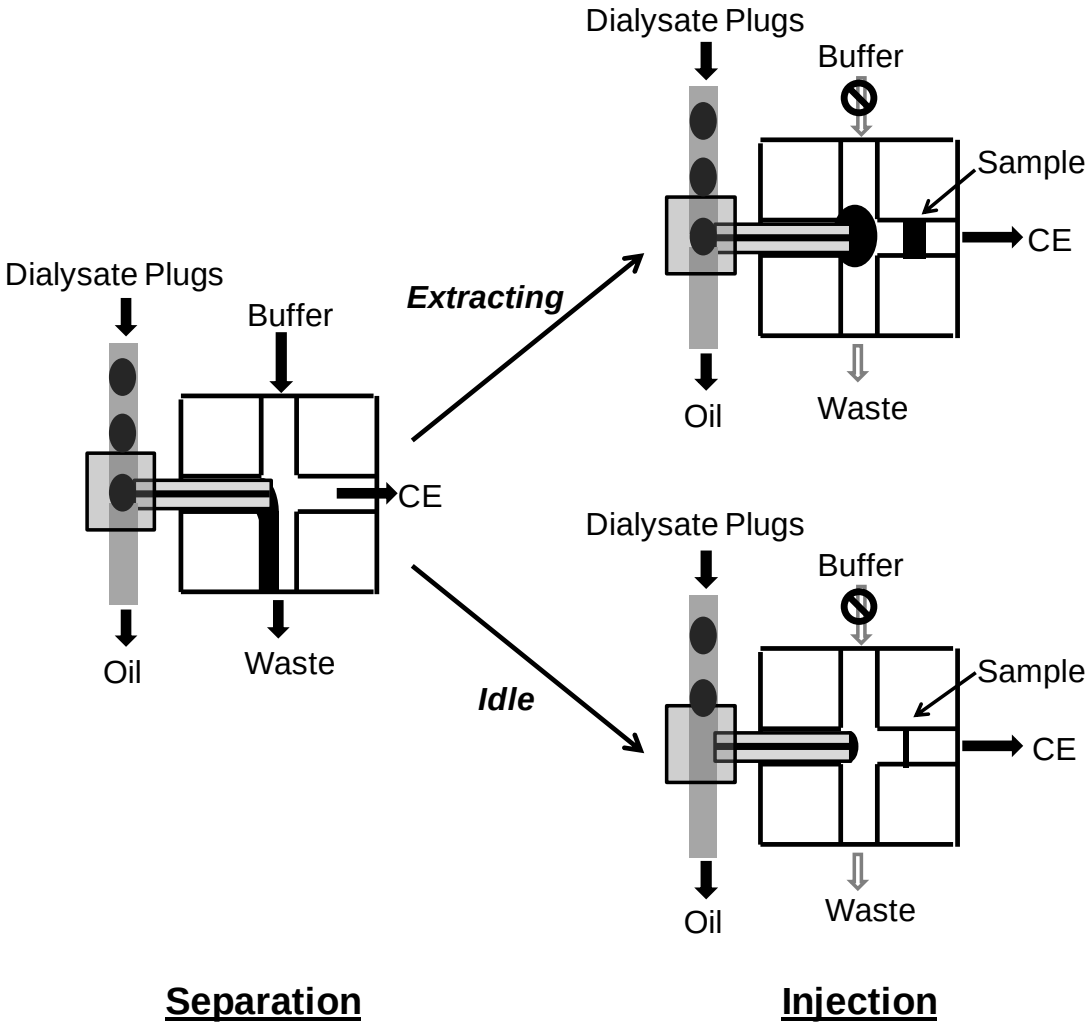

Figure 6-3. Illustration of two different situations during FG injection from segmented flow through PDMS-T interface. Detailed explanations could be found in text.

To avoid this bias, we must make sure that there was enough sample to fill the gap in the flow gate during sample accumulation time, which was 0.5 s in our case. As the approximate gap between the extraction capillary and the separation column was 30 μm, the volume of sample necessary to create a 30 μm radius sphere surrounding the inlet of the separation column was less than 0.1 nL. Since the volume of each plug was 2 nL,[276] making sure that at least one plug was extracted during the 0.5 s sample accumulation time could meet the requirements. Therefore, in theory, keeping the incoming plug frequency higher than 2 Hz was necessary to ensure reproducible CE injections.

Figure 6-4 (A) shows the values of peak height RSDs of 2 μM glutamate standard from multiple CE injections at different sampling flow rates. Plug frequency at the given flow rate was also noted in the graph. At 0.3 μL/min, when plug frequency was just above the 2 Hz threshold, peak height RSD was below 4%, which represented an acceptable reproducibility with standard solution. Using higher sampling flow rate with higher plug frequencies further lowered the RSD value. This was probably because that a larger volume of sample filling the gap during accumulation time would create a more uniform sample concentration zone at the separation column inlet, resulting in more reproducible injections. Therefore, based on the needed criterion for reproducibility, different sampling flow rates equal to or higher than 0.3 μL/min could be selected. In the following experiments, we used 1 μL/min because it produced more stable injections and had decent relative recovery with 3 mm microdialysis probes for all the targeted neuroactive amino acids to be detected in vivo.

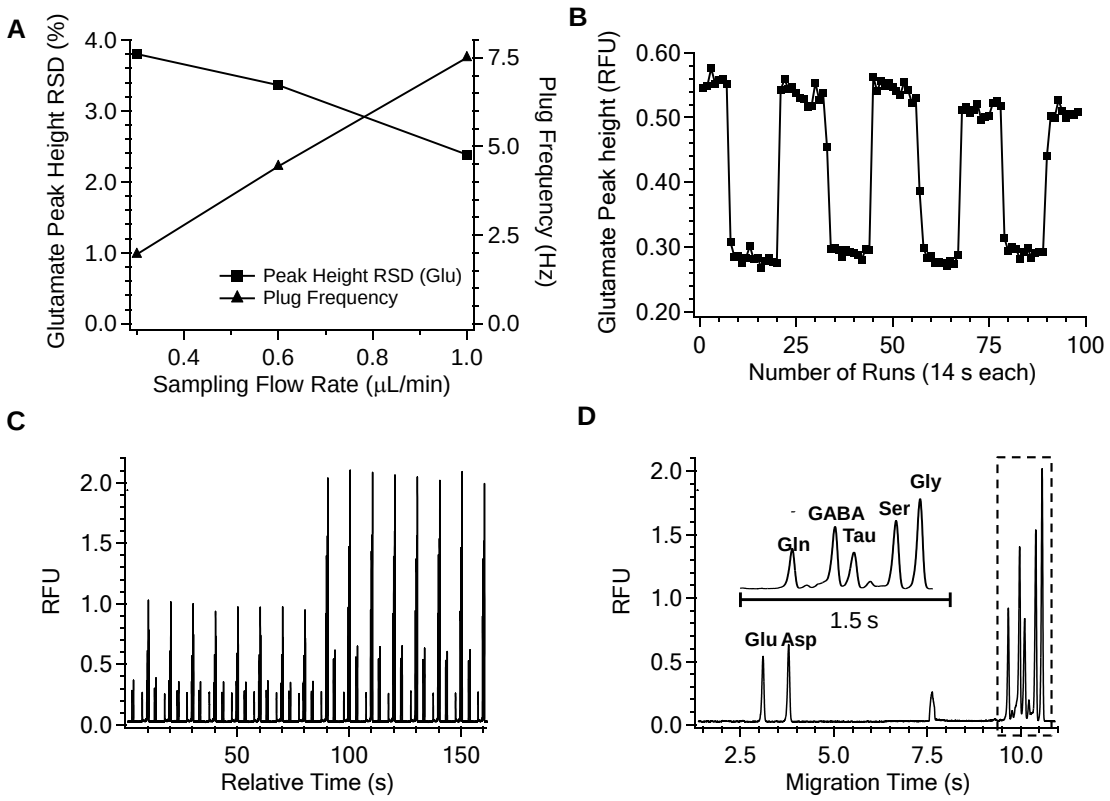

Figure 6-4. In vitro test of injection stability and system temporal resolution. (A) Dependence of injection stability of 2 μM glutamate standard on sampling flow rate and plug frequency. (B) Recorded peak height of glutamate during multiple switch between 2 and 10 μM amino acid standards at the surface of a 3 mm microdialysis probe sampling at 1 μL/min. (C) Multiple electropherograms from back-to-back injections during a concentration switch from 2 to 10 μM amino acid standard solutions at the same condition as in (B). (D) Electropherogram of 7 amino acid standards. Separation buffer was 40 mM borate with 0.9 mM HP-β-CD at pH 10.5. Electric field was 2.1 kV/cm.

Temporal Resolution of SF-MD Coupled to On-line FG-CE

The overall temporal resolution of SF-MD coupled to on-line FG-CE system was determined by two factors: the temporal resolution of SF-MD and the interval time between FG injections. From Chapter 5, temporal resolution with a 3 mm probe using SF-MD was 5.5 - 19 s at sampling flow rates of 1 - 0.3 μL/min. With current CE system,

FG injection, which lasted for 3 s, was made every 11 s. Therefore, it was expected that at 1 μL/min sampling flow rate, temporal resolution was limited by CE injection intervals and was 14 s. This was verified in Figure 6-4 (B-C). When amino acid standard solution was switched between 2 and 10 μM, step changes were generally observed in only one injection, as shown in the trace of glutamate responses in Figure 6-4 (B). Figure 6-4 (C) shows multiple electropherograms of 7 amino acids (Figure 6-4 (D)) resulted from back-to-back injections during one of such step changes. Again, the transition occurred in only one electropherogram.

When no segmented flow was included in the system, dispersion during sample transportation between the probe and the flow-gated injection interface resulted in 30 s overall temporal resolution at 1 μL/min sampling flow rate (data not shown). By simply including the PDMS-T interface to couple SF-MD into the system, we could improve temporal resolution by 2 fold without altering other operational procedures or performance parameters. Actually, we could further lower sampling flow rate (e.g. to 0.3 μL/min) for higher recovery while maintaining the same temporal resolution, as long as the temporal resolution at the sampling stage was higher than the 14 s interval time between CE injections.

Comparison of Neurotransmitter Dynamics between Long Term and Short Puffs of Potassium Stimulations in the Striatum of Freely-Moving Rats Using SF-MD Coupled to On-line FG-CE

The validity of the methods discussed above for in vivo chemical monitoring was examined by applying potassium stimulations to the striatum of freely-moving rats and

recording the responses of multiple neuroactive amino acids in real time. 3 mm microdialysis probe operated at 1 μL/min sampling flow rate was used. In vivo electropherograms at basal and elevated level during K^+ stimulation are shown in Figure 6-5. In long term potassium stimulation, 75 mM K^+ aCSF was delivered by reverse microdialysis for 10 min. An example of responses of glutamate (A), aspartate (B), GABA (C), taurine (D), glycine (E) and serine (F) during one set of such stimulation is shown in Figure 6-6. As generally observed, glutamate, aspartate and GABA were obviously elevated immediately upon K^+ infusion. For taurine, percentage of increase was also high (signal exceeded dynamic range of the detector at the peak) but the response was considerably delayed relative to the onset of stimulation. Glycine was only slightly increased during K^+ stimulation while no response in serine level was observed. These results were similar to other reports for K^+ application by reverse microdialysis.[43, 275]

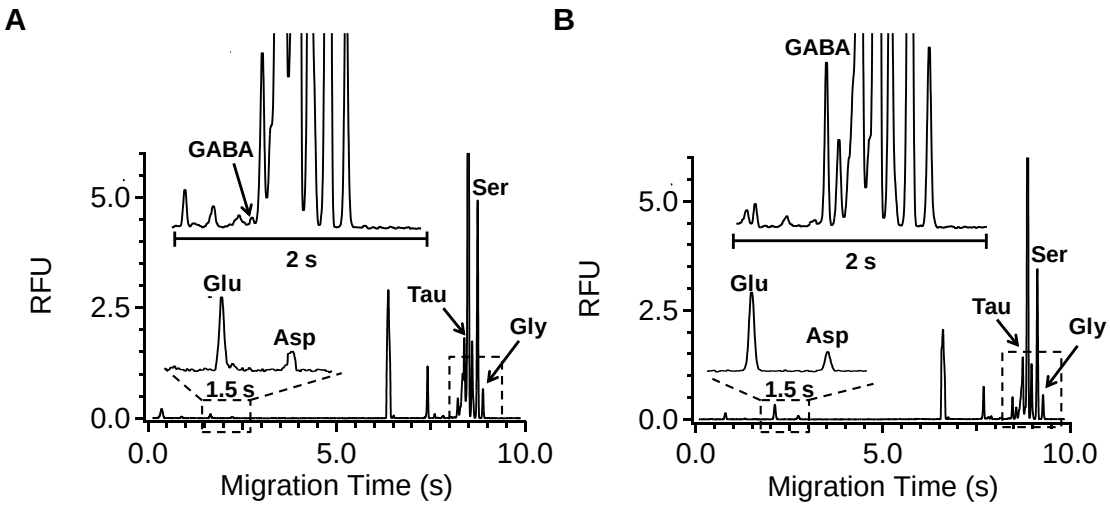

Figure 6-5. In vivo electropherograms collected from the striatum of freely moving rats. (A) basal level; (B) elevated level during K^+ stimulation. Insets show enlarged

electropherograms in the dotted box. Sampling flow rate was 1 μL/min with 3 mm microdialysis probe. Separation conditions were the same as in Figure 6-4.

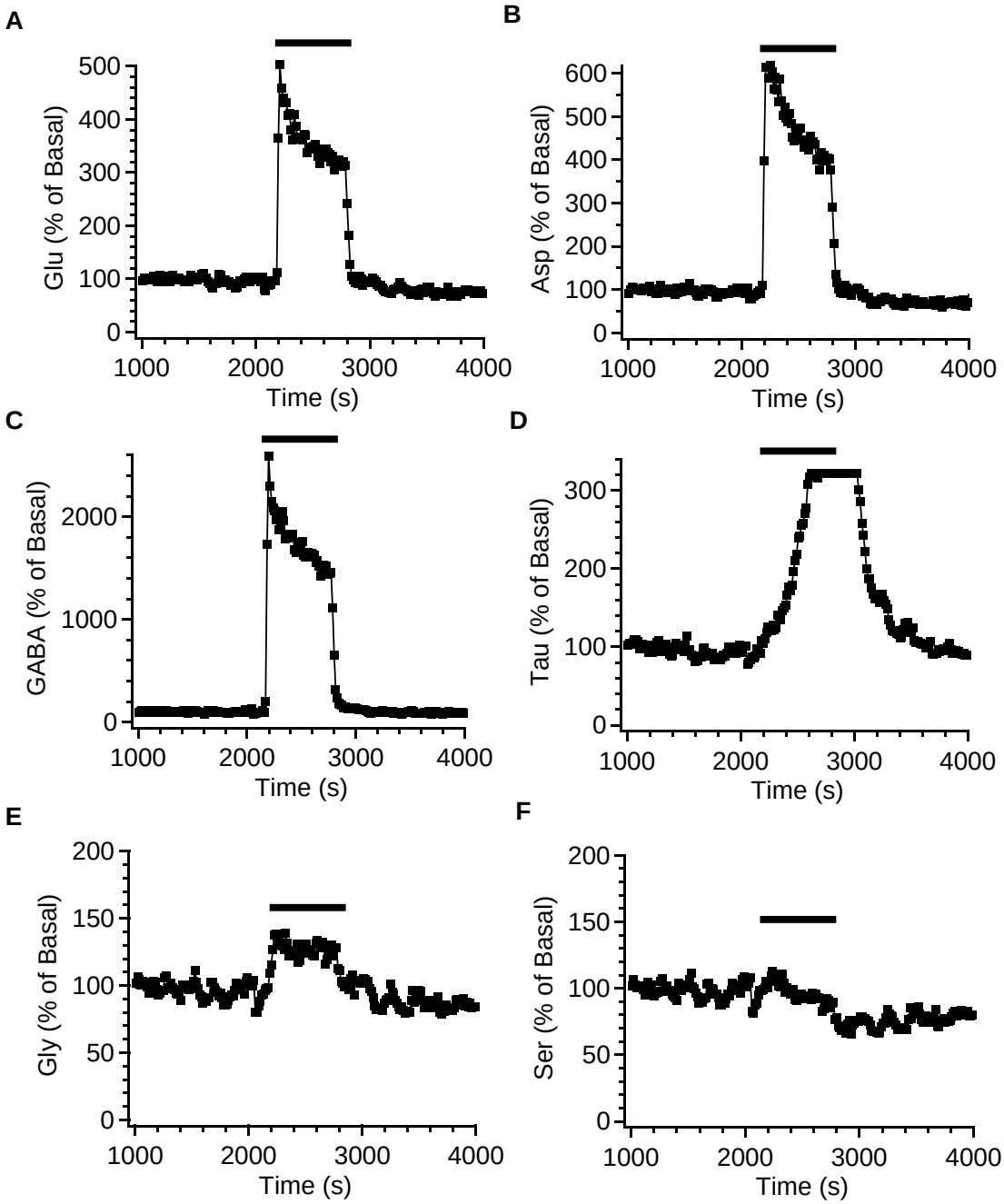

Figure 6-6. Long term potassium stimulation. An example showing the effect of delivering 75 mM potassium aCSF through microdialysis probe for 10 min on the

responses of glutamate (A), aspartate (B), GABA (C), taurine (D), glycine (E), and serine (F). Data are expressed as percentage of basal level. Black bars indicate the time period of potassium delivery by reverse microdialysis.

Short puffs of potassium stimulations were applied by microinjecting 200 nL of 75 mM K^+ aCSF to the striatum for multiple times, with 3 min intervals between adjacent injections. Responses for the same set of neurotransmitters are shown in Figure 6-7. Due to improved temporal resolution using SF-MD method, each injection induced rapid spikes of responses in glutamate, aspartate and GABA within only 1-2 CE injections, corresponding to 28-42 seconds. Interestingly, with short puffs of potassium, no increase in taurine level was detected. Instead, together with glycine and serine, a slight decrease in taurine level was recorded at the time of injection. This lack of response in taurine during short puffs of potassium injections in agreement with our previous reports (see Chapter 5).[276] More work is underway to reveal the reason and mechanism behind this phenomenon.

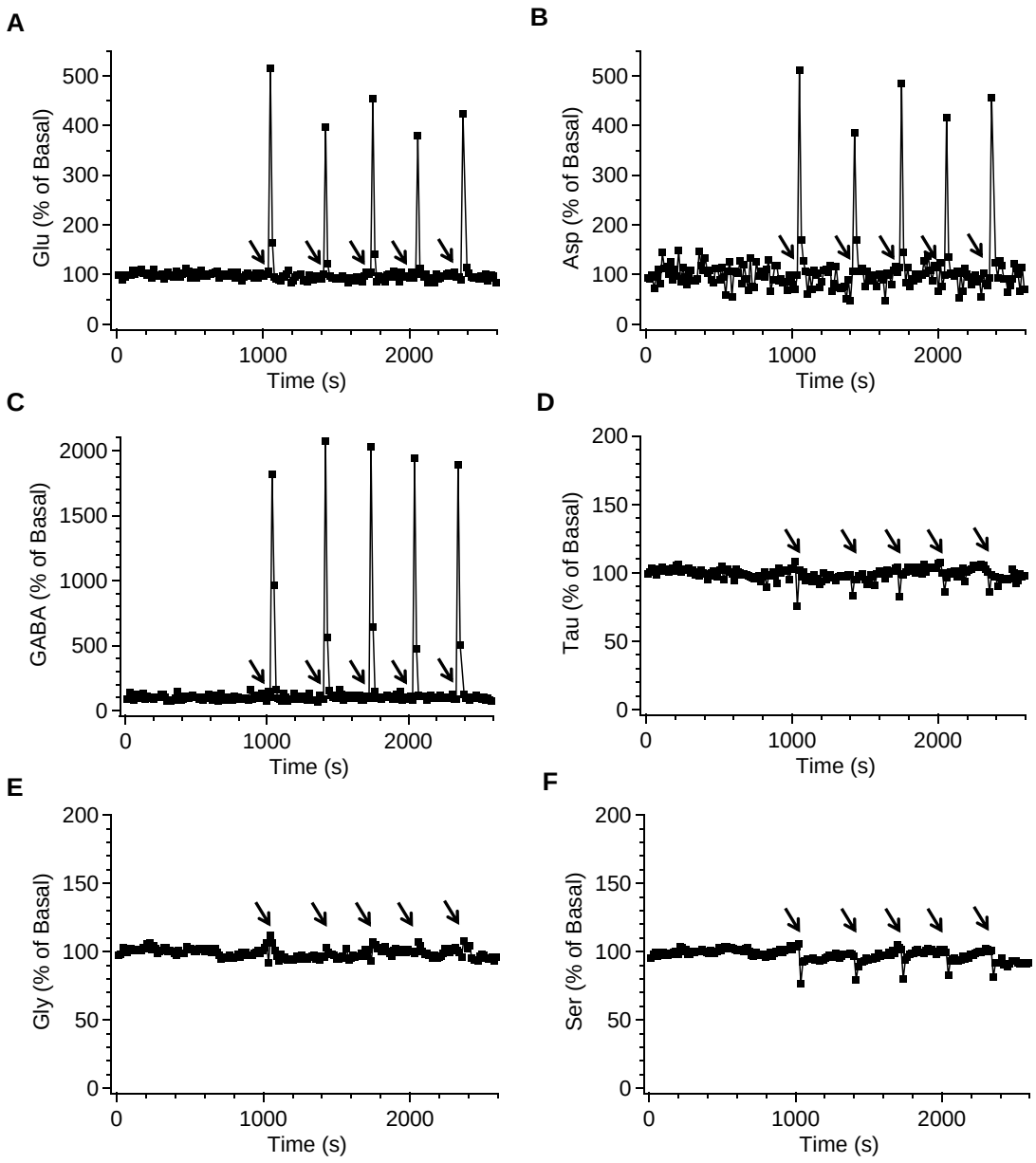

Figure 6-7. Short puffs of potassium stimulation. An example showing the effect of microinjecting 200 nL 75 mM potassium for multiple times on responses of glutamate (A), aspartate (B), GABA (C), taurine (D), glycine (E), and serine (F). Data are expressed as percentage of basal level. Black arrows indicate the start of microinjection. There was 3 min waiting time between adjacent injections.

Conclusion

In this chapter, we introduced the fabrication, characterization and usage of a PDMS-T interface to couple segmented flow microdialysis to capillary based electrophoresis system with flow-gated injection. This method improved temporal resolution of this "separation-based sensing" technique by 2 fold while offering the room of using lower sampling flow rate for high relative recovery. The robustness of the interface was verified in animal experiments, which proved that pharmacological and behavioral studies could be routinely performed with the method with 14 s temporal resolution. The comparison of neuroactive amino acid responses during long term and short puffs of potassium infusion provided a lively example on how high temporal resolution monitoring could facilitate new neurobiological findings.

CHAPTER 7

FUTURE DIRECTIONS

In this dissertation, the implementation of segmented flow microdialysis (SF-MD) in vivo and the analysis of fractionated dialysate by both microchip and conventional CE have been explored step by step. While the feasibility of the methods has been validated with a number of animal experiments, automation in dialysate collection/loading and elongation in the operational life of microchip CE are still desirable for carrying out long-term in vivo measurements. The segmented flow CE chip described in this dissertation can also be coupled to other in vivo sampling techniques such as low flow push-pull perfusion (LF-PPP), which offers higher spatial resolution than microdialysis. SF-MD coupled to on-line flow-gated CE (FG-CE) can be routinely applied for a variety of pharmacological and behavioral studies.

Automated Dialysate Fraction Collection

In the demonstration of off-line dialysate fraction collection, a piece of HPFA tubing was used. While HPFA or Teflon tubing was the perfect medium for storing segmented flow, the length of the tubing used in one continuous collection event is limited, as the excessive back pressure resulted from long collection tubing could cause adverse effect on microdialysis sampling. Therefore, depending on the sampling flow rate, samples collected over 2-20 min can generally be stored in one piece of collection

tubing before manual switch to another piece is necessary. To save the labor of tubing switching, fraction collection in an automated fashion is desirable. Figure 7-1 shows the proposed design of a "smart" microfluidic device with self-regulating valves for this purpose. The long serpentine channel used for dialysate plug collection is divided into several sections. Each section is accessible to a common inlet and outlet through an solenoid-controlled pneumatic valve.[105] Under a fixed sampling flow rate, these valves can be computer-programmed to open and close according to the time needed for sample plugs to fill each section. Since it is only necessary to pump sample against one section of the total length at a time, back pressure is constantly maintained below the tolerance threshold of the microdialysis membrane, while the total sample collection time is extended to the sum of the collection time in all sections.

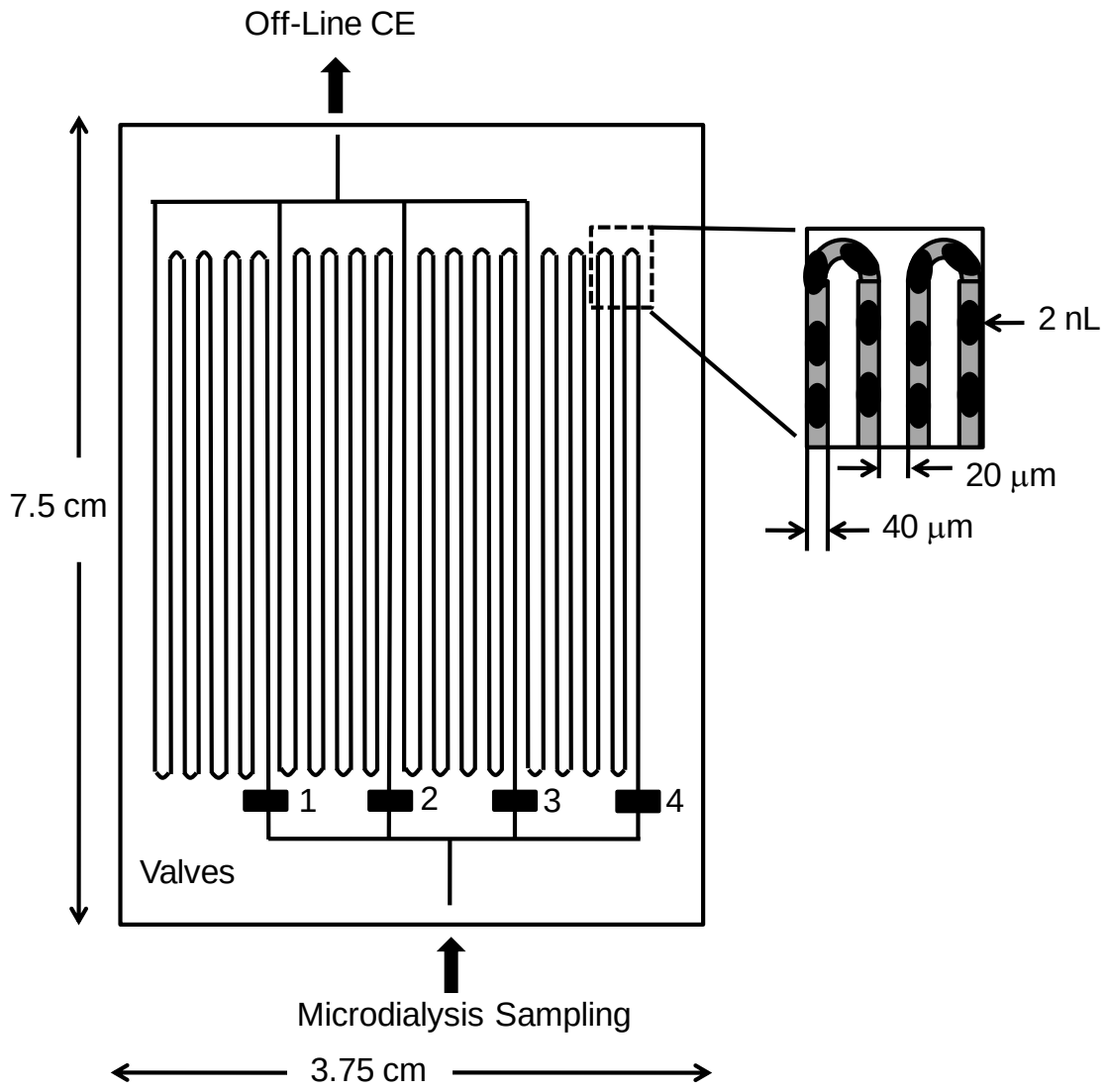

Figure 7-1. A microfluidic device for automated collection of dialysate plugs. Inset shows close-up of channel interior with plugs collected. Operation details are described in text. Channel lines are not to scale with chip dimensions for clarity.

For visualization, only 4 sections are shown in the drawing in Figure 7-1. However the density on the actual device could be much higher. These chips should be able to hold sufficient fractions for long experiments on single animals or a series of samples from different individuals. For example, if each channel is 40 μm wide and 40

μm deep, then a channel (7.5 cm long) can accommodate 16 nL/cm. From data in Chapter 4, a sample plug is 2 nL and there is 5 nL oil gap between plugs, which means that the chip could hold ~2 sample/cm. If the chip is 3.75 cm by 7.5 cm, and each channel occupies 60 μm width (40 μm for the channel and 20 μm for spacing), then the chip could contain ~625 7.5 cm long segments corresponding to 9,375 samples. From Chapter 4, we can learn that plug frequency is 1.5 Hz at 200 nL/min sampling flow rate and 0.29 water fraction. Therefore, 9,375 samples correspond to 1.7 hrs of sample collection at 200 nL/min flow rate. As noted previously, the number of sections could be increased so that 8-10 hrs of sample collection could be achieved.

If needed, sample fractions could be stored according to the principles discussed in Chapter 5. However, further investigation of freezing and thawing procedures might be needed, since a different storing material (PDMS) is used. For the analysis of stored fractions, the same computer-controlled approach could be taken to automate the sample loading process from this device onto segmented flow CE chip or other analytical systems.

Long-term Operation of Microchip CE

A drawback of microchip CE is its relatively short operation time (typically < 2hr). This comes from various reasons such as buffer evaporation, change of buffer ionic strength, or siphoning effect due to uneven buffer levels in reservoirs.[285] To extend the operation life of microchip CE, our group previously reported a chip design that can continuously supply fresh buffer and remove waste to maintain a constant buffer composition and level in multiple reservoirs for stable CE operation over 24 hrs.[286] In the

same manner, such design could be integrated into the segmented flow CE chip described in Chapter 3 to extend the time of continuous analysis of sample fractions off-line (Figure 7-2). This improvement can be combined with the self-loading fraction-collection chip described in the previous section, so that a huge amount of human labor will be saved in sample analysis. It is envisioned that the overall throughput of off-line in vivo monitoring can be greatly improved by carrying out sampling during the day and analysis over night. In such automated and high-throughput manner, off-line pumping flow rate can be further slowed down (see Chapter 4 and 5) to allow for second to second measurement of neurochemical dynamics in response to behavioral changes and drug administrations.

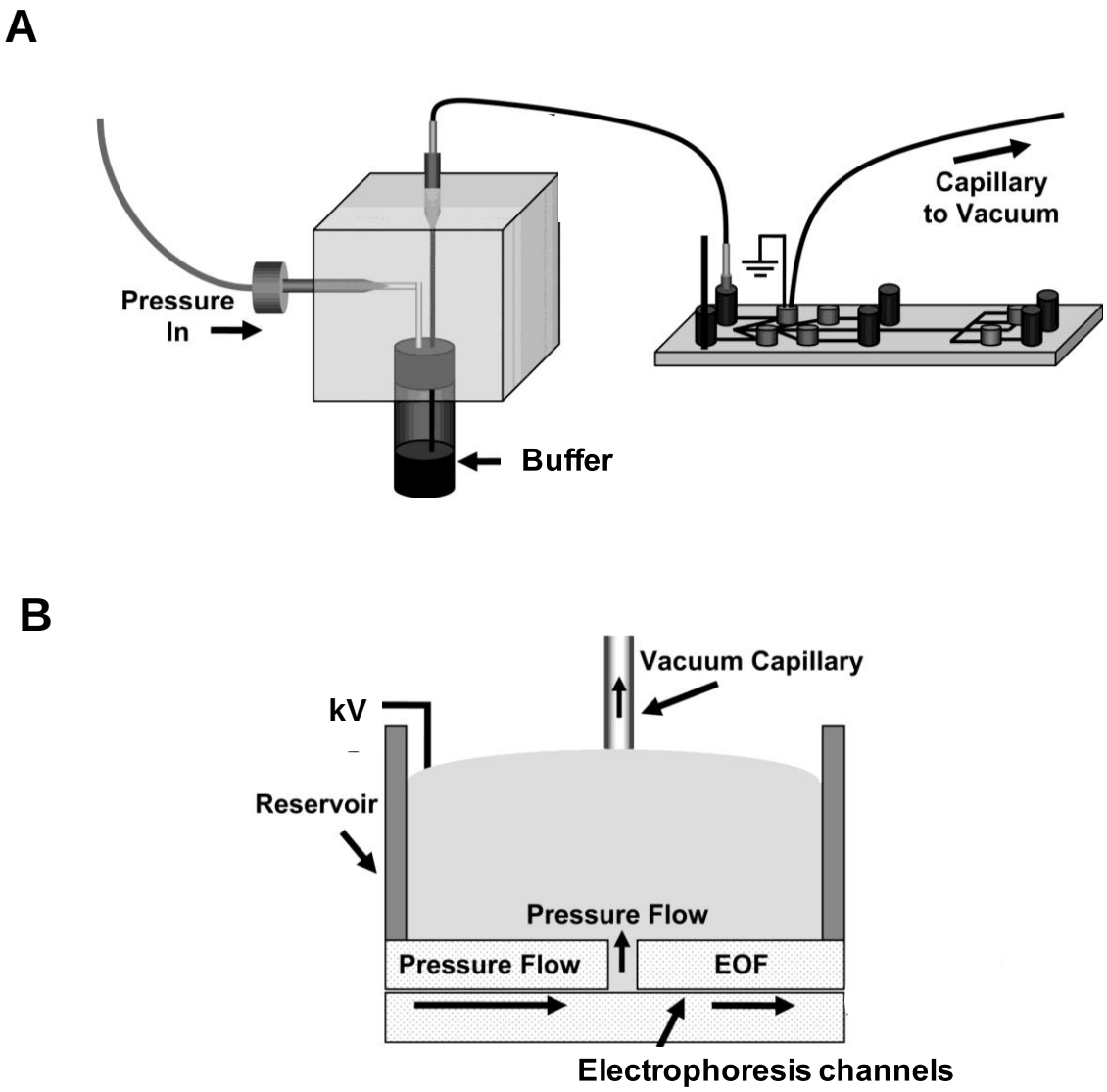

Figure 7-2. Microfluidic chip for long-term electrophoresis operation. (A) Illustration of using pressure-driven fluid to continuously supply fresh buffer to chip reservoirs for CE separation. Excess solution is constantly removed by vacuum. (B) Side view of the reservoir. The combination of pressure-driven buffer supply and vacuum keeps buffer fresh and fluid level constant over a long time. Graphs are adapted from Reference 286.

Coupling Segmented Flow Microchip CE to Samples from Push-Pull Probe

Although spatial resolution could be greatly improved with miniaturized microdialysis probe (0.5 mm sampling length) described in Chapter 5, LF-PPP sampling is considered to have even higher spatial resolution because sampling only takes place at the tip of the probe.[37, 39] Together with SF-MD reported in this dissertation, our group is also working on coupling segmented flow to push-pull probes, with the off-line sample collection scheme shown in Figure 7-3 (A). Therefore, it is natural to think that segmented flow microchip CE can also be used to analyze sample plugs collected from this such sampling method.

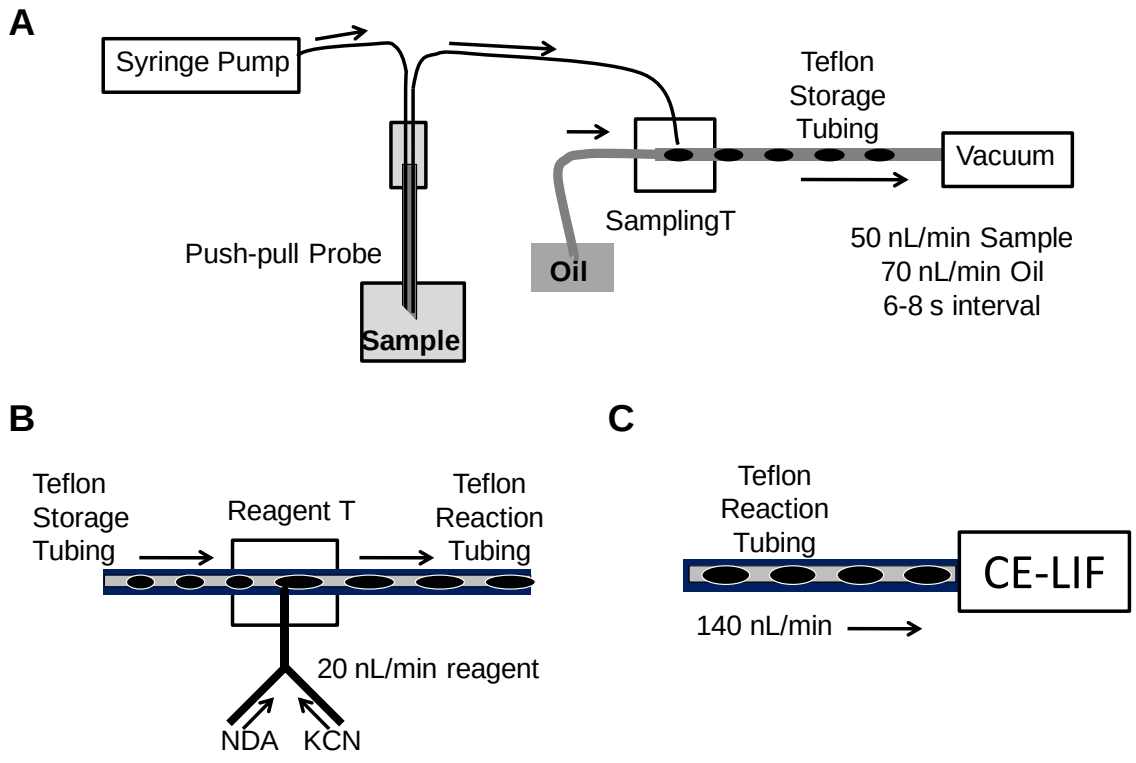

Figure 7-3. CE analysis of sample plugs collected from a push-pull probe. (A) Scheme of off-line sample plug collection from a push-pull probe. (B) Addition of derivatization reagents to sample plugs using a T interface. (C) Pumping the derivatized

samples into microchip for CE analysis. Typical operational flow rates are labeled in the graphs. Courtesy of Thomas Slaney.

A challenge with this approach, though, is the low sampling flow rate of push-pull perfusion and low frequency of resulted segmented flow. For example, in a developed method, sample fraction is collected every 6-8 second with a total segmented flow rate of ~120 nL/min. Temporal resolution with this sampling technique is 6-12 s. This means that in order to preserve such temporal resolution, every sample plug is needed to be analyzed by CE, which places stringent requirement on the speed of separation. With current CE method developed for NDA-AAs, in which a minimum of 30 s is needed to resolve all the neuroactive amino acids (Chapter 5), a trade-off between separation time and the number of resolvable analytes would have to be made. For example, Figure 7-4 (A-B) illustrate two electropherograms of AA standards recorded at different points along the separation channel, and therefore, with different separation times. A 7 s separation could only resolve glutamate and aspartate (Figure 7-4 (A)), while a 14 s sepaeration could also monitor serine and glycine (Figure 7-4 B)). After the reagent addition step demonstrated in Figure 7-3 (B), the pumping flow rate of sample plugs into CE chip (Figure 7-3 (C)) could be tuned to match the aimed separation time. For example, if the 7 s separation is chosen, pumping flow rate can be 140 nL/min, which is the flow rate after sampling and reagent addition for real-time monitoring. Under such condition, theoretically every plug is analyzed by CE. Figure 7-4 (C) shows the resulted responses observed as glutamate and aspartate peak heights in electropherograms when step changes of amino acid concentration were made at the probe during sampling. As

expected, the step changes occurred over one or two CE injections corresponding to 7-14 s, which denoted conserved temporal resolution with CE analysis. If one wants to resolve more analytes besides glutamate and aspartate, e.g. serine and glycine as in Figure 7-4 (B), the pumping flow rate would need to be slowed down to 70 nL/min, so as to permit plug-by-plug CE analysis with 14 s separations.

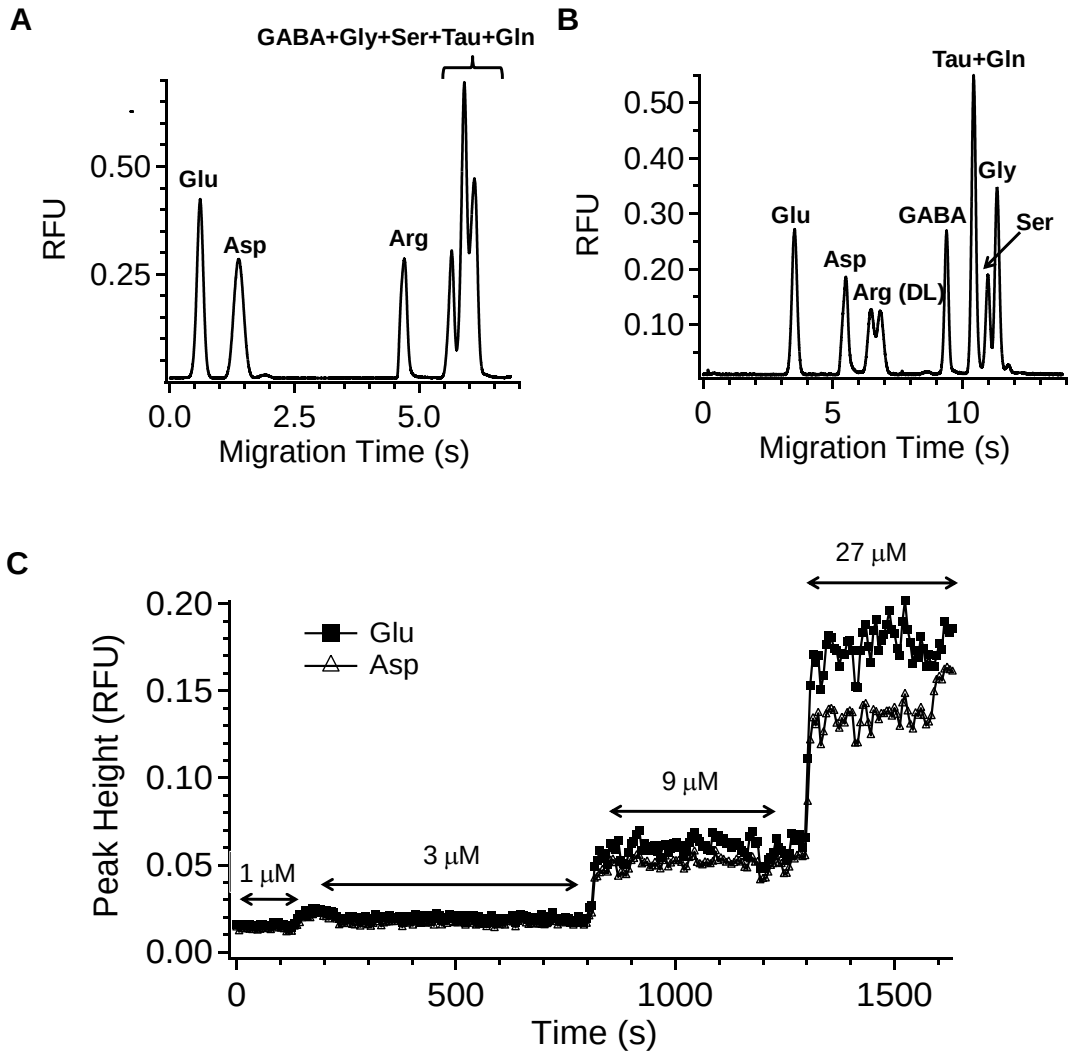

Figure 7-4. Conserving the temporal resolution of push-pull sampling with CE analysis. (A) and (B) are electropherograms of amino acid standards at 1.5 cm and 4.5 cm separation length, respectively. (C) Reponses of glutamate and aspartate when sample plugs from the push-pull probe were analyzed using 7 s separation (as in (A)) to

achieve 7-14 s overall temporal resolution. A series of step changes of solution concentration were made at the probe during sample collection. Samples were derivatized by NDA/CN and then pumped to CE chip at 140 nL/min. Each data point represents peak height of the analyte in one electropherogram. Separation buffer was 40 mM borate with 0.9 mM HP-β-CD at pH 10. Electric field was 650 V/cm and injection time was 0.08 s.

These primary data demonstrated the feasibility of monitoring push-pull perfusion samples by CE to acquire the merits of high temporal resolution, high spatial resolution and multi-analyte detection. Further improvements include achieving faster CE separation and resolving more analytes, as well as the application of this technique to animal studies.

Pharmacological and Behavioral Studies with SF-MD coupled to FG-CE

While some technical developments in microchip CE based analysis system are desirable before routine in vivo measurements, the capillary-based system that couples SF-MD from freely-moving rats with on-line FG-CE (Chapter 6) has already demonstrated its robustness for pharmacological and behavioral investigations. In fact, such system is now being used by another lab member in the group to study long-term changes in brain and behavior produced by repeated exposure to cocaine, and the role these play in the development of addiction. It is expected that the improved temporal resolution with SF-MD could offer better insight into the understanding of such behavioral problem.

APPENDIX

Sampling and Electrophoretic Analysis of Segmented Flow Streams in a Microfluidic Device

Data was produced by Gregory T. Roman

Prior to the development of the microfluidic CE chip described in Chapter 3, a microchip with an alternative design had been invented for sampling and electrophoresis of segmented flow streams. This design is inferior to the later generation in terms of separation efficiency, but offers the unique feature to carry out droplet-by-droplet analysis without desegmentation step prior to CE injection. Such approach has proven useful in drug screening by CE, as demonstrated in a later publication.[287] Therefore, the operation of the device is discussed in this appendix section. As most of the fabrication and operation procedures were the same as those detailed in Chapter 3, only differences between the two are pointed out.

Microchip Fabrication

The microfluidic devices used in this work had two depths of channel, a deeper channel for segmented flow and a shallower channel for electrophoresis, that overlapped

as shown in Figure A-1 (A). To prepare such chips, channels were made at a given depth in two different glass plates, which were then bonded together as shown in Figure A-1 (B). The result was a microfluidic network capable of generating segmenting flow and coalescing the aqueous plugs into an electrophoresis stream.

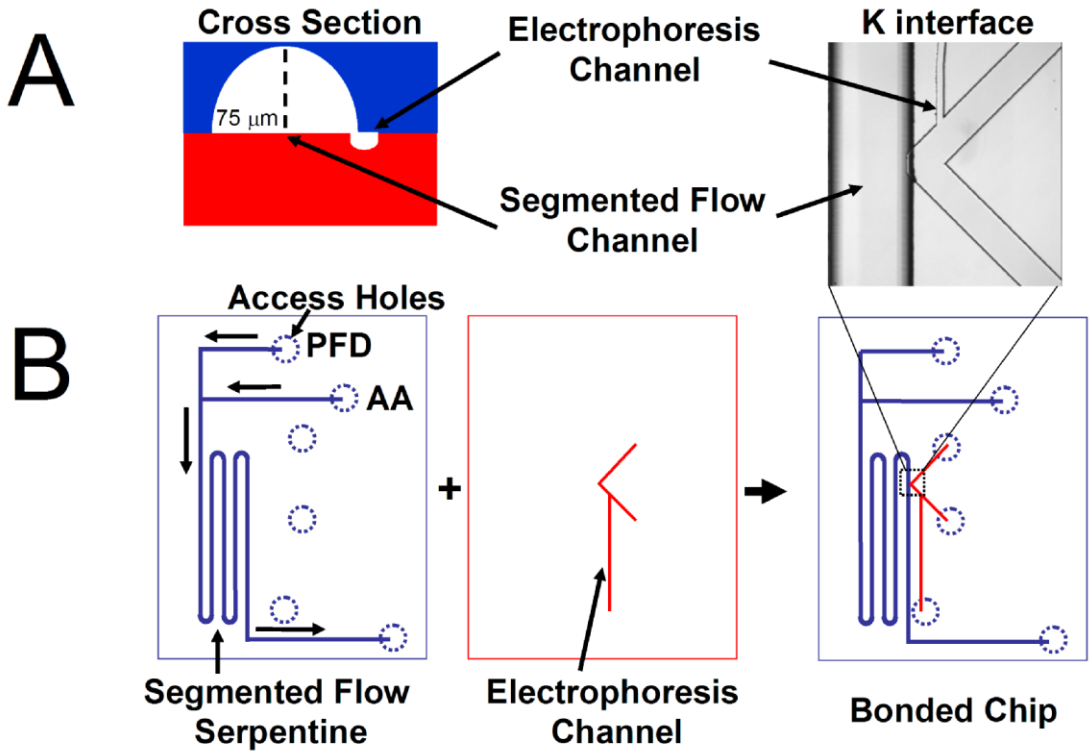

Figure A-1. Glass chip fabrication. (A) Cross section of the fabricated fluidic manifold at the K interface between the segmented flow and electrophoresis channels. The segmented flow channels are etched to 75 μm depths and 250 μm widths. The separation channels have 7.5 μm depths and 20 μm widths. (B) The fabrication scheme for the fluidic manifold. The segmented flow and electrophoresis channels are etched on separate substrates and are aligned and bonded. Perfluorodecalin (PFD) reservoir, and the amino acid (AA) reservoir are labeled. The T junction that connects these two reservoirs serves to breakup AA into plugs that are transported downstream in a continuous stream of perfluorodecalin. Arrows indicate direction of flow. After generation, these plugs are pumped into the segmented flow serpentine prior to coalescence at the K interface. Inset shows photomicrograph of the K-interface.

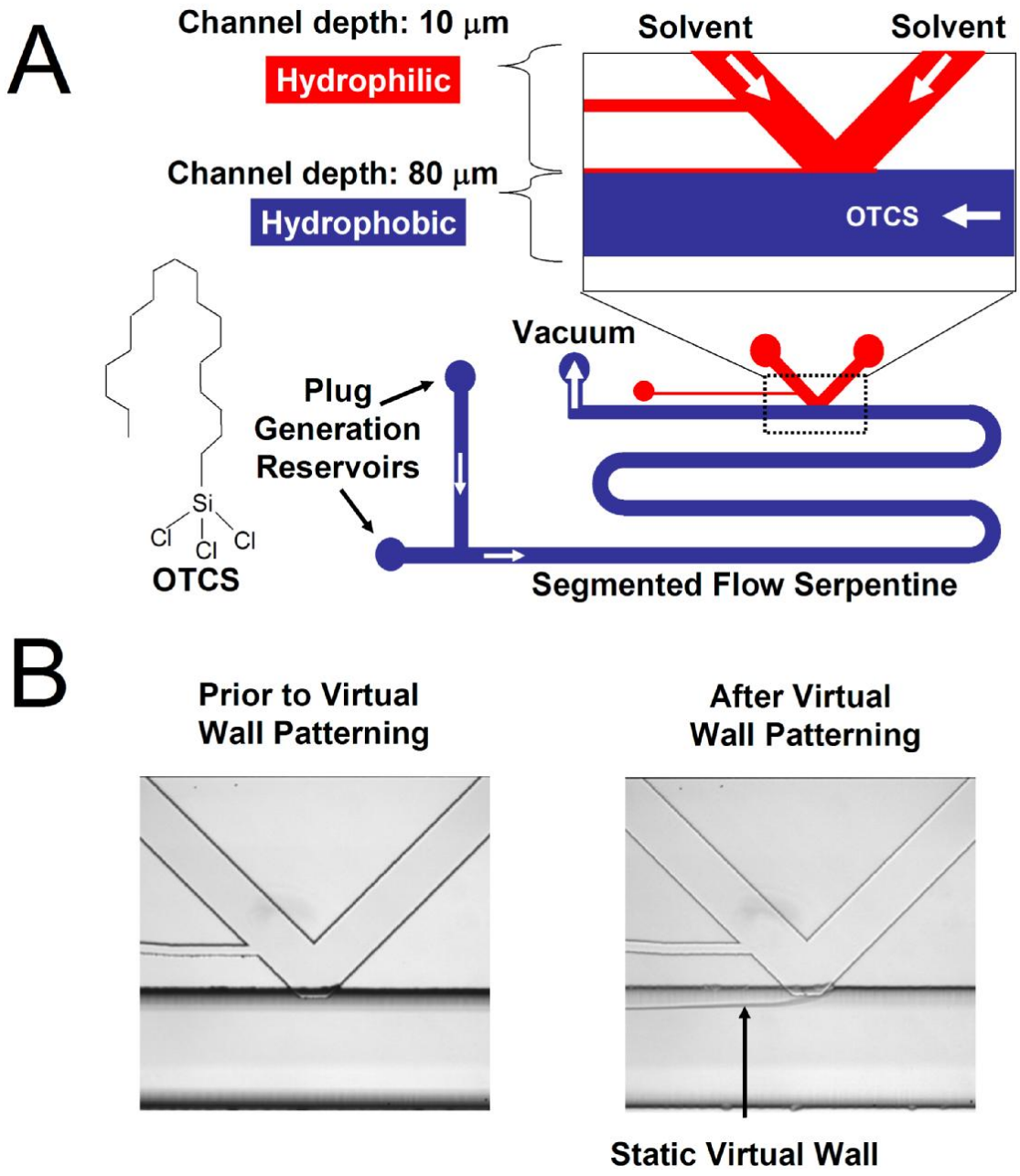

Figure A-2. Patterning of hydrophobic regions on a glass microfluidic channel using laminar flow. (A) A vacuum was applied to the common waste reservoir on the manifold to flow octadecyltrichlorosilane (OTCS) solution through the segmented flow channel. Solvent was also simultaneously pumped through the electrophoresis channels to the K interface as shown in the inset. (B) Micrographs showing virtual wall formation. Picture on left shows the K interface region filled with air. Picture on the right shows the virtual wall formed when oil and water are pumped into the interface.

Virtual Wall Fabrication

To achieve stable segmented flow, the deeper channels were selectively derivatized with octadecyltrichlorosilane (OTCS). Figure A-2 illustrates the patterning techniques and the final product.

Direct Injector

Figure A-3 (A-B) illustrates operation of direct injection. In this method an aqueous electrophoresis buffer and oil stream form a stable interface by flowing parallel to each other in the junction of a K-shaped fluidic element illustrated in Figure. A-3 (A). Electric field applied from one arm of the K to the electrophoresis channel outlet pulls electrophoresis buffer and sample into the channel by electroosmotic flow (EOF) and drives the separation. Excess buffer driven by syringe pump flows past the electrophoresis channel inlet to waste. When an aqueous plug in the segmented flow stream flows by the interface, an aliquot is transferred into the aqueous stream creating a sample zone that is carried past the separation channel inlet. As the zone passes the electrophoresis channel inlet a portion is drawn into the channel for injection with the remaining portion passing to waste. This sequence is illustrated by the fluorescence images in Figure A-3 (C). In this way, a series of samples can be injected without using relays or changing any parameters such as applied voltage. A series of sample plugs can be sampled and analyzed with 5.8% RSDs of peak area as illustrated by the sequence of traces in Figure A-3 (D). At least 800 plugs could be injected without interruption in this system.

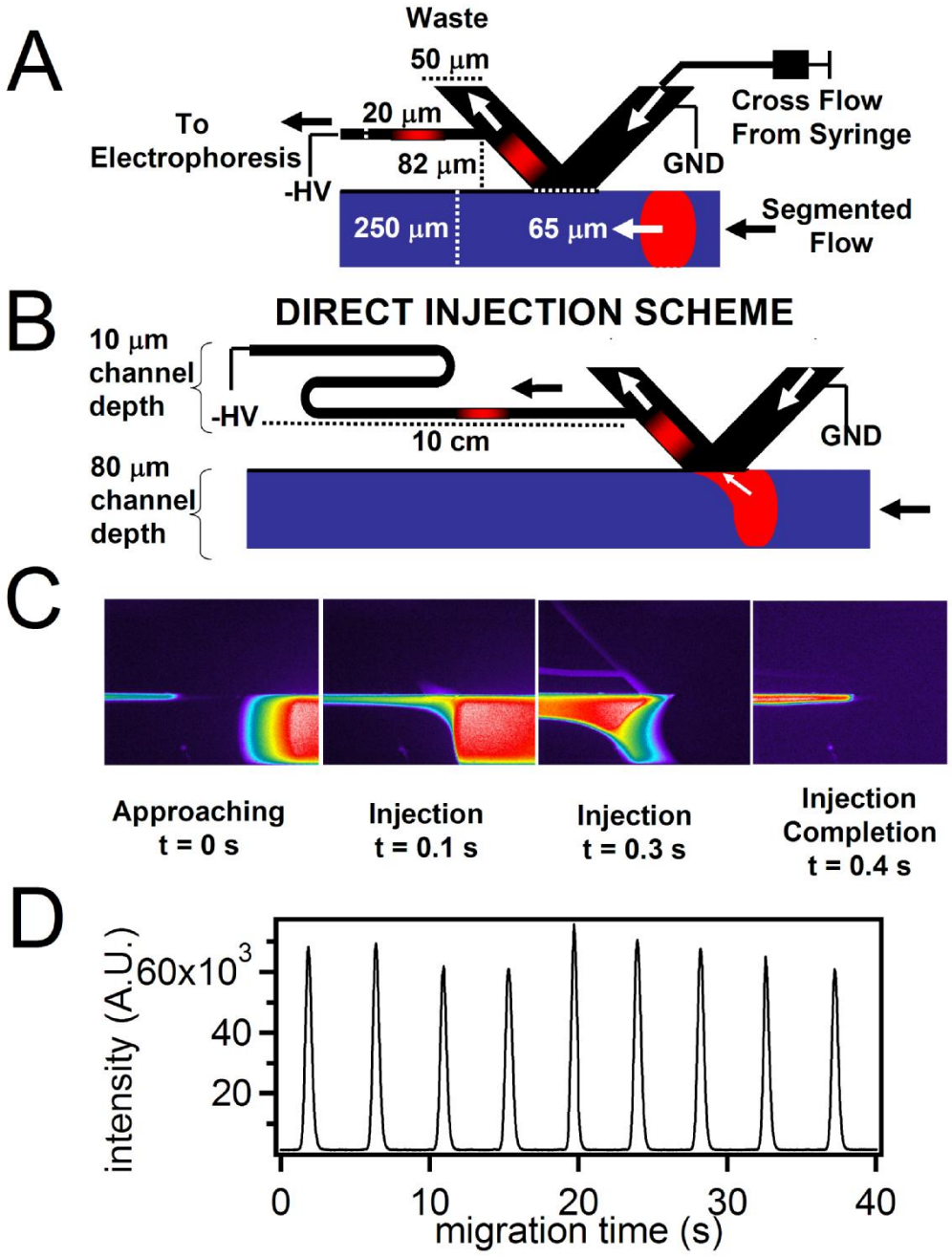

Figure A-3. Illustration of coalescence and direct injection using the K interface. (A-B) The microfluidic scheme for the direct injection scheme with a 10 cm separation channel. (C) Micrographs illustrating the coalescence of plugs using a cross flow of 100 nL/min. (D) Series electropherograms resulting from sampling and injection of plugs using the direct injector. CE separation was done on a 5 cm long separation channel at 500 V/cm with 10 mM sodium tetraborate, pH 9.0 separation buffer. The fluorescent plugs consist of 1 μM serine derivatized with FITC

Virtual Wall Formation

A key to developing reproducible injections was forming a stable virtual wall in the K-interface. Virtual walls have previously been reported with application to extraction[288-292] and membrane synthesis.[293] The stability of a virtual wall depends on several variables including the contact angle of the modified surfaces, surface tension, viscosity, and microfluidic channel depth.[236] For our work, we used differential etching to create a segmented flow channel that was ~ 8 fold deeper than the separation channel (see Figure A-1 (A)). The difference in fluidic resistance between the segmented flow channel and the separation channel reduced the movement of the non-aqueous carrier phase into the separation channel. In addition to having a differential channel height, we also patterned the surface such that the oil (perfluorodecalin) channel was made hydrophobic by covalent attachment of octadecylsilane (C18) while the aqueous channel retained a native, hydrophilic glass surface. The former was useful ensuring that perfluorodecalin wetted the walls and eliminated inter-plug chemical communication, while the latter served to retain a surface suitable for electrophoresis. The combination of both differential surface energies and channel heights yielded a stable interface between a segmented stream with flow rates from 3.5 to 5 μl/min (linear velocities of 0.29 to 0.42 cm/s) and an aqueous stream with flow rates of 40 to 220 nL/min (linear velocities of 0.03 to 0.42 cm/s). The relative flow rates of each stream at the K interface has important implications in transport of the extracted analyte past the injector as discussed below.

Direct Injector Performance

Injection volume in the direct injector is controlled by the electric field and temporal width of the plug. The temporal width of a plug is defined as the time it takes to traverse a fixed point in space and is governed by the flow velocity and plug spatial width. Thus, the injector performance is coupled to the size of sample plugs formed. To quantify how these factors affect the separation, we examined peak efficiency and area with respect to each of these variables as summarized in Figure A-4.

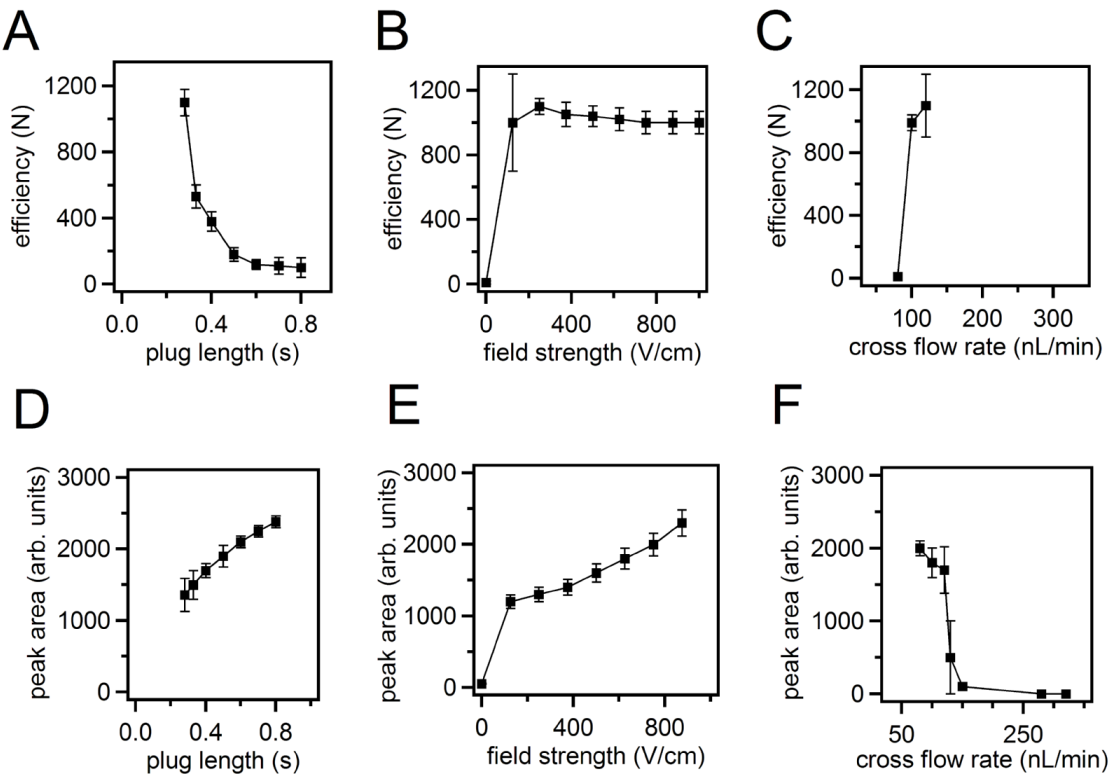

Figure A-4. Dependence of peak efficiency and area on operational parameters. (A) Effect of plug length on efficiency of peak for fluorescein dissolved in aCSF obtained using the direct injection. The flow rate for the perfluorodecalin and separation buffer was 1 µL/min and 100 nL/min, respectively, whereas the sample flow rate was varied to generate different sized plugs and ranged from 30 nL/min-500 nL/min. The plug length was calculated 500 µm from the virtual wall of the fusion interface. The electrophoresis was performed with a field strength of 1 kV/cm and a separation buffer of 10 mM sodium

tetraborate, 0.9 mM HP-β-CD at a pH of 9.7. (B-C) The relationship between the field strength and cross flow for fluorescein plugs generated using a flow rate of 1 µL/min for the PFD and 300 nL/min for the sample. Cross flow was 100 nL/min. (D-F) Peak area comparisons using the same segmentation parameters in (B-C).

Decreasing temporal plug width improved efficiency as shown in Figure A-4 (A) by decreasing injection bandwidth. Although the oil flow rate may be increased to generate even more narrow injections, this strategy is limited in at least two ways. First, faster flows decrease the interval between sample plugs and leads to overlapping electropherograms if separation time is longer than the interval time. Secondly, higher flow rates can result in unstable virtual walls. We believe that using a different method for forming plugs that allows for plugs with shorter spatial width and longer intervals would be beneficial for improving efficiency.

Efficiency of a separation is expected to increase linearly with electric field as long as Joule heating is not a factor; however, in this system we found that greater electric field strengths had relatively little effect on efficiency (Figure A-4 (B)). This is likely because even though increasing electric field improves separation efficiency, it also increases the amount injected (see Figure A-4 (E)) leading to an extra column broadening effect that negates reduced broadening in the separation channel. Fields above 600 V/cm also tended to decrease reliability of the injections due to bubble formation in the interfacial zone.

In addition to field strength and plug length, the electrophoresis buffer cross flow rate has an effect on peak area and efficiency. The cross flow serves two functions: 1) it acts to counterbalance the pressure exerted by the segmented flow stream on the virtual

wall, and 2) it washes analytes out of the coalescence interface and terminates the injection. As shown in Figure A-4 (F), as cross flow is increased above 100 nL/min (linear velocities of 0.23 cm/s) the bulk motion of the solute outstrips the electrophoretic force in the direction of the electric field and results in undetectable analyte injection. As cross flow is decreased, more analyte is injected, indicated by the increase in peak area (Figure A-4 (F)), while peak efficiency decreases (Figure A-4 (C)). The decrease of the efficiency with decreasing cross flows is a result of the longer residence time of the sample plug in the interface and longer injections. Thus, it is necessary to balance the goal of removing the analyte from the interface as soon as possible after a coalescence event, but still enabling sufficient time for electrokinetic injection into the separation channel.

To better understand the limits on separation efficiency imposed by the injector and its relationship to the band broadening in the separation channel, we examined peak variance along the channel length (Figure. A-5).[239] For this experiment, sample plugs of 1 μM fluorescein were generated at 1 Hz and coalesced with a cross flow of 100 nL/min and separated at a field strength of 250 V/cm. The linear trend with a slope of 4.1×10^{-6} cm^2/s, which is comparable to the diffusion coefficient of fluorescein,[239] suggests diffusion is the dominant source of band broadening during transport down the column. The large y-intercept of 0.001129 cm^2 indicates that extra-column effects contribute 96.5% of the total band width over a 10 cm separation length. In view of the narrow detection window and strong effects of injector conditions on the efficiency, we conclude that the injector contributes this large effect and limits efficiency.

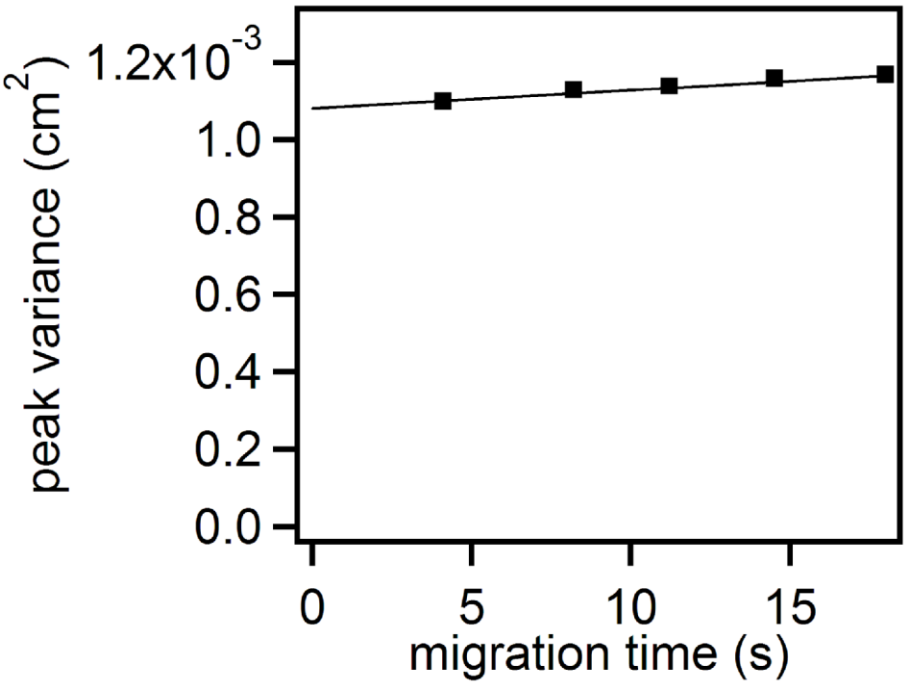

Figure A-5. Effect of migration through a 10 cm channel on peak variance. Measurements of peak variance were recorded at 0.2, 0.4, 0.6, 0.8 and 1 cm corresponding to the migration times shown. Field strength applied across the separation channel was 250 V/cm with a plug frequency of 1.5 Hz and a separation buffer of 10 mM sodium borate, 0.9 mM HP-β–CD at a pH of 10.0. Sample plug volumes were approximately 15 nL.

Based on broadening in the channel, we should be able to generate ~300,000 plates over the 10 cm separation distance at an applied electric field of 550 V/cm if the injection band width was infinitely narrow. Several improvements in this design are possible and may yield performance closer to this theoretical maximum. Methods of forming plugs that allow longer intervals with smaller plug sizes will aid efficiency by decreasing the plug width. Also, a method of manipulating voltage changes when sample is present at the interface would allow better control over the injection. In this way, lower voltage could be used to avoid over injection. Furthermore, if voltage could only

be applied when the center, most concentrated, portion of the analyte zone was passing in front of the electrophoresis channel a higher efficiency injection could be performed with less effect on sensitivity. The trade-off between peak height and efficiency could also be decreased with methods of preconcentration from sample plugs because only a small fraction of the plug is injected.

Although the peak separation efficiency is low compared to conventional EK gated injection coupled to microchip CE,[86] it is at least an order of magnitude greater than previously published plug electrophoresis[215, 229] and is compatible with a continuous stream of plugs. To illustrate separations capability, the direct injection technique was used to sample from a segmented flow stream with samples containing fluorescently-labeled amino acids. Figure A-6 demonstrate back to back coalescence, injection and separations of plugs containing 1 μM GABA, serine, and glutamic acid. These separations were performed at both 2.5 and 7.5 cm separation lengths, with plug intervals of 7 s and 12 s, respectively. These electropherograms illustrate the resolving capability of this separation technique. We envision this system to be applicable to analysis of cartridges of samples for applications requiring high-throughput.

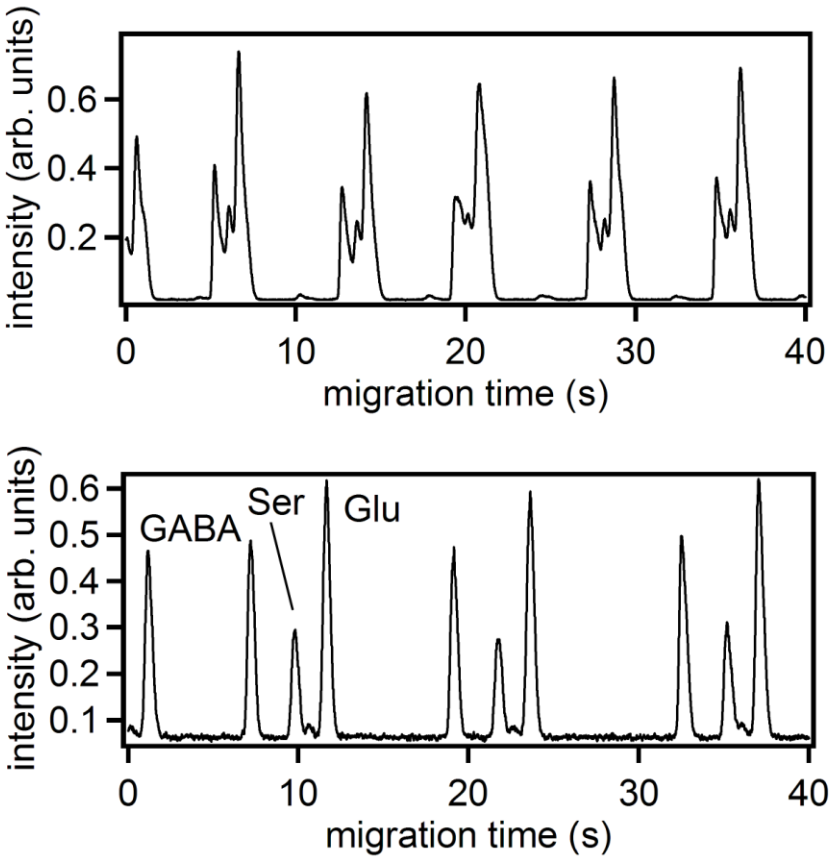

Figure A-6. : Serial plug coalescence, injection, and electrophoresis using the direct injector. NDA derivatized amines in 17 nL plugs, injected at 7 second intervals and separated at 2.5 cm (top) and injected at 12 s intervals and separated at 7.5 cm (bottom). The separation buffer was 10 mM sodium tetraborate, 0.9 mM HP-β-CD at a pH of 9.7 and the field strength of 550 V/cm.

Desegmentation Injector

The indirect injection method uses the same K-interface used for the direct injector, but cross flow velocity is reduced relative to oil flow velocity. In this way, new aqueous plugs are brought to the interface before the previous plug is washed out resulting in a continuous, secondary aqueous stream forming from the sample plugs in the sampling channel (See Figure. A-7 (A)). This secondary analyte stream is directed to a

cross-style injector.[104] A sequence of images illustrating coalescence and transfer to cross injector is shown in Figure A-7 (A). With this approach, reliable and stable injections can be achieved as illustrated in Figure A-7 (B). Using this system, it was possible to coalescence over 10,000 plugs at the K interface and make over 1,000 serial EK injections without interruption and with peak height RSD of 5.1%. Compared with the direct injector, an advantage of this approach is that injection is controlled independently of plug generation allowing optimization independent of the method of plug generation. On the other hand, plugs do not remain distinct prior to injection. Thus, this method is suited for periodic sampling of a stream of plugs rather than analysis of discrete samples.

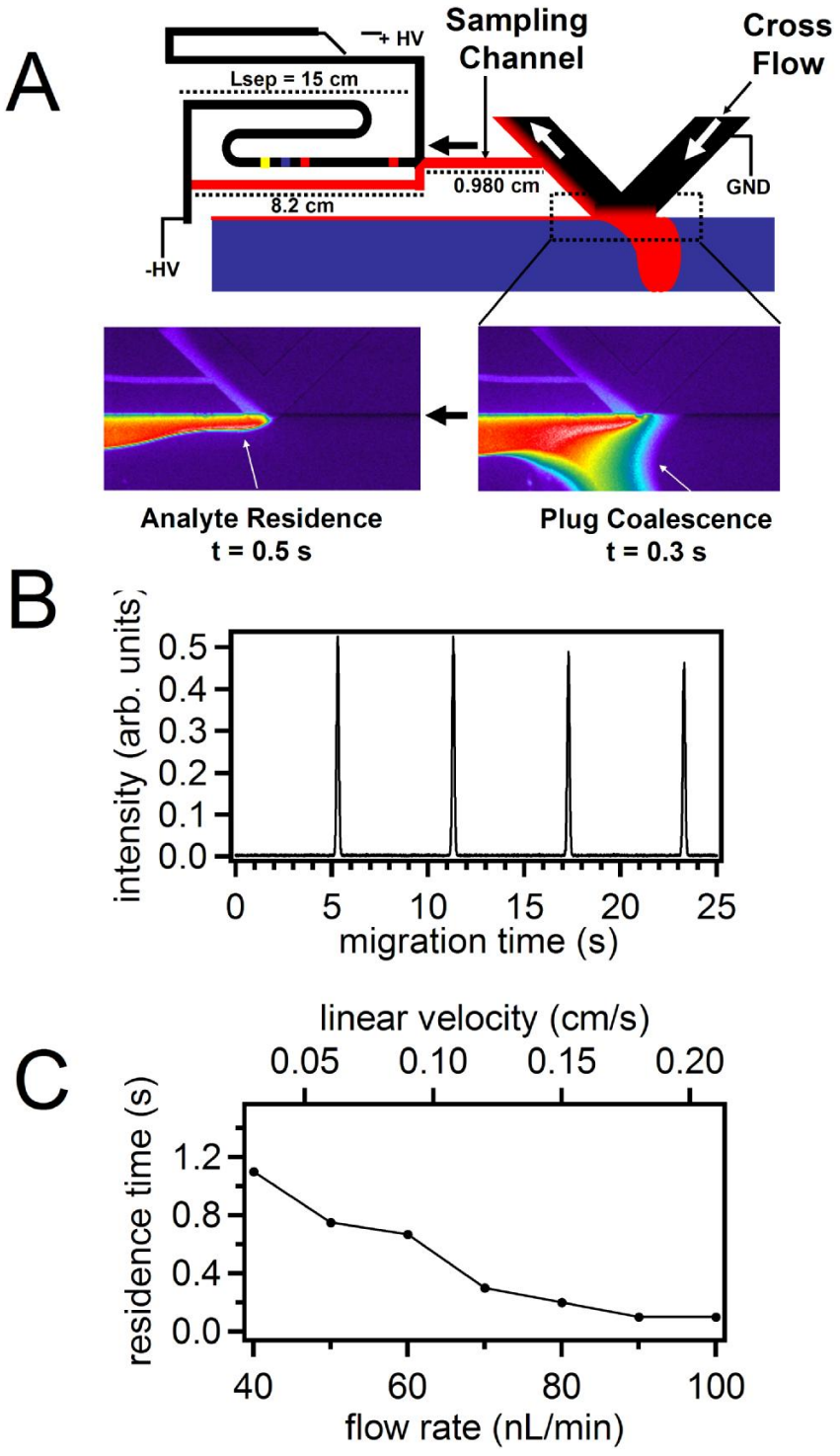

Figure A-7. Illustration of desegmentation injection and its performance. (A) Top drawing shows the lay-out of channels with addition of sampling channel and cross-style injector. Drawing illustrates a sample plug coalescing and portion being transferred to sampling channel for injection and separation. Below are two sequential fluorescence

micrographs showing coalescence of a fluorescein plug to the virtual wall illustrating "residence time". Times (t) indicate time since the plug arrived at the interface. The plugs were pumped past the coalescence interface at 5 μL/min, with a linear velocity of 0.42 cm/s. The cross flow separation buffer was pumped at a rate of 40 nL/min, with a linear velocity of 0.03 cm/s. (B) Sequential fluorescein injections performed by sampling from a K interface with a cross flow of 40 nL/min and a 1 Hz segmented flow stream. (C) Effect of cross flow rate on residence time in the sampling channel.

For tests of this system, aqueous sample plugs were generated at 1 Hz in a T junction, pumped through a serpentine, and coalesced at a K interface. Under this condition, we explored how the cross-flow rate affected the resulting secondary sample stream. As the cross flow rate is increased, the residence time of a given flow segment in the interface decreased as shown in Figure A-7 (C). The residence times provide an estimate of the plug frequency that is necessary to generate a continuous analyte stream into the EK gated injector. For example, a residence time of ~1 s at 40 nL/min suggests that droplets need to arrive at the interface at $\geq$ 1 Hz to avoid generating a discontinuous sample stream. As the cross flow rate increases, the frequency of droplet formation would have to be increased. If discontinuities occur in the secondary sample stream, it is not possible to continuously inject sample unless the injection is synchronized to match the arrival of a sample plug at the cross. Thus, for a given plug stream, the cross-flow should be kept within a fixed range to achieve reliable sampling and injection.

In this system, we observed that a minimum separation length of 15 cm for 20 μm deep channels was required to prevent flow splitting into the separation channel. Such splitting causes parabolic flow in the separation channel and must be minimized to achieve good separations. With this condition, fluorescein plugs at a concentration of 10 μM and a frequency of 0.9 Hz were coalesced to a K interface, transferred to the EK

gated injector, and electrophoresed at a field strength of 525 V/cm. Sequential injections of 10 ms produced efficiencies at 10 cm of 53,500 ± 6,400 (n = 30), shown in Figure A-6 (B). The efficiencies for these separations are limited by the injection band width and applied field strength. As with the direct injector, bubble formation above 600 V/cm prevented use of higher fields for the separation.

As suggested above, the main application of this approach to injection is sampling a stream of plugs. For example, we have recently demonstrated that temporal resolution in microdialysis sampling can be improved by segmenting dialysate prior to transport from the sampling site to the analysis system.[252] In such a case, the segmentation rate could be arbitrarily high, then sampled downstream by electrophoresis or other analytical methods at the temporal resolution desired. To demonstrate the potential for monitoring rapid concentration changes, a concentration step change was generated by filling a capillary with two known analyte solutions separated by an oil plug to mimic a sampling system that had collected a rapid change of analytes. This solution was pumped into the T junction, broken up into a segmented flow stream at 2.1 Hz, pumped into the K interface, injected at 5 s intervals with a t_{inj} of 300 ms and separated at 525 V/cm. The resulting electropherograms, shown in Figure A-8, illustrates that the change from high to low concentration of amino acids could be recorded over 10 s, or two electropherograms and cross flows of 40 nL/min and 0.03 cm/s linear velocities. The 10 s temporal resolution limit is likely due to mixing between plugs that occurs between the point at which the plugs are coalesced and the point at which the analyte is injected into the CE channel. During sampling, peak area RSDs were 5.2% RSD (n=20) for a fixed

concentration. These results demonstrate the suitability of this system for monitoring concentration changes in a sample stream.

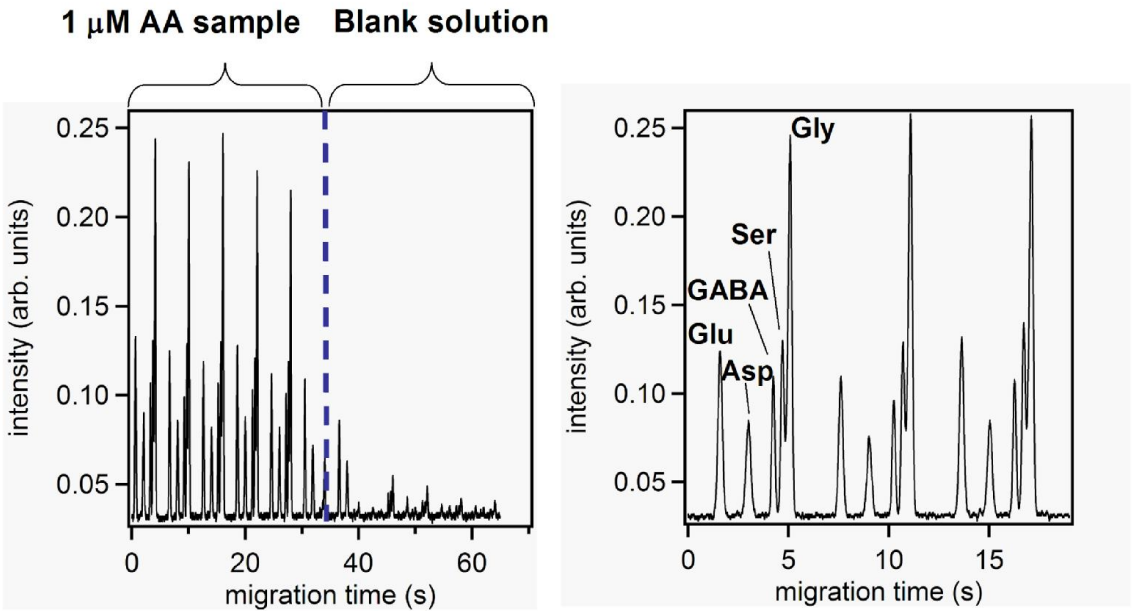

Figure A-8. Temporal resolution achieved with desegmentation injector. A 250 μm i.d. capillary was utilized with a valco union and a 100 μL Hamilton gas tight syringe to initially aspirate the sample, oil plug, and blank solution into the capillary. After the cartridge was formed it was screwed into a nanoport and pumped into the segmentation channel and analyzed using the indirect gated injector. Electropherograms recorded using a 525 V/cm field strength with 10 mM borate and 0.9 mM HP-β-CD as the separation buffer. Separation distances were 5 cm and injection widths were 200 ms.

Conclusions

The 3-dimensional microfluidic manifold with differing channel depths and patterned surface chemistry described here can be used to generate a stable interface between a segmented flow stream and aqueous buffer. The stable interface enabled reproducible sampling of plugs that passed through the interface and transfer to an

aqueous stream. Such sampling may be used for a variety of applications. We used this sampling method in developing two types of injectors for electrophoretic analysis of streams of plugs. The direct injection method enables serial electrophoretic analysis of individual droplets or plugs with ~1,050 theoretical plates and 5% RSDs. Analysis of the injection method suggests potential routes to improving efficiency including use of different plug formation method and voltage control at the injector. The indirect method performs a fluidic "digital to analog conversion" by transforming a stream of plugs into a continuous aqueous stream that is then periodically injected using a conventional electokinetic scheme. This method produced higher efficiencies of ~52,000 plates with comparable RSDs. This method is suited for periodic analysis of high frequency plug streams. Both methods showed good stability for analysis of long sequences of plugs. This approach advances the state-of-the-art for analyzing sample plugs confined in oil streams. They also provide a new approach to manipulating samples prior to electrophoresis samples. These new injection methods could have many applications including high-throughput screening, measuring products of in-plug reactions, monitoring reactions, process analytical technology, and microdialysis sampling.

BIBLIOGRAPHY

(1) Zoli, M.; Torri, C.; Ferrari, R.; Jansson, A.; Zini, I.; Fuxe, K.; Agnati, L. F. The emergence of the volume transmission concept. *Brain Research Reviews* **1998**, *26*, 136-147.

(2) Schultz, K. N.; Kennedy, R. T. Time-resolved microdialysis for in vivo neurochemical measurements and other applications. *Annual Reviews of Analytical Chemistry* **2008**, *1*, 627-661.

(3) Heien, M. L. A. V.; Khan, A. S.; Ariansen, J. L.; Cheer, J. F.; Phillips, P. E. M.; Wassum, K. M.; Wightman, R. M. Real-time measurement of dopamine fluctuations after cocaine in the brain of behaving rats. *Proceedings of the National Academy of Sciences of the United States of America* **2005**, *102*, 10023-10028.

(4) Silva, E.; Hernandez, L.; Contreras, Q.; Guerrero, F.; Alba, G. Noxious stimulation increases glutamate and arginine in the periaqueductal gray matter in rats: a microdialysis study. *Pain* **2000**, *87*, 131-135.

(5) Rossell, S.; Gonzalez, L. E.; Hernandez, L. One-second time resolution brain microdialysis in fully awake rats: Protocol for the collection, separation and sorting of nanoliter dialysate volumes. *Journal of Chromatography B* **2003**, *784*, 385-393.

(6) Tucci, S.; Rada, P.; Sepulveda, M. J.; Hernandez, L. Glutamate measured by 6-s resolution brain microdialysis: capillary electrophoretic and laser-induced fluorescence detection application. *Journal of Chromatography B: Biomedical Sciences and Applications* **1997**, *694*, 343-349.

(7) Bruno, J. P.; Gash, C.; Martin, B.; Zmarowski, A.; Pomerleau, F.; Burmeister, J.; Huettl, P.; Gerhardt, G. A. Second-by-second measurement of acetylcholine release in prefrontal cortex. *European Journal of Neuroscience* **2006**, *24*, 2749-2757.

(8) Venton, B. J.; Wightman, R. M. Pharmacologically induced, subsecond dopamine transients in the caudate–putamen of the anesthetized rat. *Synapse* **2007**, *61*, 37-39.

(9) Burmeister, J. J.; Palmer, M.; Gerhardt, G. A. Ceramic-based multisite microelectrode array for rapid choline measures in brain tissue. *Analytica Chimica Acta* **2003**, *481*, 65-74.

(10) Kandel, E. R.; Schwartz, J. H.; Jessell, T. M. *Principles of neural science*, Fourth ed.; McGraw-Hill, 2000.

(11) Hu, Y.; Mitchell, K. M.; Albahadily, F. N.; Michaelis, E. K.; Wilson, G. S. Direct measurement of glutamate release in the brain using a dual enzyme-based electrochemical sensor. *Brain Research* **1994**, *659*, 117-125.

(12) Mitchell, K.; Oke, A. F.; Adams, R. N. In vivo dynamics of norepinephrine release-reuptake in multiple terminal field regions of rat brain. *Journal of Neurochemistry* **1994**, *63*, 917-926.
(13) Westerink, B. H. C.; Cremers, T. I. F. H. *Handbook of microdialysis*, First ed.; Academic Press: New York, 2007.
(14) Robinson, T. E.; Justice, J. B. J. *Microdialysis in the neurosciences*; Elsevier: Amsterdam, 1991.
(15) Ungerstedt, U. *Measurement of neurotransmitter release in vivo*; John Wiley and Sons: New York, 1984.
(16) Watson, C. J.; Venton, B. J.; Kennedy, R. T. In vivo measurements of neurotransmitters by microdialysis sampling. *Analytical Chemistry* **2006**, *78*, 1391-1399.
(17) Benveniste, H.; Hansen, A. J.; Ottosen, N. S. Determination of brain interstitial concentrations by microdialysis. *Journal of Neurochemistry* **1989**, *52*, 1741-1750.
(18) Bungay, P. M.; Morrison, P. F.; Dedrick, R. L. Steady-state theory for quantitative microdialysis of solutes and water in vivo and in vitro. *Life Sciences* **1990**, *46*, 105-119.
(19) Justice, J. B. Quantitative microdialysis of neurotransmitters. *Journal of Neuroscience Methods* **1993**, *48*, 263-276.
(20) Chen, A.; Lunte, C. E. Microdialysis sampling coupled on-line to fast microbore liquid chromatography. *Journal of Chromatography A* **1995**, *691*, 29-35.
(21) Davies, M. I.; Cooper, J. D.; Desmond, S. S.; Lunte, C. E.; Lunte, S. M. Analytical considerations for microdialysis sampling. *Advanced Drug Delivery Reviews* **2000**, *45*, 169-188.
(22) Bert, L.; Parrot, S.; Robert, F.; Desvignes, C.; Denoroy, L.; Suaud-Chagny, M. F.; Renaud, B. In vivo temporal sequence of rat striatal glutamate, aspartate and dopamine efflux during apomorphine, nomifensine, NMDA and PDC in situ administration. *Neuropharmacology* **2002**, *43*, 825-835.
(23) Bert, L.; Robert, F.; Denoroy, L.; Stoppini, L.; Renaud, B. Enhanced temporal resolution for the microdialysis monitoring of catecholamines and excitatory amino acids using capillary electrophoresis with laser-induced fluorescence detection Analytical developments and in vitro validations. *Journal of Chromatography A* **1996**, *755*, 99-111.
(24) Bowser, M. T.; Kennedy, R. T. In vivo monitoring of amine neurotransmitters using microdialysis with on-line capillary electrophoresis. *ELECTROPHORESIS* **2001**, *22*, 3668-3676.
(25) Boyd, B. W.; Witowski, S. R.; Kennedy, R. T. Trace-level amino acid analysis by capillary liquid chromatography and application to in vivo microdialysis sampling with 10-s temporal resolution. *Analytical Chemistry* **2000**, *72*, 865-871.
(26) Church, W. H.; Justice, J. B. J. Rapid sampling and determination of extracellular dopamine in vivo. *Analytical Chemistry* **1987**, *59*, 712-716.
(27) Hernandez, L.; Tucci, S.; Guzman, N.; Paez, X. In-vivo monitoring of glutamate in the brain by microdialysis and capillary electrophoresis with laser-induced fluorescence detection. *Journal of Chromatography A* **1993**, *652*, 393-398.

(28) Kennedy, R. T.; Watson, C. J.; Haskins, W. E.; Powell, D. H.; Strecker, R. E. In vivo neurochemical monitoring by microdialysis and capillary separations. *Current Opinion in Chemical Biology* **2002**, *6*, 659-665.
(29) Lada, M. W.; Vickroy, T. W.; Kennedy, R. T. High temporal resolution monitoring of glutamate and aspartate in vivo using microdialysis on-line with capillary electrophoresis with laser-induced fluorescence detection. *Analytical Chemistry* **1997**, *69*, 4560-4565.
(30) Parkin, M.; Hopwood, S.; Jones, D. A.; Hashemi, P.; Landolt, H.; Fabricius, M.; Lauritzen, M.; Boutelle, M. G.; Strong, A. J. Dynamic changes in brain glucose and lactate in pericontusional areas of the human cerebral cortex, monitored with rapid sampling on-line microdialysis: relationship with depolarisation-like events. *Journal of Cerebral Blood Flow & Metabolism* **2005**, *25*, 402-413.
(31) Hogan, B. L.; Lunte, S. M.; Stobaugh, J. F.; Lunte, C. E. Online coupling of in vivo microdialysis sampling with capillary electrophoresis. *Analytical Chemistry* **1994**, *66*, 596-602.
(32) O'Shea, T. J.; Weber, P. L.; Bammel, B. P.; Lunte, C. E.; Lunte, S. M.; Smyth, M. R. Monitoring excitatory amino acid release in vivo by microdialysis with capillary electrophoresis- electrochemistry. *Journal of Chromatography A* **1992**, *608*, 189-195.
(33) Lada, M. W.; Vickroy, T. W.; Kennedy, R. T. Evidence for neuronal origin and metabotropic receptor-mediated regulation of extracellular glutamate and aspartate in rat striatum in vivo following electrical stimulation of the prefrontal cortex. *Journal of Neurochemistry* **1998**, *70*, 617-625.
(34) Robert, F.; Bert, L.; Lambás-Señas, L.; Denoroy, L.; Renaud, B. In vivo monitoring of extracellular noradrenaline and glutamate from rat brain cortex with 2-min microdialysis sampling using capillary electrophoresis with laser-induced fluorescence detection. *Journal of Neuroscience Methods* **1996**, *70*, 153-162.
(35) Shou, M.; Ferrario, C. R.; Schultz, K. N.; Robinson, T. E.; Kennedy, R. T. Monitoring dopamine in vivo by microdialysis sampling and on-line CE-laser-induced fluorescence. *Analytical Chemistry* **2006**, *78*, 6717-6725.
(36) Norton, L. W.; Yuan, F.; Reichert, W. M. Glucose recovery with nare and hydrogel-coated microdialysis probes: Experiment and simulation of temporal effects. *Analytical Chemistry* **2007**, *79*, 445-452.
(37) Kottegoda, S.; Shaik, I.; Shippy, S. A. Demonstration of low flow push-pull perfusion. *Journal of Neuroscience Methods* **2002**, *121*, 93-101.
(38) Kennedy, R. T.; Thompson, J. E.; Vickroy, T. W. In vivo monitoring of amino acids by direct sampling of brain extracellular fluid at ultralow flow rates and capillary electrophoresis. *Journal of Neuroscience Methods* **2002**, *114*, 39-49.
(39) Cellar, N. A.; Burns, S. T.; Meiners, J. C.; Chen, H.; Kennedy, R. T. Microfluidic chip for low-flow push-pull perfusion sampling in vivo with on-Line analysis of amino acids. *Analytical Chemistry* **2005**, *77*, 7067-7073.
(40) Yang, H.; Peters, J. L.; Allen, C.; Chern, S.-S.; Coalson, R. D.; Michael, A. C. A theoretical description of microdialysis with mass transport coupled to chemical events. *Analytical Chemistry* **2000**, *72*, 2042-2049.

(41) Yang, H.; Peters, J. L.; Michael, A. C. Coupled effects of mass transfer and uptake kinetics on in vivo microdialysis of dopamine. *Journal of Neurochemistry* **1998**, *71*, 684-692.
(42) Benveniste, H. Brain microdialysis. *Journal of Neurochemistry* **1989**, *52*, 1667-1679.
(43) Lada, M. W.; Kennedy, R. T. Quantitative in vivo monitoring of primary amines in rat caudate nucleus using microdialysis coupled by a flow-gated interface to capillary electrophoresis with laser-induced fluorescence detection. *Analytical Chemistry* **1996**, *68*, 2790-2797.
(44) Lada, M. W.; Kennedy, R. T. Quantitative in vivo measurements using microdialysis on-line with capillary zone electrophoresis. *Journal of Neuroscience Methods* **1995**, *63*, 147-152.
(45) Parsons, L. H.; Justice, J. B. Extracellular concentration and in vivo recovery of dopamine in the nucleus accumbens using microdialysis. *Journal of Neurochemistry* **1992**, *58*, 212-218.
(46) Nandi, P.; Lunte, S. M. Recent trends in microdialysis sampling integrated with conventional and microanalytical systems for monitoring biological events: A review. *Analytica Chimica Acta* **2009**, *651*, 1-14.
(47) Miele, M.; Berners, M.; Boutelle, M. G.; Kusakabe, H.; Fillenz, M. The determination of the extracellular concentration of brain glutamate using quantitative microdialysis. *Brain Research* **1996**, *707*, 131-133.
(48) Zilkha, E.; Obrenovitch, T. P.; Koshy, A.; Kusakabe, H.; Bennetto, H. P. Extracellular glutamate: on-line monitoring using microdialysis coupled to enzyme-amperometric analysis. *Journal of Neuroscience Methods* **1995**, *60*, 1-9.
(49) Yao, T.; Suzuki, S.; Nishino, H.; Nakahara, T. On-line amperometric assay of glucose, L-glutamate, and acetylcholine using microdialysis probes and immobilized enzyme reactors. *Electroanalysis* **1995**, *7*, 1114-1117.
(50) Fellows, L. K.; Boutelle, M. G.; Fillenz, M. Extracellular brain glucose levels reflect local neuronal activity: A mcrodialysis study in awake, freely moving rats. *Journal of Neurochemistry* **1992**, *59*, 2141-2147.
(51) van der Kuil, J. H. F.; Korf, J. One-line monitoring of extracellular brain glucose using microdialysis and a NADPH-linked enzymatic assay. *Journal of Neurochemistry* **1991**, *57*, 648-654.
(52) Boutelle, M. G.; Fellows, L. K.; Cook, C. Enzyme packed bed system for the on-line measurement of glucose, glutamate, and lactate in brain microdialyzate. *Analytical Chemistry* **1992**, *64*, 1790-1794.
(53) Davies, M. I. A review of microdialysis sampling for pharmacokinetic applications. *Analytica Chimica Acta* **1999**, *379*, 227-249.
(54) Kennedy, R. T.; German, I.; Thompson, J. E.; Witowski, S. R. Fast analytical-scale separations by capillary electrophoresis and liquid chromatography. *Chemical Reviews* **1999**, *99*, 3081-3132.
(55) Skold, K.; Svensson, M.; Kaplan, A.; Bjorkesten, L.; Astrom, J.; Andren, P. E. A neuroproteomic approach to targeting neuropeptides in the brain. *Proteomics* **2002**, *2*, 447-454.

(56) Li, Q.; Zubieta, J.-K.; Kennedy, R. T. Practical aspects of in vivo detection of neuropeptides by microdialysis coupled off-line to capillary LC with multistage MS. *Analytical Chemistry* **2009**, *81*, 2242-2250.
(57) Perry, M.; Li, Q.; Kennedy, R. T. Review of recent advances in analytical techniques for the determination of neurotransmitters. *Analytica Chimica Acta* **2009**, *653*, 1-22.
(58) Porkka-Heiskanen, T.; Strecker, R. E.; Thakkar, M.; BjÃ¸rkum, A. A.; Greene, R. W.; McCarley, R. W. Adenosine: A mediator of the sleep-inducing effects of prolonged wakefulness. *Science* **1997**, *276*, 1265-1268.
(59) Emmett, M. R.; Andrén, P. E.; Caprioli, R. M. Specific molecular mass detection of endogenously released neuropeptides using in vivo microdialysis/mass spectrometry. *Journal of Neuroscience Methods* **1995**, *62*, 141-147.
(60) Andrén, P. E.; Caprioli, R. M. Determination of extracellular release of neurotensin in discrete rat brain regions utilizing in vivo microdialysis/electrospray mass spectrometry. *Brain Research* **1999**, *845*, 123-129.
(61) Tao, L.; Thompson, J. E.; Kennedy, R. T. Optically gated capillary electrophoresis of *o*-phthalaldehyde/*beta*-mercaptoethanol derivatives of amino acids for chemical monitoring. *Analytical Chemistry* **1998**, *70*, 4015-4022.
(62) Jorgenson, J. W.; Lukacs, K. D. Zone electrophoresis in open-tubular glass capillaries. *Analytical Chemistry* **1981**, *53*, 1298-1302.
(63) Landers, J. P. *Handbook of capillary electrophoresis*, Second ed.; CRC Press, Inc.: Bica Raton, 1997.
(64) Cheng, Y. F.; Dovichi, N. J. Subattomole amino acid analysis by capillary zone electrophoresis and laser-induced fluorescence. *Science* **1988**, *242*, 562-564.
(65) Ewing, A. G.; Mesaros, J. M.; Gavin, P. F. Electrochemical detection in microcolumn separations. *Analytical Chemistry* **1994**, *66*, 527A-537A.
(66) Fenn, J. B.; Mann, M.; Meng, C. K.; Wong, S. F.; Whitehouse, C. M. Electrospray ionization–principles and practice. *Mass Spectrometry Reviews* **1990**, *9*, 37-70.
(67) Moore, A. W.; Jorgenson, J. W. Study of zone broadening in optically gated high-speed capillary electrophoresis. *Analytical Chemistry* **1993**, *65*, 3550-3560.
(68) Liu, J.; Dolnik, V.; Hsieh, Y. Z.; Novotny, M. Experimental evaluation of the separation efficiency in capillary electrophoresis using open tubular and gel-filled columns. *Analytical Chemistry* **1992**, *64*, 1328-1336.
(69) Monnig, C. A.; Jorgenson, J. W. On-column sample gating for high-speed capillary zone electrophoresis. *Analytical Chemistry* **1991**, *63*, 802-807.
(70) Lemmo, A. V.; Jorgenson, J. W. Transverse flow gating interface for the coupling of microcolumn LC with CZE in a comprehensive two-dimensional system. *Analytical Chemistry* **1993**, *65*, 1576-1581.
(71) Weibel, D. B.; Whitesides, G. M. Applications of microfluidics in chemical biology. *Current Opinion in Chemical Biology* **2006**, *10*, 584-591.
(72) Roman, G. T.; Kennedy, R. T. Fully integrated microfluidic separations systems for biochemical analysis. *Journal of Chromatography A* **2007**, *1168*, 170-188.

(73) Harrison, D. J.; Fluri, K.; Seiler, K.; Fan, Z. H.; Effenhauser, C. S.; Manz, A. Micromachining a miniaturized capillary electrophoresis-nased chemical-analysis system on a chip. *Science* **1993**, *261*, 895-897.
(74) Manz, A.; Harrison, D. J.; Verpoorte, E. M. J.; Fettinger, J. C.; Paulus, A.; Lüdi, H.; Widmer, H. M. Planar chips technology for miniaturization and integration of separation techniques into monitoring systems: Capillary electrophoresis on a chip. *Journal of Chromatography A* **1992**, *593*, 253-258.
(75) Chabinyc, M. L.; Chiu, D. T.; McDonald, J. C.; Stroock, A. D.; Christian, J. F.; Karger, A. M.; Whitesides, G. M. An integrated fluorescence detection system in poly(dimethylsiloxane) for microfluidic applications. *Analytical Chemistry* **2001**, *73*, 4491-4498.
(76) Wenclawiak, B. W.; Puschl, R. J. Sample injection for capillary electrophoresis on a micro fabricated device/on chip CE injection. *Analytical letters* **2006**, *39*, 3 - 16.
(77) Harrison, D. J.; Manz, A.; Fan, Z.; Luedi, H.; Widmer, H. M. Capillary electrophoresis and sample injection systems integrated on a planar glass chip. *Analytical Chemistry* **1992**, *64*, 1926-1932.
(78) Jacobson, S. C.; Hergenroder, R.; Koutny, L. B.; Warmack, R. J.; Ramsey, J. M. Effects of injection schemes and column geometry on the performance of microchip electrophoresis devices. *Analytical Chemistry* **1994**, *66*, 1107-1113.
(79) Jacobson, S. C.; Koutny, L. B.; Hergenroeder, R.; Moore, A. W.; Ramsey, J. M. Microchip capillary electrophoresis with an integrated postcolumn reactor. *Analytical Chemistry* **1994**, *66*, 3472-3476.
(80) Ermakov, S. V.; Jacobson, S. C.; Ramsey, J. M. Computer simulations of electrokinetic injection techniques in microfluidic devices. *Analytical Chemistry* **2000**, *72*, 3512-3517.
(81) Jacobson, S. C.; Ermakov, S. V.; Ramsey, J. M. Minimizing the mumber of voltage sources and fluid reservoirs for electrokinetic valving in microfluidic devices. *Analytical Chemistry* **1999**, *71*, 3273-3276.
(82) Alarie, J. P.; Jacobson, S. C.; Ramsey, J. M. Electrophoretic injection bias in a microchip valving scheme. *ELECTROPHORESIS* **2001**, *22*, 312-317.
(83) Slentz, B. E.; Penner, N. A.; Regnier, F. Sampling Bias at channel junctions in gated flow injection on chips. *Analytical Chemistry* **2002**, *74*, 4835-4840.
(84) Effenhauser, C. S.; Manz, A.; Widmer, H. M. Glass chips for high-speed capillary electrophoresis separations with submicrometer plate heights. *Analytical Chemistry* **1993**, *65*, 2637-2642.
(85) Culbertson, C. T.; Jacobson, S. C.; Ramsey, J. M. Dispersion sources for compact geometries on microchips. *Analytical Chemistry* **1998**, *70*, 3781-3789.
(86) Culbertson, C. T.; Jacobson, S. C.; Ramsey, J. M. Microchip devices for high-efficiency separations. *Analytical Chemistry* **2000**, *72*, 5814-5819.
(87) Paegel, B. M.; Hutt, L. D.; Simpson, P. C.; Mathies, R. A. Turn geometry for minimizing band broadening in microfabricated capillary electrophoresis channels. *Analytical Chemistry* **2000**, *72*, 3030-3037.
(88) Guihen, E.; O'Connor, W. T. Capillary and microchip electrophoresis in microdialysis: Recent applications. *ELECTROPHORESIS* **2010**, *31*, 55-64.

(89) Xu, H.; Ewing, A. A rapid enzyme assay for beta-galactosidase using optically gated sample introduction on a microfabricated chip. *Analytical and Bioanalytical Chemistry* **2004**, *378*, 1710-1715.
(90) Venton, B. J.; Robinson, T. E.; Kennedy, R. T. Transient changes in nucleus accumbens amino acid concentrations correlate with individual responsivity to the predator fox odor 2,5-dihydro-2,4,5-trimethylthiazoline. *Journal of Neurochemistry* **2006**, *96*, 236-246.
(91) Hapuarachchi, S.; Premeau, S. P.; Aspinwall, C. A. High-speed capillary zone electrophoresis with online photolytic optical injection. *Analytical Chemistry* **2006**, *78*, 3674-3680.
(92) Shou, M.; Smith, A. D.; Shackman, J. G.; Peris, J.; Kennedy, R. T. In vivo monitoring of amino acids by microdialysis sampling with on-line derivatization by naphthalene-2,3-dicarboxyaldehyde and rapid micellar electrokinetic capillary chromatography. *Journal of Neuroscience Methods* **2004**, *138*, 189-197.
(93) Silva, E.; Hernandez, L.; Quinonez, B.; Gonzalez, L. E.; Colasante, C. Selective amino acids changes in the medial and lateral preoptic area in the formalin test in rats. *Neuroscience* **2004**, *124*, 395-404.
(94) Presti, M. F.; Watson, C. J.; Kennedy, R. T.; Yang, M.; Lewis, M. H. Behavior-related alterations of striatal neurochemistry in a mouse model of stereotyped movement disorder. *Pharmacology Biochemistry and Behavior* **2004**, *77*, 501-507.
(95) Lapainis, T.; Sweedler, J. V. Contributions of capillary electrophoresis to neuroscience. *Journal of Chromatography A* **2008**, *1184*, 144-158.
(96) Robert, F.; Bert, L.; Denoroy, L.; Renaud, B. Capillary zone electrophoresis with laser-induced fluorescence detection for the determination of nanomolar concentrations of noradrenaline and dopamine: application to brain microdialyzate analysis. *Analytical Chemistry* **1995**, *67*, 1838-1844.
(97) Qian, J.; Wu, Y.; Yang, H.; Michael, A. C. An integrated decoupler for capillary electrophoresis with electrochemical detection: Application to analysis of brain microdialysate. *Analytical Chemistry* **1999**, *71*, 4486-4492.
(98) Léna, I.; Parrot, S.; Deschaux, O.; Muffat-Joly, S.; Sauvinet, V.; Renaud, B.; Suaud-Chagny, M. F.; Gottesmann, C. Variations in extracellular levels of dopamine, noradrenaline, glutamate, and aspartate across the sleep–wake cycle in the medial prefrontal cortex and nucleus accumbens of freely moving rats. *Journal of Neuroscience Research* **2005**, *81*, 891-899.
(99) Parrot, S.; Sauvinet, V.; Riban, V.; Depaulis, A.; Renaud, B.; Denoroy, L. High temporal resolution for in vivo monitoring of neurotransmitters in awake epileptic rats using brain microdialysis and capillary electrophoresis with laser-induced fluorescence detection. *Journal of Neuroscience Methods* **2004**, *140*, 29-38.
(100) Kostel, K. L.; Lunte, S. M. Evaluation of capillary electrophoresis with post-column derivatization and laser-induced fluorescence detection for the determination of substance P and its metabolites. *Journal of Chromatography B: Biomedical Sciences and Applications* **1997**, *695*, 27-38.
(101) Dawson, L. A.; Stow, J. M.; Palmer, A. M. Improved method for the measurement of glutamate and aspartate using capillary electrophoresis with laser induced fluorescence detection and its application to brain microdialysis. *Journal of Chromatography B: Biomedical Sciences and Applications* **1997**, *694*, 455-460.

(102) Huynh, B. H.; Fogarty, B. A.; Lunte, S. M.; Martin, R. S. On-Line coupling of microdialysis sampling with microchip-based capillary electrophoresis. *Analytical Chemistry* **2004**, *76*, 6440-6447.
(103) Huynh, B. H.; Fogarty, B. A.; Nandi, P.; Lunte, S. M. A microchip electrophoresis device with on-line microdialysis sampling and on-chip sample derivatization by naphthalene 2,3-dicarboxaldehyde/2-mercaptoethanol for amino acid and peptide analysis. *Journal of Pharmaceutical and Biomedical Analysis* **2006**, *42*, 529-534.
(104) Sandlin, Z. D.; Shou, M.; Shackman, J. G.; Kennedy, R. T. Microfluidic electrophoresis chip coupled to microdialysis for in vivo monitoring of amino acid neurotransmitters. *Analytical Chemistry* **2005**, *77*, 7702-7708.
(105) Unger, M. A.; Chou, H.-P.; Thorsen, T.; Scherer, A.; Quake, S. R. Monolithic microfabricated valves and pumps by multilayer soft lithography. *Science* **2000**, *288*, 113-116.
(106) Mecker, L. C.; Martin, R. S. Integration of microdialysis sampling and microchip electrophoresis with electrochemical detection. *Analytical Chemistry* **2008**, *80*, 9257-9264.
(107) Li, M. W.; Huynh, B. H.; Hulvey, M. K.; Lunte, S. M.; Martin, R. S. Design and characterization of poly(dimethylsiloxane)-based valves for interfacing continuous-flow sampling to microchip electrophoresis. *Analytical Chemistry* **2006**, *78*, 1042-1051.
(108) Xu, J.-J.; Wang, A.-J.; Chen, H.-Y. Electrochemical detection modes for microchip capillary electrophoresis. *TrAC Trends in Analytical Chemistry* **2007**, *26*, 125-132.
(109) Gunther, A.; Jensen, K. F. Multiphase microfluidics: from flow characteristics to chemical and materials synthesis. *Lab on a Chip* **2006**, *6*, 1487-1503.
(110) Teh, S.-Y.; Lin, R.; Hung, L.-H.; Lee, A. P. Droplet microfluidics. *Lab on a Chip* **2008**, *8*, 198-220.
(111) Song, H.; Chen, D. L.; Ismagilov, R. F. Reactions in droplets in microfluidic channels. *Angewandte Chemie International Edition* **2006**, *45*, 7336-7356.
(112) Shui, L.; Eijkel, J. C. T.; van den Berg, A. Multiphase flow in micro- and nanochannels. *Sensors and Actuators B: Chemical* **2007**, *121*, 263-276.
(113) Belder, D. Towards an integrated chemical circuit. *Angewandte Chemie International Edition* **2009**, *48*, 3736-3737.
(114) Baroud, C. N.; Gallaire, F.; Dangla, R. Dynamics of microfluidic droplets. *Lab on a Chip* **2010**, *10*, 2032-2045.
(115) Huebner, A.; Sharma, S.; Srisa-Art, M.; Hollfelder, F.; Edel, J. B.; deMello, A. J. Microdroplets: A sea of applications? *Lab on a Chip* **2008**, *8*, 1244-1254.
(116) Cramer, C.; Fischer, P.; Windhab, E. J. Drop formation in a co-flowing ambient fluid. *Chemical Engineering Science* **2004**, *59*, 3045-3058.
(117) Utada, A. S.; Fernandez-Nieves, A.; Stone, H. A.; Weitz, D. A. Dripping to jetting transitions in coflowing liquid streams. *Physical Review Letters* **2007**, *99*, 094502.
(118) Shelley, L. A.; Nathalie, B.; Howard, A. S. Formation of dispersions using "flow focusing" in microchannels. *Applied Physics Letters* **2003**, *82*, 364-366.

(119) Ward, T.; Faivre, M.; Abkarian, M.; Stone, H. A. Microfluidic flow focusing: Drop size and scaling in pressure versus flow-rate-driven pumping. *ELECTROPHORESIS* **2005**, *26*, 3716-3724.
(120) Thorsen, T.; Roberts, R. W.; Arnold, F. H.; Quake, S. R. Dynamic pattern formation in a vesicle-generating microfluidic device. *Physical Review Letters* **2001**, *86*, 4163.
(121) Garstecki, P.; Fuerstman, M. J.; Stone, H. A.; Whitesides, G. M. Formation of droplets and bubbles in a microfluidic T-junction-scaling and mechanism of break-up. *Lab on a Chip* **2006**, *6*, 437-446.
(122) Lorenz, R. M.; Fiorini, G. S.; Jeffries, G. D. M.; Lim, D. S. W.; He, M.; Chiu, D. T. Simultaneous generation of multiple aqueous droplets in a microfluidic device. *Analytica Chimica Acta* **2008**, *630*, 124-130.
(123) Hong, J.; Choi, M.; Edel, J. B.; deMello, A. J. Passive self-synchronized two-droplet generation. *Lab on a Chip* **2010**, *10*, 2702-2709.
(124) Xu, J. H.; Luo, G. S.; Li, S. W.; Chen, G. G. Shear force induced monodisperse droplet formation in a microfluidic device by controlling wetting properties. *Lab on a Chip* **2006**, *6*, 131-136.
(125) Stan, C. A.; Tang, S. K. Y.; Whitesides, G. M. Independent control of drop size and velocity in microfluidic flow-focusing generators using variable temperature and flow rate. *Analytical Chemistry* **2009**, *81*, 2399-2402.
(126) He, M.; Kuo, J. S.; Chiu, D. T. Effects of ultrasmall orifices on the electrogeneration of femtoliter-volume aqueous droplets. *Langmuir* **2006**, *22*, 6408-6413.
(127) Baroud, C. N.; Delville, J.-P.; Gallaire, F.; ccedil; ois; Wunenburger, R.; eacute; gis. Thermocapillary valve for droplet production and sorting. *Physical Review E* **2007**, *75*, 046302.
(128) Zeng, S.; Li, B.; Su, X. o.; Qin, J.; Lin, B. Microvalve-actuated precise control of individual droplets in microfluidic devices. *Lab on a Chip* **2009**, *9*, 1340-1343.
(129) Shestopalov, I.; Tice, J. D.; Ismagilov, R. F. Multi-step synthesis of nanoparticles performed on millisecond time scale in a microfluidic droplet-based system. *Lab on a Chip* **2004**, *4*, 316-321.
(130) Khan, S. A.; Gunther, A.; Schmidt, M. A.; Jensen, K. F. Microfluidic synthesis of colloidal silica. *Langmuir* **2004**, *20*, 8604-8611.
(131) Rhee, M.; Burns, M. A. Drop mixing in a microchannel for lab-on-a-chip platforms. *Langmuir* **2007**, *24*, 590-601.
(132) Liau, A.; Karnik, R.; Majumdar, A.; Cate, J. H. D. Mixing crowded biological solutions in milliseconds. *Analytical Chemistry* **2005**, *77*, 7618-7625.
(133) Casadevall i Solvas, X.; Srisa-Art, M.; deMello, A. J.; Edel, J. B. Mapping of fluidic mixing in microdroplets with 1 s time resolution using fluorescence lifetime imaging. *Analytical Chemistry* **2010**, *82*, 3950-3956.
(134) Fidalgo, L. M.; Abell, C.; Huck, W. T. S. Surface-induced droplet fusion in microfluidic devices. *Lab on a Chip* **2007**, *7*, 984-986.
(135) Lorenz, R. M.; Edgar, J. S.; Jeffries, G. D. M.; Zhao, Y.; McGloin, D.; Chiu, D. T. Vortex-trap-induced fusion of femtoliter-volume aqueous droplets. *Analytical Chemistry* **2007**, *79*, 224-228.

(136) Zagnoni, M.; Cooper, J. M. On-chip electrocoalescence of microdroplets as a function of voltage, frequency and droplet size. *Lab on a Chip* **2009**, *9*, 2652-2658.
(137) Niu, X.; Gielen, F.; deMello, A. J.; Edel, J. B. Electro-coalescence of digitally controlled droplets. *Analytical Chemistry* **2009**.
(138) Niu, X.; Gulati, S.; Edel, J. B.; deMello, A. J. Pillar-induced droplet merging in microfluidic circuits. *Lab on a Chip* **2008**, *8*, 1837-1841.
(139) Wang, W.; Yang, C.; Li, C. M. On-demand microfluidic droplet trapping and fusion for on-chip static droplet assays. *Lab on a Chip* **2009**, *9*, 1504-1506.
(140) Mazutis, L.; Baret, J.-C.; Griffiths, A. D. A fast and efficient microfluidic system for highly selective one-to-one droplet fusion. *Lab on a Chip* **2009**, *9*, 2665-2672.
(141) Christopher, G. F.; Bergstein, J.; End, N. B.; Poon, M.; Nguyen, C.; Anna, S. L. Coalescence and splitting of confined droplets at microfluidic junctions. *Lab on a Chip* **2009**, *9*, 1102-1109.
(142) Link, D. R.; Anna, S. L.; Weitz, D. A.; Stone, H. A. Geometrically mediated breakup of drops in microfluidic devices. *Physical Review Letters* **2004**, *92*, 054503.
(143) Choi, J.-H.; Lee, S.-K.; Lim, J.-M.; Yang, S.-M.; Yi, G.-R. Designed pneumatic valve actuators for controlled droplet breakup and generation. *Lab on a Chip* **2009**, *10*, 456-461.
(144) Nie, J.; Kennedy, R. T. Sampling from nanoliter plugs via asymmetrical splitting of segmented flow. *Analytical Chemistry* **2010**, *82*, 7852-7856.
(145) Adamson, D. N.; Mustafi, D.; Zhang, J. X. J.; Zheng, B.; Ismagilov, R. F. Production of arrays of chemically distinct nanolitre plugs via repeated splitting in microfluidic devices. *Lab on a Chip* **2006**, *6*, 1178-1186.
(146) Baret, J.-C.; Miller, O. J.; Taly, V.; Ryckelynck, M.; El-Harrak, A.; Frenz, L.; Rick, C.; Samuels, M. L.; Hutchison, J. B.; Agresti, J. J.; Link, D. R.; Weitz, D. A.; Griffiths, A. D. Fluorescence-activated droplet sorting (FADS): efficient microfluidic cell sorting based on enzymatic activity. *Lab on a Chip* **2009**, *9*, 1850-1858.
(147) Zhang, K.; Liang, Q.; Ma, S.; Mu, X.; Hu, P.; Wang, Y.; Luo, G. On-chip manipulation of continuous picoliter-volume superparamagnetic droplets using a magnetic force. *Lab on a Chip* **2009**, *9*, 2992-2999.
(148) Chabert, M.; Viovy, J. L. Microfluidic high-throughput encapsulation and hydrodynamic self-sorting of single cells. *Proceedings of the National Academy of Sciences of the United States of America* **2008**, *105*, 3191-3196.
(149) Issadore, D.; Humphry, K. J.; Brown, K. A.; Sandberg, L.; Weitz, D. A.; Westervelt, R. M. Microwave dielectric heating of drops in microfluidic devices. *Lab on a Chip* **2009**, *9*, 1701-1706.
(150) Sgro, A. E.; Chiu, D. T. Droplet freezing, docking, and the exchange of immiscible phase and surfactant around frozen droplets. *Lab on a Chip* **2010**, *10*, 1873-1877.
(151) Stan, C. A.; Schneider, G. F.; Shevkoplyas, S. S.; Hashimoto, M.; Ibanescu, M.; Wiley, B. J.; Whitesides, G. M. A microfluidic apparatus for the study of ice nucleation in supercooled water drops. *Lab on a Chip* **2009**, *9*, 2293-2305.

(152) He, M.; Sun, C.; Chiu, D. T. Concentrating solutes and nanoparticles within individual aqueous microdroplets. *Analytical Chemistry* **2004**, *76*, 1222-1227.
(153) Jeffries, G. D. M.; Kuo, J. S.; Chiu, D. T. Controlled shrinkage and re-expansion of a single aqueous droplet inside an optical vortex trap. *The Journal of Physical Chemistry B* **2007**, *111*, 2806-2812.
(154) Jeffries, G. D. M.; Kuo, J. S.; Chiu, D. T. Dynamic dodulation of chemical concentration in an aqueous droplet. *Angewandte Chemie International Edition* **2007**, *46*, 1326-1328.
(155) Boukellal, H.; Selimovic, S.; Jia, Y.; Cristobal, G.; Fraden, S. Simple, robust storage of drops and fluids in a microfluidic device. *Lab on a Chip* **2009**, *9*, 331-338.
(156) Frenz, L.; Blank, K.; Brouzes, E.; Griffiths, A. D. Reliable microfluidic on-chip incubation of droplets in delay-lines. *Lab on a Chip* **2009**, *9*, 1344-1348.
(157) Huebner, A.; Bratton, D.; Whyte, G.; Yang, M.; deMello, A. J.; Abell, C.; Hollfelder, F. Static microdroplet arrays: a microfluidic device for droplet trapping, incubation and release for enzymatic and cell-based assays. *Lab on a Chip* **2009**, *9*, 692-698.
(158) Li, L.; Boedicker, J. Q.; Ismagilov, R. F. Using a multijunction microfluidic device to inject substrate into an array of preformed plugs without cross-contamination: Comparing theory and experiments. *Analytical Chemistry* **2007**, *79*, 2756-2761.
(159) Song, H.; Li, H. W.; Munson, M. S.; Van Ha, T. G.; Ismagilov, R. F. On-chip titration of an anticoagulant argatroban and determination of the clotting time within whole blood or plasma using a plug-based microfluidic system. *Analytical Chemistry* **2006**, *78*, 4839-4849.
(160) Angelescu, D. E.; Mercier, B.; Siess, D.; Schroeder, R. Microfluidic capillary separation and real-time spectroscopic dnalysis of specific components from multiphase mixtures. *Analytical Chemistry* **2010**, *82*, 2412-2420.
(161) Castell, O. K.; Allender, C. J.; Barrow, D. A. Liquid-liquid phase separation: characterisation of a novel device capable of separating particle carrying multiphase flows. *Lab on a Chip* **2009**, *9*, 388-396.
(162) Fidalgo, L. M.; Graeme, W.; Bratton, D.; Kaminski, C. F.; Abell, C.; Huck, W. T. S. From microdroplets to microfluidics: selective emulsion separation in microfluidic devices. *Angewandte Chemie International Edition* **2008**, *47*, 2042-2045.
(163) Zhu, Y.; Fang, Q. Integrated Droplet Analysis System with Electrospray Ionization-Mass Spectrometry Using a Hydrophilic Tongue-Based Droplet Extraction Interface. *Analytical Chemistry* **2010**, *82*, 8361-8366.
(164) Tice, J. D.; Song, H.; Lyon, A. D.; Ismagilov, R. F. Formation of droplets and mixing in multiphase microfluidics at low values of the reynolds and the capillary numbers. *Langmuir* **2003**, *19*, 9127-9133.
(165) Song, H.; Tice, J. D.; Ismagilov, R. F. A microfluidic system for controlling reaction networks in time. *Angewandte Chemie International Edition* **2003**, *42*, 768-772.
(166) Chiu, D. T.; Lorenz, R. M.; Jeffries, G. D. M. Droplets for ultrasmall-volume analysis. *Analytical Chemistry* **2009**, *81*, 5111-5118.

(167) Chiu, D. T.; Lorenz, R. M. Chemistry and biology in femtoliter and picoliter volume droplets. *Accounts of Chemical Research* **2009**, *42*, 649-658.
(168) Song, H.; Ismagilov, R. F. Millisecond kinetics on a microfluidic chip using nanoliters of reagents. *Journal of American Chemical Society* **2003**, *125*, 14613-14619.
(169) Mazutis, L.; Baret, J.-C.; Treacy, P.; Skhiri, Y.; Araghi, A. F.; Ryckelynck, M.; Taly, V.; Griffiths, A. D. Multi-step microfluidic droplet processing: kinetic analysis of an in vitro translated enzyme. *Lab on a Chip* **2009**, *9*, 2902-2908.
(170) Srisa-Art, M.; deMello, A. J.; Edel, J. B. High-throughput DNA droplet assays using picoliter reactor volumes. *Analytical Chemistry* **2007**, *79*, 6682-6689.
(171) Hsieh, A. T.-H.; Hori, N.; Massoudi, R.; Pan, P. J.-H.; Sasaki, H.; Lin, Y. A.; Lee, A. P. Nonviral gene vector formation in monodispersed picolitre incubator for consistent gene delivery. *Lab on a Chip* **2009**, *9*, 2638-2643.
(172) Dittrich, P. S.; Jahnz, M.; Schwille, P. A new embedded process for compartmentalized cell-free protein expression and on-line detection in microfluidic devices. *ChemBioChem* **2005**, *6*, 811-814.
(173) Zhang, Y.; Bailey, V.; Puleo, C. M.; Easwaran, H.; Griffiths, E.; Herman, J. G.; Baylin, S. B.; Wang, T.-H. DNA methylation analysis on a droplet-in-oil PCR array. *Lab on a Chip* **2009**, *9*, 1059-1064.
(174) Mazutis, L.; Araghi, A. F.; Miller, O. J.; Baret, J.-C.; Frenz, L.; Janoshazi, A.; Taly, V.; Miller, B. J.; Hutchison, J. B.; Link, D.; Griffiths, A. D.; Ryckelynck, M. Droplet-based microfluidic systems for high-throughput single DNA molecule isothermal amplification and analysis. *Analytical Chemistry* **2009**, *81*, 4813-4821.
(175) Kumaresan, P.; Yang, C. J.; Cronier, S. A.; Blazej, R. G.; Mathies, R. A. High-throughput single copy DNA amplification and cell analysis in engineered nanoliter droplets. *Analytical Chemistry* **2008**, *80*, 3522-3529.
(176) Chabert, M.; Dorfman, K. D.; deCremoux, P.; Roeraade, J.; Viovy, J. L. Automated microdroplet platform for sample manipulation and polymerase chain reaction. *Analytical Chemistry* **2006**, *78*, 7722-7728.
(177) Kiss, M. M.; Ortoleva-Donnelly, L.; Beer, N. R.; Warner, J.; Bailey, C. G.; Colston, B. W.; Rothberg, J. M.; Link, D. R.; Leamon, J. H. High-throughput quantitative polymerase chain reaction in picoliter droplets. *Analytical Chemistry* **2008**, *80*, 8975-8981.
(178) Li, L.; Mustafi, D.; Fu, Q.; Tereshko, V.; Chen, D. L.; Tice, J. D.; Ismagilov, R. F. Nanoliter microfluidic hybrid method for simultaneous screening and optimization validated with crystallization of membrane proteins. *Analytical Chemistry* **2006**, *103*, 19243-19248.
(179) Zheng, B.; Ismagilov, R. F. A microfluidic approach for screening submicroliter volumes against multiple reagents by using preformed arrays of nanoliter plugs in a three-phase liquid/liquid/gas flow. *Angewandte Chemie International Edition* **2005**, *44*, 2520-2523.
(180) Hatakeyama, T.; Chen, D. L.; Ismagilov, R. F. Microgram-scale testing of reaction conditions in solution using nanoliter plugs in microfluidics with detection by MALDI-MS. *Journal of American Chemical Society* **2006**, *128*, 2518-2519.

(181) Xu, J. H.; Li, S. W.; Tan, J.; Wang, Y. J.; Luo, G. S. Preparation of highly monodisperse droplet in a T-junction microfluidic device. *American Institute of Chemical Engineers Journal* **2006**, *52*, 3005-3010.
(182) Chan, E. M.; Alivisatos, A. P.; Mathies, R. A. High-temperature microfluidic synthesis of CdSe nanocrystals in nanoliter droplets. *Journal of American Chemical Society* **2005**, *127*, 13854-13861.
(183) Zhan, Y.; Wang, J.; Bao, N.; Lu, C. Electroporation of cells in microfluidic droplets. *Analytical Chemistry* **2009**, *81*, 2027-2031.
(184) Edd, J. F.; Carlo, D. D.; Humphry, K. J.; Koster, S.; Irimia, D.; Weitz, D. A.; Toner, M. Controlled encapsulation of single-cells into monodisperse picolitre drops. *Lab on a Chip* **2008**, *8*, 1262-1264.
(185) He, M.; Edgar, J. S.; Jeffries, G. D. M.; Lorenz, R. M.; Shelby, J. P.; Chiu, D. T. Selective encapsulation of single cells and subcellular organelles into picoliter- and femtoliter-volume droplets. *Analytical Chemistry* **2005**, *77*, 1539-1544.
(186) Tan, Y. C.; Hettiarachchi, K.; Siu, M.; Pan, Y. R.; Lee, A. P. Controlled microfluidic encapsulation of cells, proteins, and microbeads in lipid vesicles. *Journal of American Chemical Society* **2006**, *128*, 5656-5658.
(187) Shi, W.; Qin, J.; Ye, N.; Lin, B. Droplet-based microfluidic system for individual Caenorhabditis elegans assay. *Lab on a Chip* **2008**, *8*, 1432-1435.
(188) Jeffries, G. D. M.; Edgar, J. S.; Zhao, Y.; Shelby, J. P.; Fong, C.; Chiu, D. T. Using polarization-shaped optical vortex traps for single-cell nanosurgery. *Nano Letters* **2006**, *7*, 415-420.
(189) Chen, D. L.; Ismagilov, R. F. Microfluidic cartridges preloaded with nanoliter plugs of reagents: an alternative to 96-well plates for screening. *Current Opinion in Chemical Biology* **2006**, *10*, 226-231.
(190) Pei, J.; Dishinger, J. F.; Roman, D. L.; Rungwanitcha, C.; Neubig, R. R.; Kennedy, R. T. Microfabricated channel array electrophoresis for characterization and screening of enzymes using RGS-G protein interactions as a model system. *Analytical Chemistry* **2008**, *80*, 5225-5231.
(191) Pei, J.; Li, Q.; Kennedy, R. T. Rapid and label-free screening of enzyme inhibitors using segmented flow electrospray ionization mass spectrometry. *Journal of the American Society for Mass Spectrometry* **2010**, *21*, 1107-1113.
(192) Churski, K.; Korczyk, P.; Garstecki, P. High-throughput automated droplet microfluidic system for screening of reaction conditions. *Lab on a Chip* **2010**, *10*, 816-818.
(193) Sun, M.; Fang, Q. High-throughput sample introduction for droplet-based screening with an on-chip integrated sampling probe and slotted-vial array. *Lab on a Chip* **2010**, *10*, 2864-2868.
(194) Boedicker, J. Q.; Li, L.; Kline, T. R.; Ismagilov, R. F. Detecting bacteria and determining their susceptibility to antibiotics by stochastic confinement in nanoliter droplets using plug-based microfluidics. *Lab on a Chip* **2008**, *8*, 1265-1272.
(195) Kreutz, J. E.; Li, L.; Roach, L. S.; Hatakeyama, T.; Ismagilov, R. F. Laterally mobile, functionalized self-assembled monolayers at the fluorous-aqueous interface in a plug-based microfluidic system: Characterization and testing with

membrane protein crystallization. *Journal of the American Chemical Society* **2009**, *131*, 6042-6043.
(196) Choi, C.-H.; Jung, J.-H.; Kim, D.-W.; Chung, Y.-M.; Lee, C.-S. Novel one-pot route to monodisperse thermosensitive hollow microcapsules in a microfluidic system. *Lab on a Chip* **2008**, *8*, 1544-1551.
(197) Kralj, J. G.; Schmidt, M. A.; Jensen, K. F. Surfactant-enhanced liquid-liquid extraction in microfluidic channels with inline electric-field enhanced coalescence. *Lab on a Chip* **2005**, *5*, 531-535.
(198) Kumemura, M.; Korenaga, T. Quantitative extraction using flowing nano-liter droplet in microfluidic system. *Analytica Chimica Acta* **2006**, *558*, 75-79.
(199) Castell, O. K.; Allender, C. J.; Barrow, D. A. Continuous molecular enrichment in microfluidic systems. *Lab on a Chip* **2008**, *8*, 1031-1033.
(200) Barikbin, Z.; Rahman, M. T.; Parthiban, P.; Rane, A. S.; Jain, V.; Duraiswamy, S.; Lee, S. H. S.; Khan, S. A. Ionic liquid-based compound droplet microfluidics for 'on-drop' separations and sensing. *Lab on a Chip* **2010**, *10*, 2458-2463.
(201) Prakash, M.; Gershenfeld, N. Microfluidic bubble logic. *Science* **2007**, *315*, 832-835.
(202) Zagnoni, M.; Cooper, J. M. A microdroplet-based shift register. *Lab on a Chip* **2010**, *10*, 3069-3073.
(203) Um, E.; Park, J.-K. A microfluidic abacus channel for controlling the addition of droplets. *Lab on a Chip* **2009**, *9*, 207-212.
(204) Easley, C. J.; Rocheleau, J. V.; Head, W. S.; Piston, D. W. Quantitative measurement of zinc secretion from pancreatic islets with high temporal resolution using droplet-based microfluidics. *Analytical Chemistry* **2009**.
(205) Chen, D.; Du, W.; Liu, Y.; Liu, W.; Kuznetsov, A.; Mendez, F. E.; Philipson, L. H.; Ismagilov, R. F. The chemistrode: A droplet-based microfluidic device for stimulation and recording with high temporal, spatial, and chemical resolution. *Proceedings of the National Academy of Sciences of the United States of America* **2008**, *105*, 16843-16848.
(206) Liu, Y.; Ismagilov, R. F. Dynamics of coalescence of plugs with a hydrophilic wetting layer induced by flow in a microfluidic chemistrode. *Langmuir* **2009**, *25*, 2854-2859.
(207) Edgar, J. S.; Graham, M.; Yiqiong, Z.; Chaitanya, P. P.; David, S. W. L.; Chiu, D. T. Compartmentalization of chemically separated components into droplets. *Angewandte Chemie International Edition* **2009**, *48*, 2719-2722.
(208) Li, Q.; Pei, J.; Song, P.; Kennedy, R. T. Fraction collection from capillary liquid chromatography and off-line electrospray ionization mass spectrometry using oil segmented flow. *Analytical Chemistry* **2010**, *82*, 5260-5267.
(209) Niu, X. Z.; Zhang, B.; Marszalek, R. T.; Ces, O.; Edel, J. B.; Klug, D. R.; deMello, A. J. Droplet-based compartmentalization of chemically separated components in two-dimensional separations. *Chemical Communications* **2009**, 6159-6161.
(210) Pei, J.; Li, Q.; Lee, M. S.; Valaskovic, G. A.; Kennedy, R. T. Analysis of samples stored as individual plugs in a capillary by electrospray ionization mass spectrometry. *Analytical Chemistry* **2009**, *81*, 6558-6561.

(211) Kelly, R. T.; Page, J. S.; Marginean, I.; Tang, K.; Smith, R. D. Dilution-free analysis from picoliter droplets by nano-electrospray ionization mass spectrometry. *Angewandte Chemie International Edition* **2009**, *48*, 6832-6835.
(212) Fidalgo, L. M.; Whyte, G.; Ruotolo, B. T.; Benesch, J. L. P.; Stengel, F.; Abell, C.; Robinson, C. V.; Huck, W. T. S. Coupling microdroplet microreactors with mass spectrometry: Reading the contents of single droplets online. *Angewandte Chemie International Edition* **2009**, *48*, 3665-3668.
(213) Liu, S.; Gu, Y.; Le Roux, R. B.; Matthews, S. M.; Bratton, D.; Yunus, K.; Fisher, A. C.; Huck, W. T. S. The electrochemical detection of droplets in microfluidic devices. *Lab on a Chip* **2008**, *8*, 1937-1942.
(214) Kautz, R. A.; Goetzinger, W. K.; Karger, B. L. High-throughput microcoil NMR of compound libraries using zero-dispersion segmented flow analysis. *Journal of Combinatorial Chemistry* **2004**, *7*, 14-20.
(215) Edgar, J. S.; Pabbati, C. P.; Lorenz, R. M.; He, M.; Fiorini, G. S.; Chiu, D. T. Capillary electrophoresis separation in the presence of an immiscible boundary for droplet analysis. *Analytical Chemistry* **2006**, *78*, 6948-6954.
(216) Abdelgawad, M.; Watson, M. W. L.; Wheeler, A. R. Hybrid microfluidics: A digital-to-channel interface for in-line sample processing and chemical separations. *Lab on a Chip* **2009**, *9*, 1046-1051.
(217) Watson, M. W. L.; Jebrail, M. J.; Wheeler, A. R. Multilayer hybrid microfluidics: A digital-to-channel interface for sample processing and separations. *Analytical Chemistry* **2010**, *82*, 6680-6686.
(218) Plock, N.; Kloft, C. Microdialysis--theoretical background and recent implementation in applied life-sciences. *European Journal of Pharmaceutical Sciences* **2005**, *25*, 1-24.
(219) Ungerstedt, U.; Pycock, C. Functional correlates of dopamine neurotransmission. *Bull. Schweiz. Akad. Med. Wiss.* **1974**, *30*, 44-55.
(220) During, M. J. *Microdialysis in the neurosciences*; Elsevier Science Publishers BV: New York, 1991.
(221) Wages, S. A.; H., C. W.; Justice, J. B. J. Sampling considerations for on-line microbore liquid chromatography of brain dialysis. *Analytical Chemistry* **1986**, *58*, 1649-1656.
(222) Gunther, A.; Khan, S. A.; Thalmann, M.; Trachsel, F.; Jensen, K. F. Transport and reaction in microscale segmented gas-liquid flow. *Lab on a Chip* **2004**, *4*, 278-286.
(223) Gunther, A.; Thalmann, M.; Jhunjhunwala, M.; Schmidt, M. A.; Jensen, K. F. Micromixing of miscible liquids in segmented gas-liquid flow. *Langmuir* **2005**, *21*, 1547-1555.
(224) Kralj, J. G.; Sahoo, H. R.; Jensen, K. F. Integrated continuous microfluidic liquid-liquid extraction. *Lab on a Chip* **2007**, *7*, 256-263.
(225) Shim, J. u.; Cristobal, G.; Link, D. R.; Thorsen, T.; Jia, Y.; Piattelli, K.; Fraden, S. Control and measurement of the phase behavior of aqueous Solutions using microfluidics. *Journal of American Chemical Society* **2007**, *129*, 8825-8835.
(226) Zheng, B.; Tice, J. D.; Roach, L. S.; Ismagilov, R. F. A droplet-based, composite PDMS/glass capillary microfluidic system for evaluating protein crystallization

conditions by microbatch and vapor-diffusion methods with on-chip X-ray diffraction. *Angewandte Chemie International Edition* **2004**, *43*, 2508-2511.
(227) Gerdts, C. J.; Sharoyan, D. E.; Ismagilov, R. F. A synthetic reaction network: Chemical amplification using nonequilibrium autocatalytic reactions coupled in time. *Journal of American Chemical Society* **2004**, *126*, 6327-6331.
(228) Zheng, B.; Roach, L. S.; Ismagilov, R. F. Screening of protein crystallization conditions on a microfluidic chip using nanoliter-size droplets. *Journal of American Chemical Society* **2003**, *125*, 11170-11171.
(229) Burns, M. A.; Johnson, B. N.; Brahmasandra, S. N.; Handique, K.; Webster, J. R.; Krishnan, M.; Sammarco, T. S.; Man, P. M.; Jones, D.; Heldsinger, D.; Mastrangelo, C. H.; Burke, D. T. An integrated nanoliter DNA analysis device. *Science* **1998**, *282*, 484-487.
(230) Sugiura, S.; Oda, T.; Izumida, Y.; Aoyagi, Y.; Satake, M.; Ochiai, A.; Ohkohchi, N.; Nakajima, M. Size control of calcium alginate beads containing living cells using micro-nozzle array. *Biomaterials* **2005**, *26*, 3327-3331.
(231) Sia, S. K.; Whitesides, G. M. Microfluidic devices fabricated in Poly(dimethylsiloxane) for biological studies. *ELECTROPHORESIS* **2003**, *24*, 3563-3576.
(232) Whitesides, G. M.; Ostuni, E.; Takayama, S.; Jiang, X.; Ingber, D. E. Soft lithography in biology and biochemistry. *Annual Review of Biomedical Engineering* **2001**, *3*, 335-373.
(233) Anderson, J. R.; Chiu, D. T.; Jackman, R. J.; Cherniavskaya, O.; McDonald, J. C.; Wu, H.; Whitesides, S. H.; Whitesides, G. M. Fabrication of topologically complex three-dimensional microfluidic systems in PDMS by rapid prototyping. *Analytical Chemistry* **2000**, *72*, 3158-3164.
(234) Duffy, D. C.; McDonald, J. C.; Schueller, O. J. A.; Whitesides, G. M. Rapid prototyping of microfluidic systems in poly(dimethylsiloxane). *Analytical Chemistry* **1998**, *70*, 4974-4984.
(235) McDonald, J. C.; Whitesides, G. M. Poly(dimethylsiloxane) as a material for fabricating microfluidic devices. *Accounts of Chemical Research* **2002**, *35*, 491-499.
(236) Zhao, B.; Moore, J. S.; Beebe, D. J. Surface-directed liquid flow inside microchannels. *Science* **2001**, *291*, 1023-1026.
(237) Shackman, J. G.; Watson, C. J.; Kennedy, R. T. High-throughput automated post-processing of separation data. *Journal of Chromatography A* **2004**, *1040*, 273-282.
(238) Wilkes, J. O. In *Fluid Mechanics for Chemical Engineers*; Pearson Education, Inc.: Upper Saddle River, NJ, 2006, pp 414-419.
(239) Culbertson, C. T.; Jacobson, S. C.; Michael Ramsey, J. Diffusion coefficient measurements in microfluidic devices. *Talanta* **2002**, *56*, 365-373.
(240) Paxinos, G.; Watson, C. *The rat brain in stereotaxic coordinates*; Academic Press, 1998.
(241) Stenken, J. A.; Topp, E. M.; Southard, M. Z.; Lunte, C. E. Examination of microdialysis sampling in a well-characterized hydrodynamic system. *Analytical Chemistry* **1993**, *65*, 2324-2328.
(242) Fox, P. T.; Raichle, M. E.; Mintun, M. A.; Dence, C. Nonoxidative glucose consumption during focal physiologic neural activity. *Science* **1988**, *241*, 462-464.

(243) Korol, D. L.; Gold, P. E. Glucose, memory, and aging. *The American Journal of Clinical Nutrition* **1998**, *67*, 764S-771.
(244) McNay, E. C.; Fries, T. M.; Gold, P. E. Decreases in rat extracellular hippocampal glucose concentration associated with cognitive demand during a spatial task. *Proceedings of the National Academy of Sciences of the United States of America* **2000**, *97*, 2881-2885.
(245) Hopwood, S. E.; Parkin, M. C.; Bezzina, E. L.; Boutelle, M. G.; Strong, A. J. Transient changes in cortical glucose and lactate levels associated with peri-infarct depolarisations, studied with rapid-sampling microdialysis. *Journal of Cerebral Blood Flow & Metabolism* **2005**, *25*, 391-401.
(246) McNay, E. C.; Gold, P. E. Extracellular glucose concentrations in the rat hippocampus measured by zero-net-flux: Effects of microdialysis flow rate, strain, and age. *Journal of Neurochemistry* **1999**, *72*, 785-790.
(247) Darbin, O.; Carre, E.; Naritoku, D.; Risso, J. J.; Lonjon, M.; Patrylo, P. R. Glucose metabolites in the striatum of freely behaving rats following infusion of elevated potassium. *Brain Research* **2006**, *1116*, 127-131.
(248) Uehara, T.; Sumiyoshi, T.; Itoh, H.; Kurachi, M. Dopamine D1 and D2 receptors regulate extracellular lactate and glucose concentrations in the nucleus accumbens. *Brain Research* **2007**, *1133*, 193-199.
(249) Weiss, D. J.; Lunte, C. E.; Lunte, S. M. In vivo microdialysis as a tool for monitoring pharmacokinetics. *TrAC Trends in Analytical Chemistry* **2000**, *19*, 606-616.
(250) Bhatia, R.; Hashemi, P.; Razzaq, A.; Parkin, M. C.; Hopwood, S. E.; Boutelle, M. G.; Strong, A. J. Application of rapid-sampling, online microdialysis to the monitoring of brain metabolism during aneurysm surgery. *Neurosurgery* **2006**, *58*, ONS-313-321.
(251) Deeba, S.; Corcoles, E.; Hanna, B.; Pareskevas, P.; Aziz, O.; Boutelle, M.; Darzi, A. Use of Rrpid sampling microdialysis for intraoperative monitoring of bowel ischemia. *Diseases of the Colon & Rectum* **2008**, *51*, 1408-1413.
(252) Wang, M.; Roman, G. T.; Schultz, K.; Jennings, C.; Kennedy, R. T. Improved temporal resolution for in vivo microdialysis by using segmented flow. *Analytical Chemistry* **2008**, *80*, 5607-5615.
(253) Skeggs, L. T., Jr. An automatic method for colorimetric analysis. *American Journal of Clinical Pathology* **1957**, *28*, 311-322.
(254) Rada, P.; Tucci, S.; Perez, J.; Teneud, L.; Chuecos, S.; Hernandez, L. In vivo monitoring of gabapentin in rats: A microdialysis study coupled to capillary electrophoresis and laser-induced fluorescence detection. *ELECTROPHORESIS* **1998**, *19*, 2976-2980.
(255) Roman, G. T.; Wang, M.; Shultz, K. N.; Jennings, C.; Kennedy, R. T. Sampling and electrophoretic analysis of segmented flow streams using virtual walls in a microfluidic device. *Analytical Chemistry* **2008**, *80*, 8231-8238.
(256) Roper, M. G.; Shackman, J. G.; Dahlgren, G. M.; Kennedy, R. T. Microfluidic chip for continuous monitoring of hormone secretion from live cells using an electrophoresis-based immunoassay. *Analytical Chemistry* **2003**, *75*, 4711-4717.
(257) De Montigny, P.; Stobaugh, J. F.; Givens, R. S.; Carlson, R. G.; Srinivasachar, K.; Sternson, L. A.; Higuchi, T. Naphthalene-2,3-dicarboxyaldehyde/cyanide ion: a

rationally designed fluorogenic reagent for primary amines. *Analytical Chemistry* **1987**, *59*, 1096-1101.

(258) Zhou, S. Y.; Zuo, H.; Stobaugh, J. F.; Lunte, C. E.; Lunte, S. M. Continuous in vivo monitoring of amino acid neurotransmitters by microdialysis sampling with online derivatization and capillary electrophoresis separation. *Analytical Chemistry* **1995**, *67*, 594-599.

(259) Yassine, O.; Morin, P.; Dispagne, O.; Renaud, L.; Denoroy, L.; Kleimann, P.; Faure, K.; Rocca, J. L.; Ouaini, N.; Ferrigno, R. Electrophoresis PDMS/glass chips with continuous on-chip derivatization and analysis of amino acids using naphthalene-2,3-dicarboxaldehyde as fluorogenic agent. *Analytica Chimica Acta* **2008**, *609*, 215-222.

(260) Freed, A. L.; Cooper, J. D.; Davies, M. I.; Lunte, S. M. Investigation of the metabolism of substance P in rat striatum by microdialysis sampling and capillary electrophoresis with laser-induced fluorescence detection. *Journal of Neuroscience Methods* **2001**, *109*, 23-29.

(261) Bings, N. H.; Wang, C.; Skinner, C. D.; Colyer, C. L.; Thibault, P.; Harrison, D. J. Microfluidic devices connected to fused-silica capillaries with minimal dead volume. *Analytical Chemistry* **1999**, *71*, 3292-3296.

(262) Li, H.-F.; Liu, J.; Cai, Z.; Lin, J.-M. Coupling a microchip with electrospray ionization quadrupole time-of-flight mass spectrometer for peptide separation and identification. *ELECTROPHORESIS* **2008**, *29*, 1889-1894.

(263) Tsai, J.-H.; Lin, L. Active microfluidic mixer and gas bubble filter driven by thermal bubble micropump. *Sensors and Actuators A: Physical* **2002**, *97-98*, 665-671.

(264) Anderson, J. J.; DiMicco, J. A. The use of microdialysis for studying the regional effects of pharmacological manipulation on extracellular levels of amino acids - some methodological aspects. *Life Sciences* **1992**, *51*, 623-630.

(265) Butcher, S. P.; Sandberg, M.; Hagberg, H.; Hamberger, A. Cellular origins of endogenous amino acids released into the extracellular fluid of the rat striatum during severe insulin-induced hypoglycemia. *Journal of Neurochemistry* **1987**, *48*, 722-728.

(266) Massieu, L.; Morales-Villagran, A.; Tapia, R. Accumulation of extracellular glutamate by inhibition of its uptake is not sufficient for inducing neuronal damage: an in vivo microdialysis study. *Journal of Neurochemistry* **1995**, *64*, 2262-2272.

(267) Rawls, S. M.; McGinty, J. E. L-*trans*-pyrrolidine-2,4-dicarboxylic acid-evoked striatal glutamate levels are attenuated by calcium reduction, tetrodotoxin, and glutamate receptor blockade. *Journal of Neurochemistry* **1997**, *68*, 1553-1563.

(268) Wang, M.; Roman, G. T.; Perry, M. L.; Kennedy, R. T. Microfluidic chip for high efficiency electrophoretic analysis of segmented flow from a microdialysis probe and in vivo chemical monitoring. *Analytical Chemistry* **2009**, *81*, 9072-9078.

(269) Smith, A.; Watson, C. J.; Frantz, K. J.; Eppler, B.; Kennedy, R. T.; Peris, J. Differential increase in taurine levels by low-dose ethanol in the dorsal and ventral striatum revealed by microdialysis with on-line capillary electrophoresis. *Alcoholism: Clinical and Experimental Research* **2004**, *28*, 1028-1038.

(270) Zhou, J.; Heckert, D. M.; Zuo, H.; Lunte, C. E.; Lunte, S. M. On-line coupling of in vivo microdialysis with capillary electrophoresis/electrochemistry. *Analytica Chimica Acta* **1999**, *379*, 307-317.
(271) Del Arco, A.; Mora, F. Effects of endogenous glutamate on extracellular concentrations of GABA, dopamine, and dopamine metabolites in the prefrontal cortex of the freely moving rat: Involvement of NMDA and AMPA/KA receptors. *Neurochemical Research* **1999**, *24*, 1027-1035.
(272) Segovia, G.; Del Arco, A.; Mora, F. Endogenous glutamate increases extracellular concentrations of dopamine, GABA, and taurine Through NMDA and AMPA/kainate receptors in striatum of the freely moving rat: A microdialysis study. *Journal of Neurochemistry* **1997**, *69*, 1476-1483.
(273) Day, B. K.; Pomerleau, F.; Burmeister, J. J.; Huettl, P.; Gerhardt, G. A. Microelectrode array studies of basal and potassium-evoked release of l-glutamate in the anesthetized rat brain. *Journal of Neurochemistry* **2006**, *96*, 1626-1635.
(274) Nickell, J.; Pomerleau, F.; Allen, J.; Gerhardt, G. A. Age-related changes in the dynamics of potassium-evoked L-glutamate release in the striatum of Fischer 344 rats. *Journal of Neural Transmission* **2005**, *112*, 87-96.
(275) Semba, J.; Kito, S.; Toru, M. Characterisation of extracellular amino acids in striatum of freely moving rats by in vivo microdialysis. *Journal of Neural Transmission* **1995**, *100*, 39-52.
(276) Wang, M.; Slaney, T.; Mabrouk, O.; Kennedy, R. T. Collection of nanoliter microdialysate fractions in plugs for off-line in vivo chemical monitoring with up to 2 s temporal resolution. *Journal of Neuroscience Methods* **2010**, *190*, 39-48.
(277) Nickerson, B.; Jorgenson, J. W. High sensitivity laser induced fluorescence detection in capillary zone electrophoresis. *Journal of High Resolution Chromatography* **1988**, *11*, 878-881.
(278) Sauvinet, V.; Parrot, S.; Benturquia, N.; Bravo-Moratón, E.; Renaud, B.; Denoroy, L. In vivo simultaneous monitoring of γ-aminobutyric acid, glutamate, and L-aspartate using brain microdialysis and capillary electrophoresis with laser-induced fluorescence detection: Analytical developments and in vitro/in vivo validations. *ELECTROPHORESIS* **2003**, *24*, 3187-3196.
(279) Bao, Y.; Lantz, A. W.; Crank, J. A.; Huang, J.; Armstrong, D. W. The use of cationic surfactants and ionic liquids in the detection of microbial contamination by capillary electrophoresis. *ELECTROPHORESIS* **2008**, *29*, 2587-2592.
(280) Mwongela, S. M.; Numan, A.; Gill, N. L.; Agbaria, R. A.; Warner, I. M. Separation of achiral and chiral analytes using polymeric surfactants with ionic liquids as modifiers in micellar electrokinetic chromatography. *Analytical Chemistry* **2003**, *75*, 6089-6096.
(281) Grossman, M. H.; Hare, T. A.; Bala Manyam, N. V.; Glaeser, B. S.; Wood, J. H. Stability of GABA levels in CSF under various conditions of storage. *Brain Research* **1980**, *182*, 99-106.
(282) Segovia, G.; Mora, F. Role of nitric oxide in modulating the release of dopamine, glutamate, and GABA in striatum of the freely moving rat. *Brain Research Bulletin* **1998**, *45*, 275-279.
(283) Kennedy, R. T. Bioanalytical applications of fast capillary electrophoresis. *Analytica Chimica Acta* **1999**, *400*, 163-180.

(284) Chen, D.; Dovichi, N. J. Single-molecule detection in capillary electrophoresis: Molecular shot noise as a fundamental limit to chemical analysis. *Analytical Chemistry* **1996**, *68*, 690-696.
(285) Mayer, B. X. How to increase precision in capillary electrophoresis. *Journal of Chromatography A* **2001**, *907*, 21-37.
(286) Reid, K. R.; Kennedy, R. T. Continuous operation of microfabricated electrophoresis devices for 24 hours and application to chemical monitoring of living cells. *Analytical Chemistry* **2009**, *81*, 6837-6842.
(287) Pei, J.; Nie, J.; Kennedy, R. T. Parallel electrophoretic analysis of segmented samples on chip for high-throughput determination of enzyme activities. *Analytical Chemistry* **2010**, *82*, 9261-9267.
(288) Aota, A.; Hibara, A.; Kitamori, T. Pressure balance at the liquid-liquid interface of micro countercurrent flows in microchips. *Analytical Chemistry* **2007**, *79*, 3919-3924.
(289) Aota, A.; Nonaka, M.; Hibara, A.; Kitamori, T. Countercurrent laminar microflow for highly efficient solvent extraction. *Angewandte Chemie International Edition* **2007**, *119*, 896-898.
(290) Hibara, A.; Iwayama, S.; Matsuoka, S.; Ueno, M.; Kikutani, Y.; Tokeshi, M.; Kitamori, T. Surface modification method of microchannels for gas-liquid two-phase flow in microchips. *Analytical Chemistry* **2004**, *77*, 943-947.
(291) Liang, D.; Hongrui, J. Tunable and movable liquid microlens in situ fabricated within microfluidic channels. *Applied Physics Letters* **2007**, *91*, 041109.
(292) Xiao, H.; Liang, D.; Liu, G.; Guo, M.; Xing, W.; Cheng, J. Initial study of two-phase laminar flow extraction chip for sample preparation for gas chromatography. *Lab on a Chip* **2006**, *6*, 1067-1072.
(293) Atencia, J.; Beebe, D. J. Controlled microfluidic interfaces. *Nature* **2005**, *437*, 648-655.